A bioengineered novel human functional neuromuscular junction platform for drug testing and diabetes studies

M Abd Al Samid

PhD 2020

A bioengineered novel human functional neuromuscular junction platform for drug testing and diabetes studies

Marwah Abd Al Samid

A thesis submitted in partial fulfilment of the requirements of the Manchester Metropolitan University for the degree of Doctor of Philosophy

Department of life sciences
Faculty of Science and Engineering
Manchester Metropolitan University

2020

Table of Contents

Acknowledgements

Firstly, thank you to my director of studies Dr Nasser Al-Shanti for the opportunity to pursue my academic career and all the support and guidance throughout this project.

Special thanks to Prof. Jamie S McPhee, Prof. Tristan McKay for their help and time throughout this project.

Special thanks for my husband Eng. Noor Al-Beldawe for his continued help and support throughout my PhD and motivation to pursue excellence in all aspects of my life.

Most importantly, thank you to my family, my father Mr. Mohamed Abd Al Samid, mother Mrs. Bushra Abd Al Jabbar and my siblings Mrs. Yasmin Abd Al Samid, Mr. Ahmed Abd Al Samid, Dr May Abd Al Samid, Eng. Ali Abd Al Samid and Eng. Fatimah Abd Al Samid for their past, present, and future support.

Lastly, thank you to my daughter Jinan Al-Beldawe and son Fanar Al-Beldawe for motivating me to pursue excellence in all aspects of my life.

Publications

Original Research Paper

Abd Al Samid, M., McPhee, J. S., Saini, J., McKay, T. R., Fitzpatrick, L. M., Mamchaoui, K., Bigot, A., Mouly, V., Butler-Browne, G. and Al-Shanti, N. (2018) 'A functional human motor unit platform engineered from human embryonic stem cells and immortalized skeletal myoblasts.' Stem Cells Cloning, 11 pp. 85-93.

Contributing Author

Saini, J., Faroni, A., **Abd Al Samid, M**., Reid, A. J., Lightfoot, A. P., Mamchaoui, K., Mouly, V., Butler-Browne, G., McPhee, J. S., Degens, H. and Al-Shanti, N. (2019) 'Simplified *in vitro* engineering of neuromuscular junctions between rat embryonic motoneurons and immortalized human skeletal muscle cells.' Stem Cells Cloning, 12 pp. 1-9.

Declaration

With the exception of any statements to the contrary, all the data presented in this report are the results of my own efforts and have not previously been submitted in candidature for any other degree or diploma. In addition, I contributed in an additional article with my colleague Dr. Jasdeep Saini, MMU as I cooperated in optimising and growing the SkMC's and optimising suitable growth and differentiation media. However, this work was before my thesis and I declare that in this thesis work presented I did all labwork and entire experiments alone.

Signed ……. **Date** …….

List of abbreviations

± SD	plus/minus standard deviation
α-BTX	α-bungarotoxin
αFF	fast-twitch fatigable motor neurons
αFR	fast-twitch fatigue-resistant motor neurons
αMN(s)	alpha motor neuron(s)
αS	slow-twitch fatigue resistant motor neurons
β-III-tubulin	class III β-tubulin
βMN(s)	beta motor neuron(s)
γMN(s)	gamma motor neuron(s)
AP(s)	action potential(s)
ACh	acetylcholine
AChR(s)	acetylcholine receptor(s)
ADP	adenosine diphosphate
ALS	amyotrophic lateral sclerosis
AR	aspect ratio
ATM	37°C with a 5% CO2 atmosphere
ATP	adenosine triphosphate
BDNF	brain-derived neurotrophic factor
C25	25-year-old immortalised human myoblasts
Ca2+	calcium ions
CF	contraction frequency
ChAT	choline acetyltransferase
CMS	congenital myasthenic syndrome
CNS	central nervous system
DAPI	4′,6-Diamidine-2′-phenylindole dihydrochloride
DHPR	dihydropyridine receptor
DM	differentiation media
DMEM	Dulbecco's modified eagle medium
DMSO	Dimethyl sulfoxide
Dok7	docking protein 7
DPBS	Dulbecco's phosphate buffered saline 1X

DS	donkey serum
ECM	extracellular matrix
EGF(s)	epidermal growth factor(s)
EPP	endplate potential
FBS	fetal bovine serum
FGF-7	fibroblast growth factor 7
FGF(s)	fibroblast growth factor(s)
FGFb	basic fibroblast growth factor
FI	fusion index
GABA	γ-aminobutyric acid
GDF-11	growth differentiation factor 11
GDNF	glial-cell-line-derived neurotrophic factor
GFAP	glial fibrillary acidic protein
GM	complete growth media
GS	goat serum
HBSS	Hanks' balanced salt solution
hESC(s)	human embryonic stem cell(s)
HGF(s)	Hepatocyte growth factor(s)
hiPSC(s)	human induced pluripotent stem cell(s)
HMC(s)	hypaxial motor column(s)
HS	horse serum
ICC	immunocytochemistry
IGF-1	insulin-like growth factor 1
IGFBP(s)	insulin-like growth factor-binding protein(s)
IP	inorganic phosphate
K+	potassium ions
LEMS	Lambert-Eaton myasthenic syndrome
L-Glut	L-glutamic acid
LMC(s)	lateral motor column(s)
LMCl	lateral lateral motor column
LMCm	medial lateral motor column
LRP4	low-density lipoprotein receptor-related protein 4
MA	myotube area
MEP(s)	motor endplate(s)

MMC(s)	medial motor column(s)
MN(s)	motor neuron(s)
MNT(s)	motor neuron terminal(s)
MHC	myosin heavy chain
MRF4	myogenic regulatory factor 4
MRF(s)	myogenic regulatory factor(s)
MG	myasthenia gravis
MuSK	muscle-specific tyrosine kinase
Myf5	myogenic factor 5
Na+	sodium ions
ND	neurodegenerative
NFH	neurofilament heavy
NGF	nerve growth factor
NM	neuromuscular
NMJ(s)	neuromuscular junction(s)
NT3	neurotrophin 3
NT4	neurotrophin 4
NT5	neurotrophin 5
Pax3	paired box protein 3
Pax7	paired box protein 7
Pen/Strep	penicillin-streptomycin
PGC	preganglionic column
PlGF	placental growth factor
PMC	phrenic motor column
PWB	Prem/Wash buffer
Rapsyn	43 kDa receptor-associated protein of the synapse
RyR	ryanodine receptor
SC(s)	satellite cell(s)
SCE(s)	spinal cord explants
SkM	skeletal muscle
SkMC(s)	skeletal muscle cell(s)
SMA	spinal muscular atrophy
SMN1	survival motor neuron 1
SMN2	survival motor neuron 2

SOD1	superoxide dismutase 1
SR	sarcoplasmic reticulum
Sty1	synaptotagmin 1
T-tubule	transverse tubule
TGFβ	transforming growth factor beta
TX100	Triton X-100
VAChT	vesicular acetylcholine transporter
VEGF	vascular endothelial growth factor

List of Figures

List of Tables

Abstract

Background: The neuromuscular junction (NMJ) is a unique chemical synaptic connection between muscle fibre and motor neurons. NMJ is a complex structure that serves to efficiently communicate the electrical impulse from the motor neuron to the skeletal muscle to signal contraction making it difficult to isolate and dissect to enable the understanding of the underlying mechanisms and factors affecting neurodegeneration and muscle wasting associated with ageing and diseases (i.e. cancer and diabetes). Despite several decades of NMJs research, the prospect of *in vivo* NMJ studies is limited and these studies are challenging to implement. Thus, new sophisticated models are required to more efficiently trial novel drugs and compounds designed to enhance muscle growth and regeneration.
Objective: The aim of this project is to establish a novel functional human NMJs platform, which is serum and neural complex media/neural growth factor-free, using human immortalised myoblasts and human embryonic stem cells (hESCs)-derived neural progenitor cells (NPCs) which could be used as disease model to study diseases associated with NMJ dysfunction. **Methods:** immobilised human myoblasts were co-cultured with hESCs for 7 days in serum and neural growth factors free differentiation media. In this co-culture model, functional NMJs form, myotubes exhibit advanced differentiation into muscle tissue and they undergo nerve-evoked contractions. The model fully characterised using different antibodies against specific markers for NMJ formation and for motor neurons and myoblast differentiation. The functionality of the NMJ was assessed using different pharmacological drugs. Finally, the model was evaluated as diabetic specific model using advanced glycation end products and cross-talk between muscle and motor neurons and endogenously secreted neural growth factors were investigated.
Results: It was confirmed that the NPCs had matured into cholinergic motor neurons using choline acetyltransferase and βIII-tubulin immunostaining. Multiple NMJ innervation sites were formed from neuronal axon sprouting branched along the myotubes resulting in extensive, spontaneous contractile activity shown in the myotubes. Postsynaptic site of NMJs was further characterised by staining dihydropyridine receptors, ryanodine receptors, and acetylcholine receptors by α-bungarotoxin (α-BTX). The functional assessments using different agonists and antagonists pharmacological drugs (L-glutamic acid, α-BTX and Tubocurarine) showed that this system behaved physiologically and muscle contraction was motor neurons-driven. The model was successfully applied as diabetic platform in which the bi-directional communications between myotubes and motor neurons were impaired and consequently essential neural growth factor levels were detrimentally affected.
Conclusion: A functional entirely human motor unit serum and neural growth factors free platform was successfully established and characterised for *in vitro* investigations and validated as a diabetic platform that replicate the diabetes in human.

Chapter 1 Introduction

1.0 Skeletal muscle myogenesis

Skeletal muscle is an extremely specialised tissue which consists of multi-nucleated, post-mitotic, non-dividing muscle fibres (Shadrach & Wagers, 2011). The contractions of the skeletal muscle fibres are controlled by the somatic nervous system, and they play the role of regulating the body's voluntary movement, locomotion, breathing, and sustaining posture (Reece et al., 2011).

The skeletal muscle cells development (also referred to as myocytes) happens inside in uterus during embryonic myogenesis (Bentzinger et al., 2012). Myoblasts are formed from myogenic antecedents produced from the mesoderm and arise in the somites. Myoblasts are sometimes called skeletal muscle stem cells satellite cells (SCs) (Chen & Goldhamer, 2003). In the embryonic myogenesis' initial stages, satellite cells go through widespread propagation up to a time when the myofibrillar protein synthesis threshold is reached (Bentzinger et al., 2012). At this point, the myoblasts leave the cell proliferation loop and fuse together to create elongated tubular multi-nucleated fibres. These eventually produce myofibres, the skeletal muscle's contractile unit (Mizuno et al., 2010; Le Grand & Rudnicki., 2007). Once the myogenesis is complete, the myofibres are no longer able to proliferate. Thus, the number of myofibres an individual has been determined before that individual is born. After birth, the growth of muscle happens through adaptation and remodelling of fibres that already exist (Tedesco et al., 2010). In maturity, skeletal muscle is heterogeneous and is made up of Type 1 and Type 2 myofibers, which can be divided further into specific physiological subtypes,

which include fatigue-resistant fibres, slow contracting, fatigable fibres, and fast contracting fatigue-resistant fibres (Pette & Staron, 2000).

After birth, satellite cells still exist and can be found in the basal lamina. In typical physiological settings, satellite cells are in dormancy, neither differentiating nor dividing (Kuang et al., 2007). In the event of muscle trauma, the dormant cells are activated, and the dedicated satellite cells migrate out of the basal lamina and start proliferating by re-entering the cells recycle (Tedesco et al., 2010). This process produces a population of myoblasts, which move to the damaged site and either amalgamate with the existing injured myofibres to deliver more nuclei for muscle hypertrophy or join together and produce de novo myofibers, which supplant the myofibres that have been destroyed during muscle hyperplasia (Siegal et al., 2011; Adams, 2006). Added to injury of, extrinsic mechanical stretch to fibres of the muscle resulting from resistance training has been shown to trigger skeletal muscle hypertrophy, resulting in an escalation of satellite cell activity and the accumulation of myonuclei to the myofibers undergoing the process of hypertrophy (Hawke & Garry, 2001; Aagaard et al., 2002; Le Grand & Rudnicki, 2007).

1.0.1 Anatomy

SkM is the largest metabolically active tissue in the human body accounting for approximately 50% of the mass in healthy adult human males (Yin et al., 2013) and comprising over 650 designated muscles, different from both muscle types (cardiac and smooth); SkM is governed through the somatic nervous system, paving the way foe individualised functional commands. Preparation, regulation and implementation of voluntary movement of the body is governed in the motor cortex region of the brain (Biswal et al., 1995). Upper motor neurons relay signals from the motor cortex of the brain via the spinal cord to peripheral motor neurons. Even though the chief function of SkM is to command physical movement, it is also responsible for

regulation of metabolism through macronutrient storage and substrate oxidation to replenish used-up adenosine triphosphate (ATP) stores (Leto and Saltiel, 2012). It is also responsible for effecting critical respiratory and endocrine functions (Pedersen and Febbraio, 2008). Local and systematic environments in the body are also influenced by growth factors, cytokines, and myokines produced by SkM fibres into the Extra cellular matrix (ECM) (Pedersen, 2011). Formation of SkM involves the merging of myoblasts to multinucleated fibres known as myotubes, eventually developing into myofibres. These singular contractile cells of SkM are innervated by a motor neuron (MN). A single MN can innervate hundreds of muscle fibres, but just one MN innervates each fully developed muscle individually. This system of an MN and all of the muscle fibres being innervated by that neuron is called a functional motor unit (Stifani, 2014). Individual myofibres are unsheathed by endomysium and stacked in bundles. Muscle fascicle, bundles of myofibres, are bound by perimysium. Subsequently are bound and held together by the fibrous outer connective tissue called epimysium to produce a whole muscle as shown in Figure 1.0, with several motor units located around it (Light and Champion, 1984; McComas et al., 1971).

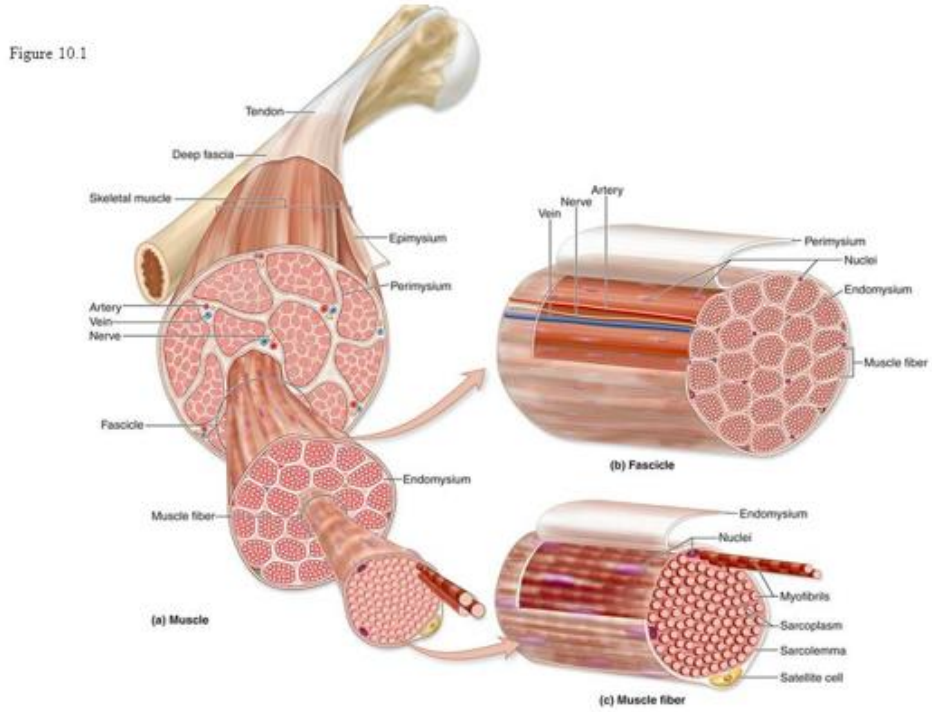

Figure 1.0: Gross anatomy of a skeletal muscle belly. A dedicated cell membrane called the sarcolemma binds the individual skeletal muscle fibres. The fibres are held together by a fine coating of connective tissue called the endomysium, which is also responsible for transporting nerve axons, oxygen and nutrients through blood and lymphatic vessels. Wrapped muscles are held together with perimysium, a thin fibrous layer of connective tissue which separates a muscle belly into fascicles. The muscle fascicles are then enclosed by the dense fibrous epimysium to form a complete skeletal muscle. Image available for free public reuse at Quizlet (https://quizlet.com/230045074/chapter-10-muscle-tissue-and-organization-diagram/).

1.0.2 Skeletal Muscle Fibres

Fully formed myofibres are made up of sequences of myofibrils, which contain the thick filament protein, and titin and thin filaments protein, actin (Rayment et al., 1993), reinforced by the protein titin. The repeated system of these proteins in the myofibrils are called sarcomeres, which are single contractile units within myofibres (Figure 1.1), showing as striations on the myofibres. Actin molecules at the edges of a sarcomere are held to a position called the Z-discs, which are the distinct borders between each sarcomere. Actin bound to Z-

discs at one edge of the sarcomere projects toward the M-line at the centre. Myosin filaments, which intermingle with the fixed actin filaments, are situated centred over the M-line, with the myosin filament edges precisely connected to the Z-discs by titin. When stimulated through nervous input, a cross-bridge is formed and the actin filaments are drawn and move along the myosin filaments, shortening the sarcomere to cause contraction of the myofibre (Denoth et al., 2002).

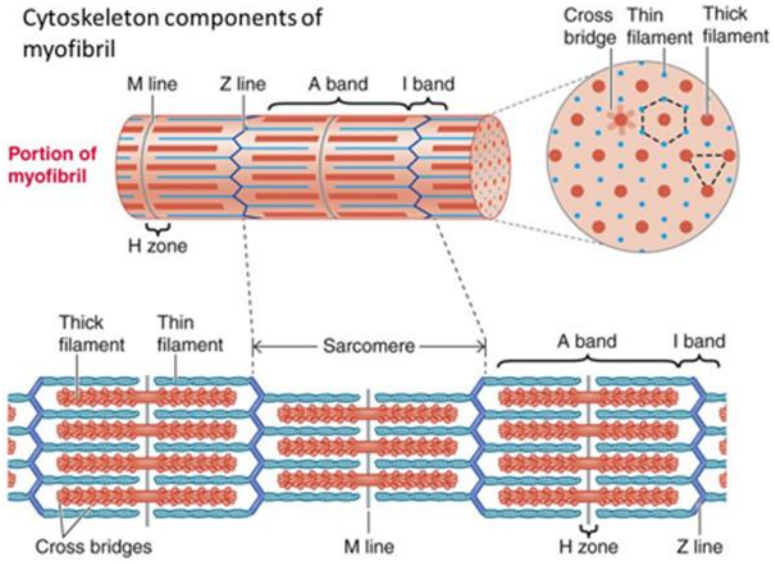

Figure 1.1: Cytoskeleton components of a myofibril. A muscle fibre is filled with myofibrils, which are made up of individual sarcomeres joined in series. One sarcomere is situated between a set of Z-disks, making a distinctive contractile unit, comprising of a thin (actin) filament and a thick (myosin) filament. The I-band of the sarcomere is the area where the myosin does not overlap the actin, resulting in a lightened appearance on the muscle fibre. The A-band looks visually darker on the muscle fibre as it has the anisotropic myosin protein. This alternate banding gives muscle fibres the appearance of striations. The H-zone is located within the A-band where there is no actin. The M-line appears in the middle of the sarcomere within the H-zone for structural integrity (Quadri, 2020).

1.0.3 Embryonic Myogenesis

The creation of skeletal muscle cells (SkMCs) is triggered during the development of the embryo. The embryonic germ layers of the early embryo pave the way for the paraxial

mesoderm, which in turn causes the formation of somites (Aulehla and Pourquié, 2010). The formation of somites are triggered by factors emanating from neural tube, dorsal ectoderm, and notochord to differentiate further (Buckingham et al., 2003; Pourquie, 2001). During the transformation of the somite, the dorsal region makes dermomyotome, which has the precursors of the SkM progenitor cells.

1.0.4 Adult Myogenesis

The ability of SkM to mend and regenerate is strictly controlled process involving 4 precisely predetermined phases. They are: deterioration, inflammation, repair-restoration, and remodelling (Carosio et al., 2011). Injury of SkM triggers instant necrosis of SkMCs, which results in gradual infiltration of SkM by inflammatory cells, producing an inflammatory reaction in the injured region (Tidball, 2005). Upon inflammation, a renewing phase is caused by the activation of latent SCs. Under normal physiological circumstances, upstream embryonic myogenesis produces Px7 manifesting cells within the dermomyotome, which form the SC population of SkM stem cells that are present after birth and are needed for subsequent SkM regeneration. The specialised latent SCs are found amongst the basal lamina and sarcolemma of SkM fibres and are regulated by the same genetic order as embryonic myogenesis. Thusly, SkM renewal can only occur when the mitotically quiescent SCs are stimulated and mature into myoblasts (Siegel et al., 2011). Upon stimulation, the SCs turn into proliferative myoblasts and rapidly re-enter the cell cycle and begin proliferation (Sousa-Victor et al., 2015). As the proliferative limit for myofibrillar protein is attained, a population of SCs experiences self-regeneration and replenishment of the SkM stem cell pool. This population of SCs return to the margins of the muscle fibres and remain in a state of latency as they await to respond to future muscle injures following subsequent activation (Relaix and

Zammit, 2012). After numerous rounds of proliferation the dedicated myoblasts leave the cell cycle, they relocate to the area of injury and start fusing into myocytes and then myotubes. As the myotubes develop, they merge with pre-existing undamaged myofibres as a scafolding and replenish the damaged region to complete the muscular repair and regeneration process (Simionescu and Pavlath, 2011). Finally, the restored myofibres continue to develop, renovation of other extracellular matrix (ECM) occurs, and function is restored (Carosio et al., 2011). There are several parallels between embryonic myogenesis and SkM restoration, which are both governed by genetic and myogenic transcription features. In the process of SkM renewal, SCs manifest the myogenic regulator Pax7 in the early stages of activation (Seale et al., 2000).

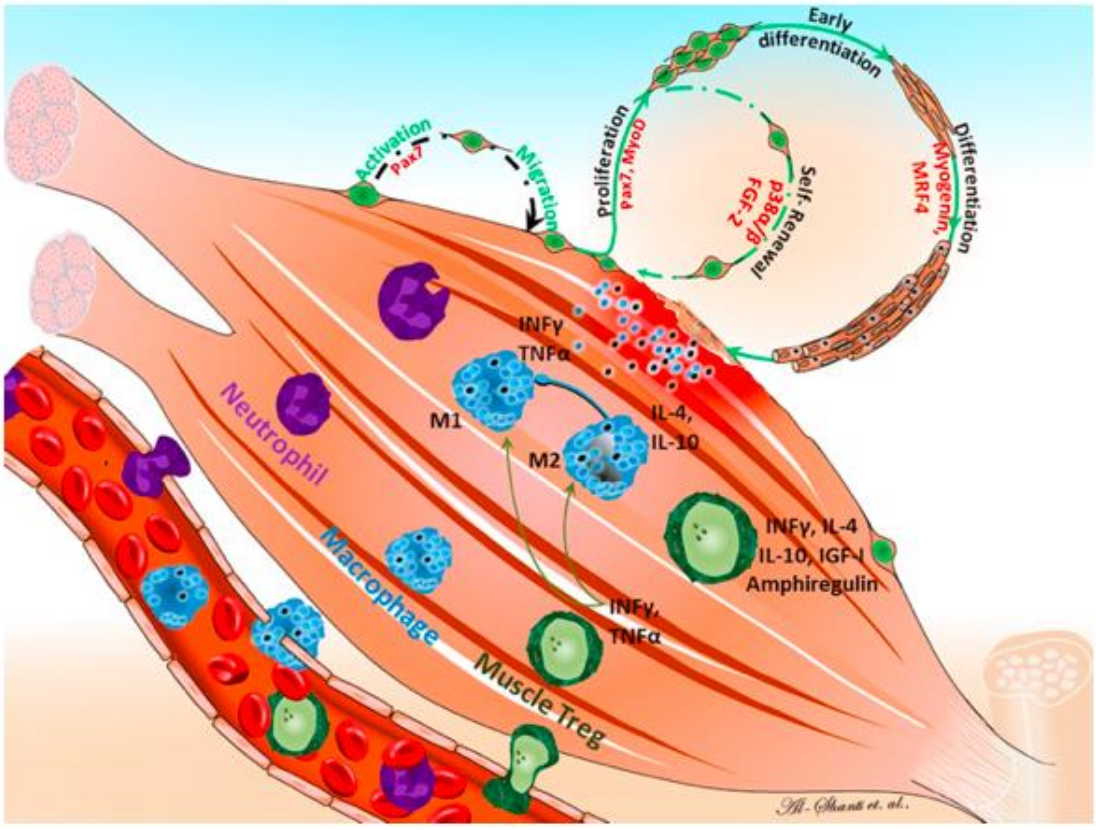

Figure 1.2: Summary of overall communication muscle cells and immune cells after acute muscle injury. The image shows the interaction of cells following muscle damage (Saini et al., 2016).

1.0.5 Skeletal muscle growth and maintenance

The growth and maintenance of skeletal muscle depend on the activation of satellite cells, which itself is influenced by such hormones as IGF-1. With a structure that is the same as insulin, IGF-1 is a polypeptide protein hormone. It is primarily expressed the skeletal muscle regulating autocrine and the liver or paracrine properties (Schiaffino & Mammucari, 2011). The regulation and preservation of IGF-1 levels in circulation is the responsibility of the growth hormone (GH)-dependent hepatic synthesis (Arvat et al., 2000).

IGF-1 is able to prompt both the differentiation and proliferation of skeletal muscle. It connects to the IGF-1 receptor (IGF-1R) on the surface of the myocyte, in the process triggering the insulin receptor substrate protein 1 (IRS-1) and their succeeding tyrosine phosphorylation (Singleton & Feldman, 2001). Thus, it is noted that IGF-1 triggers a torrent of intercellular signalling conduits, which include the mitogen-activated protein kinase (MAPK), resulting in the activation of satellite cells, the proliferation of myoblasts, and the phosphatidylinositol 3-kinase (PI3K) flow, resulting in differentiation and fusion of myotubes (Glass, 2005) (figure 1.3). Both *in vitro* and *in vivo* studies has illustrated that IGF-1 boosts protein synthesis conduits resulting in the regeneration and hypertrophy of skeletal muscle (Barton et al., 2002).

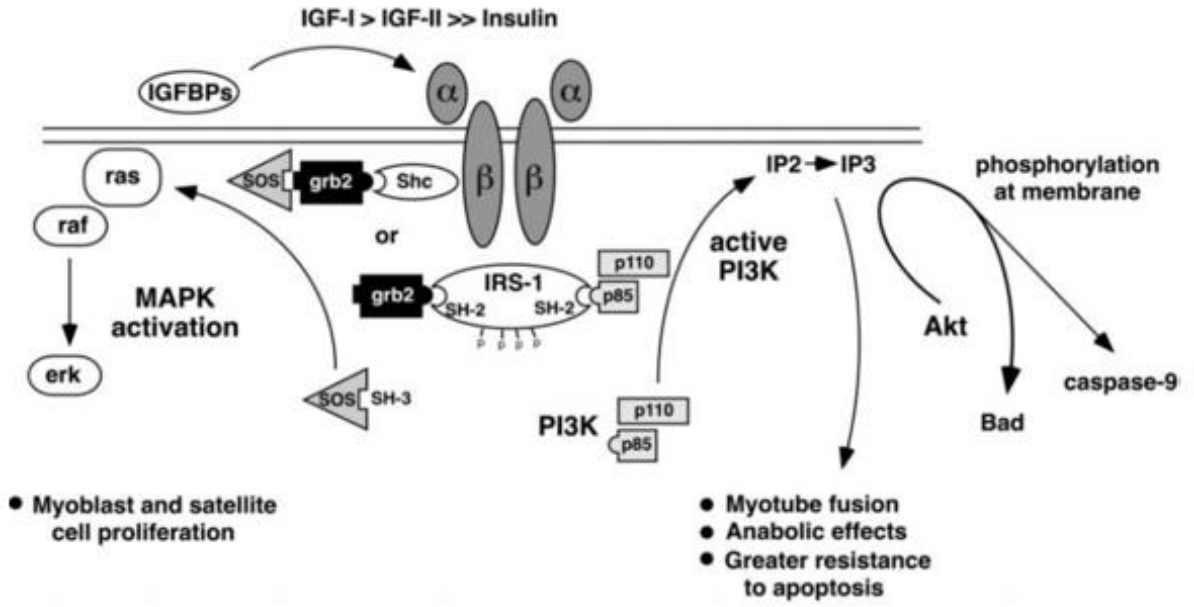

Figure 1.3: IGF-1 signalling pathways leading to skeletal muscle hypertrophy. Adapted from (Singleton & Feldman, 2001).

IGF-1 and -2 bioavailability is controlled by insulin-like growth factor-binding proteins (IGFBPs). Both IGF-1 and 2 can bind to the IGF-IR, in the process promoting tyrosine phosphorylation, and binding of insulin receptor substrate (IRS) proteins-1 and proteins-2. In IRS-1 are found docking sites for Src homology-2 (SH2). Then the adaptor protein growth factor receptor-bound protein 2 (Grb2) binds to SH2, prompting the MARK FLOW. This is followed by the Grb2 binding to Son of Sevenless (SoS), in the process triggering Raf-1, resulting in the prompting of MAPK's, ERK1 and ERK2. MAPK is responsible for the regulation of the proliferation induced by IGF. A docking station for 85-kDa regulatory subunit of P13K, 100kDa subunit catalyses inositol conversion, 100kDa subunit catalyses inositol conversion, can also be found in IRS-1. Akt is activated and phosphorylated by P13K, resulting in the prompting of caspase-9 and Bad (both pro-apoptotic proteins), prompting differentiation (Zha & Lackner, 2010; Singleton & Feldman, 2001).

1.0.6 Activation and proliferation of satellite cells

When responding to injury, skeletal muscle has an outstanding ability to repair, duplicating the formation of muscle during embryogenesis (Hawke & Garry, 2001). This potential to regenerate is credited to satellite cells as the dormant satellite cells are prompted and proliferate fast (Partridge, 2002). This creates a population of myoblasts. Estimates indicate that about a fifth of the satellite cells restock the dormant cell store for future regeneration, whilst the other four-fifths move to the damaged area and start differentiating into myocytes, contributing to the repair of muscle (Kuang et al., 2007). Pax7 is activated by both the dormant and activated cells. Nonetheless, the expression of Pax7 is down-regulated during myogenic differentiation. It was observed that Pax7 -/- mice have a total absence of satellite cells. Postnatally, their skeletal muscle does not grow, a situation that results in a huge reduction in the mass of muscle and eventually to death within the first 14 days after birth (Holterman & Rudnicki, 2005). In Pax7 mutant mice, flawed reformative myogenesis has been noted (Wen et al., 2012), indicating the crucial role played by the expression of Pax7 in the specification, maintenance, and survival of satellite cells. A close Pax7 homology is Pax3, which is expressed during satellite cell activation and proliferation. Pax3 prompts the c-Met a tyrosine kinase receptor expression, which is vital for myoblast migration, sustenance, and proliferation. Research has indicated that the skeletal muscle formation of the diaphragm and limb of c-Met null mice failed, as a result of the failure of migration of myoblast (Bladt et al., 1995; Boutet et al., 2007).

Responding to muscle trauma and damage, it is thought that injured skeletal muscle cells discharge soluble factors including fibroblast growth factor (FGF); hepatocyte growth factor (HGF), and platelet-derived growth factor (PDGF), attracting the inflammatory cells in

circulation to the site of injury with the aim of clearing the dead or damaged fibres and prompting the satellite cells to start the proliferation process (Siegal et al., 2011). Through its tyrosine kinase receptor c-Met, HGF fills the vital role of activating cells following injury, prompting their proliferation while hindering their differentiation (Allen et al., 1995). It was observed that the activating factor in the damaged muscle extract was HGF (Holterman & Rudnicki, 2005). It is also thought that PDGF and FGF are effective mitogens for satellite cells as they have illustrated their ability to intercede the myogenic proliferation and deter differentiation (Tatsumi et al., 1998; Sheehan & Allen, 1999). On the other hand, both myogenic differentiation and proliferation have been shown to be depressed by transforming growth factor-beta (TGF-β) (Allen & Boxhorn, 1989).

During postnatal myogenesis, Notch-1 signalling controls myogenic cell fate. It has been shown *in vivo* studies that Notch 1 facilitates the proliferation of satellite cells expressing the myoblast marker Pax3 while deterring differentiation until an adequate amount of cells becomes available for the repair of muscle (Conboy & Rando, 2002). It was noted that *in vitro* differentiation of the murine C2C12 cell line is deterred by cells that express the Notch ligands (Luo at al., 2005). It has been concluded from *in vitro* research that the myogenic precursor cell proliferation is promoted by Foxo1 expression of the forkhead transcription factors. This is accomplished through the repression of Foxo4, which results in the down-regulation of the cell cycle inhibitor, p21 (Hribal et al., 2003). Cell proliferation and differentiation will be examined during the study in different conditions such as in diabetes condition.

1.0.7 Maintenance of skeletal muscle, disease, and ageing

Skeletal muscle can be about two-fifths of an average human being's mass. Thus, it is vital that muscle is maintained and repaired for an individual to remain healthy. Skeletal muscle has the ability to respond and adapt to an array of physiological strains and stimuli. However, it also has the ability to respond to pathological conditions, which could be credited to age, muscular dystrophies, injury, cancer, and cachexia (Thomas, 2007; Shadrach & Wagers, 2011). Such pathological conditions can result in muscle loss or wasting, a situation that can have a detrimental effect on the strength of the individual and loss of functional skeletal muscle, something that could even lead to death (Reece et al., 2011).

The degeneration of muscle mass as a result of ageing is called sarcopenia. The condition is accompanied by a decrease in functional features like power, endurance, and strength (Rolland et al., 2008). Sarcopenia is a normal condition as human beings age, usually resulting in disability, frailty, and reduction in the ability to deal with severe illness and mortality for the elderly (Roubenoff, 2000). It has been concluded that both extrinsic and intrinsic factors are changed in ages muscle and could be a factor resulting in age-related decline in muscle mass because it has a reduced ability to regenerate (Lang et al., 2010; Marcell, 2003). It has also been noted that an physical delays increases at the beginning of sarcopenia (Morley et al., 2001). The exponential increase in the number of elderly people across the world the wasting of muscle is turning into a big health challenge, which is resulting in an increase in the cost of healthcare. It is on this basis that the development of a new approach to both treatment and prevention of sarcopenia is needed. Thus, the development of a novel treatment for skeletal muscle using nanotechnology as the system of delivery is an attractive proposal with regards to assisting in improving the lifestyle and health of the elderly.

1.1 Muscle Contraction

Excitation-contraction coupling is the programmed molecular interaction and exchange that occurs during SkM contraction. Nervous stimulation results in depolarisation of the muscle fibre membrane called sarcolemma (Figure 1.4), the resultant action potential (AP) journeys down the invaginated transverse tubule (T-tubule) of the sarcolemma into the cells. As the AP moved down the T-Tubule and into the sarcoplasm of the muscle fibre, it initiates the opening of voltage-gated L-type calcium channels, leading to the depolarisation of the interior of the muscle fibre. The inner depolarisation of the muscle cell causes the opening of calcium channels in the terminal cisternae of the sarcoplasmic reticulum (SR). Given calcium ions (Ca^{2+}) are highly concentrated in it the SR than in the cell sarcoplasm, they quickly diffuse into the sarcoplasm. The Ca^{2+} then wrap with the protein troponin, which is situated on the actin filaments. The Ca^{2+} wrapped troponin results in the conformational change of the troponin-tropomyosin-complex, thus exposing active binding sites for the myosin filament heads along the body of the actin filament, to facilitate cross-bridge formation and cycling (Figure 1.5).

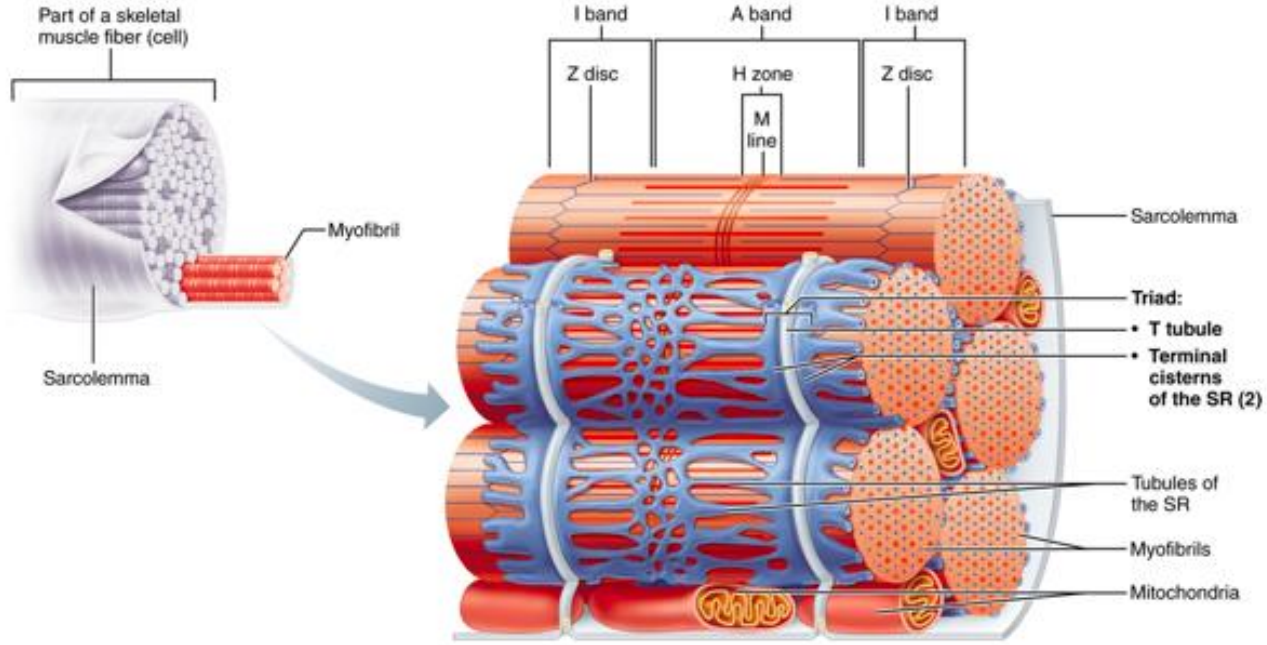

Figure 1.4: Arrangement and assembly of skeletal muscle triads. A triad ensues when a transverse tubule originating from the sarcolemma is inserted between tow terminal cisternae of the sarcoplasmic reticulum. This tight formation facilitates the efficient relay of nerve signal, depolarisation, and opening of gated ion channels.

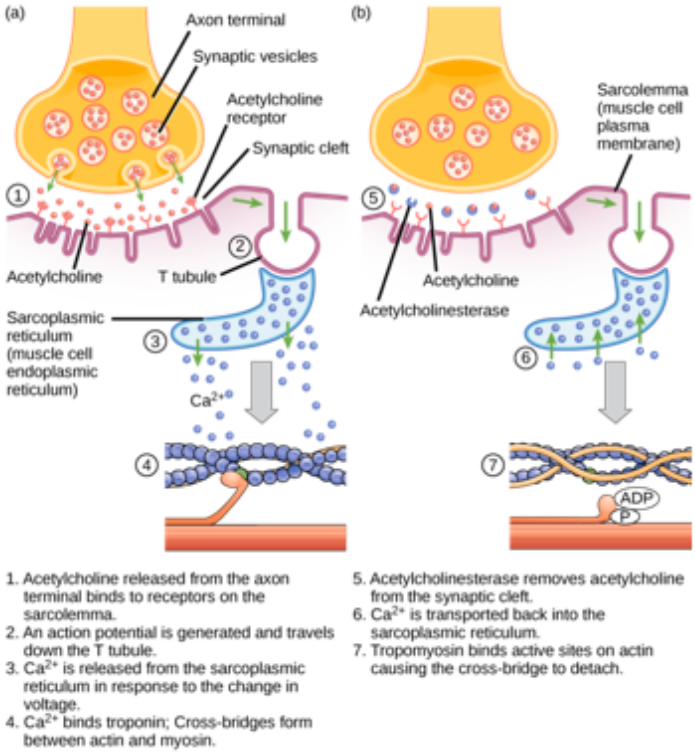

Figure 1.5: Cross-bridge formation. Depolarisation initiates calcium ions inflow into the cytosol of the muscle fibre. The calcium binds with troponin and changes the position of tropomyosin to expose binding site for myosin to form the cross-bridge required for muscle contraction. Image available for free public reuse at Lumen (https://courses.lumenlearning.com/boundless-biology/chapter/muscle-contraction-and-locomotion/).

A cross-bridge cycle can only form after the myosin head has been initiated. An ATP molecule wrapping with the myosin head, which is hydrolysed to adenosine diphosphate (ADP) and inorganic phosphate (IP), initiates activation via the energy releasing action potential of ATP hydrolysis, which sets the myosin head in a 'cocked' formation. A cross-bridge emerges between the activated myosin head and actin; the IP is then released causing the binding capacity of the myosin head to and actin filament to increase. The ADP is then released resulting in the pivoting of the myosin head. The Actin filament then slides toward the middle of the sarcomere, a movement called the 'power stroke.' Another ATP then binds with the

myosin head, the cross-bridge is destabilised and the myosin head disengages from the binding site, before being activated again for subsequent cross-bridge formation (Figure 1.6). Cross-bridge cycling will last to re-engage while the binding sites on the actin filament remain free. Repeated cycling brings the actin filaments together and the sarcomere shortens, causing muscle contraction. The ending of cross-bridge cycling occurs when Ca^{2+} ions are actively returned to the SR. The troponin-tropomyosin-complex returns to its initial configuration, blocking the myosin binding sites on the actin filaments, resulting in muscle contraction (ter Keurs et al., 2003). Muscle contraction will be examined in this study in terms of frequency and in diabetic condition.

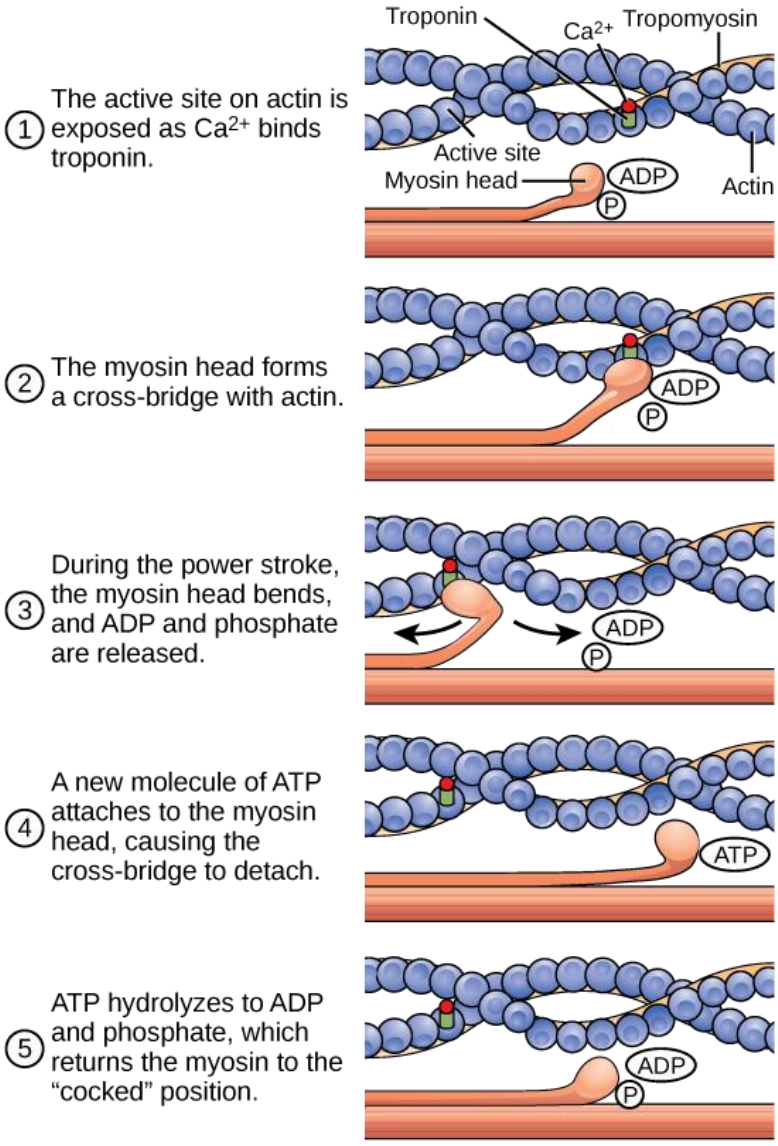

Figure 1.6: Molecular mechanisms of muscle contraction. a) Ca^{2+} ions bind with troponin, triggering a change in the structural position of the tropomyosin, exposing the actin binding sites. B) Cross-bridge formation happens between the binding sites on the myosin heads and actin filaments. c) the power stroke is effected via the release of inorganic phosphate (IP) then adenosine diphosphate (ADP). d) The engagement of adenosine triphosphate (ATP) disengages the binding of myosin and actin. e) The conversion of ATP to ADP and IP alters the myosin head for cross-bridge formation and cycling. Image available for free public reuse at Lumen (https://courses.lumenlearning.com/boundless-biology/chapter/muscle-contraction-and-locomotion/).

1.1.1 Motor Neurons

Motor neurons (MNs) are neural cells that stem from the central nervous system (CNS) and project axons into the periphery to form synapses with their target tissues. Critical for all vertebrates, optimal and accurate MN function and signal relay with target tissues in the periphery, such as SkM, is needed for essential behaviours such movement and breathing. While typically regarded as a distinct cell type, MNs have vast diversity with different manifestation of genes, target muscles, and molecular profiles. This varied nature of MNs facilitates separate innervation of the vast individual SkM groups in the vertebrate body (Kanning et al., 2010). For instance, in humans there are over 600 SkM throughout the body with most muscles making up one part of the bilateral pair (Frontera and Ochala, 2015). Thusly, strict control of the CNS signal relay to MN and MN outputs to the target SKM is essential for the sophisticated, organised motor control observed in complex motor behaviours. Some studies have suggested that MN subtype identity governs the MNs innervation sequence and connection with the target SkM (Milner and Landmesser, 1999; Landmesser, 2001). Ergo, MN subtype range ought to be understood to appreciate the function of MNs and their motor units.

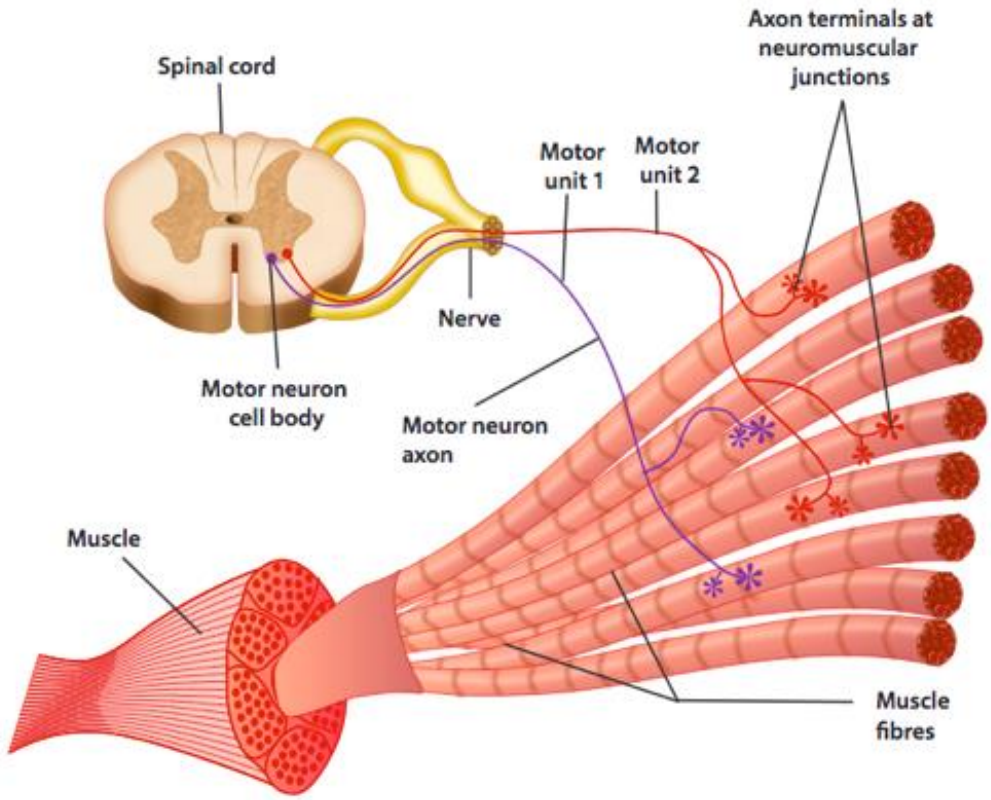

Figure 1.7: The motor unit. Motor neurons axon that extend from the spinal cord to the muscle. Each axon divides into multiple axon terminals forming NMJ with muscle fibres scattered via the muscle (Stratton., 2015).

1.1.2 Specific markers for motor neuron characterisation

The synthesis and transmission of ACh in MNs depends on the choline acetyltransferase (ChAT) and vesicular acetylcholine transporter (VAChT) to deliver the needed neurotransmitter for release into the synaptic divide (Brandon et al., 2003; Maeda et al., 2004). Analysis of synaptic vesicle proteins such as Synaptotagmin 1 (Syt1) can lead to the detecting of presynaptic MNT activity. This is an example protein is a Ca2+ sensor that stimulates amalgamation of the vesicles containing acetylcholine (ACh) and MNT membrane (Brose et al., 1992; Yu et al., 2013). NMJ models, previously developed *in vitro*, generally tend to overlook the features of innervated myotubes for advanced markers of differentiation.

These kinds of markers involve transversal triad development, nuclei found on the fringes, and striated myotubes. Moreover, the structures of the post-synaptic apparatus beyond AChRs are not usually described in-depth. For example, the post-synaptic elements stimulated by agrins such as 43 kDa receptor-associated protein of the synapse (Rapsyn) and muscle-specific tyrosine kinase (MuSK), are vital for the formation of AChRs. These markers will be used in this project to detect motor neuron and neuromuscular junction existence.

1.2 The Neuromuscular junction

To appreciate the essential role of neuromuscular junctions (NMJs) and the cellular differentiation they exhibit, the intricate regulation of NMJ formation, growth, and maturation ought to be understood within the context of essential cellular and molecular mechanisms. The CNS regulates SkM contractions. MNs relay communications from the CNS through nerve impulses to SkM fibres to initiate contractile activity in the muscle. The merging of a MNT with the MEP of an SkM fibre creates a highly differentiated chemical synapse where signal relay occurs (Figure 1.8).

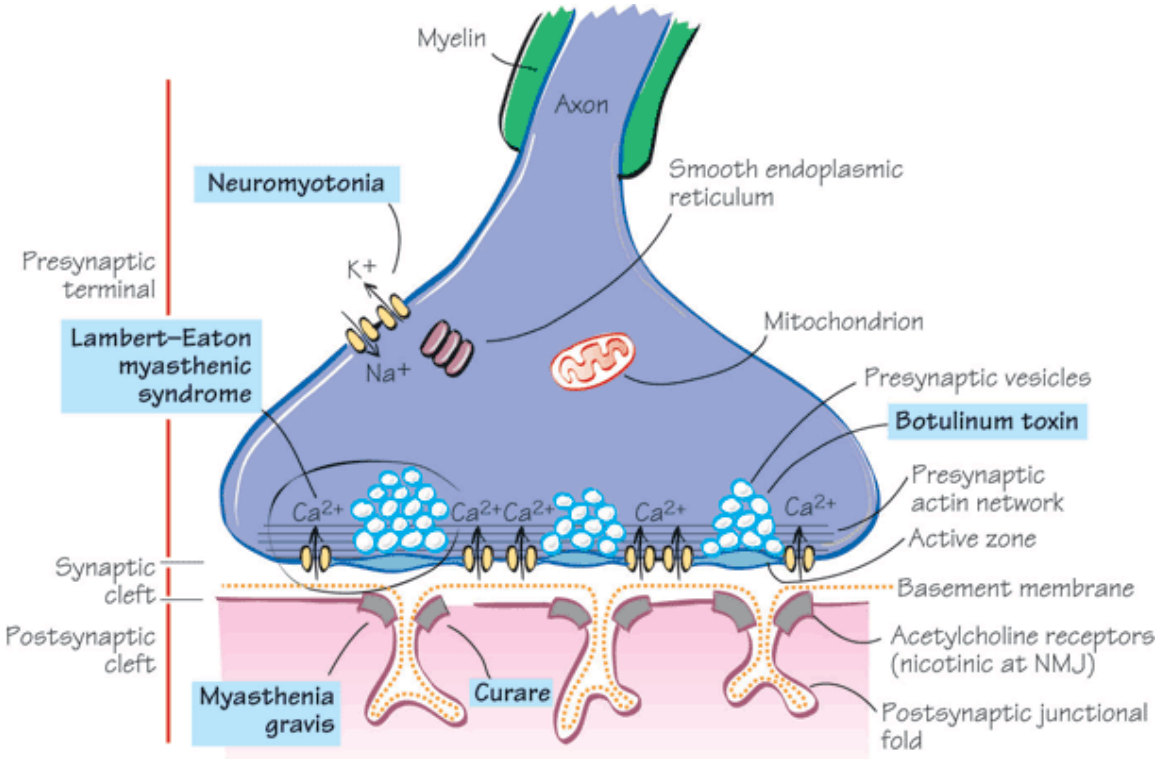

Figure 1.8: Neuromuscular junction signal transmission. 1) The action potential (AP) spreads down the motor neuron (MN) to the axon terminal. 2) Calcium channels are opened upon the arrival of the AP at the axon terminal, including inflow of calcium ions (Ca^{2+}) into the presynaptic terminal. 3) Elevated intracellular calcium presence at the axon terminal triggers synaptic vesicle merging with the membrane of the axon terminal. 4) Following the merging, the vesicle secrets acetylcholine (ACh) into the synaptic cleft. 5) ACh traverses the synaptic cleft to bind with acetylcholine receptors (AChRS), opening sodium ion (Na^{+}) channels on the motor end plate (MEP). 6) An AP generating muscle contraction is formed. 7) Termination of synaptic relay happens following the degradation of ACh through acetylcholinesterase and presynaptic reuptake. The highlighted diseases are NMJ disorders which can be examined by applying the model in this project (Barker & Cicchetti, 2012).

This synapse is one of the initial ones to emerge during embryonic development and is referred to as neuromuscular junction (NMJ). While initial NMJ formation happens early, complete maturation takes several weeks of molecular and structural configuration (Sanes and Lichtman, 2001). The NMJ maturation process is markedly longer than that witnessed in

CNS synapses formations, which occurs in just hours and exhibit a rapid turnover rate. Upon NMJ maturation, the synapse persists throughout life for optimum signal relay (Sanes and Lichtman, 1999). As a result, flawed formation, growth, or impaired sustenance through ageing could cause muscle weakness, paralysis, or manifest as various neurodegenerative (ND) or neuromuscular (NM) diseases. Conditions that directly affect the NMJs function are typically autoimmune (e.g. myasthenia gravis Lambert-Eaton myasthenic syndrome), genetic (e.g. congenital myasthenia), or neurotoxic (e.g. botulism). Furthermore, certain conditions of the NM system target MNs directly, resulting in presynaptic signal relay impairment, such as amyotrophic lateral sclerosis, (ALS) or spinal muscular atrophy (SMA). There are also 9 major types of muscular dystrophy (i.e. Becker, myotonic, limb-girdle, Duchenne, facioscapulohumeral, Emery-Dreifuss, oculopharyngeal, distal, , congenital) that attack the postsynaptic SkM MEP. The peripheral nerve is also susceptible to MN disorders that impair myelination (e.g. Charcot-Marie-Tooth disease). NMJ disorders can be examined by applying the model in this project.

The NMJ shares essential similarities with chemical synapses found throughout the central and marginal nervous system. The presynaptic MNT of the NMJ hosts vesicles containing the neurotransmitter acetylcholine (ACh). The synaptic cleft, whose width is approximately ~50-80 nm, acts as a border between presynaptic terminal and postsynaptic SkMC sarcolemma. The MEP has deep indentations known as junctional folds that are saturated with AChRs; the binding of ACh with AChRs opens sodium channels. The flow of sodium ions (Na^+) into the sarcoplasm causes the depolarisation of the MEP at the junctional folds, initiating an AP on the flanking sarcolemma, extents outward from the NMJ (Flucher and Daniels, 1989).

The basal lamina and ECM coating SkM fibres have a specialised muscle-specific composition, made up of molecules drawn from the SkMCs. Accordingly, the ECM constituents at the synaptic cleft have their own specialised molecular components, as secreted molecules at the cleft are drawn from the SkMCs and MNs (Patton et al., 1997). Together with SkMCs and MNs, the composition of NMJ *in vivo* is comprised of two other fundamental cell types, kranocytes and the terminal Schwann cells. Schwann cells originating from the NMJ are unique non-myellinating neuroglia that engulfs the MNT, producing their own unique basal lamina, which interacts with the ECM of SkMCs in close proximity to the NMJ. Finally, the inadequately comprehended kranocytes engulf the Schwann cells, enclosing the entire NMJ (Figure 1.9). both the kranocytes and the Schwann cells are involved in the maintenance of NMJ stability and reconstruction following injury (Son et al., 1996; Court et al., 2008). For seamless relay of nervous input at the NMJ, an AP induces Ca^{2+} influx in the MNT. The Ca^{2+} inflow stimulates synaptic vesicles to merge with the MNT membrane at certain locations called the 'active zones'. The ACh secreted into the synaptic cleft by the membrane-bound vesicles rapidly flow across and binds with AChRs on the SkMC. As highlighted, AChRS open sodium channels, but are also porous to Ca^{2+} as well as potassium ions (K^{+}) to some extent. The fusion and secretion of ACh from a single presynaptic vesicle, known as quantal release of ACh is referred to as miniature endplate current, which is the lowest stimulation that can be relayed between neurons. The fusion and secretion of ACh from a group of membrane-bound vesicles simultaneously produces what is referred to as the endplate potential (EPP). The EPP is produced when a presynaptic AP prompts vesicles are released to produce a current that is hundreds of nanoamperes and causes SkMCs to depolarise by approximately ~30–40 mV. The EPP generated is substantially larger than required to produce an AP in SkMCs. This greater

than needed EPP is known as the ‘safety factor’ and enables NM relay to remain operational through varying physiological conditions and stressors (Wood and Slater, 2001).

The scale of the safety factor is dictated by the morphology and physiology of the NMJ. Firstly, the number of active zones at the MNT and the scale of calcium channels, dictated by the size of the MNT. The density of synaptic vesicle fusion following stimulation of an AP and the quantity of ACh secreted also determine safety factor. The intensity of AChRs in the postsynaptic SkMC also governs the quantal current amplitude via a non-sequential fashion, as the concentration of AChRs is typically greater than needed for optimal recruitment of ACh from the synaptic cleft. In addition, sodium channels and AChRs on the junctional folds of MEPs arrange in a unique manner, with AChRs positioned at the peak of the fold and sodium channels in the trenches (Flucher and Daniels, 1998). This formation guarantees seamless relay and steadfast initiation of the AP in the sarcolemma (Slater, 2008). Muscle contraction will be examined in this project.

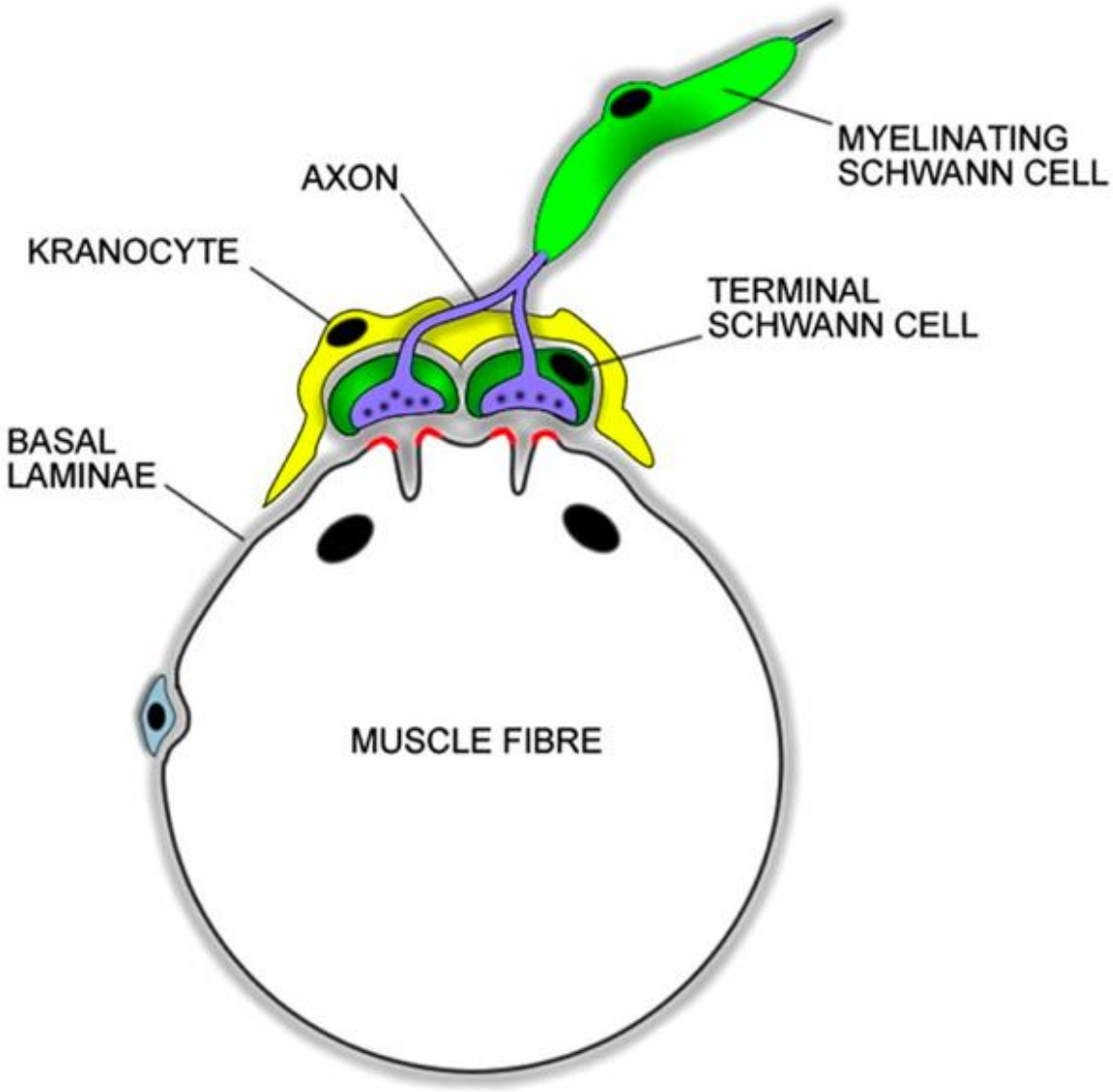

Figure 1.9: Cells comprising the neuromuscular Junction. The composition of the *in vivo* NMJs is made up of the four primary cell types—the Schwann cells, motor neurons, muscle fibres, and kranocytes. (Court et al., 2008).

1.3 Molecules involved in NMJ stabilisation

1.3.0 Agrin

The early stage of NMJ formation, groups of acetylcholine receptors (AChRs) form centrally on myofibres in advance of nervous input in a process known as intrinsic pre-patterning of muscle (Lin et al., 2001). While this preliminary pre-patterning happens without nervous input, the differentiation of postsynaptic configurations can only happen following the

formation of synapse and presynaptic input. One of the essential components responsible for the regulation of postsynaptic differentiation is *agrin.* It is an essential heparin sulphate proteoglycan required for NMJ formation and is produced and secreted by motor neuron terminals (MNTs) (Bezakova and Ruegg, 2003). The necessity of agrin has been captured in agrin-deficient mice, which manifests as failed NMJ formation and death (Gautam et al., 1996). Mice devoid of agrin also fail to undergo presynaptic differentiation and have persistent MN growth. Studies have suggested that a lack of regressive termination signallling from postsynaptic configurations and the lack of intrinsic agrin termination signals result in the failure of presynaptic differentiation and exessive axon growth (Campagna et al., 1995; Campagna et al., 1997). Even so, when agrin deficient exhibit a diminished form of agrin from their developing SkMCs, which have muscle-specific tyrosine kinase activating domains needed for AChR clustering, rejuvenation of NMJ formation is observed (Lin et al., 2008). Similarly, the involuntary overexpression of agrin in non-synaptic areas of SkMCs results in the formation of postsynaptic configurations usually only observed at the NMJ, such as mature junctional folds (Bezakova et al., 2001). There is also genetic manifestation of AChR genes typically only observeed at the synapse (Jones et al., 1997). These research works support the hypothesis that secretion of agrin from MNs to agrin-receptive SkMCs prompts the initial formation of NMJs. Formation and matuarion of the NMJ is enabled by agrin via the binding of the dystrophin-glycoprotein complex, which is dystrophin-associated transmembrane glycoproteins, namely dystroglycan (Bowe et al., 1994; Gee et al., 1994). Other studies have also suggested that the downregulation of agrin, enabled by proteolytic cleavage, governs maturation of the NMJ by modifying AChR clusters and the topology of junctional fold (Bolliger et al., 2010).

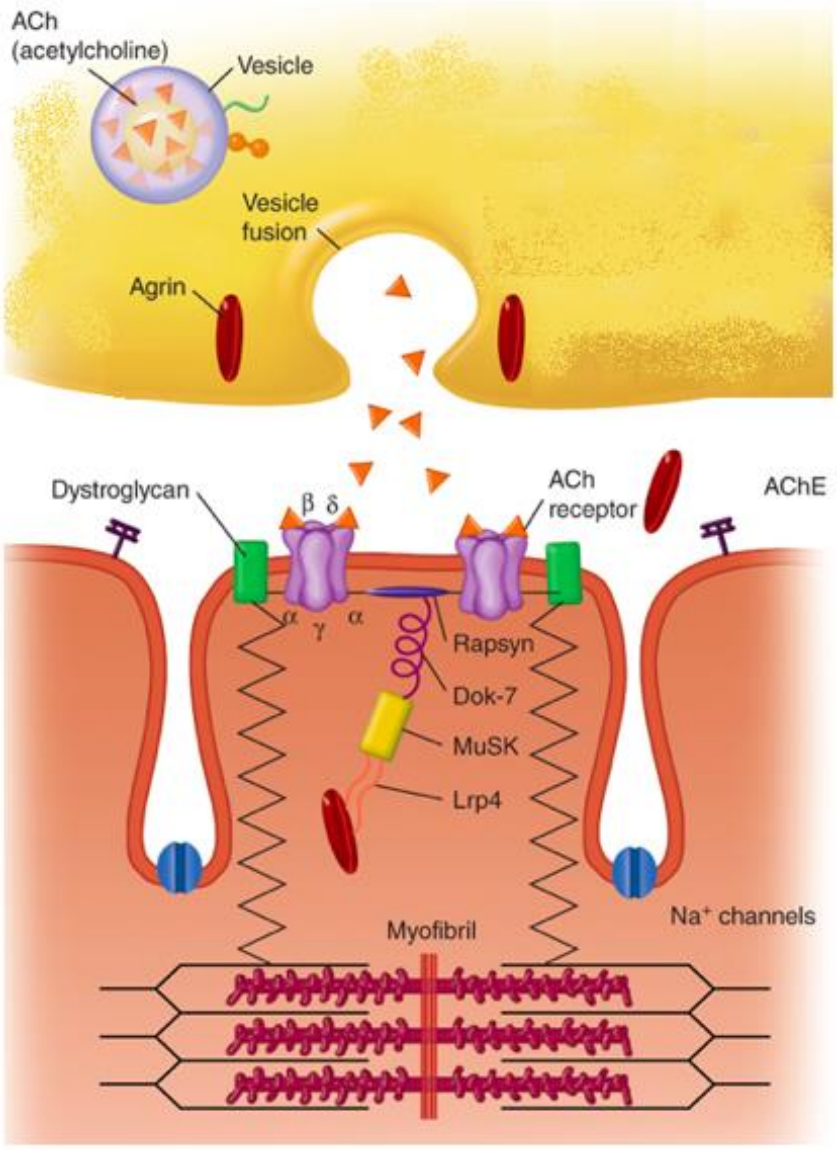

Figure 1.10: The Agrin-MuSK–LRP4–Dok7–rapsyn-AChR complex. Acetylcholine (ACh) and agrin are secreted by the motor end plate. Muscle-specific tyrosine kinase (MuSK phosphorylation happens after the binding of agrin and low-density lipoprotein receptor-related protein 4 (LRP4), which induces the organisation of MuSK-LRP4. The assembling of docking protein 7 (Dok7) steadies MuSK vial dimerization. As a result, activated MuSK zones bind AChRs with 43kDa receptor-associated protein of the synapse (rapsyn) after the tyrosine phosphorylation of Dok7. (Amato, 2018).

1.3.1 43 kDa Receptor-Associated Protein of the Synapse

Rapsyn, which is manifested in SkMCs throughout the initial development of NMJs in mature SkM, is a cytoplasmic support protein underlying the postsynaptic cytoskeleton, with manifestation chiefly limited to the synapse. A high-density protein construct is made by the inflexible binding of rapsyn with dystroglycan and AChRs (Unwin, 2013; Bartoli et al., 2001). This intricate formation is thought to sustain cytoskeletal-anchoring of AChRs. However, the AChR-rapsyn clustering caused by MuSK activation is yet to be understood from the molecular signalling pathways standpoint. Both *in vivo* and *in vitro* research works have established rapsyn as a compulsory protein in the development of AChR clusters. Therefore, notable failure of postsynaptic specialisation of the NMJ in mice devoid of rapsyn is observed (Gautam et al., 1995). Unlike the stark phenotypes exhibited in LRP4-, MuSK- and Dok7-deficient mice, mice devoid of rapsyn have some respiratory function and laboured breathing, thus sustaining life only for a few hours. Examination of the failed MEP revealed a lack of cytoskeletal differentiation and inappropriate AChR clusterisation. Nonetheless, aggregations of synaptic basal lamina components such as acetylcholinesterase and laminin-β2 are still availed in abundance. Interestingly, a gathering of MuSK below the MNT and overexpression of AChR genes by the synaptic myonuclei are exhibited (Apel et al., 1995). These findings revealed that rapsyn does not take part in the synaptic gene transcription but is essential for the affixation of AChRs at the MEP apparatus. They also suggest that the miniature muscle contractions are possible at underdeveloped NMJs prior to complete anchoring of AChRs by rapsyn.

1.3.2 Acetylcholine Receptors

In addition to the essential functions AChRs are involved in during signal relay, they are also responsible for MEP creation during NMJ development. Rapsyn has been found to form create clusters in non-myogenic cells when forced elevated expression is induced. However, SkMCs need AChRs to activate clusterisation. For example, a loss of associated rapsyn clusters happens when AChRs are eliminated from *in vitro* myotube cell membranes using laser of antibodies to initiate AChR depletion (Bruneau et al., 2008; Marangi et al., 2001). Studies have also demonstrated that AChRs are joined with and accompanied by rapsyn initially in the exocytotic route (Marchand et al., 2002; Moransard et al., 2003). Other findings reinforce the idea that AChRs are essential for the creation of the MEP, given deletion of the AChR γ-subunit gene, which is responsible for fabrication of physiological AChRs during embryogenesis, causes rampant MN growth (Liu et al., 2008). Worth noting is that mice in these studies still exhibited clustering of MuSK at the diaphragm, whereas clustering of rapsyn was undetectable. Ultimately, AChRs are seen to take part in the differentiation of MEP, as well as facilitation of rapsyn distribution to the MEP apparatus. The synthesis and transmission of ACh in MNs depends on the choline acetyltransferase (ChAT) and vesicular acetylcholine transporter (VAChT) to deliver the needed neurotransmitter for release into the synaptic divide (Brandon et al., 2003; Maeda et al., 2004). These markers will be used in this project to detect motor neuron and neuromuscular junction existence.

Analysis of synaptic vesicle proteins such as Synaptotagmin 1 (Syt1) can lead to the detection of presynaptic MNT activity. This example protein is a Ca2+ sensor that stimulates amalgamation of the vesicles containing acetylcholine (ACh) and MNT membrane (Brose et al., 1992; Yu et al., 2013). NMJ models, previously developed *in vitro*, generally tend to overlook the features of innervated myotubes for advanced markers of differentiation. These

kinds of markers involve transversal triad development, nuclei found on the fringes, and striated myotubes. Moreover, the structures of the post-synaptic apparatus beyond AChRs are not usually described in-depth. For example, the post-synaptic elements stimulated by agrins such as 43 kDa receptor-associated protein of the synapse (Rapsyn) and muscle-specific tyrosine kinase (MuSK), are vital for the formation of AChRs. These markers will be used in this project to detect motor neuron and neuromuscular junction existence.

1.4 Bi-directional communications between muscle and motor neurons in formation of NMJ

The bi-directional relay between MNs and SkMCs (which are interdependent tissues) plays a critical role in the regulation of voluntary muscle movements in the human motor system. Ergo, muscle composition and function change significantly via muscle innervation and re-innervation (Cisterna et al., 2014). Conversely, NMJs are made and maintained by muscle-dependent trophic, axon pathfinding signals, and cell adhesion, suggesting that the addition of exogenous GNFs in other nerve-muscle co-culture models can affect and alter the treatment and development of DMY and DN (Das et al., 2007; Guo et al., 2011; Guo et al., 2014; Rumsey et al., 2010; Puttonen et al., 2015). Nonetheless, GNFs produced endogenously are universally known to govern muscle differentiation, flexibility, neural survival, and expansion *in vivo* (Oppenheim, 1991; Reichardt, 2006). Ergo, numerous experiments have suggested that these factors play pivotal roles in cell populations of myriad of tissues. SkM populations have hence provoked much curiosity, as they exhibit receptors for severla growth factors, cytokines, and neurotrophins, suggesting that neurotropic signalling takes place in SkMCs via productio, expansion and innervation (Griesbeck et al., 1995; Chevrel et al., 2006; Gonzalez et al., 1999). An experiment performed on mice gastrocnemius muscles with and without a local supply of neurotrophin-3 (NT-3) revealed that NT-3-induced axonal

rejuvenation through stimulation of differentiation of muscle fibre, preventing muscle atrophy in NMJs (Sterne et al., 1997).

There are two types of IGF ligands— IGF-I and IGF-II—both which play an important role in the growth and development of human beings (Duan et al., 2010). A 30% drop in body weight has been observed when rats lack both types of IGF ligands (Liu et al., 1993; Baker et al., 1993). Whereas IGFs were initially thought to be necessaty for SkM growth, subsequent studies have shown that they are also vital for the survical of MNs, funcitonal development of the CNS, and the stabilisation of NMJs (Dobrowolny et al., 2005). Absence of IGF-I is associated with mental impairments, hypertrophic muscle tissue, and growth deficiencies (Wood et al., 1996): Duan et al., 2010). Additionally, IGFBPs are a group of proteins specifically produced to bind to IGF-I and IGF-II, playing the role of carrier proteins that synchronise IGF turnover, transport, and the half-lives of circulating IGFs (Jones and Clemmons, 1995). The IGF-IGFBP complexes can control blood glucose level through inhibition of cross-binding of circulating IGF to the insulin receptor (Rajaram et al., 1997). Several studies have noted that lack of one of these IGFBPs (not all) does no result in severe effects on total body mass owing to efficient compensation by other IGFBPs. An experiment with IGFBP-2 null mice revealed elevated IGFBP-1, -3, -5, and -4 concentrations (Wood et al., 2000; DeMambro et al., 2008).

1.4.0 Impact of diabetes on cross-talk between muscle and motor neurons

The manifestation pattern of GNFs in diabetes has been observed in both humans and animals. Evidence from subsequent studies suggest that down-regulation of NT-3 is linked to muscle impairment in the diabetic group (Middlemas et al., 2003; Andreassen et al., 2009). Moreover, nerve cells are significantly imparied by the reduction of NT-3, which suffers from diminisedh communication within NMJs (Dey et al., 2013),), whilst irregular increase in growth hormone (GH) levels was observed in diabetes. This increase has been linked to the

diminished levels of IGF-I and IGFBP-3 (Hanaire-Broutin., 1996), while IGFBP-1 is increased in diabetes, resulting in a reduction in IGF-I bioavailability. As a result, IGF-I function is hampered in diabetes (Thrailkill, 2000). Additionally, a significant drop in serum levels of IGF-I has been observed at around 86% in Streptozotocin-induced diabetic mice, which was linked to a drop in IGF-I mRNA transcripts and alterations to the components of IGF system (Leinninger et al., 2004). One experiment demonstrated that a drop in IGF-I levels is due to DN (both sensory and motor) (Chu et al., 2008). Surprisingly, overexpression of GDNFRα and GDNF has been detected in denervated SkMs and marginal neuropathies (Lie and Weis, 1998; Yamamoto et al., 1998). Therefore, the chief concern is how out innovative co-culture system produced free of serum and GNFs, as my approach had not included them artificially. This development suggest that they were produced endogeneously by MNs and SKMCs, which are needed to initiate nerve axonal sprouting and production of NMJs with myotubes. Cross-talk between motor neurons and skeletal muscle will be examined in this project to investigate the relationship between them in neuromuscular junction.

1.5 Human NMJ model versus Animal model

Animal model and cell culture are limited models in their capacity to reflect human ageing, physiology, carcinogenesis and progressive wasting disorders nevertheless, they remain a core part of clinical research due to ethical and practical concerns related to human models (Mak et al., 2014). Animal investigation gives limited results in predictions of human clinical trials and most of the animal research is not re-tested in human trials (Ledford, 2011). In addition, negative results are not published in relation to animal studies *(Mak et al., 2014)*. The most common animal used in pre-clinical and research tools are mice however, mice are poor models for most human diseases, this is due to critical cellular, genetic, molecular and

immunologic differences between rodents and humans *(Seok et al., 2013)*. Mouse models duplicate parts of a disease progression or exact process of the physiological performance however, they do not demonstrate the whole variety of physiological changes occurring in human disease.

Animal models can serve as an important source of *in vivo* information, but alternative translational approaches have emerged that may eventually replace the link between *in vitro* studies and clinical applications. *In vitro* human cell and tissue cultures are more relevant to humans, faster and more cost effective in comparison to animal cell and tissue cultures. Human cell cultures have showed significant progression in research for multitude purposes as it has improved knowledge of human disease (Mak et al., 2014: Ledford, 2011). The main benefit of *in vitro* research is that it allows generalisation of the process of the disease, permitting focusing on a small number of components *(Ledford, 2011)*. Tissues or cells obtained from volunteers' patients, surgical operations, post-mortem specimens and biopsies are used for *in vitro* studies and offers an *in vitro* model of the tissue in a clear environment for analysis. Non-commercial human cell lines are very useful within laboratories for example Henrietta's cells have become standard laboratory techniques. It is essential to take benefit of human models without resulting in harm to patients or volunteers. Many patients with different diseases are willing to volunteer for treatment development and discovering new drugs therefore human clinical researches shows that there is no shortage of volunteers. Ethical standards are highly concerned when working with human tissues or human cell lines. However, a lack of human model for skeletal muscle research is still an issue *(Mak et al., 2014)*.

All drugs must be tested on animal by law, before released onto the pharmaceutical market. However, despite animal testing one of the key causes of death is reactions and side effects

in developed countries. Therefore, it is essential to address the concern that high numbers of drugs that work on animals, subsequently fail when outcomes are tested in human patients *(neavs, 2017)*.

Co-culture models that use primary human SkM SCs (i.e. primary myoblasts), which are obtained from muscle biopsy present certain weaknesses. They tend to suffer from restricted proliferative capacity, low purity of cells, and display cellular senescence as a result of the expansion of the cells (Mouly et al., 2005; Webster & Blau, 1990). These limitations could potentially be mitigated by progress in the use of cells obtained from MNs (Stockmann et al., 2013) and hiPSCs, and hESCs to produce myoblasts (Tanaka et al., 2013). However, apart from the ethical considerations that come with the use of hESCs, monocultures of stem cell obtained from MNs tend to be extremely delicate in culture and need manifold culture media constructions with compulsory growth and neurotrophic factors. As a result, in the event that they are co-cultured with myoblasts, these trophic elements have a negative effect on the differentiation of SkMC. Added to this, myoblasts co-cultures with stem cell-derived MNs create inferior NMJs which are not suitable for long-term studies of both the evolution and preservation of NMJ (Li et al., 2005). It is for this reason that it be suggested that employing immortalised human myoblasts in a co-culture model presents a number of benefits. Examples of such advantages include being less expensive, they are easy to use, and deliver a limitless source of material with the least amount of ethical considerations linked with using human tissue. A population of pure cells is also provided by cell lines, a desirable scenario since it delivers a reliable sample and its results are reproducible (Kaur and Dufour, 2012). For these reasons it was decided that the model established in the project will be human based.

1.6 NMJ Serum free media platform

Researchers usually add animal serum to culture media as a nutrients source, foetal calf serum or foetal bovine serum (FBS) are most common serum used in culture media as it contains low y-globulin and strong growth promoting driver *(Ferruzza et al., 2012)*. Despite serious ethical and scientific concerns, serum is an essential supplement in cell culture media *(Brunner et al., 2010)*. Serum used in culture media has technical disadvantages as it is not fully known what molecules are resident which increases risk of contamination *(Hadwe, 2009)*. Moreover, ethical issues are concerned as serum collection can make the animal suffer therefore it is highly important to avoid using serum in culture media *(Riebelinng et al., 2011)*. Many serum free media use chemical components as a replacement for serum in mammalian cell lines and primary cultures. However, manufacturer search is needed to determine appropriate formulation of medium and it is time consuming *(Brunner et al., 2010).* Additionally, when serum is used in nerve-muscle co-culture systems that are characteristically established (Daniels et al., 2000; Dutton et al., 1995; Giller et al., 1973, Li et al., 2001; Nelson et al., 1993) it presents unspecified variables as a result of the variances in the composition of serum which decreases the investigational reproducibility and could also disrupt the impact of the experimental treatments on the system. Hence, adding a serum into a co-culture system makes it unfeasible to describe the minimum factors needed for generating *in vitro* NMJs. Evidence has shown that lagging MN myelination *in vitro* could be the reason why there is serum in the culture system (Rumsey et al., 2009).

Inclusion of serum complicates the reproducibility/ interpretation of the experiments in particular drug screening as serum contains tens of proteins that may interfere with drug discovery experiments in addition to many factors that cannot be controlled (Dutton et al.,

1995). Serum in cell culture may alter the experimental outcomes in a direct or indirect way hence, it does not represents physiological conditions of the cells therefore, in many cases, serum may not be appropriate buffer to use in cell culture (Li et al., 2001). The serum obtained from cows contains different factors for each cow furthermore the serum for each cow are different during the year due to different factors such as diet etc. therefore, the probability to obtain similar lot for an entire project or experiment is very low due to the genetic variability and environmental changes (Dutton et al., 1995). A research by Ham in 1960s tried to re-move the serum from cell cultures however, using a serum free media has been difficult (Li et al., 2001). Therefore, there are a limited number of serum-free media designed for a specific cell line. Development of a specific media requires a selection of serial clonal for each cell line (Sargent., 2015).

1.7 The impacts of diabetes on skeletal muscle, motor neuron and NMJ

Skeletal muscle is responsible for coordination of body movement through the generation of contractile forces. They govern the body's metabolism by storing up to 80% of total glycogen and aiding in insulin absorption and catabolism of amino acids (Jensen et al., 2011). The lengthy and sustained functioning of skeletal muscle fibres and their subsequent exposure to different biochemical and physical stimulants results in substantial muscle changes (Shadrach and Wagers, 2011). In a healthy human being, 70-80% of ingested glucose is absorbed by skeletal muscles aided by an insulin-controlled mechanism (Deshmukh, 2016). Type 2 diabetes mellitus (T2DM) is a metabolic illness that causes elevated levels of glucose in blood or hyperglycaemia, and the absence of glucose within tissues (Shadrach and Wagers, 2011). Diabetes mellitus markedly reduces the myogenic functionality of satellite cells within the skeletal muscle (Abdul-Ghani and DeFronzo, 2010). Studies have highlighted a host of

mechanisms that can trigger damage to the health of the skeletal muscle. They include dangerously low-grade inflammation profile (CLIP), oxidative stress (shown in Figure 1.12), and impaired extracellular matrix modelling (D'Souza et al., 2013). In diabetes mellitus, this functionality is compromised owing to insulin resistance (Abdul-Ghani and DeFreonzo, 2010). Additionally, it hampers muscle metabolism resulting in reduction in intermyofibrillar mitochondrial content and function as well as elevated levels of abnormal lipid deposition. Subsequently, this hampers switching between fat and carbohydrate oxidation in response to insulin. These changes render muscles metabolically inflexible, a state which has far-reaching implications for the maintenance of an active and healthy lifestyle (Kelley and Mandarino, 2000).

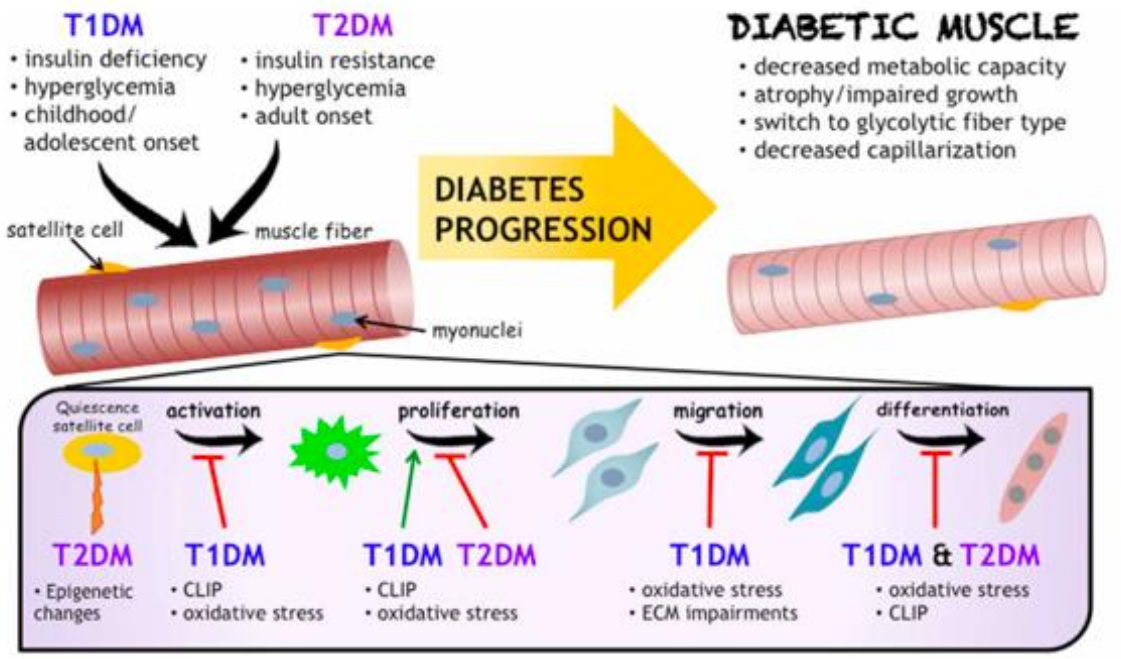

Figure 1.11: Impact of diabetes mellitus on skeletal muscle health. Chronic low-grade inflammation (known as chronic low-grade inflammatory profile or CLIP), oxidative and impaired extracellular matrix remodelling are the common mechanisms that causes muscle impairment and decreases satellite cell functionality in diabetes mellitus (D'Souza et al., 2013).

A prevalent, often neglected complication of diabetes mellitus is the diminishing healthy skeletal muscle content and functions, a condition referred to as diabetic myopathy (D'Souza et al., 2013). Additionally, hyperglycaemia can result in damages to the neurons and alter neuromuscular relay causing muscle atrophy and weakness in persons with diabetes, a complication referred to as diabetic neuropathy (could take the form of motor or sensory neuropathy) (Callaghan et al., 2012). Notably, myriad of factors have been shown to result in muscle and neural wasting in T2DM. Such factors include: hyperinsulinemia, hyperglycaemia, and hormonal fluctuations like glucocorticoids (Kalyani et al., 2014). In healthy and young SkMC advanced differentiation are observed where the nuclei position are located at the periphery of the myofiber beneath the plasma membrane. Nevertheless, the nuclei stop being evenly distributed during formation of the NMJ and in formation of myotendinous junction. However, the periphery position of the nuclei are lost in old SkMC and abnormal cells. Muscle contractions are delayed or stops completely in multiple muscle disorders caused by interruption of the nuclear position, hence, the signalling between the cells are interrupted due to the nuclei being relocated in the centre of the cells leading to hindering of the signal (Roman and Gomes., 2018).

1.7.0 Diabetic myopathy and neuropathy

Persons with diabetic myopathy typically present with alternative extended-term symptoms of diabetes, such as cardiovascular conditions, peripheral vascular disease as well as neuropathy (Delaney-Sathy et al., 2000; Ahmad et al., 2014). The link between motor neurons and skeletal muscle is called neuromuscular junction (NMJ), which is an essential link in the human motor system governing voluntary muscular movement (Gonzalez-Freire et al., 2014). Muscle denervation, re-innervation or inhibited NMJ severely alter muscle

physiology (Cadot et al., 2015). The morphological and operational changes to NMJ in diabetes is linked to muscle inferiority (diabetic myopathy) (which is a muscle originated from the inferior part of the tendinous ring, with nerve supply from the oculomotor nerve to input the sclera of the eye, and whose action directs the pupil downward and medialward) as well as neural weakening or peripheral neuropathy (diabetic neuropathy) (which is a result of damage to the nerves outside of the brain and spinal cord, often causes weakness, pain and numbness). In association with muscle weakness diabetic neuropathy is linked with functional and morphological changes of NMJ (Gonzalez-Freire et al., 2014). Differences of NMJ relay would facilitate the progressing weakness of flexor and extensor muscles within diabetes (Andersen, 2009).

The unique mechanisms underlying the progress of diabetic peripheral neuropathy (DPN) have yet to be understood. Even so, DPN is likely a consequence of diabetes-related muscular or metabolic inhibitions which are not mutually exclusive and could be related or synergistic (Zochodne, 2008). Such mechanisms lead to axonal loss through dying-back or retrograde deprivation, in addition to peripheral nerve demyelination (Zochodne, 2008). Notably, T2DM leads to long-term deficiency and malfunctioning of various tissues (Calcutt et al., 2009). Particularly, neural deficiency resulting from diabetes (motor as well as sensory nerve) comprises a major type of neuropathy (Andersen, 2009). Moreover, mitochondrial malfunction linked to oxidative stress caused by hyperglycaemia or hyperlipidaemia are hypothesised to have a huge impact in DPN (Figure 1.12) (Picard et al., 2013).

Diabetes mellitus comprises a prevalent reason for motor myopathy (impairment of the motor nerve) leading to muscle atrophy and weakness (Andersen, 2009). A lack of muscle strength, which is linked to wasting of the distal portions of the lower body owing to denervation caused by the loss of motor axons and insufficient re-innervation has been

attributed to motor neuropathy (Ramji et al., 2007). The ability of the body to coordinate motion may be affected by motor neuropathy, especially during walking. The foot condition known as Charcot foot may advance owing to walking while suffering from neuropathy (Said, 2007). Therefore, persons with diabetes are more likely to experiences greater loss of muscle content, strength and eminence with time, compared to the diabetes free ones (Kalyani et al., 2010). The most prevalent type of diabetic neuropathy is the length-dependent symmetrical neuropathy with significant involvement of sensory fibres (said, 2007) and motor fibres in the severe forms (Dyck et al., 2011). These effects of diabetes on muscle on muscle could explain why persons with diabetes are at a greater risk of developing exhibiting functional impairment and movement restrictions (Kalyani et al., 2014). Additionally, the cause of this deterioration of in muscle function in persons with diabetes has yet to be understood. The model established in this study can be used as a diabetic platform to understand disorders in diabetes patients.

Among humans, loss of motor axon or motor unit (MU) (illustrated in Figure 1.7) has been investigated by employing the extensor digitorum brevis (EDB) (Power et al., 2010; Wang et al., 2014). Even so, within intrinsic foot muscles like the EDB, it can be difficult to differentiate axonal loss stemming from physical trauma from impairment caused by biochemical factors linked to diabetes (Wang et al., 2014). Also, examination of MU loss within muscles with more functions such as tibialis anterior facilitates the assessment if alternative related physiological and clinical factors including strength and fatigability (Wilson and Wright, 2014). It is thought that hyperglycaemia, which is a preliminary sign of progress in diabetes, weakens nerves and causes muscle weakness and the loss of mass and strength (Gumy et al., 2008). Notably, muscular wastage and weakness associated with T2DM could be partly result from motor unit as well as motor axon loss (Allen et al., 2016).

1.7.1 The Effect of AGEs in inducing diabetic myopathy and neuropathy

Advanced glycation end products (AGEs), a vast group of compounds formed through a non-enzymatic glycation process called the Maillard reaction (figure 1.14), have a huge impact on the aetiology of diabetic complications (Chiu et al., 2015). However, hyperglycaemia leads to glycation of enzymes and proteins needed for various cellular processes (Ashraf et al., 2014; Ashraf et al., 2015). Also, the endogenous metabolites, methylglyoxal (MG), glyoxal, as well as 3-deosyglucosone (3DG) are reactive glycating agents secreted via auto-oxidation of glucose, which further converts sugars to AGEs (Ashraf et al., 2016; Beisswenger et al., 2005). Non-enzymatic glycation commences with the formation of Schiff bases that are further converted into amadori products and then to AGEs (Ahmed and Thornalley, 2007), and steady accumulation of AGEs within organs and muscle promotes the formation of reactive oxygen species (ROS) causing oxidative stress, which is mostly a consequence of NF-κB signalling pathway resulting in mitochondrial malfunction (Vlassara and Palace, 2002; de M. Bandeira et al., 2013).

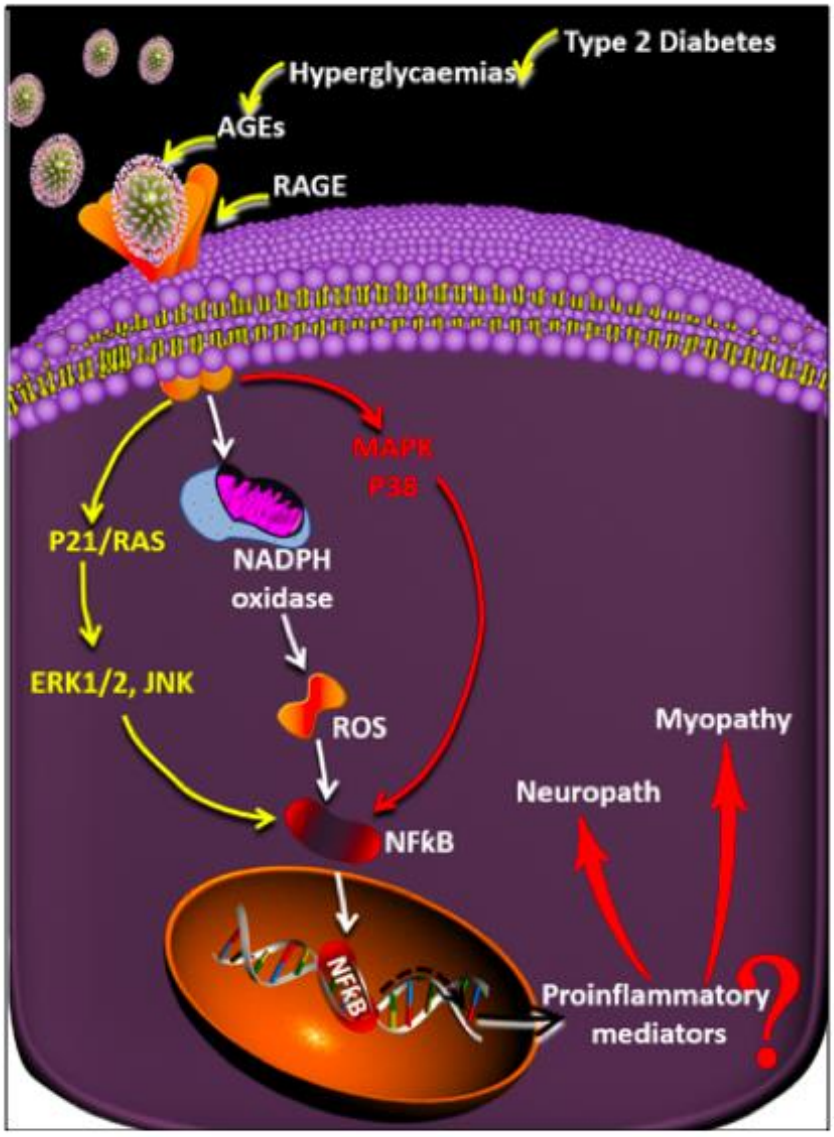

Figure 1.12: Mechanisms of diabetic neuropathy. AGEs/RAGE signalling pathway showing engagement of RAGE that activates many signalling pathways which promote the activation of NFkB which promote the transcription of several proinflammatory proteins which are involved in diabetic complications (Generated by our research group).

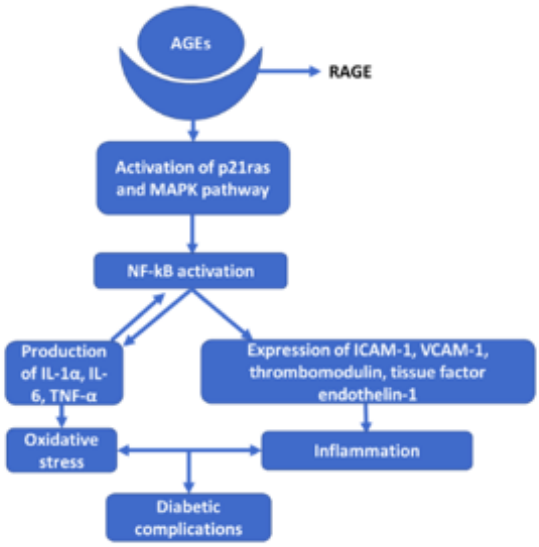

Figure 1.13: Cascades resulting from AGEs and RAGE binding. Cross-links between AGEs and RAGE cause oxidative stress and induce inflammation cascade, including triggering of mitogen-activated protein kinase (MAPK) pathway, nuclear factor-kB (NF-kB), interleukin-1 a (IL-6), and tumour necrosis factor-a (TNF-a), expression of intercellular adhesion molecule 1 (ICAM-1) and Vascular cell adhesion protein 1 (VCAM-2) resulting eventually in diabetic complications (Singh et al., 2014).

Figure 1 The various reaction steps which lead to the formation of AGEs

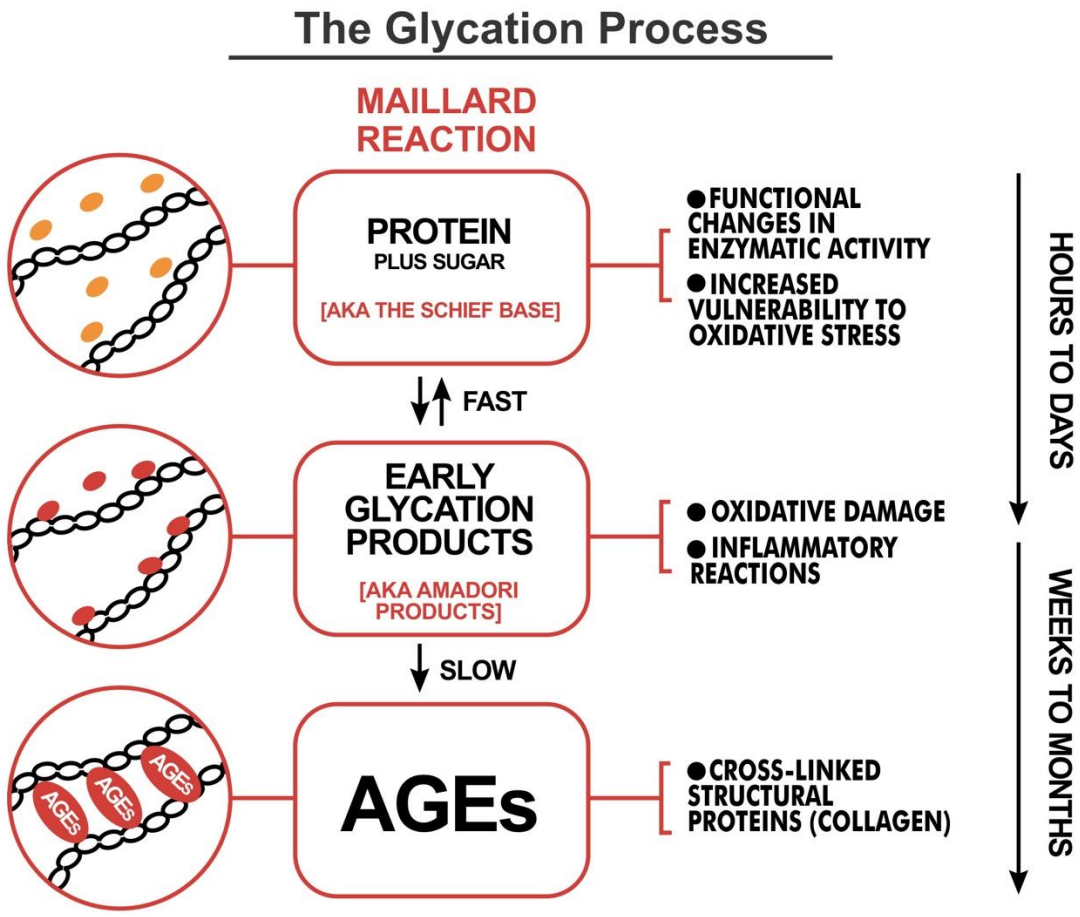

Figure 1.14 Millard reaction. Enzymatic glycation process called the Maillard reaction https://line.17qq.com/articles/shhahcucx.html.

AGE-altered proteins bind to RAGE (AGE-receptors on the outside of the cell) and elevated expression to RAGE has been observed on the cardiac myocytes, endothelial cells and skeletal muscle cells in persons with diabetes (Ramasamy et al 2005). AGEs and RAGE have also been observed to arouse prompt genetic expression, intracellular signalling and generation of free radicals as well as pro-inflammatory cytokine. Ergo, this interaction is believed to play a significant role in the development and progress of diabetes (Kim et al., 2005). The accumulation of AGE takes place or is enhanced under oxidative stress (Snow et al., 2007). Overall, the AGEs accumulation is tissue specific, changes the configuration features of

protein, while decreasing their tendency to breakdown (Singh et al., 2014). Beside their role within the pathogenesis of diabetic impediments, current research suggest that AGEs could hamper insulin activity through various cellular pathways; they intrude in the intricate insulin pathway, modify the insulin molecule and diminish secreted insulin (Cassese et al., 2008). The skeletal muscle cells comprise a significant portion of the insulin stimulated glucose utilisation (Uribarri et al., 2011). Consequently, a faction of studies, which have hypothesised that the myofibrillar protein glycosylation involves a feasible mechanism reinforcing the reduction in muscle functioning linked to age, have also observed the accumulation of AGEs within the skeletal muscle of ageing mice (Ramamurthy and Larsson, 2013). Additionally, various studies have observed deposits of AGEs within the myofibres of the extensor digitorum longus of ageing mice (Snow et al., 2007) as well as the soleus muscles of mice with diabetes (Snow and Thompson, 2009). Accumulation of AGES within the skeletal muscles has also been observed among ageing human subjects, coupled with diminished muscle strength (Dalal et al., 2009). A further investigation revealed that rats with streptozotocin-induces diabetes with extensive aggregation of AGEs in muscles of hind limbs exhibited significant diminished muscle mass, endurance of muscles as well as regenerative ability, suggesting that AGEs have an important link with the damage in mass and force of muscles, which supported findings of a previous study (Chiu et al., 2016).

Studies on rats with diabetes have revealed that myelin structure in the central as well as marginal nervous system undergoes non-enzymatic glycation (Ramasamy et al., 2005). It has also been suggested that AGE-associated marginal nerve myelin is susceptible to phagocytosis from macrophages, and this triggers macrophages to secrete protease, which could aid demyelination within diabetic neuropathy (Sango et al., 2017). Main axonal cytoskeletal proteins such as tubulin and actin, in addition to neurofilament, also undergo glycation. Such

axonal proteins are necessary for the maintenance of axonal functioning and arrangement, meaning their alteration via glycation could interfere with the structural as well as functional features of the axon, thus facilitating wastage and degeneration of the axon, in addition to the deterioration of axon signalling (Sugimoto et al., 2008). However, studies on the implications of AGEs for the function of skeletal muscle within diabetic rodents as well as humans are limited (Semba et al., 2010; Sugimoto et al., 2008). Therefore, AGEs will be used in this study to establish diabetes-specific NMJ model.

1.8 Aim and objectives

The primary **aim** of this project is to engineer and characterise entirely human *in vitro* nerve-muscle co-cultures that generate functional NMJs, thus providing a viable NMJ platform for e.g. diabetes studies.

The main **objectives** are:

1- Establishing media and generating neural progenitor cells (NPCs)

2-Establishment of *in vitro* NMJ between NPCs and immortalised human myoblasts.

3-Characterisation of *in vitro* NMJs using immunofluorescence and confocal microscopy to confirm SkMC innervation and NMJ formation via staining of pre- and post-synaptic proteins.

4-Functional Assessment of *in vitro* NMJs between neural progenitor cells and immortalised human myoblasts using agonist and antagonist drugs.

5-Investigating the cross communications between motor neurons and muscle co-culture model using ELISA-based microarray (identifying the concentrations of endogenously secreted growth and neurotrophic factors).

6-Establishing physiologically diabetes-specific NMJ platform.

Chapter 2: Materials and Methods

2.0 Materials

2.0.0 Cell Lines

A major element of this study is the utilisation of immortalised human skeletal muscle myoblasts (HSMM), (access made possible by Professor Browne Paris) (Mamchaoui et al., 2011). The Institute of Myology (Paris, France) provided the two immortalised human skeletal muscle cell (SkMC) lines used in this project. Young SkMC lines were produced with young myoblasts gathered anonymously from Myobank. The Myobank is a store of tissues associated with Eurobiobank and is accredited by the Ministry of Research in France (authorisation # AC-2013-1868). The primary myoblasts were obtained from a man aged 25 with no disease of genetic defects. Telomerase-expressing kinase 4-expressing vector transduction and cyclin-dependent (Mamchaoui et al., 2011) were used for myoblast immortalisation. Our group, in this project, was the first to make use of these cells, implying that these cell lines have not been established in the past in our laboratory. Consequently, the Institute of Myology provided training of cell culture methods for the two cell lines to my supervisor Dr. Al-Shanti. Dr. Al-Shanti trained me and provided me with one tube of cells containing 100 000cells. I expanded the number of cells myself and managed to do a stock (of passage 2) for myself which I used throughout the project.

2.1. Methods

2.1.0 Human Skeletal Muscle Cell Culture

The Class II, Type A2 biosafety cabinet provided the setting for all cell culture work. Aseptic practices and techniques were strictly adhered to. From liquid nitrogen storage, two cryovials were obtained, with $1x10^6$ 25-year-old immortalised human myoblasts (C25) in each. In 10% Dimethyl sulfoxide (DMSO) and 1 mL suspension of 90% fetal bovine serum (FBS), the cells were cryopreserved. Before being quickly thawed in two minutes, the frozen vials were put in a water bath set at 37°C for 1min. Following this, the thawed myoblasts were moved into separate 15 mL tubes. The next task involved adding 9 mL of pre-prepared complete growth media (GM) (Table 2.0) into each tube to prompt the process of the proliferation of myoblasts.

Table 2.0: Complete growth media for skeletal muscle cell proliferation.

Media components	Concentration
Dulbecco's modified eagle medium (DMEM)	59% (v/v)
Medium 199 with Earle's balanced salt solution	19% (v/v)
Fetal bovine serum (FBS)	20% (v/v)
L-glutamine	1% (v/v)
Penicillin-streptomycin mixture (Pen/Strep)	1% (v/v)
Fetuin from fetal bovine serum	25 µg/mL
Basic fibroblast growth factor (FGFb)	0.5 ng/mL
Epidermal growth factor (EGF)	5 ng/mL
Hepatocyte growth factor (HGF)	2.5 ng/mL
insulin	5 µg/mL
Dexamethasone	0.2 µg/mL
Gentamicin	10 µg/mL
Plasmocin	25 µg/mL

The separate 10 mL suspensions of C25 were moved into separate T175 flasks. After placing the flasks in a levelling plate, they were incubated at 37°C with a 5 % CO^2 atmosphere (ATM). The incubation continued until a cell growth density was at a confluence of 80%, as determined by the area percentage that cells covered in the entire field using the microscope

locator measurement to make sure that same field was not counted more than 1 time. microscopic field of view. The difference in the confluence percentage between the two cells lines at intervals of 24, 48, 72, and 96 hours was determined using contrast microscopy analysis with DMI6000B and Axiovert 40 C inverted microscopes. ImageJ, a processing application based on Java and developed at the National Institutes of Health and the Laboratory for Optical and Computational Instrumentation (Madison, WI, USA) (Schneider et al., 2012; Collins, 2007) provided the means to enumerate the confluence at the intervals stated earlier by computing the aggregate myoblast area. The formula used for the calculation is < [(total area of myoblasts in a field)/ (total area of the field)] (100) > (Ricotti et al., 2011; Ren et al., 2008). A DMI6000B inverted microscope with the N Plan 10x/0.25na Ph1 objective was used for visualising the entire field using the microscope locator measurement to make sure that same field was not counted more than 1 time.

.

2.1.1 Cell Count

Once the confluence of the flasks was at 80%, the GM was aspirated before the cells were washed two times using 10 mL of Dulbecco's phosphate-buffered saline 1X (DPBS). This was done to get rid of any GM components which could restrict the disassociation enzymes' functioning. Then, the cells' monolayers were disassociated from the flasks. This was accomplished through the use of 2 mL of extremely filtered, recombinant cell-dissociation TrypLE express enzyme 1X and five minutes of incubation at ATM. Once the 2 mL cell suspensions had been dissociated, they were pipetted from the flask and placed in separate 15 ml tubes. Following this, each flask was washed separately with 8 mL of GM. This was done with the aim of capturing any remaining cells that may still be in the flask following the

disassociation. From each flask, the 8 mL of GM was gathered and added to a matching 15 mL tube of C25, which had 2 mL of cells already collected. The 8 mL GM, 2 mL TrypPLE cell suspensions of both C25 were mixed separately by pipetting the cell suspension in the 15 mL tube up and down for between five and ten times before the sample was divided for cell counting. Traditional cell count procedures (Phelan & Lawler, 2001) were used for comparing the viable aggregate cells in C25.

The mixing of Trypan Blue and cell suspension (50 µL) using a ratio of 1:1 was used as the technique for counting the cells. The Trypan Blue helps identify cells that are non-viable by getting into the membrane and colouring the cell blue, while the viable cells stay transparent with the area around the membrane having a characteristic white halo. Counting the viable cells was accomplished through the use of traditional methods with a haemocytometer (Phelan & Lawler, 2001), observed with an A-Plan 10x / .25 Ph1 objective on the Axiovert 40C inverted microscope. The formula, [(Average number of live cells in eight large corner square) (dilution factor) (10^4)] was used to determine the number of viable cells/mL of cell suspension. For instance, (50)(2)(10000) = $1x10^6$ cell/mL of suspension. On this bases, it can be that 10 mL suspension of gathered cells would produce $1x10^7$ cells. Depending on the demands of the experiment, the cell suspension counted was either cryopreserved, sub-cultured, or seeded on tissue culture surfaces as needed.

2.2.2 Subculture

Once the cell counting was done, divisions of cells suspensions with $1x10^6$ cell were moved into new 15 mL tubes from the tubes of counted cells. Into the new 15 mL tubes of cells, a volume of GM required to get the aggregate volume of the suspensions to 10mL was added. Therefore, the new cells suspensions of both C25 had $1x10^5$ cells/mL as their concentrations. In their separate tubes, the suspensions of cells were homogenised, before they were

pipetted into separate T175 flasks. This was followed by incubation at ATM until a confluence of 80% was reached.

2.2.3. Cryopreservation

Huge stores of cells were produced for storage and retrieval for use in experiments when needed. For generating the cells, C25 was expanded and sub-cultured on an ongoing basis as described above. Thus, to make sure that fidelity was maintained right across this project, the myoblasts retained a low number of passages. After disassociation and counting of cells (as described in 2.2.1), the 10 mL cell suspensions of C25 were moved to separate new 50 mL tubes. Into the 50 mL tubes, the same volume of DPBS was added, in the process diluting and washing the cells in the suspension. Then, at 300 x g, the 50 mL tubes were centrifuged at 23^{o}C for 10 minutes.

Once the cells had been centrifuged, the aspiration of the supernatants into the tubes followed, making sure that the pelleted cells did not get disturbed. The volume of FBS needed was supplemented into the 50 mL tube so that the cells' concentration came to 1x10^{6} cell/mL, depending on the quantity of the cells before centrifugation. Then, the cell pellet was fully distributed and homogenised in the FBS through up and down pipetting of the solution in the tube ~ ten 20 times. Into each of the cryovials, 900 µL of the FBS cell suspension was pipetted before adding 100 µL of DMSO into each vial. Consequently, in each vial, there was ~1x10^{6} cells suspended, 90% FBS, and 10% DMSO. A Mr Frosty freezing container was them used to store the vials at -80°C for 24 hours. From there, the vials were moved from the -80°C storage freezer into a liquid nitrogen tank for extended storage at -200^{o}C.

2.1.4 Differentiation Parameters

Once the process of counting the cells was complete, the cells were moved into new 50 mL tubes, from 15 mL tubes. The needs of the experiment determined the number of cells placed

in the 50 mL tubes. The GM volume required for diluting the cells to a $1.5x10^5$ cells/mL concentration was supplemented to the 50 mL tubes in preparation for seeding in tissue culture plates. Before the cells were plated, a 1% Gelatin solution was used to pre-coat the 6-well plates, which were then dried for 60 minutes. This was followed by the separated pipetting of the 2 mL of the GM cell suspension of C25 in 6-well plates. As a result, in each well of the 6-well plate, the cells' concentration was $3x10^5$ cells, which could also be articulated as a density of 315 cells/mm^2. Once the cells had been seeded, the 6-well plates were put on a levelling plate before they were incubated at ATM for 24 hours. The confluence reached by the cells at this point was ~90-100%. After the incubation and the GM was aspirated from the wells, the cells were washed two times using 1 mL of DPBS. Before the cells were incubated for 96 hours at ATM, 2 mL of a simplified complete differentiation media (DM) (Table 2.1) was supplemented into each well.

Table 2.1: Complete differentiation media for immortalized human skeletal muscle cell.

Media components	Concentration
Dulbecco's modified eagle medium (DMEM)	98% (v/v)
L-glutamine	1% (v/v)
Penicillin-streptomycin mixture (Pen/Strep)	1% (v/v)
Insulin	10 µg/mL
Gentamicin	10 µg/mL
Plasmocin	25 µg/mL

To determine the proportional reduction in cell proliferation, Immunofluorescence microscopy was employed. The same technique was used to assess the phenotypic differentiation (elongation, alignment, and fusion) of C25 cell lines as they were differentiating over 96 hours. The comparison of differentiation parameters (Bullwinkel et al., 2006; Schonk et al., 1989) were measured at intervals of 24, 48, 72, and 96 hours. For each interval, from the wells, DM was aspirated before the cells were washed two times using 1

mL of DPBS. The cells were then incubated for 10 minutes at 23°C in a 500 µL 4% paraformaldehyde solution to accomplish cell fixation. Then, the paraformaldehyde was aspirated before the cells were washed three times using DPBS. Then a 1X concentration of Prem/Wash buffer (PWB) was used for cell permeabilisation. Into each well, 1 mL of PWB was supplemented before 1 mL of DPBS was used to wash the cells. This was followed by the use of 1 mL of pre-prepared blocking solution with 10% goat serum (GS) and 0.2% Triton X-100 (TX100) was supplemented to each well before incubation of the cells at 23°C for an hour. Then, the blocking solution was removed in creating conditions for antibody labelling.

A 250-µL antibody diluent solution with DPBS, 0.05% TWEEN 20, 3% GS, anti-antibody at a proportion of 1:100 was applied to the cells. This was followed by the removal of the primary antibody solution from the wells before washing the cells three times using DPBS. Fluorescent-labelled secondary antibody conjugates were then added. The volume of the secondary antibody diluent was applied into the cells before incubation at 23°C for 30 minutes was 250 µL. It contained DPBS and 4', 6-Diamidine-2'-phenylindole dihydrochloride (DAPI) at a proportion of 1:10000, phalloidin at a ratio 1:500, anti-myosin heavy chain (MHC) Alexa Fluor 488 at a ratio 1:500, and anti-rabbit Alexa Fluor 568 at a ratio 1:500.

Twice more, the stained cells were washed using DPBS. They were then kept in the DPBS for subsequent analysis. Fluorescence microscopy was used for the visualisation of the stained cells. The measuring and comparison of the differentiating parameters were accomplished with the use of ImageJ (Table 2.2).

Table 2.2: Differentiation parameters (Ren et al., 2008; Ricotti et al., 2011; Grubisic et al., 2014).

Differentiation parameters	Formula
Myotube area (MA)	[(total area of myotubes in a field)/(total area of the field)](100)
Fusion index (FI)	(total number of nuclei per myotube)/(total number of nuclei in the field)](100)
Aspect ratio (AR)	(myotube length)/(myotube width)

2.1.5 Co-culture

A dearth of nerve component imposes limitations on *in vitro* research that uses aneurally cultured SkMCs to explore muscular dysfunction. This is a situation that leads to restricted differentiation and non-contractile myotubes (Delaporte et al., 1986). If the reflection of the physiological conditions existing *in vivo* is to be obtained, SkMCs are needed for MN stimulation. Thus, to deal with the restrictions of aneurally cultured SkMCs, a novel co-culture model was established successfully by me. In this model, functional innervation of myotubes was attained through the use of NPCs (Figure, 2.1).

2.2 Generating neural progenitor cells (NPCs)

The lack of nerve element (NMJ) results in restrictions when it comes to studies on muscular dysfunction employing aneurally cultured SkMC. The consequence of this is restricted differentiation and myotubes that fail to contract (Delaporte et al., 1986). The replication of motor neuron is a requirement for the specific replication of the physiological settings established *in vivo*. To deal with the limitations of aneurally cultured SkMC, a novel co-culture model was established by me. In the new model, operational innervations of myotubes were obtained through the employment of NPC cells differentiation from neural stem cells.

2.2.0 Maintenance of MEFs and mitotic inactivation

Within complete medium (table 2.3), mouse embryonic fibroblasts (MEF, Cell Biolabs, UK) were cultured. This was followed by the passaging of cells using a ratio of 1:4. Using0.1µg/ml Mitomycin C within regular culture medium, MEFs were mitotically inactivated before they were incubated at 37°C for three hours. Following this, was four rinses using 10ml phosphate-buffered saline (PBS). Using 150µl/cm2 TrypLE, the cells were enzymatically dissociated. They were then kept in FBS 10% (v/v) dimethyl sulfoxide (DMSO) at a temperature of -80°C and a

density of ~5 x10^6 cells/ml before the embryonic stem cells were cultured at a density consisting of 5x10^4 cells/cm2 on 0.1% (w/v) Gelatin-covered tissue culture dishes.

Table 2.3: Mouse embryonic fibroblasts growth media

MEF growth media components Concentration	
Dulbecco's Modified Eagles Media (DMEM) from Lonza (Nottingham, UK)	500 ml
L-glutamine from Lonza (Nottingham, UK)	1% (v/v)
Penicillin/Streptomycin (Sigma, UK)	5ml (2mM)
Heat inactivated fetal bovine serum (FBS) from Gibo (Loughborough, UK)	10% (v/v)

2.2.1 Maintaining Shef3 hEs cells

Professor McKay provided the Human Embryonic stem cell line, which was sustained in hEs cell medium on MEFs (table 2.4). Subject to such settings, cells were kept in a pluripotent condition. The colonies passaging was attained through the use of flame-drawn glass pipette and also the dissecting microscope after a period of between five and seven days. Each colony was divided into numerous sub-divisions and re-plated on new MEFs. With the aim of adjusting hEs cells that rely on MEF to feeder-free conditions, cultures were plated and trypsinised at a high density (1:1) on human fibronectin (20 µg/ml) that was purified and covered in mTESR. Any polluting MEFs that got trapped to the flasks were lost. The passaging of feeder-free cultures was done using TrypLE after a period of between three and five days. Ahead of neural initiation, ES colonies sustain by the feeder were attuned to feeder-free circumstances with the aim of avoiding the carry-over of MEF.

Table 2.4: Human embryonic stem (hEs) media for cells on MEFs.

hES/MEF cell medium components Volume/concentration	
Dulbecco's Modified Eagles Media (DMEM)- F12 (1:1) from Lonza (Nottingham, UK)	38.5 ml
MEM Non-essential amino acids (NEAA) (Life Technologies, UK)	0.5ml (1x)
Penicillin/Streptomycin (Sigma, UK)	0.5 ml (1x)
bFGF (R&D systems, UK) (100ug/ml)	5uL (10ng/ml)
Knockout Serum Replacement (KSR) (Gibco, Life Thechnologies, UK)	10ml (20%)

2.2.2 Feeder-free Shef3 hEs cells neural induction

Seventy-two hours before the commencement of differentiation, neural induction medium (NIM), which included Poly Vinyl Alcohol (PVA) was established. The inclusion of PVA was done at a concentration of 4mg/ml to DMEM/F12 and shaken energetically for over 60 minutes. At a temperature of 4°C, the medium was kept for more than 72 hours on a roller so that the PVA could dissolve completely. Following this, it was heated to a temperature of 37°C and filtered with a 0.22 µm syringe constrained filter to sterilise. Once the filtration was done, the medium was amplified using the factors catalogued in table 2.5. The hEs feeder-free cells were enzymatically disturbed to obtain a sole cell suspension before being spun down for five minutes at 1080 xg. The suspension of the pellets was done once more in NIM and at a density of $1x10^4$ cells/well in Nunc 96 V bottom well plates. To a top intensity of 300ng/ml, the rock inhibitor was included over a time of 24 hours to facilitate the establishment of spheroids. In the 24 hours, neuroepithelial clusters were formed in the suspension. Over a time of five days, the medium was changed every day (to feed the cells with fresh media). On Day 6, the NIM on laminin (20µg/ml) covered dishes were used to re-plate the aggregates with the aim of allowing for the formation of neural rosettes (two-three days). Once formed, the rosette clusters were gathered using a 21-gauge sterile needle, centrifuged over three minutes and 200x g before re-suspension in NEM (neural expansion medium), (Table 2.6). This was done with the aim of facilitating neural stem cells (NSCs) propagation in ultra-low attachment plates. Constantly, cells were cultured as neurospheres, which can be described as groups of hollow spheroids that can be passaged through disruption that used p200 Gilson pipette. Neural stem/progenitor cells, on the other hand, were extended on tissue culture dishes treated with a monolayer culture of laminin. For a short period, cells were rinsed with PBS, trypsinised for three minutes, and resuspended with 10 ml of PBS and spun for eight minutes

at speeds of 900 rpm. After removing the supernatant, the cells were resuspended using NEM.

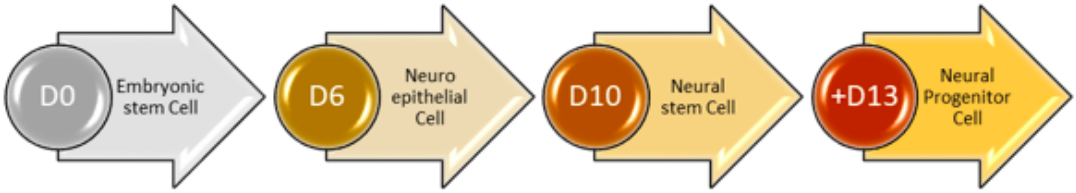

Figure 2.1: The schematic illustrates the ESC, NEC, NSC, NPC and neuron progression time scale. On Day 0, MEF cultured on hEs colonies were resuspended with the aim of producing NECs. On the sixth day, NECs were plated on pre-coated laminin dishes to permit for the production of rosettes over a time of two to three days. On the tenth day, the rosettes were manually isolated and coated as a monolayer in NEM.

Table 2.5: Neural Induction Medium (NIM)

NIM components	Volume/concentration
Dulbecco's Modified Eagles Media (DMEM)- F12 (1:1) from Lonza (Nottingham, UK)	48.5 ml
MEM Non-essential amino acids (NEAA) (Life Technologies, UK)	0.5ml (1x)
Penicillin/Streptomycin (Sigma, UK)	0.5 ml (1x)
bFGF (R&D systems, UK) (100ug/ml)	10uL (20ng/ml)
N2 supplement (Life Technologies, UK)	0.5 ml (1x)
Heparin (Sigma, UK) (2mg/ml)	50ul (2ug/ml)
Poly (vinyl alcohol) (PVA) (Sigma, UK)	4mg/ml

Table 2.6: Neural Expansion Medium (NEM)

NEM components	Volume/concentration
Dulbecco's Modified Eagles Media (DMEM)- F12 (1:1) from Lonza (Nottingham, UK)	48.5 ml
MEM Non-essential amino acids (NEAA) (Life Technologies, UK)	0.5ml (1x)
Penicillin/Streptomycin (Sigma, UK) (100x)	0.5 ml (1x)
bFGF (R&D systems, UK) (100ug/ml)	10uL (20ng/ml)
N2 supplement (Life Technologies, UK) (100x)	0.5 ml (1x)
Heparin (Sigma, UK) (2mg/ml)	50ul (2ug/ml)
B27 supplement (Life Technologies, UK) (50x)	1 ml (1x)

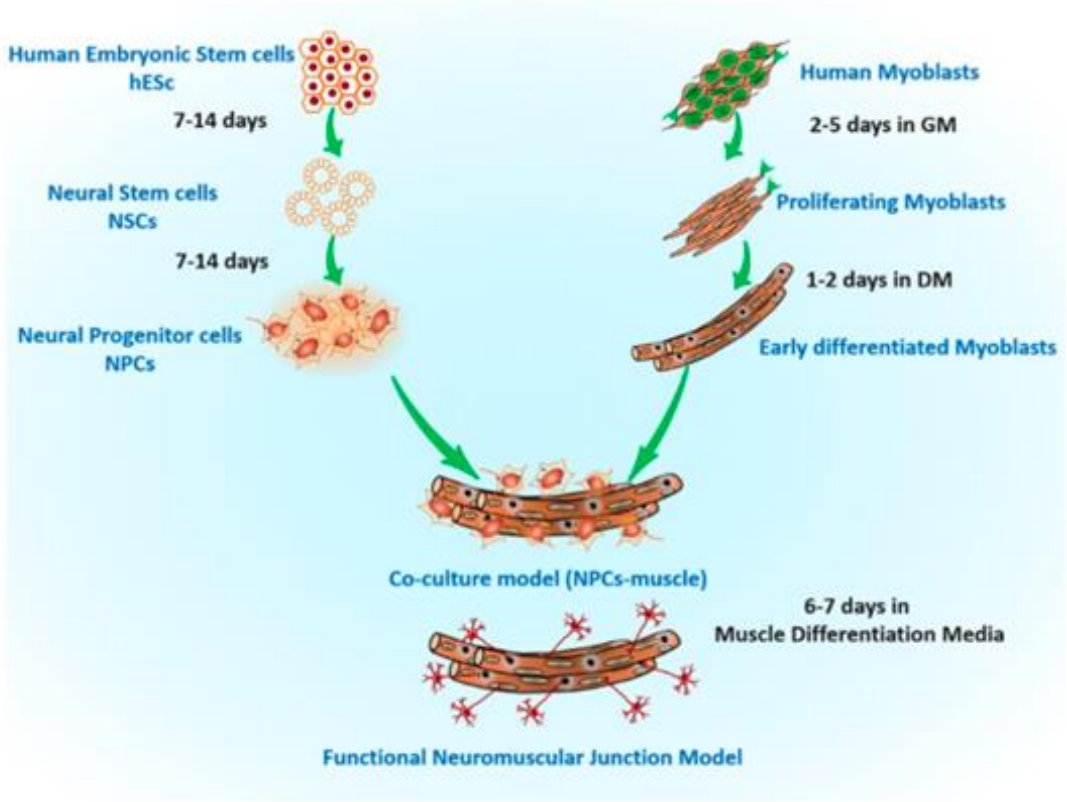

Figure 2.2: Human neuromuscular junction model (NMJ). Together with human neural progenitor cells (NPCs) derived from hESCs, human immortalized myoblasts were co-cultured. Within a time of seven days in muscle differentiation media without any serum or neural growth factors, myoblasts differentiated into myotubes while NPCs differentiated into motor neurons that spread to create numerous NMJ innervation sites along the myotubes (Adapted from our research group).

2.3 Co-culture fixation

On the seventh day following co-culture, the co-culture cells were fixed in their dishes for characterisation and analysis. This was two days following the continuous spontaneous contractions of the myotubes, although the co-cultures could be maintained beyond 30 days as long as there were regular changes to the media as described in 2.1.8. From the dishes, the DM was aspirated before the cells were washed three times using 500 µL of DPBS. At a temperature of 23°C, a 4% paraformaldehyde solution was used for incubating the cells for

12 minutes. The paraformaldehyde was them eliminated from the dishes before 500 µL of DPBS was used to wash the cells three times. For up to seven days, the fixed cells were kept in DPS solution with a temperature of 4°C. For the co-culture model's pre- and post-synaptic components of neuromuscular junction (NMJ) formation, the characterisation and evaluation was conducted through immunocytochemistry (ICC).

2.3.1 Co-culture Immunocytochemistry

Once the co-cultured cells had been fixed, under temperatures of 23°C and timelines of 30 minutes, the cells were incubated with 500 µL of a 1X concentration of PWB. Following the permeabilisation, the PWB was eliminated from the dishes before 500 µL of DPBS was used to wash the cells two times. To the cells, 500-µL of blocking solution was applied before the cells were incubated at 23°C for an hour with the aim of clocking undefined antibodies binding. In the solution was 0.2% TX100 with 10% GS or donkey serum (DS). When the incubation was complete, the blocking solution was removed before 500 µL DPBS was used to wash the cells once. Before the cells were incubated at 4°C for between 18 and 24 hours, the primary bodies (Table 2.7) and 250 µL of primary antibody diluent consisting DPBS, 3% GS or DS, 0.05% TWEEN 20 were added.

Table 2.7: Primary antibodies for co-culture.

Antibody	Concentration
Anti-calcium channel L type DHPR alpha 2 subunit (DHPR)	1:100
Anti-choline acetyltransferase (ChAT)	1:100
Anti-glial fibrillary acidic protein (GFAP)	1:100
Anti-muscle-specific kinase (MuSK)	1:100
Anti-neurofilament H (NFH)	1:100
Anti-receptor associated protein of the synapse (rapsyn)	1:100
Anti-ryanodine receptor 1 (RyR)	1:100
Anti-synaptotagmin (Syt1)	1:100
Anti-vesicular acetylcholine transporter (VAChT)	1:100

After the incubation of the primary antibody, from the dishes, the diluent was aspirated before the cells were washed three times using 500 µL of DPBS before fluorescent-labelled secondary antibodies were added. Into each dish, a secondary antibody diluent with 250 µL DPBS supplemented with DAPI at a ratio of 1:10000 and a matching antibody (Table 2.8) was supplemented to each dish and incubated under dark conditions for half an hour. From the dishes, the secondary antibodies were aspirated, and 500 µL of DPBS was used to wash the cells twice for the last time. During analysis, the cells were kept in 1 mL of DPBS. Confocal and immunofluorescence microscopy was used for the confirmation of the innervation and characterisation of the formation of the NMJ. The microscopy employed Leica DMI6000 B inverted microscope with HCX PL FLUOTAR L 20X/0.40na CORR and N Plan 10x/0.25na Ph1 objectives, and a Leica TCS SP5 confocal microscope with HCX PL APO 40x 1.25-0.75 Oil CS ∞ and HCX PL APO 63x 1.40-0.60 oil CS ∞ objectives.

Table 2.8: Secondary antibodies for co-culture.

Antibody	Concentration
Anti-β-3-tubulin Alexa Fluor® 488 conjugate	1:400
Anti-chicken IgY DyLight® 488	1:400
Anti-goat IgG Alexa Fluor® 568	1:400
Anti-MHC Alexa Fluor® 488 conjugate	1:400
Anti-mouse IgG Alexa Fluor® 555	1:400
Anti-rabbit IgG Alexa Fluor® 488	1:400
Anti-rabbit IgG Alexa Fluor® 568	1:400
α-BTX Alexa Fluor® 647 conjugate	1:400

2.3.2 Neuromuscular Junction Morphologies Quantification

Parallel experiments were done with the aim of comparing the development of the co-cultured cell's NMJ morphologies in comparisons to myotubes that were aneurally cultured. Aneural and innervated cultures were differentiated, fixed, and stained on the seventh day after they were co-cultured, using DAPI and α-bungarotoxin (α-BTX). The concentrations and methods used are described above. Distinct NMJ morphologies were enumerated into NMJ

morphology development categories already established (Valdez et al., 2010; Sahashi et al., 2012; Kummer et al., 2004; Lee et al., 2013). The categories included mature, fragmented, faint, premature, and denervated. A Leica TCS SP5 confocal microscope with an HCX PL APO 40x 1.25-0.75 Oil CS ∞ objective was used for the assessment of 20 random fields of view for each data set.

2.3.3 Transversal Triad Formation Quantification

The comparison of the development of transversal triads between natural and co-cultured myotubes was made using parallel experiments. Anural and innervated cultures were differentiated, fixed, and stained on the 7th day following co-culture for ryanodine receptors (RyR), dihydropyridine receptors (DHPR), and DAPI. The concentration and methods used are described in 2.3.1. Myotubes were said to have attained proper transversal triad formation, perceived to be an indication that differentiation is advanced when the RyR and DPHR staining was arranged in alternating order on at least half of the length of the myotubes. Twenty random fields of view were evaluated for triad formation. The visualisation was done using a TCS SP5 confocal microscope with a HCX PL APO 63x 1.40-0.60 oil CS ∞ objective.

2.3.4 Peripheral Myonuclei Quantification

In parallel experiments were done with the aim of comparing the myonuclei position in cultured myotubes in comparison to myotubes that were aneurally cultured. Any myonuclei located on the periphery is considered to be an indication of advanced differentiation. Aneural and innervated cultures were differentiated, fixed, and stained on the seventh day after the co-culture for DAPI and anti-MHC. The concentrations and techniques used are described in 2.3.1 Where myonuclei were detected to be protruding the membrane of the myotube, they were considered to be peripherally situated. The assessment and visualisation

of twenty random fields of view were done for peripherally located myonuclei using a Leica TCS SP5 confocal microscope with a HCX PL APO 40x 1.25-0.75 Oil CS ∞ objective.

2.3.5 Striation Formation Quantification

In parallel experiments were done with the aim of comparing the aneurally cultured myotubes and the stained myotubes in co-culture, considering that striations indicate advanced differentiation. On the seventh day following the co-culture, aneural and innervated cultures were differentiated, fixed, and stained for DAPI and anti-MHC. The concentrations and methods used are discussed in 2.3.1 Myotubes were recorded as striated in the event that the expression of MHC was organised in an alternating binding arrangement for at least half of the length of the myotubes. A Leica TCS SP5 confocal microscope with an HCX PL APO 40x 1.25-0.75 Oil CS ∞ objective was used to assess the striation formation of twenty random fields of view.

2.3.6 Myotube Width Quantification

In parallel experiments were done with the aim of comparing myotube thickness in aneurally cultured myotubes and myotubes in co-culture. Aneural and innervated cultures were differentiated, fixed, and stained on the seventh day after co-culture for DAPI and anti-MHC. The concentrations and methods used are described in 2.3.1 The quantification of myotube thickness was accomplished using phase-contrast microscopy with a Leica DMI6000 B inverted microscope and the ImageJ image processing software package. The HCX PL FLUOTAR L 20X/0.40na CORR objective was used to assess the entire field using the microscope locator measurement to make sure that same field was not counted more than 1 time.

2.4. Neuromuscular Junction Formation Functional Assessment

To confirm the NMJ formation, co-cultures were functionally evaluated. This was accomplished using live phase-contrast video analysis of myotube contraction frequency in reaction to agonist/antagonist treatments (table 2.9 and table 2.10). On the 7th day, the dishes with the co-cultured cells were placed in an inverted microscope stage, surrounded by an incubation chamber so that the conditions of the atmosphere could be maintained at 5% CO_2 and temperatures of 37°C. After 5 minutes of live observation of the continuous contractile activity of the myotubes, cholinergic antagonists were used for treating the myotubes to block AChRs at the NMJ.

Table 2.9: Treatments to boost or constrain myotube contraction frequency through NMJ signal transmission.

Drug	Concentration
1(S),9(R)-(−)-Bicuculline methiodide	10 µM
γ-Aminobutyric acid (GABA)	1 mM
L-Glutamic acid (L-Glut)	400 µM
(+)-Tubocurarine chloride pentahydrate	8 µM
α-Bungarotoxin (α-BTX)	1:400

Glutamatergic and γ-aminobutyric acid (GABA) was also used to treat the co-cultures with the aim of arousing glutamate and GABA receptors on the motor neurons (MNs). Previous studies were used as the basis for selecting the concentrations specified (Das et al., 2007; Borodinsky & Spitzer, 2007; Morimoto et al., 2013; Guo et al., 2011). The Hertz (Hz) is the unit measure for contraction frequency. The unit of frequency equals a single cycle per second, and for this project, it equals one contraction for each second.

The CF (contraction frequency) of the myotube was measured 30 seconds before the treatments were applied to the cells, to determine the baseline spontaneous CF. Successively, agonist or antagonist treatments were supplemented to the dishes in the middle

of the field of view. As soon as the treatment of the cells was done, CF modulation was conducted. Live measurements of CF in reaction to treatment were done again after 15 minutes, 20 minutes, 30 minutes, 45 minutes, 60 minutes and 90 minutes (observation was for 2 minutes). Ninety minutes following treatment, 500 µL of DPBS was used to wash the cells three times before new untreated DM was supplemented to the cells. The dished were put back in the microscope stage in the incubation chamber. Soon after, CF was measured at the two hours and 24-hour marks after the washout and DM resupply. Using phase-contrast microscopy that employs the DMI6000 B inverted microscope with an N Plan 10x/0.25na Ph1 objective, live video analysis was recorded. The expression of myotube contraction frequency was done as a mean ± SD.

Table 2.10 Agonist and antagonist drugs. Pharmacological drugs was used to assist pharmacological function as demonstrated in the table.

Drug	**Pre or postsynaptic effect**	**Mechanism of action**	**Agonist or Antagonist**
α-bungarotoxin	Postsynaptic	Block ACh receptor in Muscle	Antagonist
Tubocurarine	Presynaptic	Nerve impulse is blocked by alkaloid (Muscle relaxant)	Antagonist
Bicuculline	Presynaptic	Blocking ACh receptor	Antagonist
L-glutamic acid	Presynaptic	Neurotransmitter L-Glut stimulator MN	Agonist
γ-aminobutyric acid	Presynaptic	Force ACh discharge	Agonist

2.5. Human Growth Factor Array

In parallel experiments were done with the aim of comparing the concentration of 40 human growth factors (Table 2.11) in aneural myotube cultures and co-cultured myotubes. The co-cultured and aneural myotubes were prepared, seeded, and differentiated for seven days as has been described above. For assessment using a human growth factor array kit, supernatant samples were collected from both conditions. The assessment showed that spontaneous myotube contractions were initially observed contracting in harmony as a motor unit. The manufacturer guidelines were followed to do the preparation of reagents and standards in the array kit. Then, into each of the wells, 100 µl of sample diluent from the array kit was supplemented before 30 minutes of incubation at 23°C to block slides. Following this, the wells were decanted, and 100 µl of standards, controls and supernatant samples were supplemented to the individually allocated wells. After sealing, the slides were incubated at 4°C on microplate shaker fixed to 500 rpm.

After the incubation, the samples were removed from the wells. The following task involved washing the slides for five minutes, five times using 150 µl of 1X wash buffer 1. Then they were washed twice each for five minutes using 150 µl of 1X wash buffer 2. The activity that followed involved adding 80 µl of detection antibody cocktail into each well. The sides were then incubated at 23°C for 1.5 hours. After aspirating the antibody cocktail from the wells, the wash steps using buffer 1 and 2 were repeated one more time.

When the slides had been washed, 80 µl of Cy3 equivalent dye-conjugated streptavidin was supplemented into each well before it was sealed and incubated at 23°C under dark conditions for one hour. After the incubation, the wash steps were iterated once more. Then, the slides were separated from the gaskets and put inside the washer/dryer tube provided. Then, 30 mL of 1X wash buffer 1 was used to fill the tube, so that the slides were covered

completely before each tube was gently shaken for 15 minutes. From the tube, the 1X wash buffer 1 was eliminated before 30 mL of 1X wash buffer 2 was supplemented to cover the slides before they were shaken for another 5 minutes. The slides were then taken out of the washer/dryer tube, and compressed air was used to dry them so that any remaining buffer solution could be removed. This was followed by the visualisation of the array using GenePix 4000B laser scanner at 532nm wavelength. GenePix Pro 4.1 Microarray Acquisition & Analysis Software was used for processing the raw data from the visualised array images. The RayBiotech Q-Analyzer® tool Software for QAH-GF-1 was used for further statistical analysis of the data.

Table 2.11: Descriptions of the neurotrophins and the human growth factors enumerated in aneural myotube cultures and co-cultured myotube supernatant.

Growth/neurotrophin factors	
Amphiregulin (AR) (colorectum cell-derived growth factor) (CRDGF)	Insulin-like growth factor-binding protein (IBP-4) (IGF-binding protein 4) (IGFBP-4)
Brain-derived neurotrophic factor (BDNF) (Abrineurin)	Insulin-like growth factor-binding protein (IBP-6) (IGF-binding protein 6) (IGFBP-6)
Fibroblast growth factor 2 (FGF-2) (basic fibroblast growth factor) (bFGF) (heparin-binding growth factor 2)(HBGF-2)	Insulin-like growth factor I (IGF-I) (Mechano growth factor) (MGF) (Somatomedin-C)
Bone morphogenetic protein 4 (BMP-4) (Bone morphogenetic protein 2B) (BMP-2B)	Insulin [Cleaved into: Insulin B chain; Insulin A chain]
Bone morphogenetic protein 5 (BMP-5)	Macrophage colony-stimulating factor 1 receptor (CSF-1 receptor) (CSF-1-R)(CSF-1R) (M-CSF-R) (EC 2.7.10.1) (Proto-oncogene c-Fms) (CD antigen CD115)
Bone morphogenetic protein 7 (BMP-7) (osteogenic protein 1) (OP-1) (Eptotermin alfa)	Tumour necrosis factor receptor superfamily member 16 (Gp80-LNGR) (Low affinity neurotrophin receptor p75NTR) (Low-Affinity nerve growth factor receptor) (NGF receptor) (p75 ICD)
Beta-nerve growth factor (Beta-NGF)	Neurotrophin-3 (NT-3) (HDNF) (Nerve growth factor 2) (NGF-2) (Neurotrophic factor)
Pro-epidermal growth factor (EGF) [cleaved into: epidermal growth factor (Urogastrone)]	Neurotrophin-4 (NT-4) (Neurotrophin-5) (NT-5) (Neurotrophic factor 4)
Epidermal growth factor receptor (EC 2.7.10.1) (Proto-oncogene c-ErbB-1) (Receptor tyrosine-protein kinase erbB-1)	Tumour necrosis factor receptor superfamily member 11B (Osteoclastogenesis inhibitory factor) (Osteoprotegerin)
Prokineticin-1 (Endocrine-gland-derived vascular endothelial growth factor) (EG-VEGF) (Mambakine)	Platelet-derived growth factor subunit A (PDGF subunit A) (PDGF-1) (Platelet-derived growth factor A chain) (Platelet-derived growth factor alpha polypeptide)
Fibroblast growth factor 4 (FGF-4) (Heparin secretory-transforming protein 1) (HST) (HST-1) (HSTF-1) (Heparin-binding growth factor 4) (HBGF-4) (transforming protein KS3)	Placenta growth factor (PIGF)
Fibroblast growth factor 7 (FGF-7) (Heparin-binding growth factor 7) (HBGF-7) (Keratinocyte growth factor)	Kit ligand (Mast cell growth factor) (MGF) (stem cell factor) (c-Kit Ligand) [Cleaved into: Soluble KIT ligand (sKITLG)]
Growth/differentiation factor 15 (GDF-15) (Macrophage inhibitory cytokine 1) (MIC-1) (NSAID-activated gene 1 protein) (NAG-1) (NSAID-regulated gene 1 protein) (NRG-1)	Mast/stem cell growth factor receptor kit (SCFR) (EC 2.7.10.1) (Piebald trait protein) (PBT) (Proto-oncogene c-Kit) (Tyrosine-protein kinase KIT) (p145 c-kit)
Glial cell line-derived neurotrophic factor (HGDNF) (Astrocyte-derived trophic factor) (ATF)	Protransofrming growth factor alpha [cleaved into: Transforming growth factor alpha (TGF-alpha) (EGF-like TGF) (ETGF) (TGF type 1)]
Somatotropin (Growth hormone) (GH) (GH-N) (Growth hormone 1) (Pituitary growth hormone)	Transforming growth factor beta-1 (TGF-beta-1) [Cleaved into: Latency-associated peptide (LAP)]
Proheparin-binding EGF-like growth factor [cleaved into: Heparin-binding EGF-like growth factor (HB-EGF) (HBEGF) (Diphtheria toxin receptor) (DT-R)]	Transforming growth factor beta-3 (TGF-beta-3) [Cleaved into: Latency-associated peptide (LAP)]
Hepatocyte growth factor (Hepatopoietin-A) (Scatter factor) (SF) [Cleaved into: Hepatocyte growth factor alpha chain; hepatocyte growth alpha chain; hepatocyte growth factor beta chain]	Vascular endothelial growth factor A (VEGF-A) (Vascular permeability factor) (VPF)
Insulin-like growth factor-binding protein 1 (IBP-1) (IGF-binding protein 1) (IGFBP-1) (placental protein 12) (PP12)	Vascular endothelial growth factor 2 (VEGFR-2) (EC 2.7.10.1) (Fetal liver kinase 1) (FLK-1) (Kinase insert domain receptor) (KDR)
Insulin-like growth factor-binding protein (IBP-2) (IGF-binding protein 2) (IGFBP-2)	Vascular endothelial growth factor receptor 3 (VEGFR-3) (EC 2.7.10.1) (Fms-like tyrosine kinase 4) (FLT-4) (Tyrosine-protein kinase receptor FLT4)
Insulin-like growth factor-binding protein (IBP-3) (IGF-binding protein 3) (IGFBP-3)	Vascular endothelial growth factor D (VEGF-D) (c-Fos-induced growth factor) (FIGF)

.

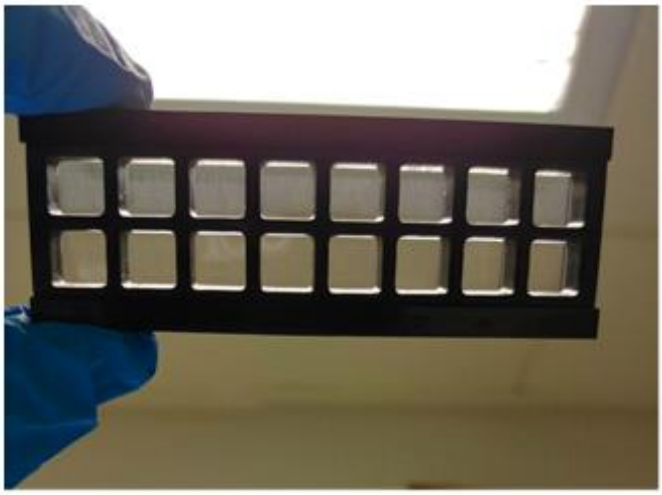

Figure 2.3: Human neurotrophic/ growth factor microarray (QAH-GF-1) slide. A single standard glass is divided to create sixteen wells of duplicate GNF antibody microarrays. Each positive control and antibody is arrayed in quadruplicate. In the slide, there is a detachable gasket with 16 wells which makes it possible to process 16 wells on one slide. With regards to GNF quantification, the array demonstrates the standards of GNF, with concentrations that were defined previously, that are available for the aim of producing a fixed curve of each GNF. Both the standard GNF and the samples are assayed simultaneously, using a sandwich ELISA technique. To determine the concentration of the GNF, the standard curve is compared to the signals of the concentrations that are unknown (Adapted from our research group).

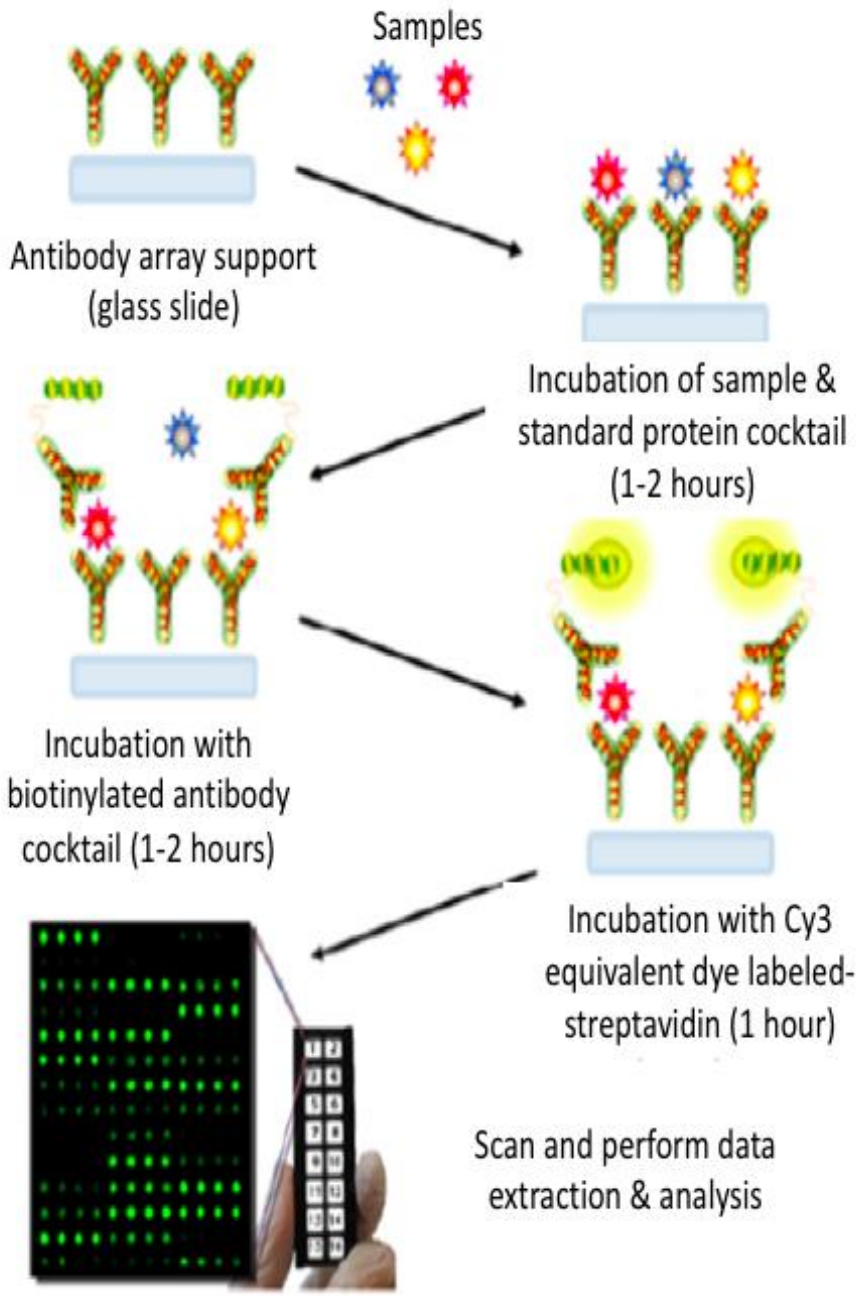

Figure 2.4: An illustration of the process of enumerating the growth/neurotrophic factors in the supernatant of both co-culture models (with AGEs/BSA treatment) using human growth/neurotrophic factor microarray (adapted from Raybiotech, 2016).

The multiplexed sandwich-based ELISA quantitative array platform is similar to the standard ELISA, which is sandwich-based, via the employment of few growth neurotrophic factors (GNF), precise antibodies for exposure. At first, the role of the capture antibody is for binding

to the glass slide. The incubation of the second biotin-labelled detection antibody has the role of helping identify the differing epitope of the same target GNF. The addition of the streptavidin-conjugated Cy3 equivalent dye makes it possible to use a laser scanner to visualise the GNF-antibody-biotin complex.

2.6. Diabetes model, Co-culture procedure: Day 2

Following step 2.1.5, the GM was aspirated after 24 hours of incubation, during which the complete adherence of the SkMCs to the wells and proliferation occurred. In the co-culture model AGE was used as a treatment, DM was used for diluting the AGEs in a concentration of 150 mg/ml, in agreement with studies done in the past (Matou-Nasri et al., 2017; Chiu et al., 2016).

On the other hand, the co-culture model treated with BSA had DM used for diluting BSA at the concentration of 150 mg/ml contingent on the AGE concentrations used in the precise trial. The AGEs was prepared using BSA as the glycation trials' model protein. The protein had been incubated for 72 hours at a temperature of 37^{o}C in methylglyoxal (MG, 0.1 M) in a sodium phosphate buffer (0.1 M, pH 7.4, with 0.1% sodium azide as a bacterial growth inhibitor). The NPCs were later added. From the flask with NPCs, Neural expansion medium (NEM) was extracted. Adding TrypLE™ to the flask was the method of dissociating the NPCs. Then, the solution was centrifuged (following dilution using DPBS) at 21°C for five minutes. The NPCs were then resuspended in NEM after the supernatant was removed. At a density of $2.5x10^4$ cells/ml, the NPCs were then moved into the 6-well plate. Figure 2.5 illustrates the procedure.

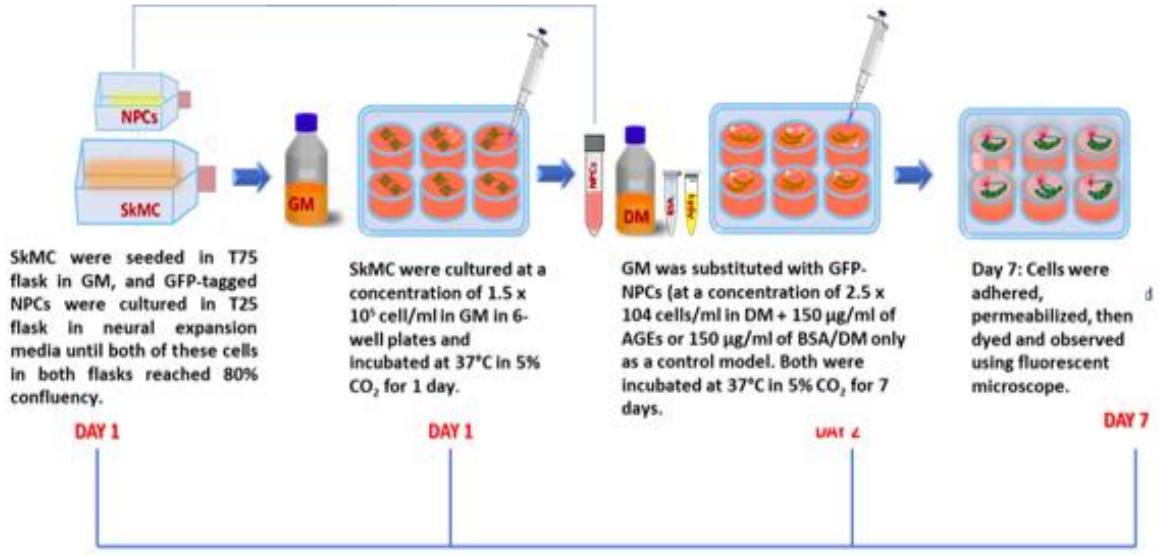

Figure 2.5: Illustration of co-culture muscles and nerves (adapted from our research group).

2.6.1 Procedure for immunofluorescence imaging

After the third and fifth days of co-culture, the cells were made ready for immunofluorescent microscopy (with AGEs and BSA). First, the DM was removed before the DPBS was used for washing the cells two times. Then the cells were fixed with 4% paraformaldehyde. For ten minutes at a temperature of 21°C, the cells were then incubated. Before DPBS was used to wash the cells two more times, the paraformaldehyde was thrown away. This was followed by a permeabilising of the cells for 60 minutes at 21°C using 10% goat serum diluted in distilled water and a 10% perm/wash buffer (from Becton & Dickinson (BD) biosciences) (Oxford, UK). The solvent was thrown away before the cells were washed twice. To the wells, a blocking solution consisting of 0.05% Tween 20 and 3% goat serum, both obtained from Sigma Aldrich (Dorset, UK), diluted in DPBS was added. At the end of the incubation period, the added solution was thrown away, before the cells were washed two more times. The Leica DMI6000 B inverted microscope, manufactured by Leica Microsystems was used for observing the immunofluorescent stains (Milton Keynes, UK).

2.6.2 Procedure for staining co-culture cells

In the co-culture models (with BSA and AGEs), the dying of the actin filaments was accomplished using the Texas Red-X manufactured by Invitrogen (Paisley, UK). At a concentration of 1:200, Phalloidin stain was used. The dying of the nuclear objects was accomplished using Diamidino-2-phenylindole dihydrochloride (DAPI).

2.6.3 Axonal Analysis

Live- cell co-culture was analysed using Leica DMI6000 B inervated microscope (for both control co-culture and AGEs treated co-culture) at 24hours, 48hours, 72hours and 120hours. Co-culture in DM, 150 g/ml BSA and 50 g/ml, 100 g/ml, 150 g/ml of AGEs were analysed were images were obtained at random fields of view at each time point. Images of 20x magnification were exported as JPEG files for ImageJ analysis. In ImageJ, the scale was set as 50 μm = 100 pixels in distance (figure 2.6A.). The length of the axons were measured using the images, the axons extending from the differentiating GFP- tagged-NPCs. The line of measurement started at the axon initial segment (AIS), an area defined as the base of the axon at which action potentials are initiated, the line was measured by hand. The line of measurement continued through the AIS to the tip ends of the terminal as shown in figure 2.6B. The lengths of the axons were recorded in mm for statistical analysis. The number under "length" was recorded as it corresponds to the axonal length in mm (figure 2.6C). Morphological features of cell cultures was analysed using Leica DMI6000 B inverted microscope and the ImageJ image processing software package. Aspect ratio, fusion index and myotube area were measured manually using imageJ, and microscope locator measurement to make sure that same field was not counted more than 1 time.

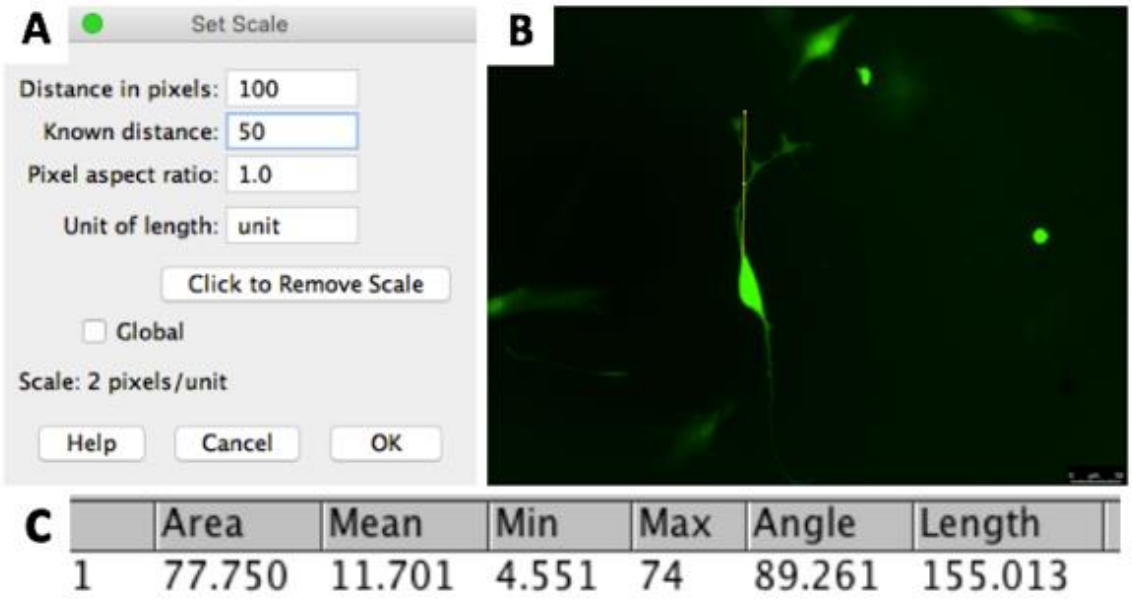

Figure 2.6: The process of measuring axonal length using ImageJ software.

2.7 Statistical Analysis

The results that the outcomes of the experiments in this project present, represent at least three independent experiments. The GraphPad Prism v6.05 statistical analysis software was used for the analysis of the results. Data are expressed as a mean plus/minus standard deviation (± SD). The analysis of statistical variances was tested for parametricity first considering equal variance and normal distribution, one the data was confirmed to be parametric, the analysis of statistical variances was done using the unpaired t-test, one-way ANOVA, split plot ANOVA, MANOVA with Tukey correction for multiple comparison test depending on what was suitable. Bonferroni post hoc pairwise comparisons was also applied were required. Split plot ANOVA was applied when analysing two or three conditions where the conditions/treatments was considered as between elements and time being within element if applicable. Furthermore, repeated measures ANOVA or split plot ANOVA was applied with a series of single measurement was applied when group measurement was analysed. NS (not significant), represents p= >0.05, *represents p=0.05-0.01, **represents p=0.01-0.001, ***represents p=0.001-0.0001 and ****represents p<0.0001.

Chapter 3: Establishment of *in vitro* Neuromuscular Junction between Neural progenitor cells and Immortalised Human Myoblasts.

3.0 Background

3.0.0 Introduction

Despite decades of intensive research to characterise the structure and function of NMJs by utilizing animals and ex vivo models (Wu et al., 2010), effective treatment of neuromuscular and neurodegenerative diseases remains a significant unmet clinical need. This is mainly due to the failure of experimental animal models to reflect complex processes of human aging and disease progression (van der Worp et al., 2010). In order to advance this field, novel, alternative, experimental models are needed. There has been recent progress toward the development of *in vitro* co-culture models using human induced pluripotent stem cells (iPSCs); (Thomson et al., 2012; Berry et al., 2015) mouse, (Umbach et al., 2012) rat, (Smith et al., 2013) and human primary myoblasts; (Demestre et al., 2015; Guo et al., 2017) and human embryonic stem cells (hESCs) (Guo et al., 2014; Santhanam et al., 2018; Happe et al., 2017) and cross-species models (Arnold et al., 2012; Vilmont et al., 2016). However, existing *in vitro* motor neuron and skeletal muscle co-culture systems typically require a complex neural growth medium that contains serum and cocktails of around 15 neural growth factors (some of which are derived from animals) (Guo et al., 2017; Guo et al., 2014; Guo et al., 2011). This further complicates drug discovery and toxicology studies due to possible cross-communication of the novel compound with factors contained within the added media, possibly explaining why many promising therapies do not translate to clinics. Another issue with existing models is that muscle contraction is induced by applied electrical or chemical

stimulation, which does not replicate the native physiological stimulation required for muscle contractions (Umbach et al., 2012; Guo et al., 2011; Miles et al., 2004; Guo et al., 2010). Recent innovation in the use of iPSCs offers the potential to derive myoblasts and motor neurons for use with *in vitro* NMJ models. However, cells derived from iPSCs may exhibit genetic inconsistency and genetic modification, which limit their use (Chin et al., 2009). Recent human iPSC-based studies have failed to recapitulate the severe neuronal loss observed in human neurodegenerative diseases (Chung et al., 2013; Kondo et al., 2013; Sareen et al., 2013). Human skeletal myoblasts which were used in some of the abovementioned models (Demestre et al., 2015; Guo et al., 2017) were obtained from primary cells (eg, muscle biopsy or surgical samples), but their life span is limited to just a few passages which restricts experimentation and necessitates repeated supply of the primary cells (Mouly et al., 2005; Webster and Blau., 1990). Furthermore, primary cells have varied cell purity (Kaur and Dufour., 2012) and experience phenotypic changes when expanded, rendering primary myoblasts a problematic choice for a consistently reproducible co-culture system (Mouly et al., 2005; Webster and Blau., 1990). Therefore, there is a clear need for a more relevant human experimental model to study motor units and NMJs to overcome the limitations of existing models.

With the aim of addressing this challenge some nerve-muscle co-culture models produced from primary human myoblasts, rat, mice, cells from hiPSCs, and cross-species systems have been established (Arnold et al., 2012; Demestre et al., 2015; Guo et al., 2014; Harper et al., 2004; Umbach et al., 2012). These types of co-culture models have the disadvantage of lacking when it comes to experimental reproducibility. This is because of the complicated character of the culture framework which calls for a range of neurotrophic and growth factors.

3.0.1 Aims

The aim of this study was to establish a novel functional human NMJs platform, which is serum and neural complex media/neural growth factor-free, using human immortalized myoblasts and human embryonic stem cells (hESCs)- NPCs that can be used to understand the mechanisms of NMJ development and degeneration.

3.1 Results

3.1.0 Confirmation of neural induction of hES- Shef 3 cells

To introduce differentiation of neural cells, human embryonic stem cells (hESc) were exposed to specific protocol (Fitzpatrick et al., 2018) to limit exogenous growth factors to achieve default neurectoderm differentiation. Figure 3.0 demonstrates the neural specification procedure. At day 0 hES cells were maintained on feeder free or MEFs. Following 6 days in neural specification medium with high concentration of FGF2 (20ng/ml), clusters shaped neuro epithelial cells (NECs) were formed within 24hr, the cluster- like shape become larger over time. NECs were cultured on pre-coated laminin dishes on day 6. Aggregates and outgrowth were observed after 24 hr. After 48 to 72 hr small clusters within adherent aggregates were observed with neural rosette shape as illustrated in figure 3.1A. All cells did not form rosettes however, as there was a high rate of rosettes observed, using a 21 gauge needle the rosettes were manually isolated under a dissecting microscope (Figure 3.1B). Pre-coated laminin dishes were used to culture isolated rosettes, neural stem cells (NSCs) in neural expansion medium (NEM) containing B27 (Figure 3.2A), cells were grow to 90-95% confluence. Figure 3.2A, 3.2B and 3.2C show cultured NSC on day 0, day 3 and day 7. Cells were neural progenitors cells (NPCs) after culture in NEM for several passages (figure 3.3A and 3.3B). Within 4 weeks of mature conditions, NPCs had the ability to terminally differentiate. To encourage terminal differentiation, low density of cells was placed on a thin

Matrigel layer with 1% horse serum replaced by FGF2. During early maturation (day 8), terminal differentiation neurons were distinguished morphologically as formation of axonal process was observed and cell bodies bundles were present at day 13 indicating formation of the neuronal network.

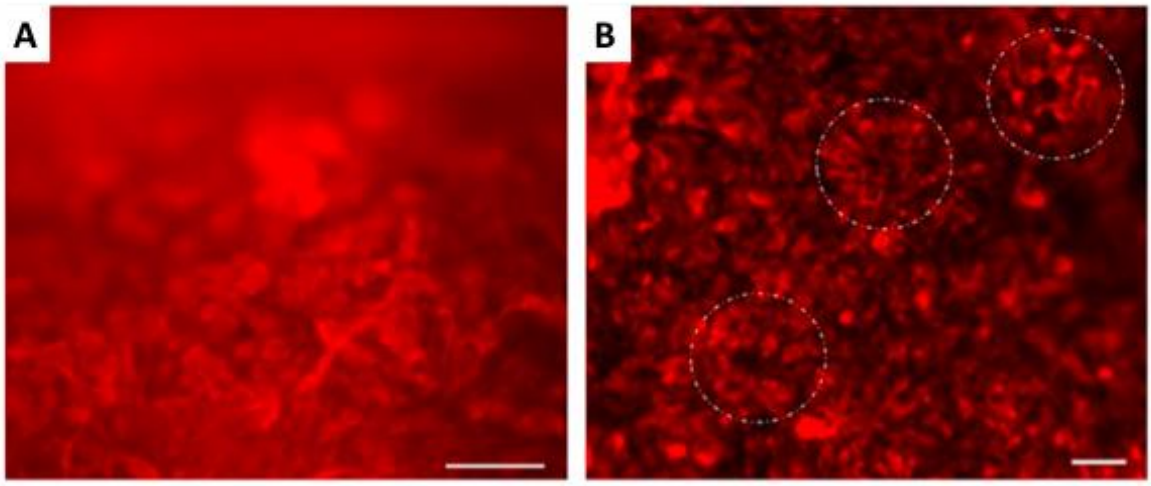

Figure 3.1 Neural differentiation of hESCs. Identification of NPCs from hESCs using nestin red colour as a specific neural differentiation marker. Day 7-10 of neuroepithelial rosettes shaped cells, plated on pre-coated laminin dishes. (**A**) NECs. (**B**) NRPCs (Neuroepithelial rosettes formation coated laminin plates). Scale bars are 100 µM.

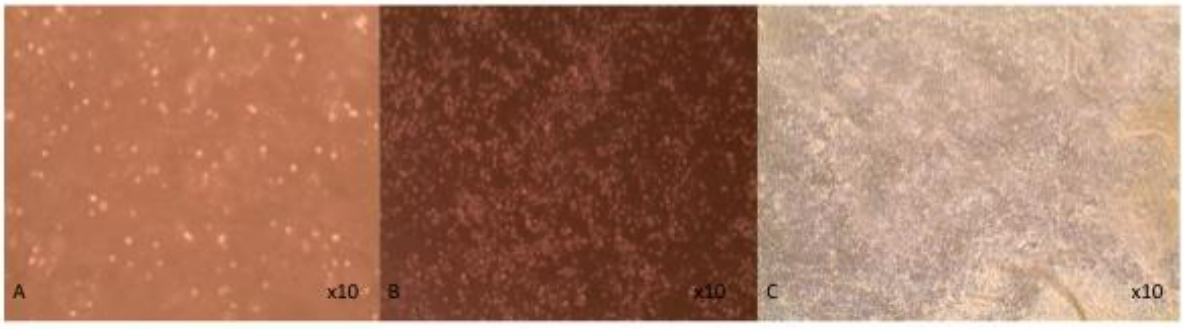

Figure 3.2 Neural Stem cells progression. Neural stem cells were observed at a magnification of x10 (EVOS microscope) (A) NSCs is suspension, day 0 (B) NSCs on day 3 (C) plated NSCs on day 7.

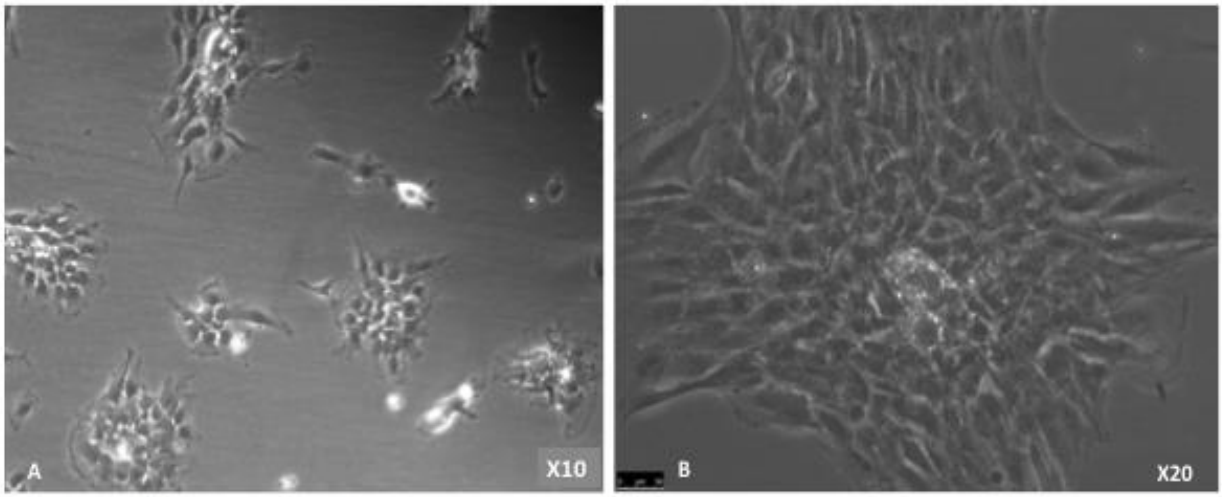

Figure 3.3 Neural progenitor cells progression (NPCs). Neural progenitor cells expanding in suspension in NEM media, NPCs was observed at a magnification of x10 and x20, Microscope Leica DMI6000B live. (A) NPCs is suspension, day 3 (B) plated NPCs on day 10.

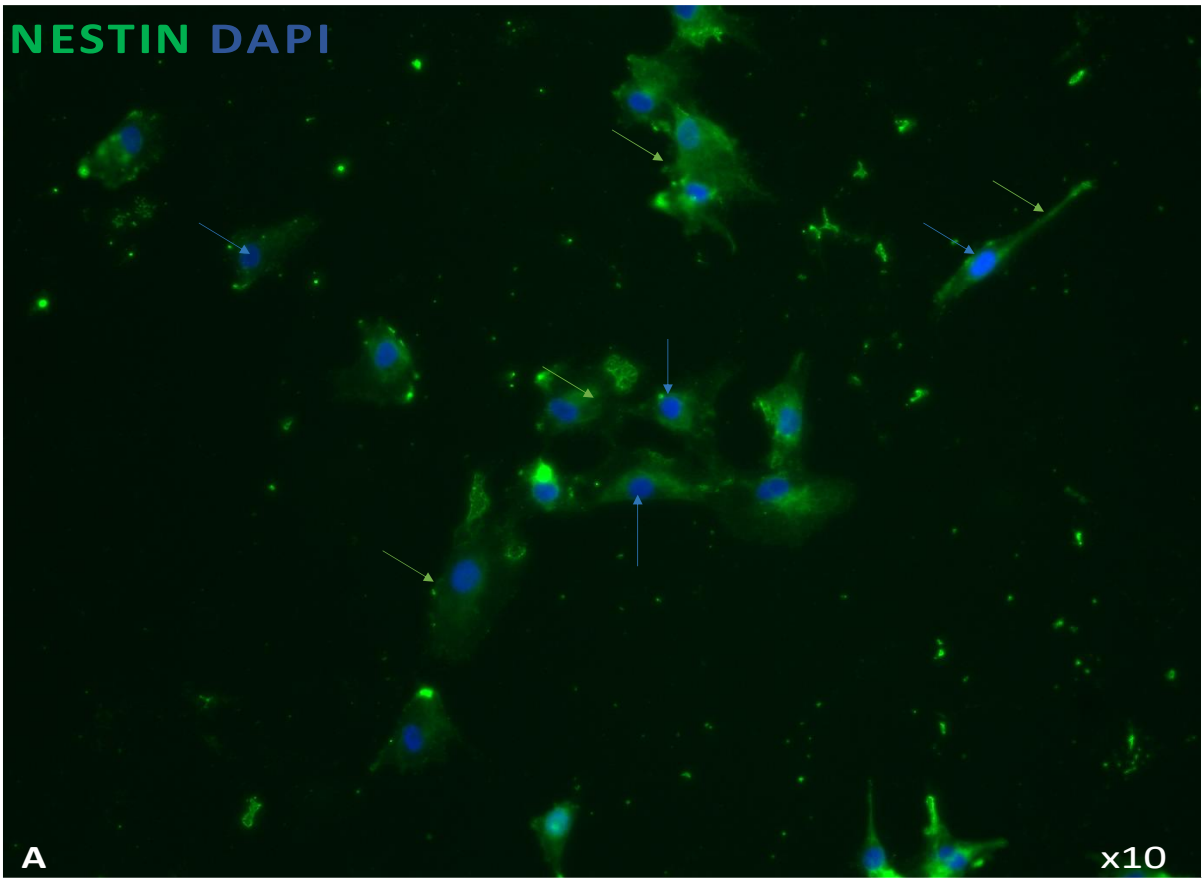

Figure 3.4 NPC marker nestin. (A) NPC stained with Nestin (green arrows) and DAPI (blue arrows) was observed at magnification of x10. Microscope Leica DMI6000B live.

3.1.1 Derivation of NPCs from hESCs and establishment of a functional human NMJ platform

The present work describes a functional human motor unit platform established using immortalised skeletal myoblasts and hESCs-derived NPCs that develop into motor neurons in muscle differentiation media (co-culture media) devoid of any complex neural growth factors or serum. To validate the platform, two monoculture controls were included, one of NPCs and the other of immortalized human myoblasts (Mamchaoui et al., 2011) with co-culture media for 7 days. Cultured GFP- transfected NPCs did not show any morphological changes or motor neuron differentiation, but instead they deteriorated and died (Figure 3.5A). The human myoblasts stained with phalloidin-DAPI showed normal morphology and differentiation features with centrally and peripherally located nuclei, but the myotubes did not spontaneously contract (Figure 3.5B).

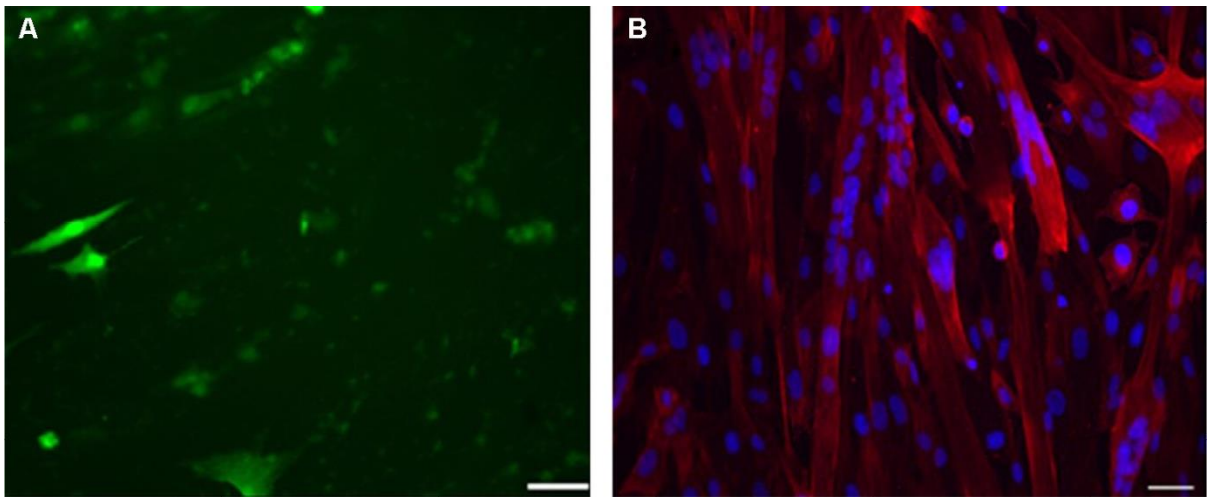

Figure 3.5 Monoculture of NPCs and myoblasts. NPCs and myoblasts were separately cultured for 7 days. The same growth media was used for monocultures and co-cultures. (**A**) A representative image of GFP- transfected NPCs. The NPCs did not exhibit any morphological changes or motor neuron differentiation; instead, they deteriorated and died after 24h. (**B**) A representative image of phalloidin-DAPi-stained human myoblasts showed normal

morphology and differentiation features with centrally and peripherally located nuclei inside the myotubes. Scale bar: 50 µM.

The NPCs were derived from hESCs, as described previously (Fitzpatrick et al., 2018). Neural differentiation of hESCs progressed through three stages of differentiation to NECs (Figure 3.1A) and NRPCs (Figure 3.1B) which were stained with Nestin red colour. To confirm that differentiated NPCs were homogeneous committed neural lineage, cells were stained with DAPI, anti-GFAP (a specific marker for glial cells) and anti-Nestin. Double-positive staining (DAPI blue and Nestin red) confirmed the formation of NPCs while single DAPI staining was not observed, which confirmed that the differentiated cells were NPCs (Figure 3.6A).

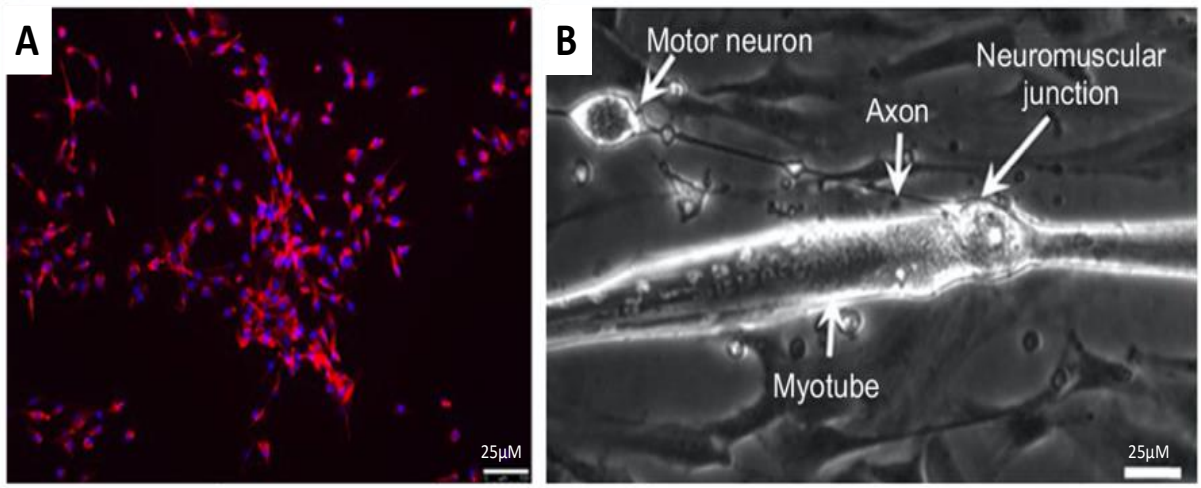

Figure 3.6 Formation of MN and NMJ in co-culture. (A) nestin-red colour for NPCs. Scale bars is 100 µM (B) A representative phase-contrast image of NMJ formation showing an axon extended to contact a myotube. White dotted circle indicates a rosette shape. Scale bars is 25 µM.

3.1.2 Spontaneous Myotube Contractions

Exploration of physiological function motor units is essential for recognising pathophysiological systems of NMJ disorders associated with diseases or age. Therefore, subsequent to SkMC line characterisation, a co-culture structure proficient in NMJ creation and myotube innervations is important to determine. The NPCs were co-cultured with human immortalised myoblasts for 7 days in co-culture media. After myogenic differentiation was initiated, the characteristics of functional motor units began to develop. This included myotube formation and axonal sprouting from the NPCs which subsequently formed NMJs along the myotubes (Figure 3.6B). The myotubes showed spontaneous muscle contractions from approximately day 7 onwards in the absence of any exogenous electrical and chemical stimuli (Video 1). Due to the force of contractions, some myotubes were detached from the culture plate, causing large spaces within the co-culture. Since the myotubes cultured without NPCs did not contract, they did not detach from the culture plate and did not open up large spaces (Figure 3.5B). Implying that the construction of myotubes worked as a single motor unit getting rushes of stimulation from MNs. Nonetheless, numerous innervation points could still be observed in distinct myotubes during this time. Fascinatingly, the myotubes which where contracting were also observed to be taking the morphological features of the three-dimensional tubes, while the aneural myotubes upheld flat two-dimensional morphology, fixed firmly to the surface of the culture plate.

3.1.3 Co-culture with serum vs Co-culture without serum

To determine if the first observable occurrences of myotube contractions (at 72 hours) in the co-culture system were due to neuron-induced morphological changes to myotubes with no effect by serum, the myotube differentiation parameters were measured (figure 3.7) for co-culture with and without fatal bovine serum (FBS). Phase contrast microscopy was utilised to quantify any significant differences in the differentiation of aneurally cultured and co-cultured myoblasts after 72 hours of incubation. Co-culture of SkMCs and NPCs with FBS where observed in (Figure 3.7a). Whereas co-cultured SkMCs and NPCs without FBS (Figure 3.7b) display visually similar myotube differentiation and neural growth similar to co-culture with serum. The fusion index (FI) did not significantly differ between the co-culture with FBS and co-culture without FBS (P= 0.528, Figure 3.7c). Additionally, no difference was detected between the myotube area (MA) of both culture environments (P = 0.455, Figure 3.7d). Finally, myotube hypertrophy was determined by evaluating the aspect ratio (AR). Both culture conditions exhibited no difference in the AR of co-cultured cells with FBS P= 0.749, Figure 3.7e).

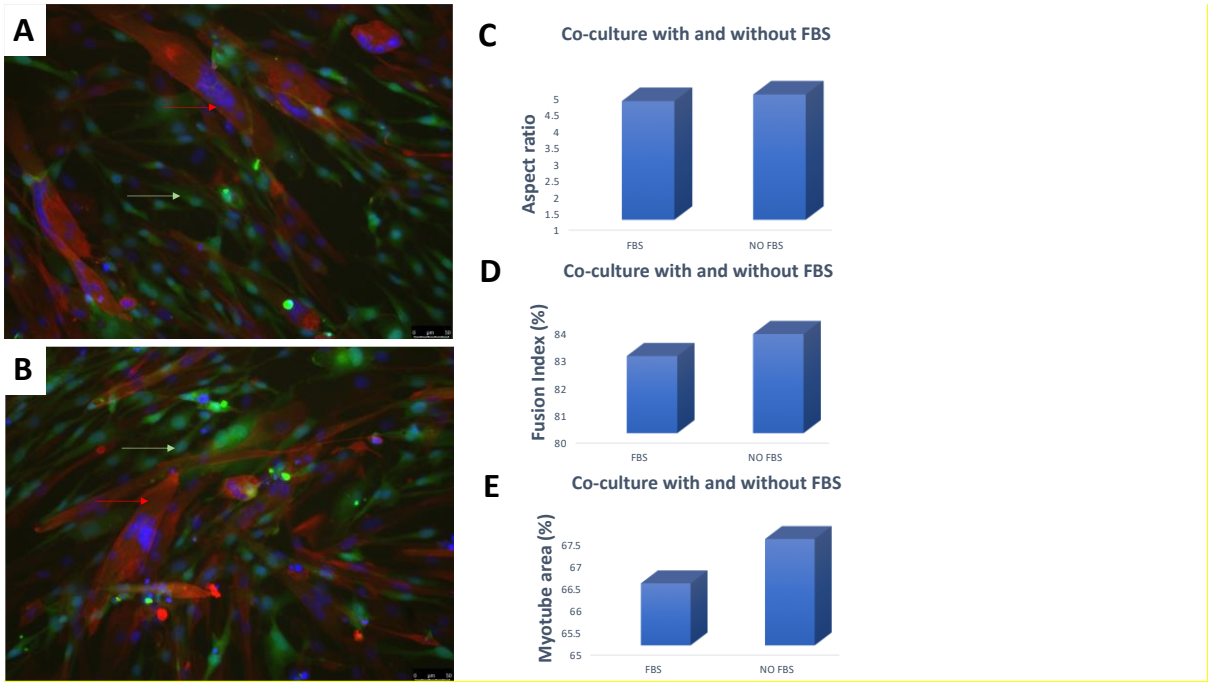

Figure 3.7: Differentiation parameters of co-culture with FBS and without FBS co-cultured with skeletal muscle cells and NPCs at 72 hours. a) The image panel displays cultured C25 with NPCs (marked with GFP) within FBS added to the media; neuronal axons (green arrows) making contact with myotubes (red arrows). b) A representative image of co-culture morphology of C25 and NPCs (marked with GFP); neuronal axons (green arrows) making contact with myotubes (red arrows) with no serum added. Nuclear are stained with DAPI and myotubes are stained with phalloidin. c) Comparison of the percentage of cellular fusion in co-cultured and aneurally-cultured myotubes at 72 hours. d) Comparison of the myotube area in co-cultured and aneurally-cultured myotubes at 72 hours. e) Comparison of the aspect ratio in co-cultured and aneurally-cultured myotubes at 72 hours. Data presented as a mean, error bars signify ± SD. n = 5 independent experiments, entire field was examined. Bar = 75 µm.

3.1.4 Formation of Preliminary Neuromuscular Junction

The findings to the effect that the SCEs, when cultured alone and in the co-culture system, secreted agrin, shows that the co-culture system had the compulsory agrin required for NMJ formation and AChR clustering (Tintignac et al., 2015; Wu et al., 2010). Hence, the experiment that followed was done with the aim of determining whether the contractions of the myotubes which were seen in the co-culture system were really driven by the MN stimulation as a result of the formation of NMJ. On the seventh day, ICC of the co-cultures provided verification when it became apparent that myotubes were contracting as a single motor entity. β-III-tubulin was used to stain the co-cultures with the aim of showing the MN. The co-cultures were also stained with α-bungarotoxin (α-BTX), which binds to nicotinic AChRs and shows the clustering of AChR on myotubes. The co-localisation of MNs produced from the SCEs with AChRs on the myotubes was by immunofluorescence microscopy and phase contrast. From the results, it could be concluded that numerous AChR clusters on myotubes that had differentiated combined with MNTs and MN axons (Figure 3.9). Occurrences of AChR and MN co-localisation could be seen in 83.4% ± 12.6 of myotubes, a situation which shows the early development of NMJs in the system of co-culture.

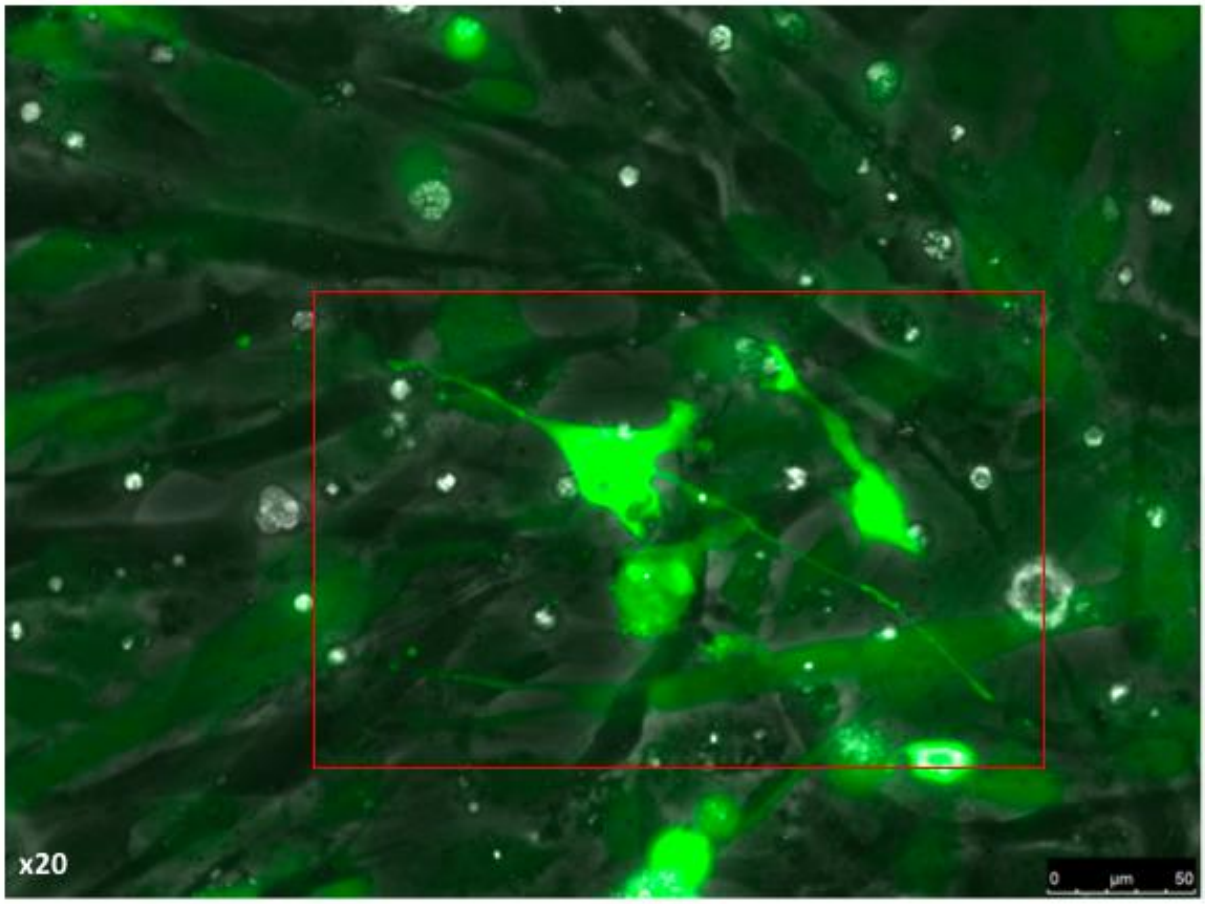

Figure 3.8 Motor neurons formation in co-culture of C25 and NPCs. Formation of motor neuron in co-culture, (red box). NPCs are marked with GFP. Bar = 50 µm.

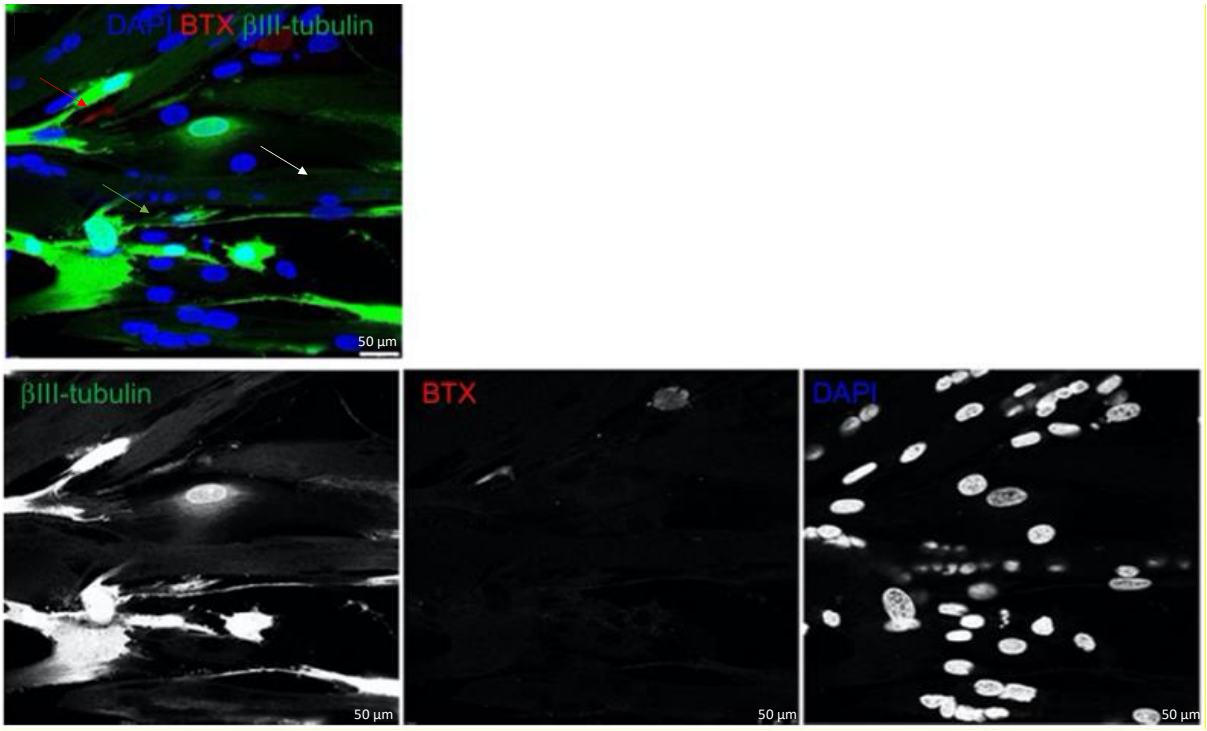

Figure 3.9: Co-localisation of motor neuron axons derived from NPCs with acetylcholine receptor clusters on myotubes at day 7. The panel on the lower left is a phase contrast image of neuronal cells in the co-culture stained for β-III-tubulin (green). The lower middle panel is phase contrast image of differentiated myotubes in the co-culture stained for α-bungarotoxin (α-BTX) (red). The lower right panel is phase contrast image of differentiated myotubes in the co-culture stained for DAPI (blue). The panel on top is a combined immunofluorescence image showing the overlap of NPCs with acetylcholine receptor (AChR) clusters on the myotubes (white arrow). The enlarged inset shows a cluster of AChRs (red arrow) interacting with neuron axons (green arrow). Bar = 50 µm (Abd Al Samid et al., 2018).

3.1.5 Contraction Frequency

To examine the time point the co-culture presented its highest frequency of contraction, the contraction frequency was recorded for the NMJ. Contraction frequency was recorded for the days where contraction was observed which started at day 5 end started to end after day 10 from co-culture. To ensure optimal innervation of co-cultured myotubes, the efficiency of co-culture with FBS and co-culture without FBS to investigate the differences in contraction for

co-culture with and without serum. The co-culture of myoblasts with FBS was compared against serum free media due to serum media being an established alternative for most of the published NMJ co-cultures *(Ferruzza et al., 2012)*. Optimal innervation of myotubes was quantified by analysing contraction frequency every 24 hours post co-culture for 5 days, using live phase contrast microscopy to assess 20 random fields of view at 10X magnification. The results revealed no observable myotube contractions in either serum or serum free co-cultured with myoblast after the first 4 days. Following 6 days of co-culture, initiation of myotube contractions were observable in the co-cultures with FBS, contracting at a frequency of 0.48 Hz. Co-culture with no added serum had a contracting frequency of 0.50 Hz. On day 6, the myotubes in the co-cultures with FBS increased contraction frequency to 0.67 Hz; co-culture with no added serum had a contracting frequency of 0.69 Hz. Day 7 observed most frequency, hence the myotubes in the co-cultures with FBS increased contraction frequency to 0.73 Hz; co-culture with no added serum had a contracting frequency of 0.74 Hz. On day 8, the myotubes in the co-cultures with FBS decreased contraction frequency to 0.74 Hz; co-culture with no added serum had a contracting frequency of 0.75 Hz. On day 9, the myotubes in the co-cultures with FBS decreased contraction frequency to 0.71 Hz; co-culture with no added serum had a contracting frequency of 0.72 Hz. On day 10, the myotubes in the co-cultures with FBS showed contraction frequency of 0.66 Hz; co-culture with no added serum had a contracting frequency of 0.66 Hz. After performing a normalisation test the data showed to be parametric. Thereafter, a split plot ANOVA was performed with a within element being time (days 5-10) and a between element (with vs without serum). In addition, to Bonferroni post hoc pairwise comparisons. There was no significant differences between the co-cultured cells in media with and without serum hence P-value was less than 0.05. However, better contraction frequency was observed in co-culture with no FBS as observed

in figure 3.10. After confirming co-cultured without serum are more efficient than co-culture with serum inducing myotube contractions, subsequent co-culture experiments where conducted without serum.

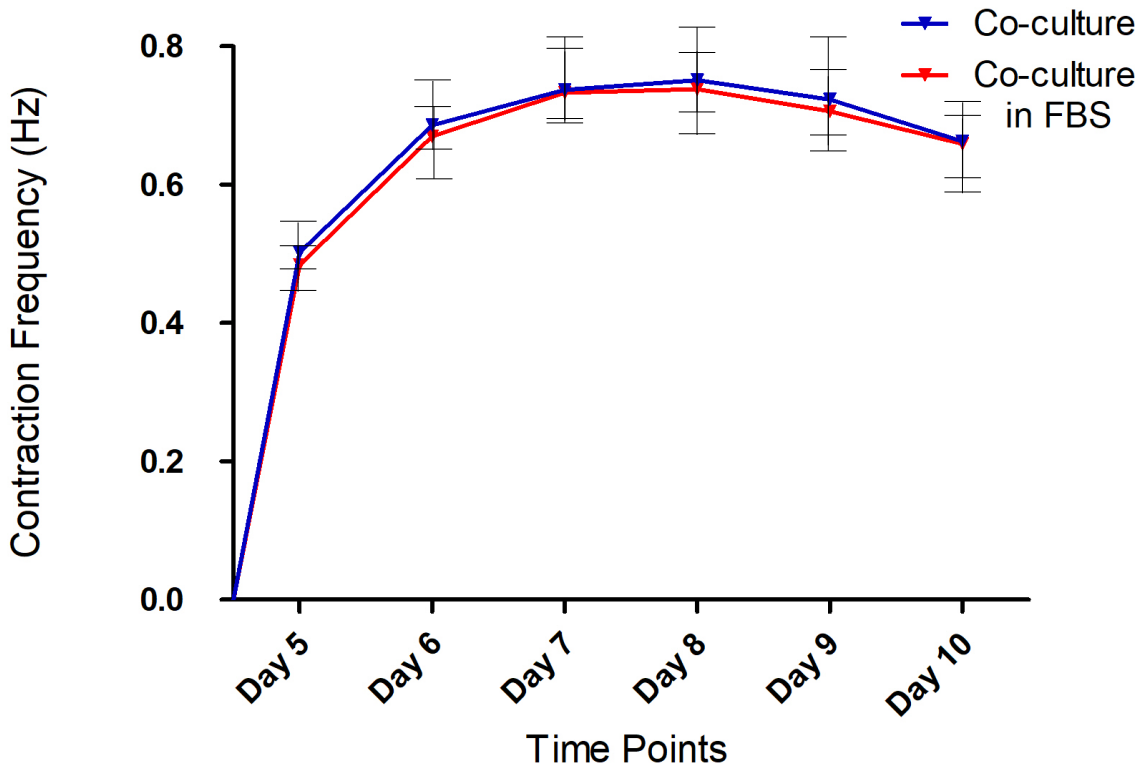

Figure 3.10: Contraction frequency in myotubes co-cultured with NPCs over 7 days. A line graph comparing the onset of myotube contractions and contraction frequency in young immortalised human myoblasts co-cultured with NPCs. Data presented as a mean, error bars signify ± SD. $P<0.05$, n = 10 independent experiments.

3.2 Discussion

Exploration of physiological function motor units is essential for recognising pathophysiological systems of NMJ disorders associated with diseases or age. Therefore, subsequent to SkMC line characterization, a co-culture structure proficient in NMJ creation and myotube innervations is important to establish. As far as we know, this structure is new as it produces NMJs *in vitro* by means of the employment of explants of human neural cells

and immortalised skeletal muscle cells from humans. This specially created model permits the scrutiny of NMJ creation as well as growth systems, in addition to offering the foundations for scrutiny of differentiation of innervated myotubes, which more precisely mirrors *in vivo* circumstances in contrast to aneural myotube differentiation research (Zhang et al., 2015). Animal models can represent parts of physiological changes in a human disease *(Mak et al., 2014)* however, *In vitro* human cell and tissue cultures are more relevant to humans with higher significantly, faster and more cost effective in comparison to animal cell and tissue cultures.

This study's findings provide details of the functional formation of a new minimalist *in vitro* nerve-muscle co-culture system that does not contain growth/neurotrophic factors and serum. The system facilitated the continued existence of the SCEs in simplified DM, boosted neuronal axons proliferation, produced contractile myotubes, and showed several occurrences of co-localisation between neuronal axons with AChRs, providing proof that there NMJ was developing. The innervation of C25 with NPCs was used to create the co-culture model. There are certain benefits delivered by this co-culture model, beyond the standard myoblast monocultures as an implement of research for the investigation of muscle wasting and MN diseases. For instance, human myotubes cultured in aneural did not contract in culture. Nonetheless, as was observed *in vivo*, this co-culture system's innervated myotubes showed endogenously stimulated contractile functionality (Feher, 2017).

Research has been done on human-nerve/muscle co-cultures discharged proteins for the treatment of human myotubes that are aneurally cultured. The result was an increase in clustering of AChR, primarily as a result of exposure to agrin (Arnold et al., 2004; Bandi et al., 2008). On the other hand, the use of protein obtained from co-cultures did not lead to any contractile function. What can be inferred from such a finding is that neuronal cell-secreted

factors like agrin, do not have the independent capability to prompt myotube contraction *in vivo*. Fascinatingly, the co-culture model which this study deals with showed the contraction of myotubes within 5 days of co-culture. This could easily be the first time contractile functionality has been noted at this stage of any nerve-muscle co-culture system's development. Hence this model shows potential to be used in clinical field. A finding such as this one implies that the de novo formation of NMJ could be as a result of the need by myotubes of MNs' nervous input to prompt contraction (Hong & Etherington, 2011). Added to the advantage which comes from the fact that this co-culture model is more comparable, physiologically, *in vivo* settings of SKM development than myotubes cultured in aneural, the system was also designed in a way that reproducibility would be easier. The media used to differentiate the NMJ did not have any neurotrophic factors, serum, and growth factors. This was the first model to produce contractile innervated myotubes through this streamlined culture media configuration, producing a radical decrease in experimental variability possible. In contrast, nerve-muscle culture system previously developed required the employment of serum or trophic factors to prompt the innervation of myotubes, formation of NMJ, and instinctive contraction of myotubes (Das et al., 2010; Guo et al., 2011; Demestre et al., 2015; Rumsey et al., 2010). Notably, the possible ease of reproducibility and experimental variability delivered by this simplified co-culture model is apparent when the culture media construction employed in the development of the co-culture model is compared with some of the leading modern substitute nerve-muscle co-culture systems that still need intricate tropical factors for them to successfully create their own system (Guo et al., 2017).

Consequently, this co-culture model delivers the epitome environment for high-throughput study of the contrivances accredited for the creation and growth of NMJs and the sophisticated contractile myotube differentiation. The techniques employed across this study

are intended to reduce the time needed to prompt discernible spontaneous contraction of myotubes and yield a profusion of functional NMJs. NPCs was established from embryonic stem cells making it possible to culture millions of NPCs which made it possible for a huge array of time points and experimental conditions to be accessed. The individual myotubes, in this co-culture model, started to contract on the fifth day. The cells that had contracted continued increasing contraction frequency could be observed by the seventh day (Video 1). Co-culture models that had been previously established involve a complex technique that needs numerous co-culture media constructions for distinct MN or myotube differentiation for a minimum of ten days ahead of co-culturing (Guo et al., 2011). Other research has presented the formation of NMJ in 21 days (Demestre et al., 2015). Such prolonged procedures can result in needless delays and potential accidental disparity in experimental processes.

3.3 Conclusion

It can be concluded that a novel physiological functional co-culture system was designed using motor neurons obtained from the NPCs for the inaugural innervation of C25, leading to the contractile myotubes with a host of possibly functional NMJs. The match to *in vivo* contractility observed in the mature myotubes in this co-culture arrangement advances research competencies into the physiology of SkM, making it possible to attain better pathophysiological interpretation, diagnosis, and cure. The simplified serum and trophic factor free culture media applied in this co-culture media make it possible to accurately manipulate the variability of the system, a situation that could result in better understanding of the formation and development of NMJ. This co-culture model makes available an appropriate method for high-throughput examination of human muscle physiology, NM pathology, and NMJ-linked disease such as diabetes.

Chapter 4: Characterisation *of in vitro* neuromuscular junctions between immortalised human myoblasts and hESCs-derived-NPCs

4.0 Background

The last chapter presented an outline of how a novel nerve-muscle co-culture system free from serum and trophic factors is established. Serum free media was able to prompt differentiated myotubes into contractile activity and show co-localisation within acetylcholine receptor (AChR), implying that neuromuscular junctions (NMJs) have been formed. The NMJ can be described as an extremely specialised outlying synapse regulating the contraction of skeletal muscle cells (SKM). It accomplishes this by facilitating the connection between SkMCs and lower motor neurons.

The NMJ, which is formed *in vivo* in the stage of prenatal development, comprises a post-synaptic motor endplate (MEP), synaptic cleft, and presynaptic motor neuron terminal (MNT). For numerous neurodegenerative (ND) and neuromuscular (NM) diseases, the target of the pathology is either the post-synaptic or presynaptic integrity of the NMJ, resulting in the deterioration of the SkM (Punga and Ruegg, 2012). Another impact of ageing is the weakening of the MEP's AChRs, which could trigger denervation and succeeding age-related muscle dysfunction and loss (Gonzalez-Freire et al., 2014). Therefore, the SkMCs' innervation is needed for the applicable SkM growth and functioning.

Studies have illustrated that there is myotube degeneration when there is no innervation of SkMCs during the development of the embryo (Ashby et al., 1993). In addition, when innervation is absent, evidence shows myotube size reduction and severe deficit in the development of secondary myotube (Condon et al., 1990; Wilson & Harris, 1993). Results from these studies deliver proof of the vital role that NMJs and motor neurons (MNs) play in the regulation of the development, maturation, and size of SKM fibre. To explore the

formation of NMJs and innervated myotubes' physiological development, fewer *in vitro* models are cultured in MNs that contain SkMCs in an attempt to repeat the formation of NMJ (Das et al., 2007; Das et al., 2010). Other models use stem cell or primarily derived myoblasts (Chipman et al., 2014; Demestre et al., 2015; Puttonen et al., 2015). Furthermore, the potential is presented by the establishment of more novel human induced pluripotent stem cell (hiPSC) NMJ models, for MN disease modelling which is specific to distinct patients or specialised drug screening (Inoue et al., 2014; Faravelli et al., 2014).

There are also possibilities presented by hiPSCs with regards to NMJ maturation and differentiation and development of SkMCs and MNs in these types of models (Siller et al., (2013). In addition, a number of these systems which have been previously established deliver proof of the development of NMJ. They do this through AChR clusters and neuronal axons co-localisation even when there is no confirmation or analysis of crucial factors in MNs required for transmission at the NMJ. For example, the vesicular acetylcholine transporter (VAChT) and choline acetyltransferase (ChAT) is needed for the transmission and synthesis of ACh in MNs, delivering the required neurotransmitter for discharge into the synaptic divide (Maeda et al., 2004; Brandon et al., 2003).

Presynaptic MNT activity can also be observed through analysing the synaptic vesicle proteins like Synaptotagmin 1 (Syt1). This example of protein is a Ca^{2+} sensor that prompts blending of the MNT membrane and the vesicles that contain acetylcholine (ACh) (Yu et al., 2013; Brose et al., 1992). NMJ models that are previously developed *in vitro* also generally ignore the innervated myotubes characteristics for advanced differentiation markers. These types of markers include the development of striated myotubes, and nuclei located in the periphery. Furthermore, post-synaptic apparatus structures beyond AChRs have seldom been described in detail. For instance, the post-synaptic elements prompted by agrins like the 43 kDa

receptor-associated protein of the synapse (Rapsyn) and muscle-specific tyrosine kinase (MuSK) are crucial. Therefore, this study's experiments were done with NPC co-cultures innervating immortalised human myoblasts (C25) aged 25 years to investigate the NMJ formation and explore the innervated myotubes' advanced innervation.

4.0.1 Aims

The present study's aim is to fully characterise the developed NMJ model in the previous chapter.. Consequently, the objectives are as follows.

(i) Determine the best timing for the characterisation of co-culture.

(ii) Characterise the NMJs formed in the co-culture system's pre- and post-synaptic elements.

(iii) Investigate innervated myotubes maturation for advanced differentiation markers.

4.1 Results

4.1.0 Determine the optimal time for co-cultures characterisation

To make sure the best innervation, formation of NMJ, and advanced differentiation of myotubes had taken place ahead of characterising of the co-cultured cells, the highest contraction frequency (CF) of the myotubes that were co-cultured was employed as a gauge of the vitality of co-culture. High contraction frequency shows that the NMJ formed are working frequently and mimic to human muscle contraction. The best co-culture characterisation conditions were determined through quantifying CF after every 24 hours following the co-culture of myotubes. From the results, it could be noted that there were no myotube contractions in the myotubes that were co-cultured within the initial four days. Five days after the co-culture, it became apparent that the myotube contraction had begun, and

the frequency was 0.30 Hz. Over the following day, it could be observed that the co-cultured myotubes were increasing gradually. On the 7th day, the frequency of myotube contractions went up to 0.73 Hz (Figure 4.0). Until the 8th day, the peak contraction frequency was maintained by the co-cultured myotubes, which was followed by a progressive reduction in innervated myotube contractile activity. Even though the contractile activity continued to be apparent until day 10 when the experiment was terminated, the contraction frequency had become lower. Moreover, contractile activity had become asynchronous. This is the reason why the decision to do the co-culture characterisation on day seven was made.

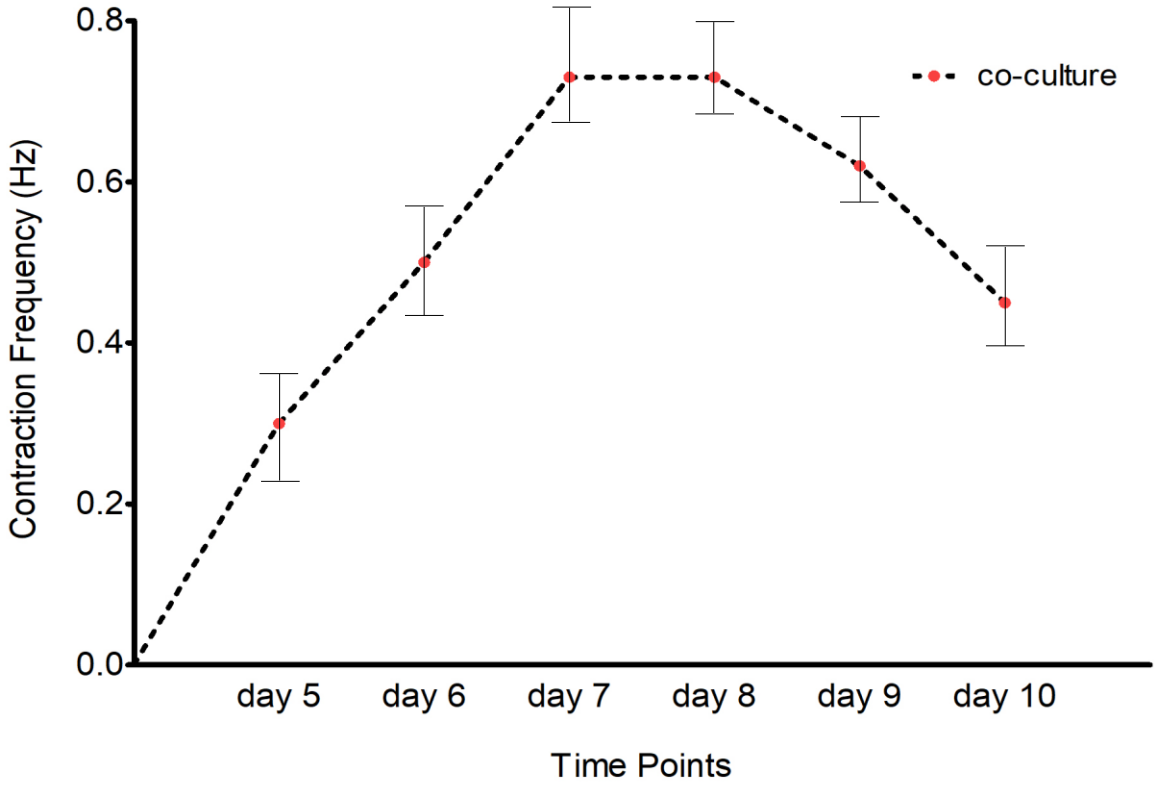

Figure 4.0 Co-cultured myotube contraction activity between the 5th and 10th days. The line graph illustrated the beginning, increase, and decrease of the frequency of myotube contraction in 25-year-old immortalised human myoblasts co-cultured with NPCs. The data is shown as an average with the errors bars standing for ± SD. n = 5 independent experiments.

4.1.1 NMJ formation characterisation

Once the co-localisation between myotubes in the co-culture system validation and characterisation was complete, experiments were done to characterise and confirm the NMJs formation. To show that there is the development of NMJs, there has to be at least one AChRs aggregation on the membrane of the myotube in MN axon terminal apposition. It is on this basis that the execution of ICC on the co-cultures was necessary and the process of staining with MNs for β-III-tubulin was used to determine the axon terminals (Figure 4.1 and 4.2). For further validation of the formation of NMJ, neurofilament heavy (NFH) was used for further staining of MNs (Figure 4.3). The neurofilament is described by Lees et al. (1988) as an intermediary filament located in the neurons' cytoplasm.

The characterisation of the AChRs accumulation on the myotubes was characterised using fluorescently labelled α-bungarotoxin (α-BTX), which has been noted to specifically attach to AChR on the membrane of the myotube (Young et al., (2003). From the results, it could be noted that terminals covering AChR clusters and MN axons gathered on the surface of the myotubes. Analogous to observations *in vivo*, the clusters of AChR in co-culture showed the highest concentrations where there was an overlapping of the clusters of the MN axons and terminals, showing that there was the successful establishment of NMJs.

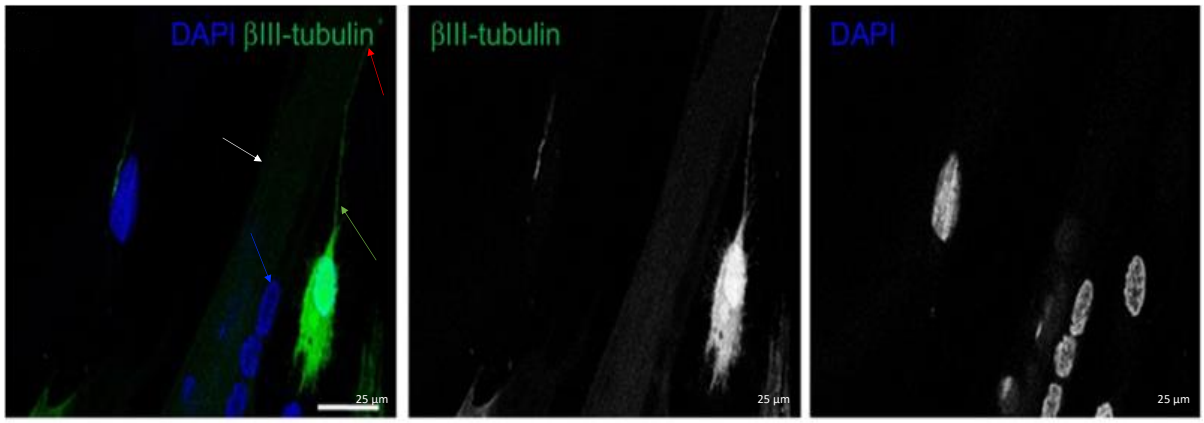

Figure 4.1 Day 7 neuromuscular junction formation characterisation. An image is representing the co-culture stained β-III-tubulin (green) and DAPI (blue). Image shows motor neuron (green arrow), nuclei (blue arrow), myotube (white arrow) and its believed that NMJ is were motor neuron interact with the myotube (red arrow). Scale bar = 25 µm.

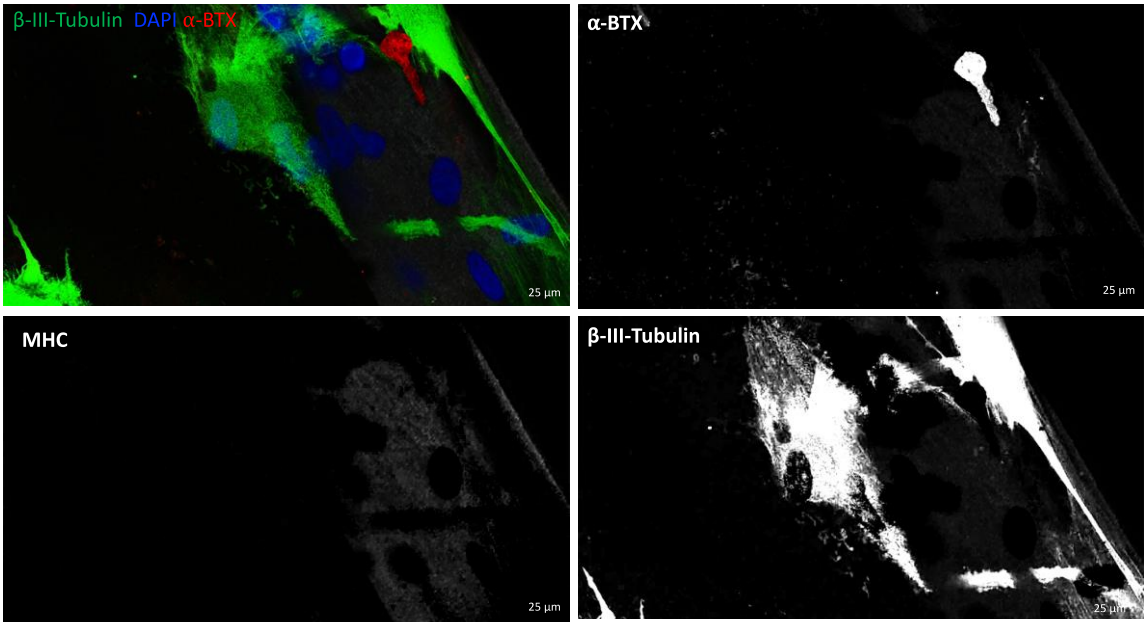

Figure 4.2 Day 7 neuromuscular junction formation characterisation of motor neuron axon. An image is representing the interaction between a single motor neuron axon terminal and a receptor cluster in culture. β-III-tubulin (green), alpha-bungarotoxin (α-BTX) (red), and DAPI (blue) were used for staining the co-cultures. Scale bar= 25 µm.

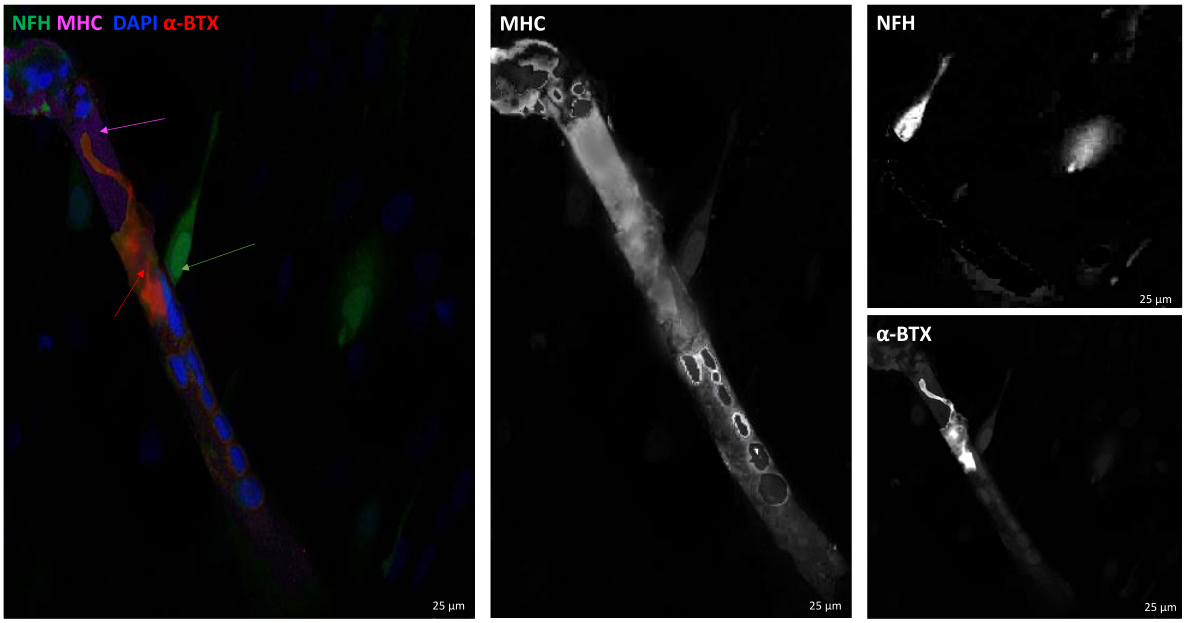

Figure 4.3 Day 7 neuromuscular junction formation confirmation and observation of Ach clusters. The image represents the interaction between motor neuron axons (green arrow) and numerous acetylcholine receptor clusters (red arrow) on a differentiated myotube (purple arrow) in culture. The co-culture were stained for DAPI (blue), neurofilament heavy (NFH) (green), alpha-bungarotoxin (α-BTX) (red), and myosin heavy chain (MHC) (purple). Scale bar = 25 µm.

4.1.2 Presynaptic Characterisation

The use of immunocytochemistry (ICC) methods in the last chapter led to the initial observation that the SCEs had sprouted neurites that clearly conveyed β-III-tubulin (Figure 4.1 and 4.2), showing that there was neuronal cells proliferation in the co-culture system. The proper establishment and development of NMJs are depicted by the cholinergic MNTs with MEPs convergence on SkMCs. Hence, the experiments that follow were done as a way of confirming that neuronal cells sprouting from SCEs actually included cholinergic MNs and as confirmation that there was localisation of SkM myotubes and cholinergic MNs in culture. The achievement of the confirmation of co-localisation was through confocal microscopy-

visualised antibody staining. To show the cholinergic MNs in the co-cultures, a cytoplasmic transferase enzyme available in raised amounts in cholinergic neurons known as ChAT (Oda, 1999) was stained to show cholinergic MNs in the co-cultures (Figure 4.4). The existence of the cholinergic MNs was validated by using VAChT, an mediator of ACh transport and storage by synaptic vesicles (Arvidsson et al., 1997) (Figure 4.5).

The validation of the existence of cholinergic MNs was achieved by the use of additional staining. The ACh storage and transport by synaptic vesicles functional mediator was VAChT (Arvidsson et al., 1997) (Figure 4.5). To indicate differentiation of myotubes, the myotubes were stained for myosin heavy chain (MHC). When the co-cultured cells were stained, it was shown that $VAChT^{+}$ and $ChAT^{+}$ cholinergic MNs, with the termination of axons taking place at differentiated myotubes. It was also noted that exon terminals were creating numerous contact points with individual myotubes, an observation that was also noted in embryonic myogenesis. Splitting axons, originating from various MNs, are the areas where myotube innervation *in vivo* happens. The innervation process's maturation results in axon pruning, a situation that leaves individual MNs to innervate many mature muscle fibres, creating a motor unit that is functional (Low & Cheng, 2006). Outstandingly, in this co-culture model, myotubes also showed numerous innervations (Figure 4.3), analogous to what is noted *in vivo* before the occurrence of axon pruning.

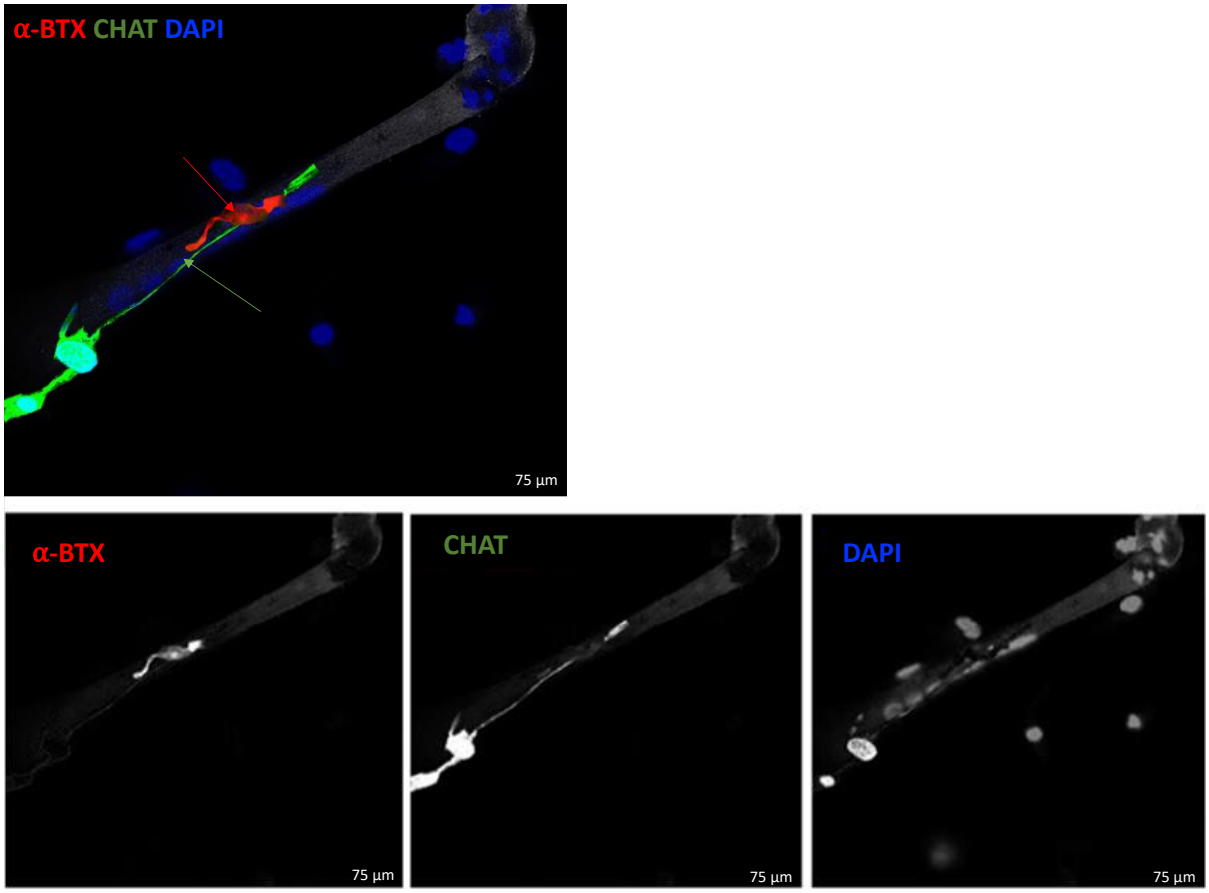

Figure 4.4 Day 7 cholinergic motor neurons co-localisation with myotubes. An image representing the termination of a single cholinergic motor neuron axon (green arrow) terminating above one differentiated myotube. ACh clusters showing NMJ (red arrow). Green shows the co-culture stained for choline acetyltransferase (ChAT), red is α-BTX, blue is DAPI, and grey is myotube. Bar = 75 µm.

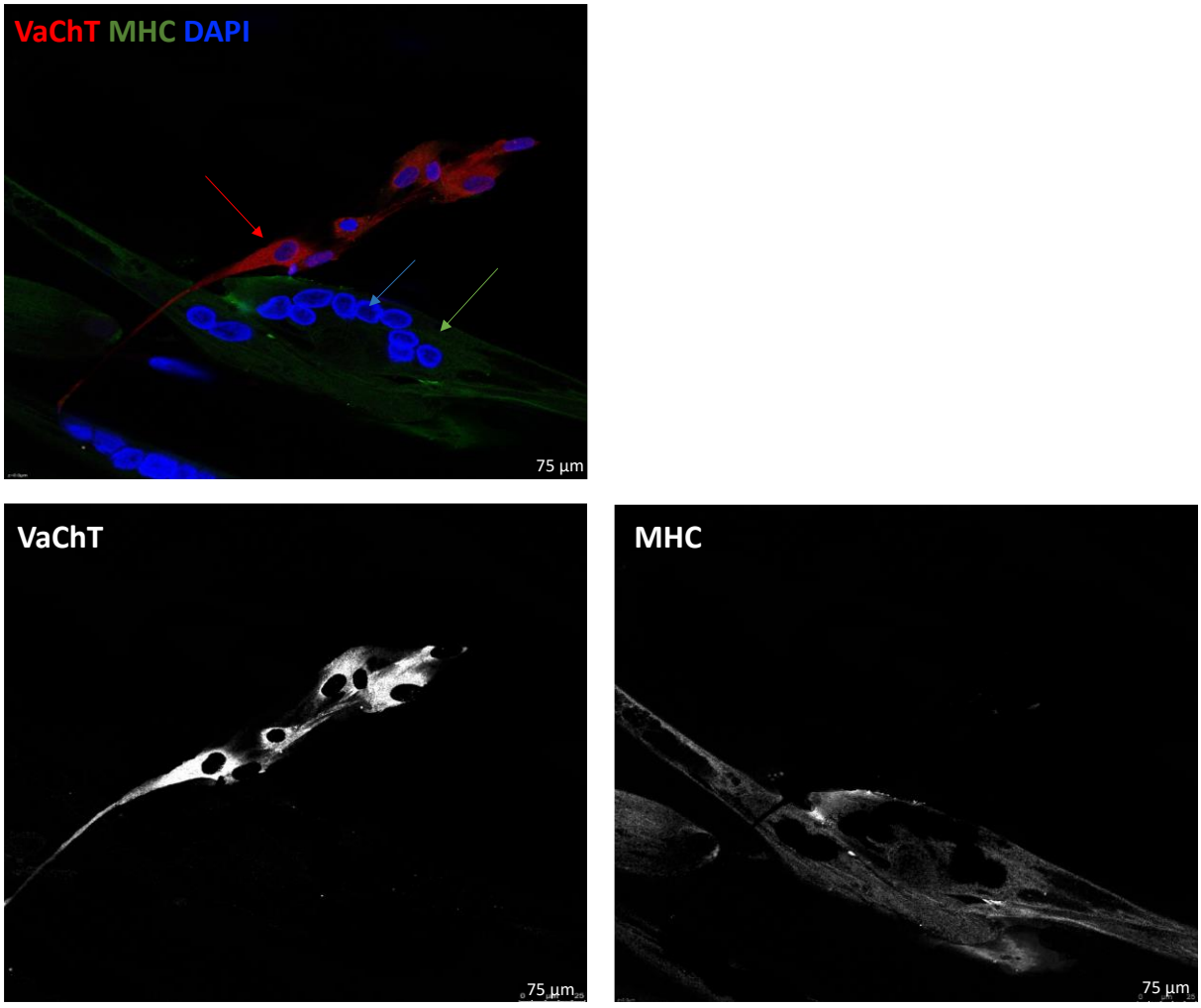

Figure 4.5 Day 7 Validation of co-localising of myotubes and cholinergic motor neurons. The image shows cholinergic motor neuron axons co-localising with differentiated myotube. The co-cultures were stained for vesicular acetylcholine transporter (VAChT) (red arrow), myosin heavy chain (MHC) (green arrow), and DAPI (blue arrow). Bar = 75 µm.

4.1.3 Presynaptic activity characterisation

Once the NMJ formation had been confirmed, later experiments were done with the aim of assessing NMJ functionality via the characterisation and examination of the presynaptic apparatus. The exocytosis, which depends on calcium comprises the exact synaptic vesicles docking to the presynaptic membrane, which is partly controlled by the calcium sensor Syt1 (Brose et al., 1992). For confirming presynaptic NMJ activity, NFH staining was employed for visualising MN axons while terminal activity was indicated by staining MN for Syt1 (Figure

4.6). From the results, it is noted that there is a higher Syt1 collected at the MNT, demonstrating NMJ presynaptic.

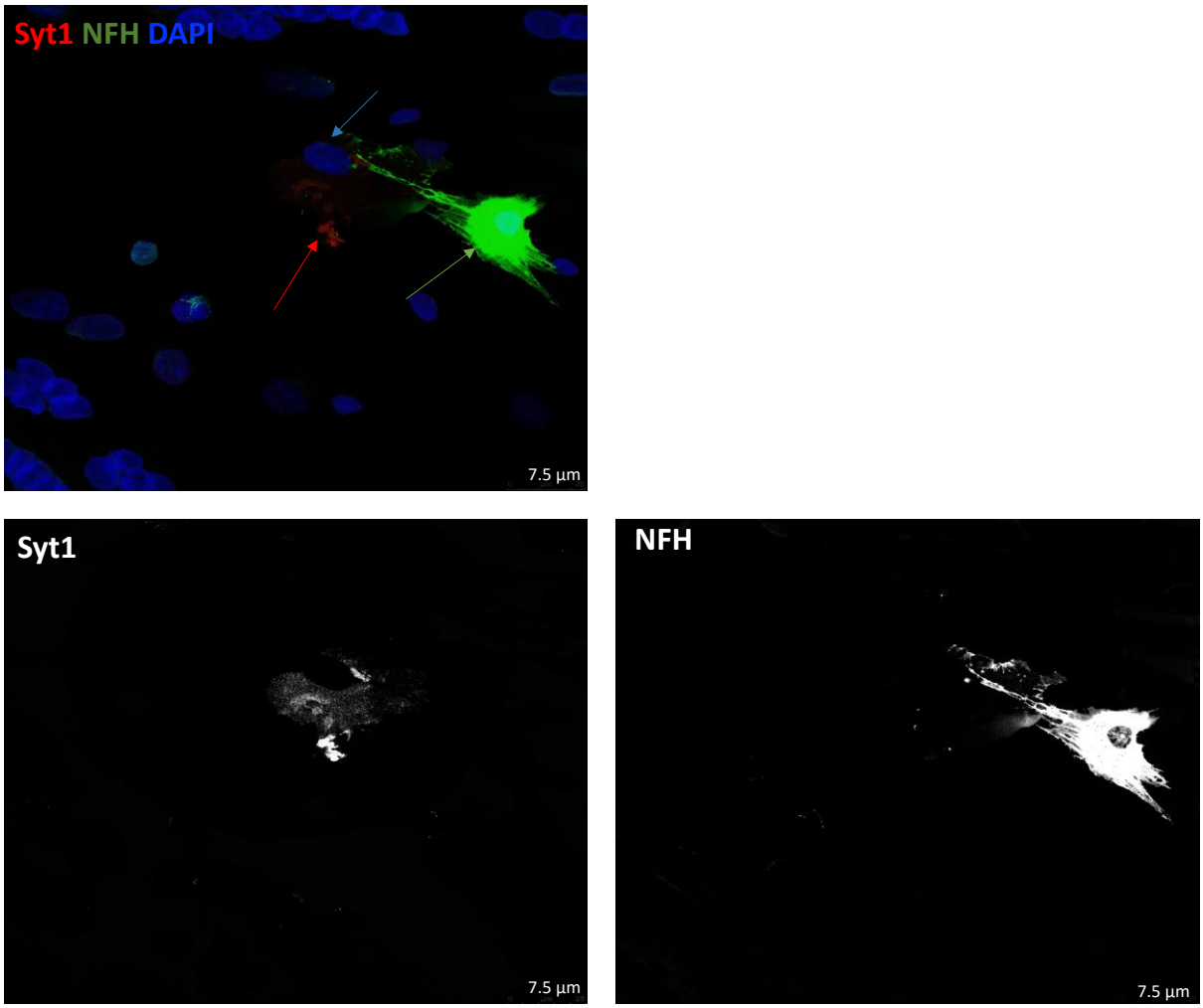

Figure 4.6 Day 7 presynaptic neuromuscular junction activity characterisation. The images show a single neuronal axon expressing activity at the axon terminal. The co-cultures were stained for DAPI (blue arrow), Synaptotagmin 1 (Syt1) (red arrow), and neurofilament heavy (NFH) (green arrow). Bar = 7.5 µm.

4.1.4 Post-synaptic elements characterisation

Once MNT was confirmed in co-cultured cells, the experiments that followed were done with the aim of identifying post-synaptic proteins recognised for co-localising with AChRs at the MEP. The clustering of AChR in the MEP depends on agrin, which is crucial for specific NMJ formation. When MNs presynaptically discharge agrin, the result is the initiation and growth

of MuSK, which creates a preliminary scaffold for Rapsyn to facilitate other post-synaptic MEP elements recruitment (Apel et al., 1997; Apel et al., 1995). To validate that there were maturation and proper MEP development, α-BTX was used to stain the co-culture to show AChRs together with Rapsyn and MuSK antibodies. From the result, it could be seen that both MuSK and Rapsyn were specifically covering the AChR clusters structure on the post-synaptic membrane (Figure 4.7).

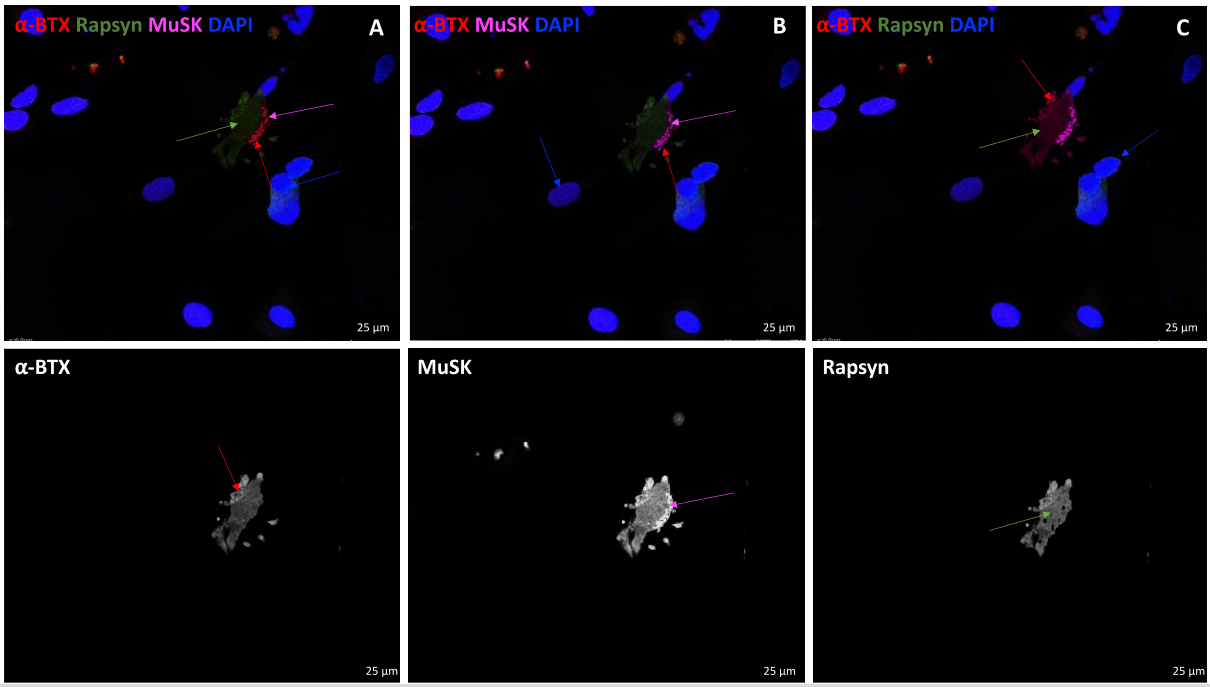

Figure 4.7 Day 7 post-synaptic neuromuscular junction formation. (a) The image shows detailed conformation and interaction of Rapsyn (green arrow) and post-synaptic proteins MuSK (magenta) at the AChR stained with α-BTX (red arrow), DAPI (blue arrow). (b) Image shows co-culture stained for DAPI (blue arrow), MuSK (magenta), and alpha-bungarotoxin (α-BTX) (red arrow). (c) The image represents co-culture stained for Rapsyn (green arrow), alpha-bungarotoxin (α-BTX) (red arrow), and DAPI (blue arrow). Scale bar = 25 µm.

4.1.5 Innervated **myotubes** characterisation

There are several features displayed by myotubes *in vivo*, which could be seen as evidence of differentiation. For example, when myotubes are appropriately developed, they feature triad, organised in a transversal way. The structural arrangement of triads identified in myotubes

that have undergone differentiation at an advanced level if moulded on each side by a transverse tubule (T tubule) with a sarcoplasmic reticulum (SR) which is called the terminal cisterna (Marty et al., 1994). To conclude whether the co-culture system permitted innervated myotubes to go through advanced differentiation analogous to the developed myotubes noted *in vivo*, both aneurally cultured and co-cultured myotubes characterisation was done using antibody staining. The identification of T-tubules was achieved through staining for dihydropyridine receptor (DHPR). DHPR is a calcium conduit found in the T-tubule membrane (Rios & Brum, 1987).

Identification of ryanodine receptor (RyR) was also achieved through the use of antibody marking. A comparison of differential co-culture myotubes to aneurally-cultured myotubes was made to determine if there were any variances in the proportions of myotubes showing advanced differentiation indicators. From the results, it could be noted that 32.6% ± 7.4 of innervated myotubes in the co-cultures had developed well and properly structured transversal treads (Figure 4.9). On the other hand, no was shown by the aneural myotubes. Together with the formation acting as a pointer of innervated myotubes developing advanced differentiation, nuclei located in the periphery were also employed for the purpose of showing advanced differentiation features.

For both aneurally cultured and co-cultured myotubes, characterisation was done using antibody staining with DAPI and MHC to determine if there were any variances in the proportion of myotubes with peripheral nuclei (Figure 4.10). In contrast, no peripheral nuclei were presented by the myotubes in the aneural cultures.

The development of striations is another feature of advanced differentiation in myotubes. Thus, the staining of myotubes was done using DAPI and MHC to find out if there were any variances in the proportions of myotubes showing striations on aneural and co-cultured

conditions. From the results, it can be noted that 57.0% ± 7.4 of the myotubes in the co-cultures had membranes with striations. The reduction ($P < 0.0001$) in the proportion of striated myotubes (18.0% ± 4.8) was significant when the aneural cultures were examined (Figure 4.11). Comparing the width of myotubes between co-cultured myotubes showing advanced differentiation features and myotubes cultured aneurally showed the innervation and the advanced differentiation that followed allowed for thicker myotubes to be formed. The myotubes with advanced differentiation's width were 20.0 µm ± 9.0. On the other hand, the myotubes cultured aneurally were substantially lower at ($P < 0.0001$) 12.0 µm ± 6.1 (Figure 4.8).

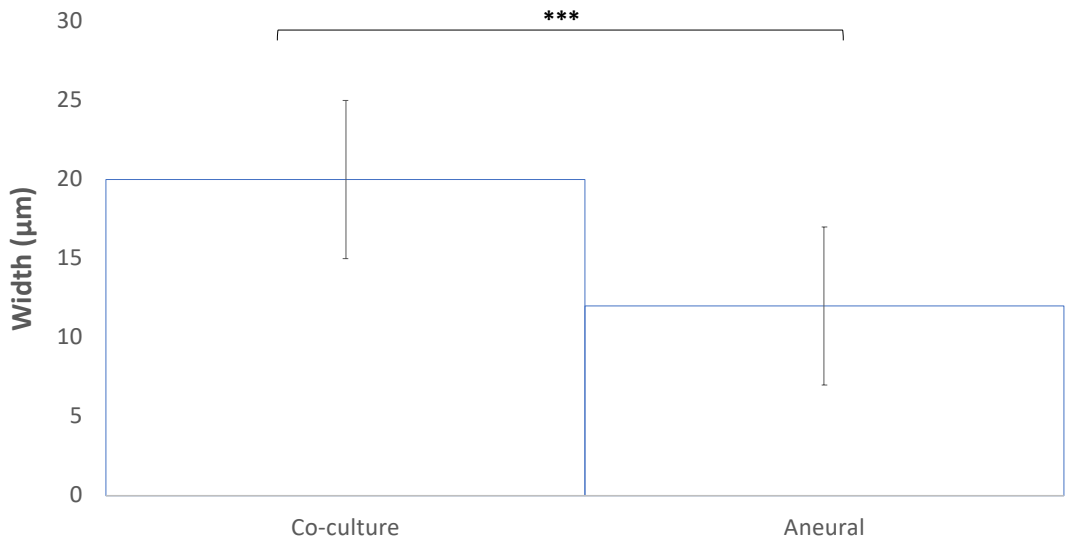

Figure 4.8 Day 7 width of myotubes: The bar graph compares myotube width showing elements of advanced differentiation in conditions of co-culture against myotubes that are aneurally cultured. The presentation of data is done as a mean. The ± SD signifies error bars. *** represents P= 0.001-0.0001. n = 4 independent experiments.

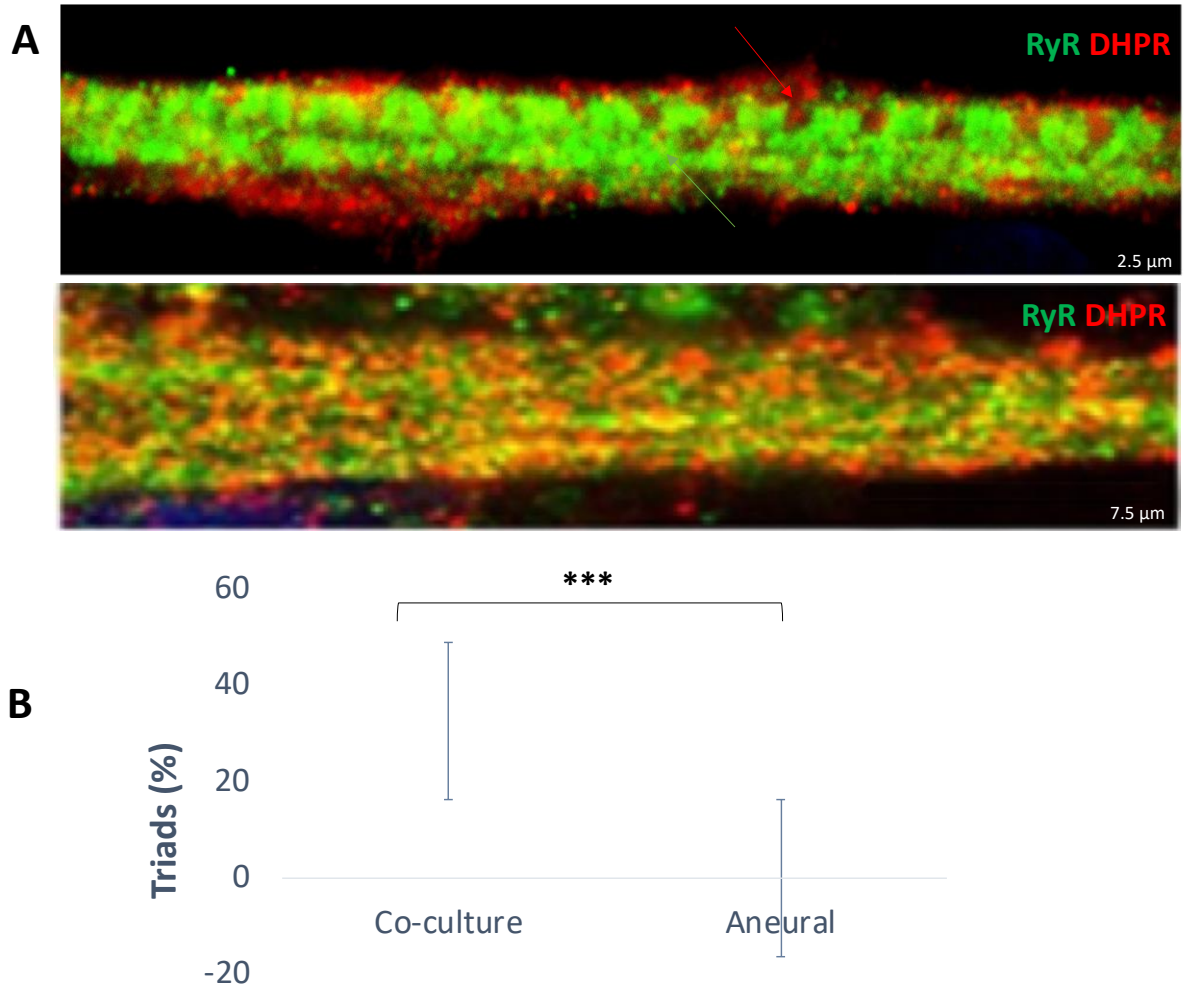

Figure 4.9 Staining of myotube with DHPR and RYR. (a) The image panel on the upper end shows a myotube that is innervated and co-cultured with NPCs explant exhibiting proper organisation of terminal cisterna and transverse tubules. The image panel, which is lower represents myotubes that are cultured aneurally showing a dearth of transversal triad's formation. Myotubes were stained for dihydropyridine receptor (DHPR) (red arrow) and ryanodine receptor (RyR) (green arrow). (b) An image presentation of a bar graph that compares the proportion of myotubes that have triad arrangement in conditions of co-culture and aneural myotube conditions. Data are shown as a mean. The ± SD signifies error bars. n = 4 distinct experiments. *** signifies P= 0.001-0.0001. Scale bars for the first image: 2.5 µm and scale bars for the second image: 7.5 µm.

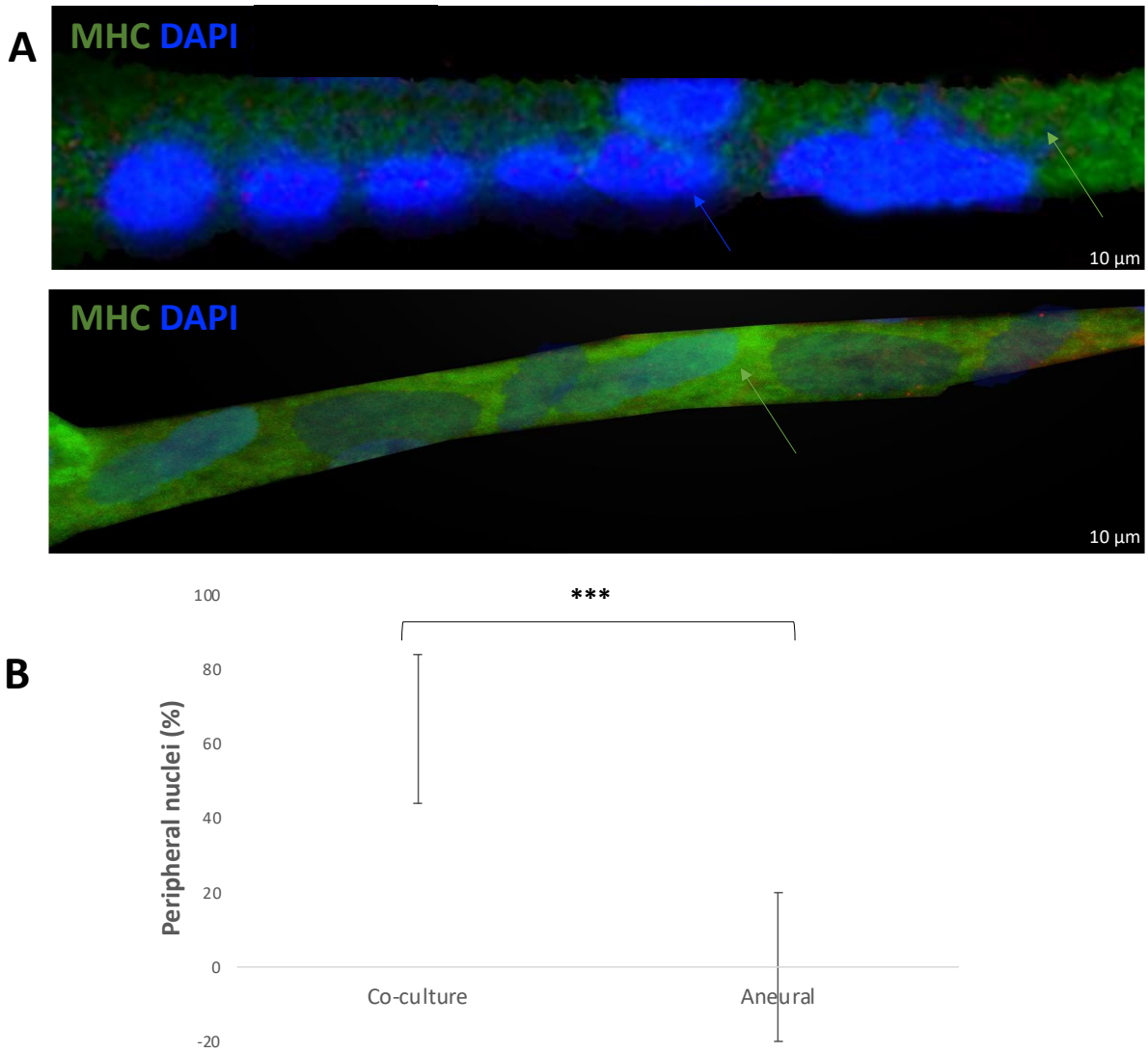

Figure 4.10 Day 7 peripheral nuclei generation. (a) The image panel on the upper end represents an innervated myotube where NPC explant showing nuclei located in the periphery extending from the myotube is used for co-culture. The image on the lower panel represents myotubes cultured aneurally with nuclei that are located at the centre. Staining of myotubes was done for DAPI (blue arrow) and myosin heavy chain (MHC) (green arrow). (b) A comparison of proportions of myotubes with nuclei on the periphery in conditions of co-culture against aneural myotube conditions. Data are shown as a mean. The ± SD signifies error bars. n =4 independent experiments. *** symbolises P= 0.001-0.0001. Bar = 10 µm.

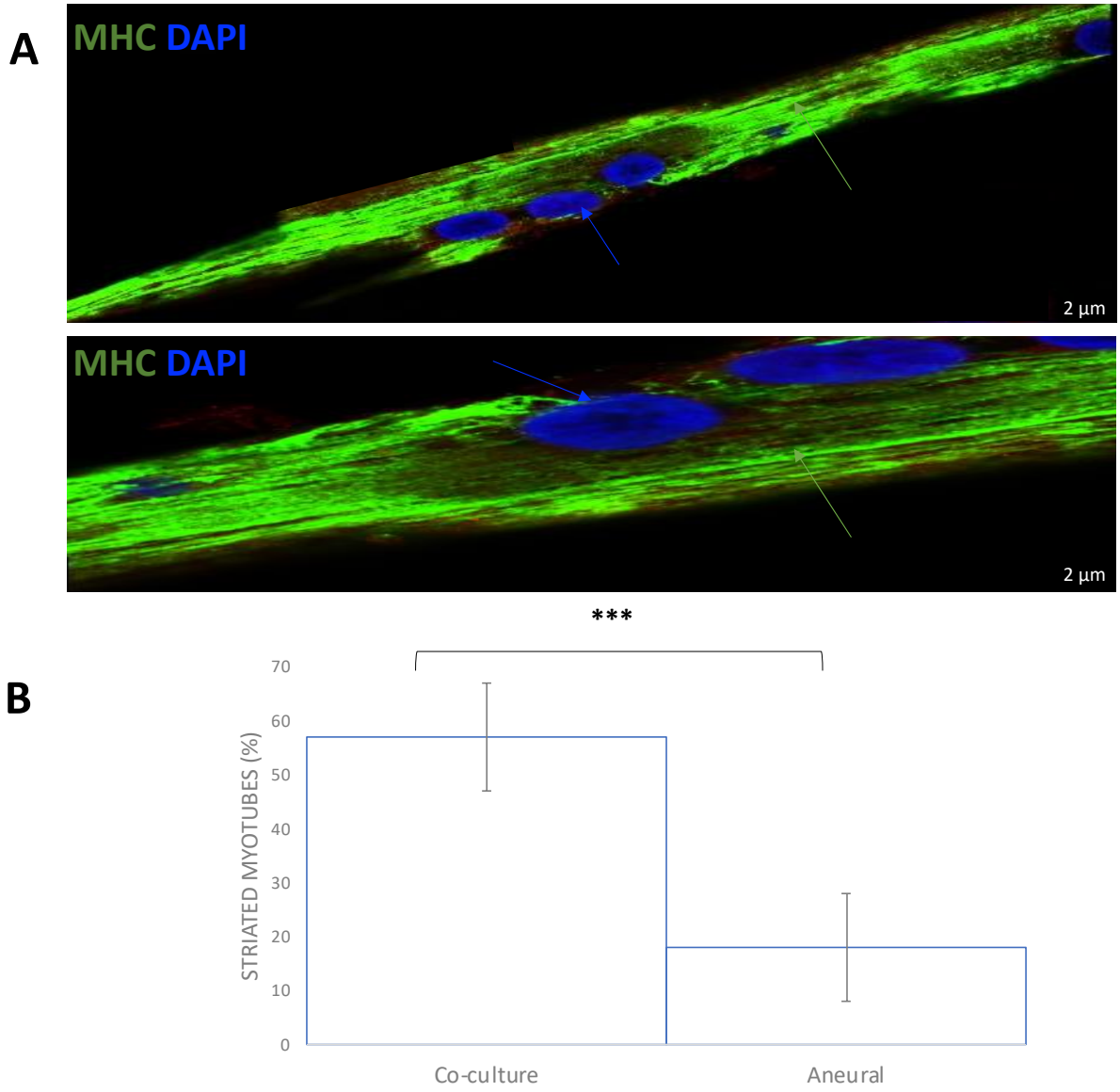

Figure 4.11 Day 7 myotube striations. (a) The image on the upper panel represents an innervated myotube co-cultured with NPCs explant displaying striations on the myotube membrane. The lower image panel represents myotubes that are cultured aneurally without striations. Myotubes were stained for DAPI (blue) and myosin heavy chain (MHC) (green). (b) The bar graph compares the proportion of striated myotubes in conditions of co-culture with aneural myotube conditions. The presentation of data is done as a mean. The ± SD shows error bars. *** signifies P= 0.001-0.0001. n = 4 independent experiments. Bar = 2 µm

4.2. Discussion

The main outcome of this chapter is the presentation of the characterisation of the *in vitro* NMJ model developed in the previous chapter. The NPCs with C25 co-cultures validated the differentiated myotubes and cholinergic MNs and facilitated the interaction between myotubes and neurons. In addition, co-cultures created the establishment of mature NMJs with presynaptic and post-synaptic physical arrangement. It was also concluded that innervated myotubes in co-cultured settings demonstrated physical characteristics showing advanced differentiation development.

When the initial experiments were done with the co-cultures with the aim of determining the best time to characterise the system, the standard for both formation and maturation of NMJ was CF. Observing that the peak of innervated myotubes was on the 7^{th} day in the co-culture system delivered proof of effective NMJ development, which was shown following the completion of characterisation and the revelation that the NMJs, MNs, and myotubes had suitably differentiated. When compared, it was noted that some co-culture systems that were established previously need over 20 days before the formation of NMJ happens and also included extensive myotube and MN differentiation beforehand, a situation that increases the experimentation timeline (Das et al., 2010; Southam et al., 2013). Furthermore, when compared to the co-culture system that this study presents, the prior co-culture models showed that NMJ development happened prematurely, leading to myotubes that lacked advanced differentiation. Notwithstanding the fact that co-cultures were characterised on the 7^{th} day, the initial experiments used when determining the best date for characterisation also showed the potential of long-term co-culture studies with this innovative and simpler framework, taking into account that the contractions of myotubes happened right up to the day when the experiment ended on Day 10, which could have been further maintained if

desired. The cholinergic MNs with ChAT and VAChT in the co-cultures characterisation lead to the observation that ACh, MNs, and myotubes took place within the system. The nerve $ChAT^{-/-}$ shows hyper-innervation of smaller MNTs, extreme presynaptic nerve branching, and an escalation of AChR aggregations quantities with less presynaptic contacts (Misgeld et al., 2002; Brandon et al., 2003). Even though structural synaptic elements existed in the $ChAT^{-/-}$, a collection of pre- and post-synaptic irregularities could be noted in the NMJ. What the results from this *in vivo* ChAT deficient NMJ research suggest is that neurotransmission is not ACh's only function and that ACh and ChAT (its biosynthetic enzyme) are needed by synaptogenesis. Studies done using VAChT-/- in nerve come to the same conclusion that there are severe irregularities in the development of NMJ (de Castro et al., 2009). As was the case in ChAT-/-, research involving excessive MN growth, enlarged MEPs, necrotic SkM tissue, showing that VAChT is required for the discharge of ACH, at the normal and synapse NMJ development. Therefore, ChAT and VAChT characterisation in co-cultures delivered details indicating similar to *in vitro* NMJs created system were an accurate illustration of NMJ development noted *in vivo*.

The correct NMJs formation needs the interaction between MEPs of myotubes, axon terminals of neurons, and terminal Schwann cells. *In vivo* research done using mutant mice with no Schwann cells shows the ability of MN axons to grow and spread in the direction of developing SkM. Nonetheless, substantial axonal defasciculation is noted. Such a result implies that Schwann cells are not needed for axonal projection in the direction of myotubes even though they are needed for nerve fasciculation. In addition, nerves lacking in Schwann had the ability to start initial NMJ formation but failed to sustain further synapse development (Morris et al., 1999; Lin et al., 2000; Riethmacher et al., 1997; Wolpowitz et al., 2000; Woldeyesus et al., 1999). What is demonstrated by these studies is that Schwann cells

are not needed to start contact between axons and neurons *in vivo*, even though they are necessary for the consequent advancement and sustenance of the synapse in development. Thus, the validation of Schwann cells in the co-culture system and the succeeding interaction between Schwann cells and MNs implies the *in vitro* formation seen in the co-cultures were matured and sustained via communication between MN and Schwann cells.

Significantly, presynaptic nerve terminals with antibodies for Syt1 characterisation happening in the co-cultured cells. Studies exploring Syt1 validate the work it accomplishes as a sensor of calcium, enabling the discharge of neurotransmitters from Ca2+-dependent vesicles, a requirement for vesicle exocytosis depending on calcium in invertebrates (Littleton et al., 1993; Geppert et al., 1994). However, $Syt1^{-/-}$ investigations showed that Syt1 was only needed for the fast synchronous discharge of neurotransmitters from Ca2+-dependent vesicles since Synaptotagmin 2 has the capability to compensate for the asynchronous exocytosis absence in Syt1-/- (Geppert et al., 1994). Studies are done with spinal muscular atrophy (SMA) mouse model to investigate the reasons behind weakened neurotransmitter discharge also showed that during the MNTs development of the muscles that were severely affected, there was downregulation of Syt1. However, this was not the case in the less susceptible muscle (Lopez-Manzaneda et al., 2016). Thus, identifying Syt1 in co-cultures provides proof that presynaptic activity at NMJs was an indication of the functionality of NMJ, as would be anticipated in proper NMJ formation and development.

In the present co-culture system, the NMJs formation was characterised on MEP with α-BTX to reveal the arrangement of AChRs' post-synaptic aggregation. Prior-established nerve-muscle co-culture systems indicate the formation of NMJ as speckled or diffused AChR clusters co-localising with MNs, particularly in the groups of premature or faint formation (Das et al., 2007; Southam et al., 2013). Nonetheless, it is recognised that on its own, co-

localisation is not a representation of NMJ formation *in vivo* (Thomson et al., 2012). NMJ research concludes that MN axons end at the MEP and overlap the AChR clusters exactly (Englander & Rubin, 1987; Sanes & Lichtman, 1999). The nuclei in the myotube are positioned regularly throughout the fiber length. While the SkMC differentiate the nuclei actively spread along the myotube at the periphery of the myofibers by microtubule motor protein (kinesin-1 and cytoplasmic dynein) (Wilson et al., 2016). Nuclei position at the periphery of the myofiber underneath the plasma membrane are observed in advanced differentiation in healthy and young SkM cells. However, when NMJ are formed and in myotendinous junction formation the nuclei are not evenly distributed anymore. In addition, nuclei lose its periphery position in abnormal cells and old SkMC, hence, interruption of nuclear location consequences in multiple muscle disorders as it delays or stops muscle contractions. This is because of the interruption in the signalling in reaching the nuclei due to the nuclei being relocated in the centre of the cells (Roman and Gomes., 2018).

Significantly, the formation of NMJ noted at the co-culture system that is presented in the current study showed MN ending on clusters of AChRs in the usual twisting knotted arrangement. What this finding does is that it signifies physiological *in vitro* NMJ formation, analogous to that which was noted *in vivo*. The confirmation that the co-cultures were capable of generating NMJs with features of AChR clusters that were maturely developed triggered the investigation of other post-synaptic NMJ elements. Required for the establishment and sustaining of the NMJ, the observation of Rapsyn and MuSK at the MEP was proof of the MuSK signalling pathways activated by the secretion of agrin from the MNT (Luo et al., 2003; Wu et al., 2010; Kim and Burden, 2008). This is a finding which is important

since it delivered a proof in the direction of successful post-synaptic differentiation at the NMJ through pre- and post-synaptic communication.

Furthermore, the connection of Rapsyn with AChRs is needed for *in vivo* AChR clustering (Apel et al., 1997). Therefore, detecting the co-localisation between MuSK, Rapsyn, and AChRs showed that the post-synaptic development noted in the co-cultures had the ability to attain maturation levels that would permit the investigators of post-synaptic NMJ manipulation in the system. Myotubes that were co-cultured also showed the morphological features of advanced differentiation. Apart from the fact that transversal triads could be observed in the innervated myotubes, the co-cultured myotubes have nuclei located in the periphery and the standard actin-myosin striations expressed in mature differentiation, all features that were noted *in vivo* (Shadrin et al., 2016; Bruusgaard et al., 2003). This important characterisation of mature innervated myotube development is a further example of the co-culture system's advantage when compared to the usual aneural *in vitro* myoblast cultures and previously established nerve-muscle co-culture models that are unable to attain advanced levels of development. This makes this co-culture system more desirable with regards to research and the accurate explanation of wasting of skeletal muscle and make the investigation of NM disorders better.

4.3 Conclusion

This report provides a characterisation of the novel *in vitro* system created from C25-co-cultured NPCs. The de novo development of NMJs was confirmed by ascertaining pre- and post-synaptic structures of the junctional apparatus. Interactions with myotubes and MN were indicated to validate the advanced innervated myotubes differentiation.

5: Functional Assessment of *in vitro* neuromuscular junctions between neural progenitor cells and immortalised human myoblasts

5.0 Background

In the previous chapter, experiments provided details of the nature of NMJs and innervated myotubes in the NPC/ C25 co-culture system. The axon of MNs will often branch to enable a single MN to synapse with multiple skeletal muscle cells. However, each muscle cells is innervated by only one MN which release acetylcholine from synaptic vesicles to stimulate muscle contraction through NMJ. In this *in vitro* NMJ model physiological muscle contraction was MN-driven distinctive from other established models by other researchers were some models used electrical pulse to stimulate muscle contraction, other models prompt contractions of the myotube through applying chemical solution to stimulate muscle contraction (Belluardo et al., 2001; Umbach et al., 2012; Guo et al., 2012;Miles et al., 2004; Guo et al., 2010). Establishment of NMJ with presynaptic cholinergic MN activity, maturation of post-synaptic motor endplate (ME P) components, together with the interaction of cells happening between SkMCs and MNs were confirmed across the co-cultures. The NMJ formation and innervated myotubes development made it possible to attain-sophisticated myotube differentiation in the co-culture system, distinguished through classification of peripheral nuclei, cross-striations on the myotubes. The heterologous co-culture model in this study indicate that antibiotics particular to humans can be employed when studying disorders which impact on the post-synaptic and/or presynaptic parts of the NMJ.

Data gathered through the description of the co-culture model as presented in this study has indicated the system's possibility to imitate applicable *in vivo* structural NMJ development and also shown enduring steadiness in culture. Nonetheless, if the co-culture model is to be

an effective system, the contractile activity of the SkMCs will have to physiologically respond to the NMJ prior to and after manipulation via pharmacological interventions.

Classic studies arrived at the conclusion that human SkMCs that are aneurally cultured, which form the leading method employed *in vitro* model in researching human SkM (Aas et al., 2013), often do not typically form differentiated post-synaptic components of NMJs or contraction under normal settings un-like animal derived SKMCs, (Kobayashi & Askanas, 1985; Delaporte et al., 1986). It is for this reason that it is generally accepted that human myotubes that are aneurally cultured do not show spontaneous contractile activity. So, if there is any evidence of contraction, it is considered to be a result of innervation (Mis et al., 2017). Remarkably, the inaugural publishing of the spontaneous aneural myotube contractions observed in differentiated human SkMCs was in 2014 (Dixon et al., 2018). According to Guo et al. (2014) at that time, the authors advanced the claim that there was no spontaneous contraction recounted from aneural human SkMCs *in vitro.*

Nonetheless, the myotubes differentiated from the C2C12 mouse myoblast cell line indicate a capability for contractile activity which is spontaneous when aneurally cultured (Manabe et al., 2012), showing that there is a potential for human myotubes that are aneurally cultured to spontaneously contract even though this may be rare. For purposes of demonstrating the functional NMJs formation, certain nerve-muscle co-culture models which were previously established have employed excitatory neurotransmitters like glutamate for the purpose of stimulating MNs, leading to an escalation in the contraction of myotubes. In a different way, the termination of myotube contraction has also been shown via the use of AChR inhibitors which are reversible of irreversible like bungarotoxin or tubocurarine (Bowman, 2006; Guo et al., 2011; Umbach et al., 2012; Miles et al., 2004).

It is interesting to note that studies which carried out recently identified glutamate decarboxylase, an enzyme that has a role in the synthesis of γ-aminobutyric acid (GABA) and a protein accredited for the GABA transportation across membranes known as GAT-2, in the vertebrate NMJ (Nurullin et al., 2018). The impact of GABA receptor antagonist like bicuculline has not been explored sufficiently. It is for this reason that this study's experiments were done with co-cultures of NPCs innervating C25 with the aim of exploring the effective reaction of NMJs to biochemical intervention. By trying different methods of stimulations. The contraction frequency was measured in hertz (Hz) in this experiment, hence the unit of frequency is equivalent to one cycle per second and in this project equal to one contraction per second. Therefore, 60 contractions/ minutes equal to 1 Hz.

5.0.1 Aims

The main aim of this chapter is to determine the functional assessment of the NMJ model using different pharmacological drugs (α-bungarotoxin, tubocurarine, bicuculline, L-glutamic acid and γ-aminobutyric acid) to confirm the extensive myotubes contractile activity is MN-driven. The present study's first aim was to confirm that spontaneous myotube contraction in the co-culture system where indeed a result of MN stimulation, as there is a likelihood that the spontaneous contractions may have been aneurally prompted. The second aim was to make sure that the NMJs produced in the co-culture arrangement respond to drug in a physiological way illustrative of *in vivo* NMJs. Hence, the objectives are as follows.

i) Establish a co-culture model exhibiting spontaneous myotube contractions.

ii) Use agonist and antagonist drugs (i.e. α-bungarotoxin, tubocurarine, bicuculline, L-glutamic acid and γ-aminobutyric acid) to treat the co-culture.

iii) Determine the functionality of NMJs generated in the co-culture system by assessing the myotube contraction frequency in response to pre- and post-synaptic NMJ manipulation via drug treatments.

5.1 Results

Pre or post synaptic effect was observed in co-culture exposed to different drugs. Some used drugs were agonist and some were antagonist. The different drugs had certain mechanism of action on the co-cultures such as blocking Ach receptor in muscle, blocking nerve impulse, force Ach discharge and neurotransmitter L-glutamic acid stimulator motor neuron.

5.1.0 Functional Assessment of NMJs with α-Bungarotoxin

α-BTX is a naturally occurring neurotoxic peptide which exists in the venom of a snake called *Bungarus multicinctus*. Exposure of NMJs to α-BTX results in an antagonistic binding between the AChRs and the neurotoxin on the NMJ's post-synaptic MEP. Hence, to determine whether the muscle contraction is MN-driven, α-BTX was applied of the SkM detected *in vivo* (Santhanam et al., 2018) used to treat the co-culture as a way of prompting permanent blockade of the post-synaptic AChRs. On the seventh day, experiments were done, at the time when maximum spontaneous contraction frequency became apparent, as determined in chapter 3 (Figure 3.6D). Ahead of having the co-cultures exposed to α-BTX treatment, the culture dishes were placed on the microscope stage within an incubation chamber with the aim of upholding a suitable atmospheric environment for spontaneous myotube contractile activity. Uninterrupted spontaneous myotube contractions could be noted for no less than five minutes ahead of taking the baseline measurements. The inclusion of this step was to make sure that any variations in myotube contraction frequency as a result of environmental conditions or temperature fluctuations were alleviated, in the process getting rid of false-positive results, considering the fact that the co-cultures are very sensitive to such instability. The measuring of baseline contraction frequency was done half a minute ahead of applying α-BTX (Figure 5.0). No differences ($P = 0.51$) were recorded in baseline contraction frequency

before the negative control and the positive controls ahead of treatment as the media was same for both at this stage. When the treated and untreated diluent to the cultured cells was introduced, all the myotube contractions in the α-BTX treated co-cultures and controls contraction immediately terminated. After 15 minutes, at 0.42 Hz the myotube contraction frequency in the controls were measured, while there were no myotube contractions detected in the co-cultures treated with α-BTX. After 20 minutes, an increase to 0.45 Hz, in myotube contractions could be detected in the controls. The contractions of the control myotubes were recorded at 0.57 Hz after 30 minutes, with no contractions detected in the cells treated with α-BTX. In the next 45 minutes following the treatment, the controls contraction frequency went back to equivalent baseline levels of 0.71 Hz. After one hour, the controls were still showing contraction frequency similar to baseline and at one and a half hours, even though there were no contractions detected in the cells treated with α-BTX at these time points.

The cells treated in α-BTX and the control were washed out before new untreated DM was introduced to the cells one and a half hours following measurement, resulting in the halting of contractions on both control and treated conditions. Measurements were done 30 minutes following the washout (2 hours following the inaugural application of treatment), it was noted that the controls were again contracting at equivalent baseline frequency of 0.63 Hz. The same observation was made 24 hours following the treatment, at which point the contraction frequency measured 0.61 Hz. Nonetheless, no contractile activity was noted in the co-cultures treated with α-BTX in either of the two last time points. After performing a normalisation test the data showed to be parametric. Thereafter, a split plot ANOVA was performed with a within element being time and a between element (control vs BTX treated culture). In addition, to Bonferroni post hoc pairwise comparisons.

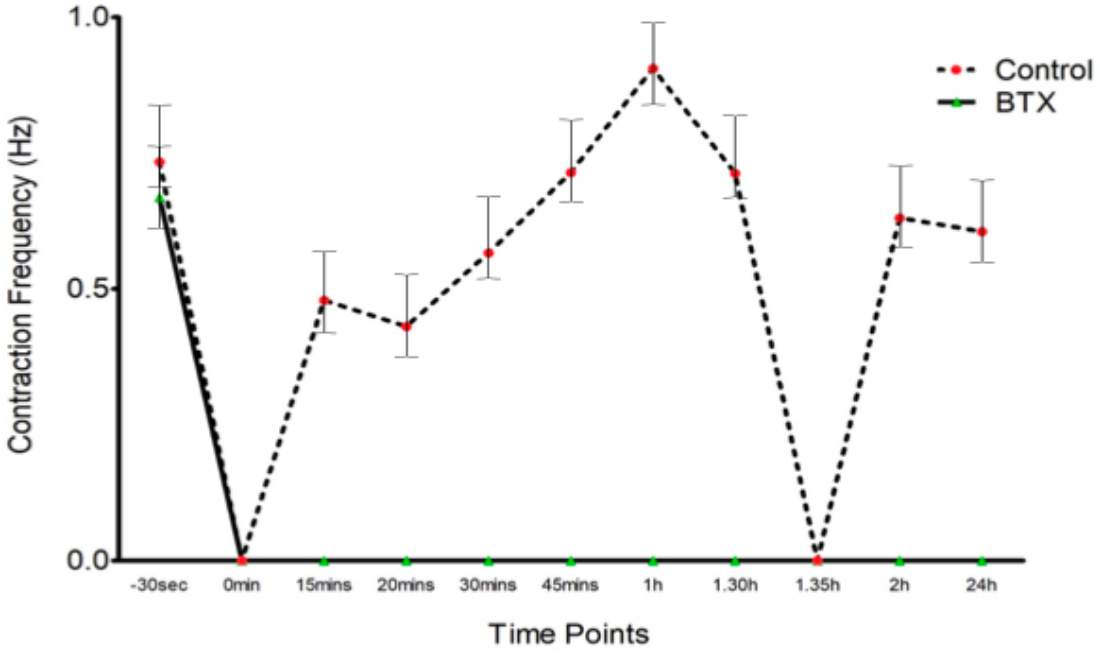

Figure 5.0 Contraction Frequency for α-bungarotoxin. Assessment of the functional effects of a 1:400 of 10nM concentration α-bungarotoxin on co-cultured myotubes. The figure presents a comparison of the contraction frequency of α-BTX-treated myotubes and untreated controls. Data are presented as a mean, with error bars denoting ± SD. n = 10 independent experiments.

5.1.1 Functional Assessment of NMJs with Tubocurarine

Tubocurarine is a toxic mono-quaternary alkaloid which is extracted from a plant known as Chondrodendron tomentosum. This toxin works through a rescindable AChRs binding at the post-synaptic NMJ (Cooke & Grinnell, 1964). In a comparable manner to the impact of α-BTX, and adequate amount of tubocurarine results in the paralysis of SkM and death due to asphyxiation as a result of the diaphragm paralysis. With the aim of finding out if innervated myotubes produced in the co-culture system matches the paralysis of SkM as noted *in vivo*, 8 µM tubocurarine (Guo et al., 2011; Santhanam et al., 2018) was used to treat the co-cultures to AChRs (Figure 5.1). No difference was noted in baseline contraction frequency between control cultured and treated myotubes recorded half a minute ahead of adding treatment solution to the cells.

Once untreated diluent was added to the control cells and tubocurarine to the treated cells, there was a termination to all notable contractions in both settings. A split plot ANOVA was performed with a within element being time and a between element (control vs Tubocurarine treated culture) showing significant differences at 15min, 20min, 30min, 45min, 60min and 90min P=<0.001. Bonferroni post hoc pairwise comparisons was also performed.

Both treated and control conditions were washed out, and the new DM was introduced to the cells. This resulted in an immediate total stoppage of myotube contractions. No difference (P = > 0.05) was observed in as measured 30 minutes following the washout: the treated cells were contracting at 0.69 Hz and the controls at 70 Hz. In a similar manner, measuring the contraction frequency 24 hours following the first treatment showed the controls were contracting at 0.72 Hz and the treated cells were contracting at 0.705 Hz with no significant variance (P = >0.05).

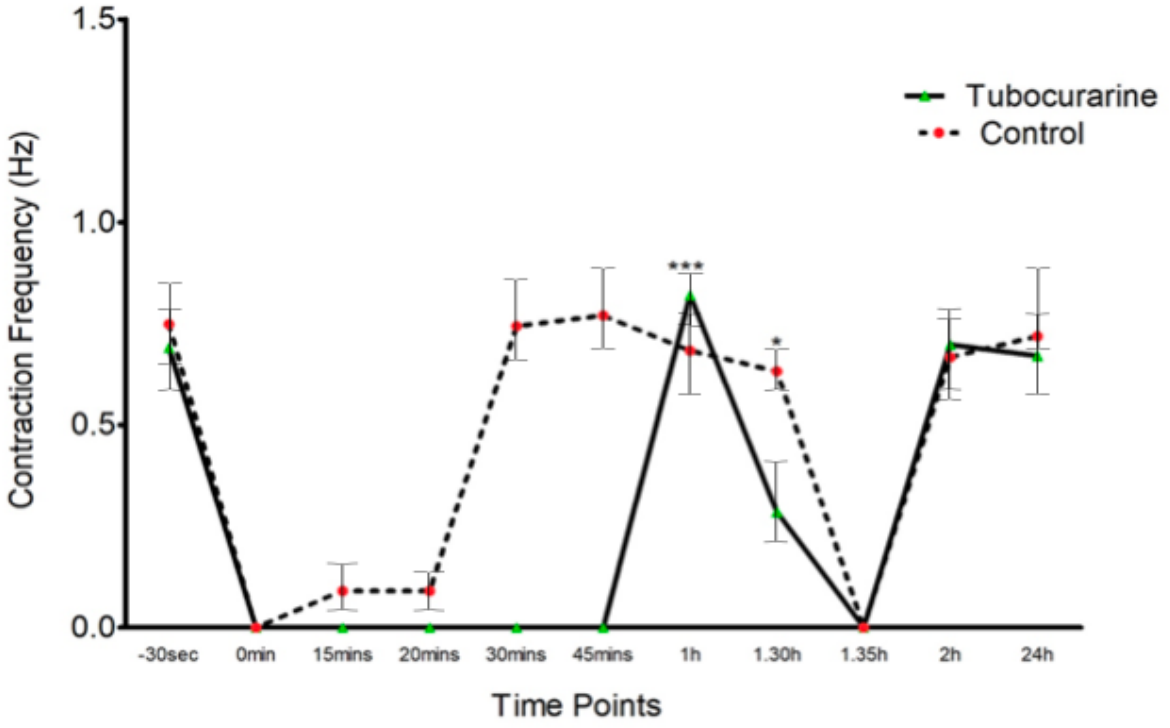

Figure 5.1 Contraction Frequency for tubocurarine. Assessment of the functional effects of 8 µM tubocurarine on co-cultured myotubes. The line graph conducts a comparison of the myotube contraction frequency between the tubocurarine-treated myotubes and the untreated myotubes. Data is displayed as a mean with error bars indicating ± SD. n = 10 independent experiments. * signifies P= 0.05-0.01; *** signifies P= 0.001-0.0001.

5.1.2 Functional Assessment of NMJs with Bicuculline

The phthalideisoquinoline alkaloid bicuculline is a competitive GABA receptor antagonist obtainable from various Fumarioideae subfamily species (Manske, 1932). Studies conducted in the past show that applying bicuculline in a homologous NMJ co-culture model has the effect of modulating contraction frequency (Mis et al., 2017). Hence, 10 µM bicuculline (Borodinsky and Spitzer., 2007) was applied to the current *in vitro* NMJ with the aim of finding out the effects it has on myotube contraction frequency in this heterologous co-culture system (Figure 5.2). Once the bicuculline or DM was introduced to both treated and untreated cells, there was an immediate halt in all contractions. A split plot ANOVA was performed with a within element being time and a between element (control vs Bicuculine treated culture)

showing significant difference between the drugged co-culture and control at the timepoint 15min, 20min, 30min, 45min 60min and 90min with P=<0.01. Bonferroni post hoc pairwise comparisons was also performed.

When a washout and replacement of DM was done, all contractions came to a complete halt. Measurements taken 30 minutes after the washout showed that there was no difference when the control and treated conditions where compared. In the same manner, no differences were noted after 24 hours between the treated and control conditions P = >0.05).

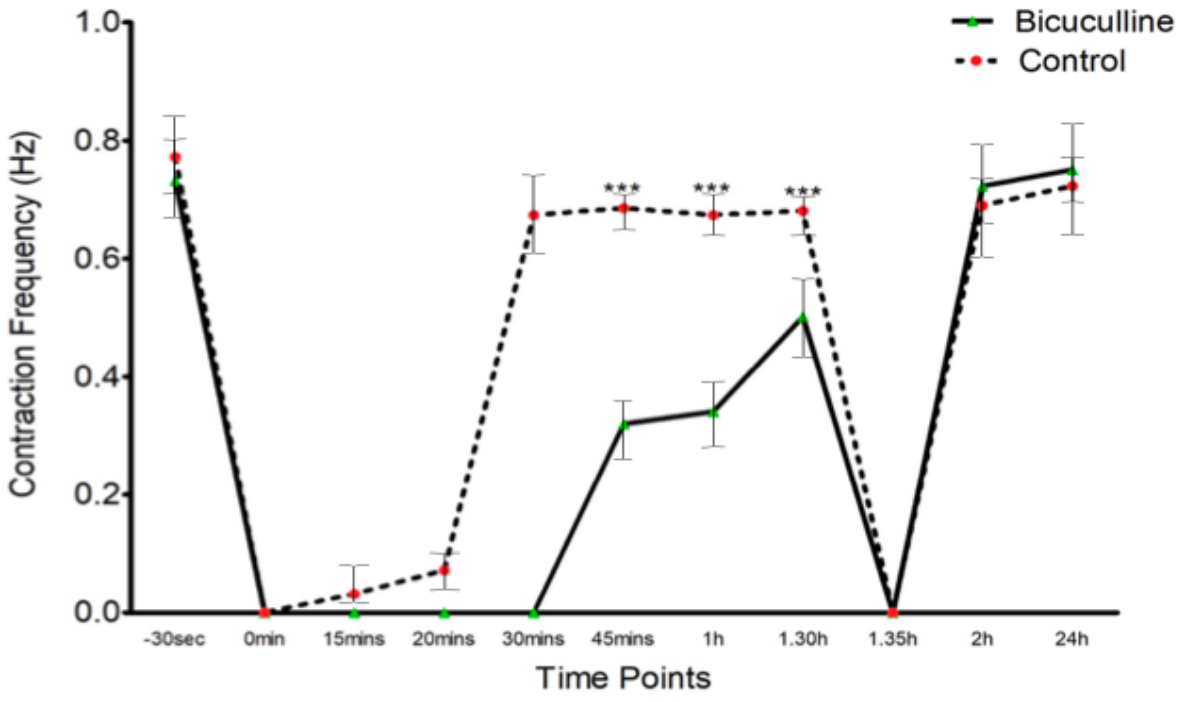

Figure 5.2 Contraction Frequency for bicuculline. Assessment of the functional effects of 10 µM bicuculline on co-cultured myotubes. The line graph presents a comparison of the contraction frequency of bicuculline-treated and untreated controls. Data is displayed as a mean, with error bars denoting ± SD. n = 10 independent experiments. *** signifies P= 0.001- 0.0001.

5.1.3 Functional Assessment of NMJs with L-Glutamic Acid

Once it was found that myotube contractile activity in the co-culture system could be decreased or halted by applying antagonist drugs that influence AChRs at the NMJ MEP, the experiment that followed was designed to find out the effect of presynaptic agonist

stimulation of the NMJ at the MNs. Hence, the excitatory neurotransmitter glutamate (400 µM L-glutamic acid (L-Glut)) (Smith et al., 2013), was applied to the co-cultures with the aim of assessing the impact of L-Glut on the co-cultured myotubes contraction frequency (Figure 5.3). Baseline measurements of contraction frequency were taken 30 seconds ahead of applying untreated diluent to the negative controls and L-Glut to the positive controls, which showed that there were no significant differences P = >0.05). Once the treatment solutions were introduced to the cultures, all contractions immediately stopped. A Split plot ANOVA was performed on the contraction frequency of controls and contractile activity of myotubes with a within element being time and a between element (control vs L-Glutamic treated culture) showing significant difference between the drugged co-culture and control at the timepoint 20min and 30min. P=<0.01. Bonferroni post hoc pairwise comparisons was also performed.

Both culture conditions were washed out, and the DM was replaced 90 minutes after the initial treatment, which resulted in a complete halt of all contractions in the cultures, measurements were taken 30 minutes following the washout, it could be noted that the rate of contraction of both the treated and control co-cultures was close when compared to the baseline P=<0.05. With regards to measurements taken 24 hours following the initial treatment, it was noted that there was no variance in contraction frequency (P= >0.05) between the L-Glut-treated cultures and controls. The spontaneous activity exhibited is the same as that of the baseline.

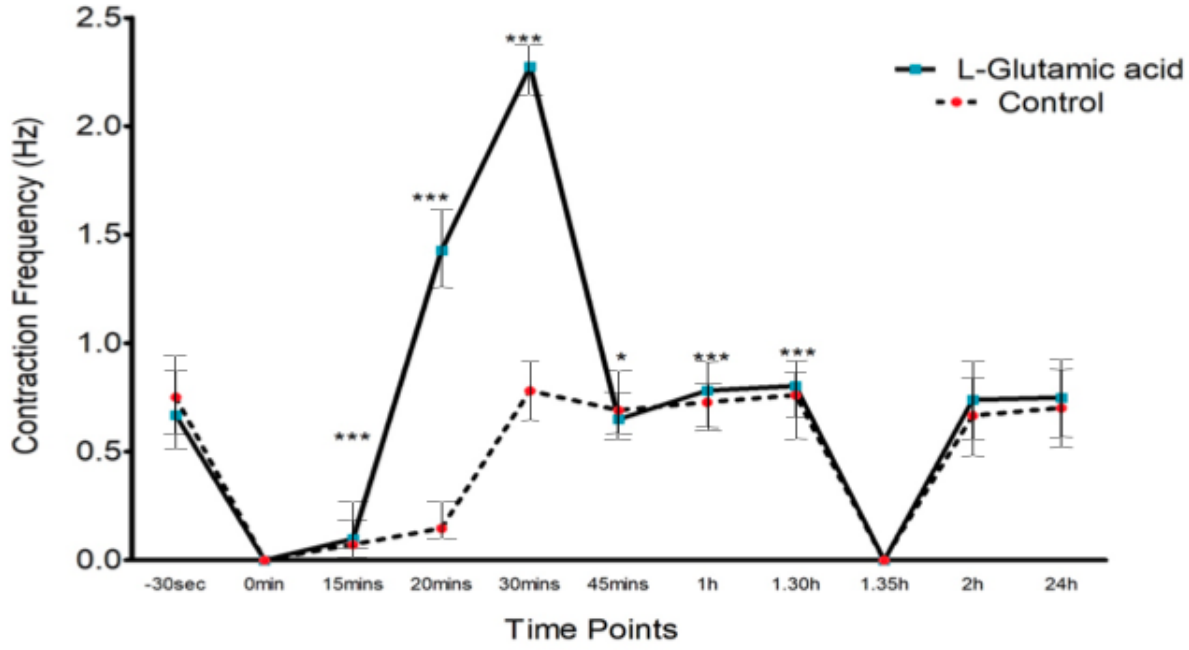

Figure 5.3 Contraction Frequency for L-glutamic acid. Assessment of the functional effects of 400 µM L-glutamic acid on co-cultured myotubes. The line graph presents a comparison of the contraction frequency between myotubes treated with L-glutamic acid and the controls that are not treated. Data is displayed as a mean, with error bars denoting ± SD. n = 10 independent experiments. * signifies P= 0.05-0.01, *** signifies P= 0.001-0.0001.

5.1.4 Functional Assessment of NMJs with γ-Amino butyric Acid

According to Obata (2013), γ-Aminobutyric Acid, the GABA's inhibitory neurotransmitter plays an important role in the manner in which the brain functions. It is mainly found in the synapses of the CNS. Previous research has indicated that GABA signalling could may occur in the periphery, with GABA transporters and receptors entangled in the process of GABA signalling being discovered in a tiny amount of exocrine and endocrine glands (Watanabe et al., 2002). Research involving molecules has come to the conclusion that $GABA_A$ receptor subunits α4 and β2/3 exist in cholinergic neurons (Park et al., 2006; Elinos et al., 2016). Notwithstanding the reality that GABA plays the role of reducing neuronal activity in the CNS, the consequence of an escalation of GABA concentration in the *in vitro* NMJ setting still needs to be clarified. It is for this reason that 1 mM GABA (Borodinsky and Spitzer., 2007) was used

to treat the co-cultures before a comparison of the contraction frequency against the control settings. A Split plot ANOVA was performed on the contraction frequency of controls and contractile activity of myotubes with a within element being time and a between element (control vs GABA treated culture) showing no significant difference between the drugged co-culture and control at the timepoint 15min P=>0.05. Significant variation was observed at 20min (P= <0.001). Bonferroni post hoc pairwise comparisons was also performed. Observations after 30 minutes showed that the myotubes contraction frequency in cultures treated with GABA were substantially higher than that of the controls with significant difference P= < 0.0001). Nonetheless, measurements taken after 45 minutes show that there were significant differences in the contraction frequency of myotubes between the GABA and non-treated controls in addition to 60 min, 90 min and 120min (P=<0.001). Furthermore, slight variance was observed at 24 hours following the treatment (Figure 5.4) with P= <0.05.

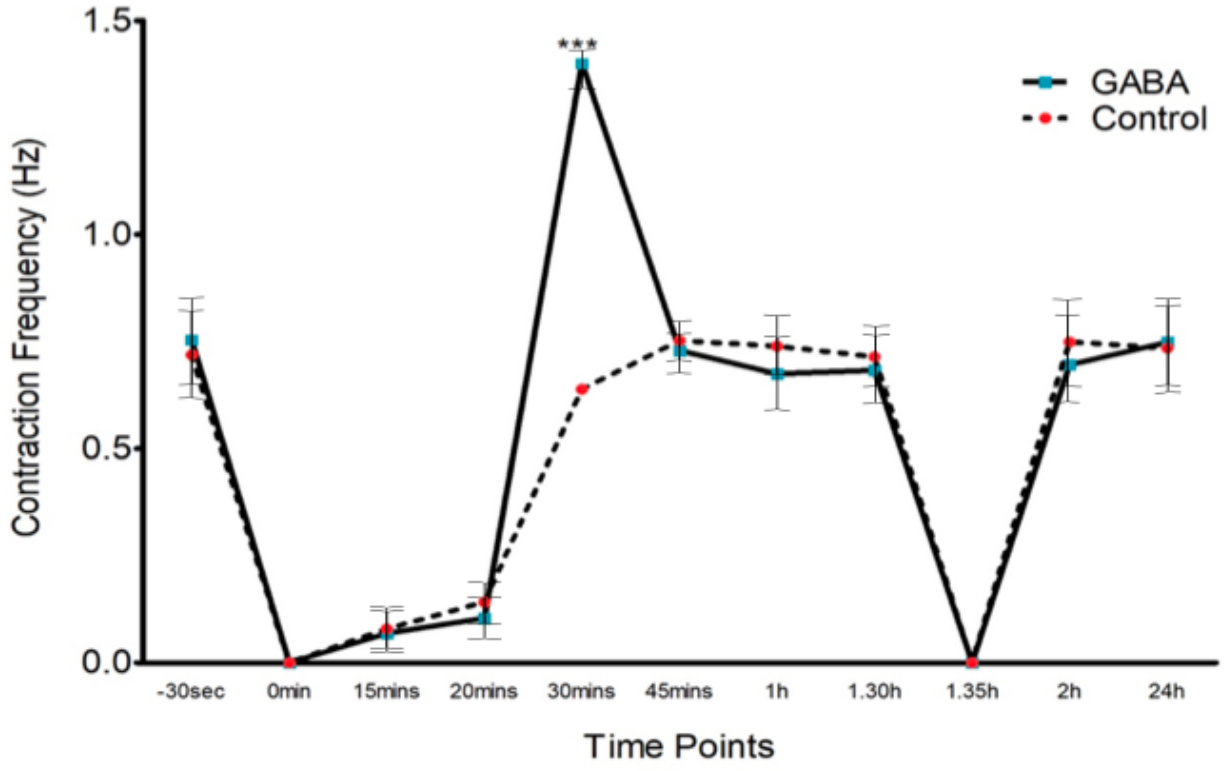

Figure 5.4 Contraction Frequency for γ-aminobutyric acid. Assessment of the functional effects of 1 mM γ-aminobutyric acid on co-cultured myotubes. The line graph presents a comparison of myotube contraction frequency when treated with γ-aminobutyric acid (GABA) and the untreated controls. Data is displayed as a mean, with error bars denoting ± SD. n = 10 independent experiments. *** signifies P= 0.001-0.0001.

Tubocurarine, α-Bungarotoxin and Bicuculline had antagonist effect whereas L-glutamic acid and GABA had agonist effect.

5.2 Discussion

From this chapter, it can be noted that the primary results demonstrate the functional capacity of NMJs produced in the nerve-muscle co-culture system, which was designed for this study. The experiments done are planned in such a way that they prove that the spontaneous myotube contractile activity is indeed mimicking the physiological contraction as consequence of MN signalling via the NMJ. It is for this reason that NMJs functionality was evaluated through analysing myotube contraction frequency modulation through the employment of agonist and antagonist (pre-and post) pharmacological interventions which act on presynaptic MNs or postsynaptically on AChRs at the NMJ. The result of introducing α-

BTX to the co-cultures was an instant and permanent halting of spontaneous myotube contractions. Such a result shows that their AChRs bind with α-BTX at the NMJ MEP, a situation that stops ACh from forming a bond with the post-synaptic receptors and eventually there is paralysis in the co-cultured innervated myotubes. Even though the α-BTX-exposed co-cultures were washed out and brought back to the standard culture conditions with new DM, the spontaneous myotube contractile activity was stopped permanently. What this shows is that the NMJs produced in this *in vitro* co-culture arrangement reacted physiologically to an irrevocable competitive antagonist at the AChRs, in agreement with the observations made in the *in vivo* mammalian NMJ (Domet et al., 1995). Added to this, introducing tubocurarine to the co-cultures resulted in an instant, even though impermanent, stoppage of endogenously produced contractions of myotubes.

Not like the α-BTX-treated cultures that failed to reinstate contractile activity, the myotubes in the co-cultures treated with tubocurarine were able to re-establish spontaneous activity, starting with low-frequency uneven spasms as opposed to the standard co-ordinated contractions seen in control conditions. Notwithstanding the fact that the reinstatement of the contractile activity was apparent (60 minutes) following tubocurarine application, the spontaneous myotube contractions failed to get back to the normal synchronous frequency until the stage where the co-cultures had been restored to the conditions that prevailed before the intervention. Research has proved that the ACh effects do not become eliminated as a result of the existence of tubocurarine, even though there is a reduction in the capacity of the ACh to open the receptor channels. This results in a situation similar to a reduction in the ACh concentration (Bowman, 2006).

In a manner that is different from the permanent receptor antagonist α-BTX that effectively makes the AChRs inactive, the role of tubocurarine is achieved through the reduction of the

likelihood of the activating the receptor as opposed to completely inactivating it. The role of tubocurarine is accomplished through repeated association and dissociation with its binding sites, in the manner that is in keeping with the character of a reversible competitive receptor antagonist as opposed to maintaining a continuous connection with AChR such as α-BTX. The myotube contractile activity's capability in the co-culture to recover from tubocurarine provides confirmation of the precise physiological character of the neurotransmission as observed in this *in vitro* NMJ arrangement.

The results obtained from analysing bicuculline application to the co-cultures shows an initial termination of myotube activity. Notwithstanding the reality that the spontaneous contractile function recovered partially, the myotube contraction frequency was substantially attenuated ahead of the bicuculline removal from the cultured cells. Prior studies (Liu et al., 1994) examining the classic GABA Type A receptor antagonist bicuculline effects on AChRs, demonstrates that bicuculline dose-dependently has a blocking effect on the whole-cell current's amplitude in the cultured NPC-skeletal muscle.

Another insight that has been obtained from this study is the bicuculline's capability to decrease the optimal inducible ACh current without changing the Kd value. Such a conclusion shows that the binding of ACh to AChRs was competitively non-competitively blocked by bicuculline. Study by Liu et al (1994) concluded that bicuculline played the role of blocking embryonic nicotinic AChR channels. Added to this, experiments designed to explore the bicuculline effect on heteromeric mouse muscle αβγδ nicotinic AChRs show that the currents prompted by ACh were reduced by bicuculline, in a speedy but reversible way, showing that bicuculline inhibits the receptor (Liu et al., 1994).

Other studies dealing with the analysis of the effect of bicuculline at varying membrane capacities prove that the inhibition of receptors depended on voltage, a situation which

shows that bicuculline blocks nicotinic AChRs non-competitively (Demuro et al., 2001). Such studies deliver evidence supporting the idea that bicuculline-induced modulation of myotube contractions, seen in the current co-culture arrangement, is a result of ACh being prevented from binding with MEP receptors, a situation which further shows that signalling at the NMJ was controlling the myotubes' contractile activity in this *in vitro* NMJ model.

Jiang et al., 1990 defines Glutamic acid as a neuron-specific excitatory neurotransmitter which prompts APs in MNs. Notwithstanding the fact that glutamate receptors were detected in mammalian NMJs, there are some studies which show that such receptors have a role to play in regulating the potentials of muscle fibre membrane through the nitric oxide synthase system (Urazaev et al., 1995), as opposed to signalling at NMJ. The examination of the stimulation of linked neurons in co-cultures through neuron-specific excitatory neurotransmitter L-Glut implementation shows that the myotube contraction frequency within the system was substantially raised. Immediately, the manner in which myotube contraction frequency is influenced by MN stimulation with L-glut could be observed, resulting in an increase in myotube activity (1.25 Hz higher) over the control in 20 minutes and an escalation to 1.5 Hz higher than the control in 30 minutes. Nonetheless, results show that myotube contraction frequency went back to levels equivalent to spontaneous activity within 45 minutes after MN stimulation with L-Glut.

For mammals, it is recognised that the stimulation of SkMC membranes happens exclusively via AChRs, a reality which shows that the effective improvement of myotube contractions in the co-cultures through introducing L-glut into the system was possibly obtained through the augmented discharge of ACh from the cultured MNs into the MN's synaptic cleft. GABA, as an inhibitory neurotransmitter in CNS synapses, plays roles in neuronal development and function through activating metabotropic and inotropic receptors (i.e. GABAA and GABAB

respectively) (Bowery et al., 2002; Obata, 2013; Olsen & Sieghart, 2008). Further studies looking into the GABA effects on quantal and non-quantal ACh discharge from MNT puts forward the view that GABA could decrease ACh discharge through activation of the GABAB receptors located in the NMJs of mammals, with phospholipase C taking the role of mediation (Malomouzhet al., 2015).

Even though studies conducted more recently show mechanisms of GABA and synthesis at the mammalian NMJs' AChRs, it could not be determined if GABA has a role to play in being a gliotransmitter at the NMJ or co-mediator of ACh (Nurullin et al., 2018). Nonetheless, the studies note that GABAB receptors' activation has an impact on the force with which ACh is discharged. Remarkably, the introduction of GABA into the co-culture system resulted in an increase in the myotubes' contractile activity. A temporary, even though substantial escalation of myotube contraction frequency was noted in the cultures treated with GABA in the initial 30 minutes after the treatment. A finding such as this shows that there was a discharge of ACh, and there was also an enhancement in the co-culture system, discrediting the conclusions in the studies mentioned above. Nonetheless, there are some studies that have come to the conclusion that $GABA_A$ receptors are in existence at the embryonic vertebrate SkMCs and there is also an existence of the expression of numerous transmitter receptor classes in the initial embryonic neuron and muscle development, including ACh, GABA, glutamate, and glycine (Borodinsky & Spitzer, 2007). Such a deeper analysis of the role and dynamic functions of GABA at the embryonic and mature mammalian NMJ is called for, for the contrivances of how NMJ is affected by GABA to be clearly understood.

Finally, it can be noted that this chapter's results deliver proof that this nerve-muscle co-culture arrangement allows for real-time assessment of NMJ functionality. In doing so, it makes available a content podium from where the evaluation of ground-breaking therapies

and *in vitro* disease modelling, and also a framework for the refinement of the understanding of how NMJ is formed and works in both disordered and healthy settings can take place.

5.3 Conclusion

This chapter has done an evaluation of the simplified *in vitro* nerve-muscle co-culture system for NMJ functionality. Initially, it was confirmed that spontaneous myotube contractions in the co-cultures resulted from MN signalling through NMJs. Added to this, it has also been verified that the co-culture model did react in a physiologically suitable way for the drugs employed in this study. This was confirmed by revocable and irrevocable paralysis of myotube contractile activity with AChRs antagonists and also supplementing myotube contractions with MN agonists.

Chapter 6: Investigating The Cross Communications between Motor neurons and Muscle in NMJ co-culture Model.

6.0 Background

The previous chapter described experiments that were conducted to confirm the NMJ physiological functionality in the *in vitro* NMJ culture that consists of NPC-co-cultured human myoblasts. Right across the co-cultures, it was confirmed that the modulation of myotube contractile activity using the NMJs manipulation with presynaptic MN agonists and post-synaptic AChR antagonists was successful. What this implies is that this *in vitro* NMJ arrangement physiologically replicates the function of NMJ in mammals as it responds to acknowledged toxins and drugs. For this reason, this novel co-culture system without growth, serum, and neurotrophic factors would be suitable *in vitro* NMJ model for selecting possible molecules and drugs used in studies related to ND and MN disorders like congenital myasthenic syndrome (CMS), spinal muscular atrophy (SMA), lambert eaton myasthenic syndrome (LEMS), amyotrophic lateral sclerosis (ALS), myasthenia gravis (MG), heart failure, diabetic neuropathy, cancer cachexia, sarcopenia, and myopathy. The streamlined character of the co-culture arrangement (i.e. free from serum and growth/neurotrophic factors), also makes it a reliable resource in drug screening procedures. Considering that introducing exogenous complex neural growth factors, as in alternate nerve-muscle co-culture models will affect the results and to understand which growth factors are truly expressed in the co-culture (Guo et al., 2011; Das et al., 2007; Puttonen et al., 2015; Guo et al., 2014; Rumsey et al., 2010).

Nonetheless, it needs to be noted that endogenously occurring neurotrophins and growth factors are crucial in the existence, growth, function, plasticity, and eventual demise of neurons *in vivo* (Reichardt, 2006; Oppenheim, 1991), and also in the maturation of myoblasts

(Syverud et al., 2016). On this basis, a substantial amount of studies have been done dealing with the neurotrophic/growth factors in the development of the nervous system and its function. Nevertheless, conclusions drawn from further studies show that such factors have a vital role in different populations of cells across numerous tissues. The SkMCs is one cell that has attracted a lot of attention. SkMCs express receptors for numerous cytokines, growth factors, and neurotrophins, implying that the signalling of neurotrophins happens inside SkMCs as they are being formed, develop, and in the innervation process (Chevrel et al., 2006; Griesbeck et al., 1995; Gonzalez et al., 1999).

As far as I know, the co-culture system that this project establishes is the inaugural co-culture model contrived with no exogenous growth factors, implying the endogenous secretion of all the factors needed for the NMJ establishment and growth, SkMCs advanced differentiation, and MN maturation. From research using neurotrophin-5 (NT-5) and neurotrophin-4 (NT-4), it can be noted that there are clear flaws in the development and function, something that could be read to mean that there is an involvement of NT-4/5 in the fibre differentiation of SKM (Carrasco & English, 2003). Furthermore, it has been suggested that neurotrophin-3 (NT-3) plays a role in muscle spindle formation (Ernfors et al., 1994) and altered nerve growth factor (NGF) has been associated with certain dystrophic muscle pathologies (Chevrel et al., 2006). For instance, studies done with healthy people and individuals suffering from multiple sclerosis indicate that BDNF in circulation increases with physical exercise (Rojas Vega et al., 2006; Ferris et al., 2007; Gold et al., 2003). In addition, research has shown that two hours of exercise with an ergometer bicycle has the capacity to spur the production of BDNF mRNA in SkM (Matthews et al., 2009). Furthermore, SkM neurotrophins concentrations are transformed in denervated muscle. Research using diabetic mice studying the same concept concludes that NGF mRNA and NTC decreases while BDNF mRNA expression increases in the

muscle (Ihara et al., 1996; Fernyhough et al., 1995; Fernyhough, et al., 1996, Fernyhough et al., 1998; Fernyhough et al., 1995).

The glial-cell-line-derived neurotrophic factor (GDNF), is recognised for playing a role in supporting CNS dopaminergic neurons (Lin et al., 1993). It has been concluded, from studies, that GDNF expression in SkM involves NMJs' hyper innervation as a result of escalation in the sprouting of MN (Nguyen et al., 1998). Suggestions have been made to the effect that GNF can play the role of maintaining cholinergic MNs right across the ageing process (Ulfhake et al., 2000) and a substantial yet fleeting GDNF expression at NMJs in the embryonic myogenesis process can also be seen *in vivo*. Fascinatingly, it has also been noted that GDNF expression escalates in denervated human SkM (Lie & Wies, 1998). Functional and characterisation results from the co-culture systems described in the previous chapters of this report deliver proof that NMJs generated in the system physiologically emulate *in vivo* structural development and functionality.

As was indicated in the previous chapters of this report, alternate established nerve-muscle co-culture models generally need intricate neural growth media containing serum or a mixture of neural growth factors (some that can be obtained from animals). This is a situation that makes toxicology studies and the drug discovery process even more complicated because of the potential cross-communication between the factors in the culture media and the novel compounds which are the subject of the study, providing a possible explanation why numerous potential treatments do not make it into clinics. Even the most contemporary systems need up to 18 trophic factors for their model to be successfully established. Added to this, numerous systems prompt contractions of the myotube through applying chemical or electrical stimulation, which fails to mirror the physiological stimulation needed for the contraction of muscles. Even though the effect of serum- free culture are not known the

hypothesis of this experiment was that it's better to avoid using serum. However, a question remains to be answered with regards to the manner in which the prevailing co-culture model that this project engineers were able to generate physiological functional NMJs with no trophic factors and serum, implying that SkMCs and MNs in the system discharge all required factors to spur the MN axons sprouting and NMJs creation with myotubes. To provide the answer to this question regarding the ability of the streamlined co-culture systems capability to create robust NMJs without involving exogenous serum, neurotrophic, and growth factors, which prior nerve-muscle co-culture systems require, the following study conducts ELISA-based microarray experiments with the aim of examining the concentration of endogenously secreted growth factors and neurotrophins in this *in vitro* NMJ system.

6.0.1 Aims

To my knowledge this is the first co-culture model engineered in the absence of serum and neural growth factors without any adverse effects, which suggests that nerve and muscle cells release all of the necessary factors needed to stimulate NPCs and myoblasts differentiation, nerve axonal sprouting and formation of NMJs with myotubes were secreted endogenously. Therefore, the aim of this chapter was to investigate the bi-directional communication between motor neuron and muscle to identify potential growth factors secreted as a result of this bi-directional communications

This, the study objectives to:

(i) Carry out ELISA-based microarray- technique to determine the neurotrophic and growth facts that occur endogenously in the co-cultures.

6.1 Results

6.1.0 Quantifying neurotrophic and growth factors

The process of determining whether there were any significant variances in the discharge of neurotrophic/growth factors in the supernatant of co-cultured, aneurally cultured NPCs, and human myoblasts that were aneurally cultured, a ELISA-based microanalysis analysis was conducted on neurotrophic/growth factor concentrations. A comparison was made between three settings. On Day 7, as is shown in Table 6.0, the quantification of the 40 neurotrophic/growth factors was done. From the results obtained from MANOVA analysis, it can be noted that 8 of the analysed factors had significant variances ($P < 0.05$) between aneural myotube cultures, co-cultures, and cultured NPCs. Followed by a series of single factor split plot ANOVA and post-doc pairwise analyses.

Below are some of the factors analysed and results show that they were significantly higher in the supernatant obtained from cultures when compared supernatant collected from cultured NPCs and aneurally-cultured myotubes. It was decided to focus on eight growth factors (listed below), seen as important factors to consider.

- Brain-derived neurotrophic factor (BDNF)
- Insulin-like growth factor-binding protein (IGFBP) -, -3, -4, -6
- Neurotrophin (NT) -3
- Growth differentiation factor -15 (GDF-15)
- Glial cell-derived neurotrophic factor (GDNF)

Table 6.0 ELISA-based microarray analysis of growth and neurotrophic factor in supernatant collected from co-cultured and aneurally-cultured myotubes on Day 7.

Growth factors	NMJ Co-culture (pg/mL)	SkMC only (pg/mL)	NPC only (pg/mL)	Fold change NMJ vs SkMC	Fold change NMJ vs NPCs	P-value NMJ vs SkMC	P-value NMJ vs NPCs	Log-Log regression standard curve (r^2)
AR	0.0 ± 0.0	0.0 ± 0.0	1.3 ± 1.9	0.0	0.0	0.999	0.198	0.99
BDNF	112.0 ± 54.5	8.5 ± 4.1	0.5 ± 0.1	13.12	233.98	0.002**	0.001**	0.98
bFGF	36.5 ± 3.3	4.6 ± 2.1	6.0 ± 0.7	7.88	6.04	<0.0001****	<0.0001****	0.94
BMP-4	5.8 ± 4.7	5.8 ± 4.9	6.5 ± 2.9	1.00	0.89	0.999	0.962	0.96
BMP-5	393.4 ± 285.6	481.6 ± 360.4	497.0 ± 278.1	0.82	0.79	0.891	0.854	1.00
BMP-7	3.8 ± 5.5	9.1 ± 3.3	7.8 ± 5.5	0.42	0.48	0.264	0.437	0.99
b-NGF	0.5 ± 0.4	0.2 ± 0.4	0.4 ± 0.3	2.80	1.23	0.393	0.942	0.99
EGF R	29.4 ± 4.1	47.4 ± 18.9	4.2 ± 1.1	0.62	6.99	0.085	0.020 *	1.00
EG-VEGF	0.13 ± 0.27	0.7 ± 0.2	0.4 ± 0.4	0.20	0.36	0.046	0.502	0.99
FGF-4	44.6 ± 31.2	30.8 ± 21.9	55.9 ± 45.7	1.45	0.80	0.798	0.858	1.00
FGF-7	211.7 ± 47.5	0.0 ± 0.0	0.1 ± 0.1	0.00	3683.15	<0.0001****	<0.0001****	1.00
GDF-15	328.2 ± 65.6	360.0 ± 95.8	0.9 ± 0.4	0.91	370.33	0.734	0.0001 ***	1.00
GDNF	25.5 ± 4.3	4.3 ± 1.7	1.4 ± 0.8	5.88	18.54	<0.0001***	<0.0001****	1.00
GH	2.6 ± 1.7	5.8 ± 2.9	4.9 ± 1.3	0.44	0.52	0.093	0.237	0.99
HB-EGF	0.1 ± 0.2	1.6 ± 0.9	1.1 ± 0.7	0.06	0.08	0.027*	0.115	0.97
HGF	6413.4 ± 93.1	33.9 ± 24.2	908.8 ± 93.1	189.14	7.06	<0.0001****	<0.0001****	0.99
IGFBP-1	5.1 ± 0.9	2.3 ± 1.1	0.3 ± 0.3	2.20	16.44	0.0023**	<0.0001****	1.00
IGFBP-2	7640.5 ± 517.8	34.5 ± 27.6	7908.9±1822.0	221.38	0.97	<0.0001****	0.917	1.00
IGFBP-3	11315.9 ±1269	2306.1 ± 805.6	816.8 ± 371.6	4.91	13.85	<0.0001****	<0.0001****	0.99
IGFBP-4	2393.2 ± 361.1	249.5 ± 189.2	1168.0 ± 500.1	9.59	2.05	<0.0001****	0.002 **	1.00
IGFBP-6	3952.7 ± 674.4	29.3 ± 20.3	268.0 ± 196.6	135.01	14.75	<0.0001****	<0.0001****	0.99
IGF-1	102.6 ± 57.0	77.5 ± 74.4	96.7 ± 61.7	1.32	1.06	0.810	0.988	0.98
Insulin	10239.8 ±5950	9061.4±8143.4	7462.1±3198.6	1.13	1.37	0.947	0.752	0.99
MCSF R	2.1 ± 2.5	7.5 ± 7.8	6.0 ± 4.2	0.29	0.36	0.306	0.513	0.99
NGF R	184.0 ± 30.5	67.5 ± 38.5	2.0 ± 0.6	2.73	91.12	0.0005 ***	<0.0001****	0.99
NT-3	18.9 ± 3.7	4.0 ± 4.4	4.0 ± 2.8	4.69	4.71	0.0005 ***	0.0005***	1.00
NT-4	2.7 ± 2.3	6.4 ± 3.1	2.1 ± 1.6	0.42	1.29	0.099	0.913	1.00
OPG	864.5 ± 113.1	884.2 ± 277.0	4.9 ± 2.7	0.98	175.85	0.98	0.0001***	1.00
PDGF-AA	260.7 ± 31.6	2065.3 ± 703.8	28.1 ± 18.7	0.13	9.27	0.0003 ***	0.647	1.00
PIGF	270.0 ± 37.3	79.8 ± 33.5	3.1 ± 0.6	3.39	87.15	<0.0001****	<0.0001****	0.99
SCF	7.2 ± 2.0	1.2 ± 0.9	1.9 ± 0.5	6.19	3.80	0.0002***	0.0005***	1.00
SCF R	4.6 ± 3.1	2.6 ± 2.4	9.0 ± 1.0	1.78	0.51	0.388	0.045*	1.00
TGFa	0.1 ± 0.1	0.2 ± 0.2	0.2 ± 0.2	0.39	0.53	0.539	0.694	0.89
TGFb1	2525.0 ± 1682.3	3191.2±2251.2	1520.5±1474.5	0.79	1.66	0.830	0.668	0.98
TGFb3	6.6 ± 2.3	2.7 ± 2.0	9.8 ± 4.1	2.44	0.68	0.154	0.272	0.98
VEGF	1131.6 ± 128.3	685.0 ± 215.5	3.6 ± 3.4	1.65	311.49	0.0034**	<0.0001****	0.96
VEGF R2	6.5 ± 5.7	10.2 ± 6.2	15.7 ± 2.7	0.63	0.41	0.511	0.056	1.00
VEGF R3	7.5 ± 4.3	9.5 ± 5.6	11.8 ± 1.3	0.78	0.63	0.712	0.288	0.99
VEGF-D	0.9 ± 0.2	1.0 ± 0.5	0.7 ± 0.4	0.93	1.34	0.978	0.549	0.99

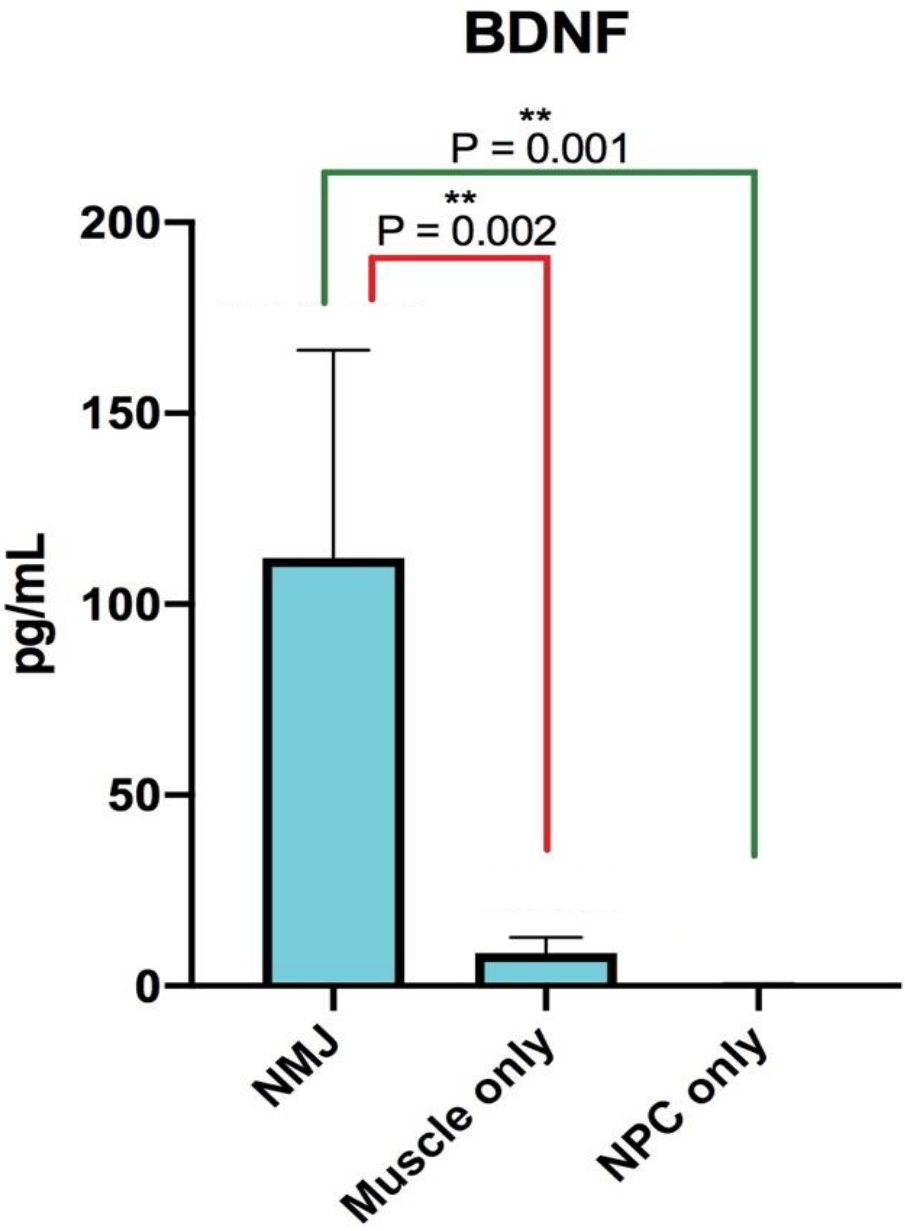

Figure 6.0 BDNF in supernatant collected from NMJ, SkMC cultured alone and NPCs cultured alone on Day 7. The above figures illustrate comparisons in the levels of the trophic factors between monoculture and CC conditions. Data is presented as a mean concentration of the trophic factor in each condition with error bars signifying ± SD. n=4 and represents the independent experiments/sample types from which the supernatant was collected. **Represents p=0.01-0.001. The red connectors indicate the comparisons between muscles only vs. co-culture conditions. The green connectors indicate the comparisons between NPC only vs. co-culture conditions.

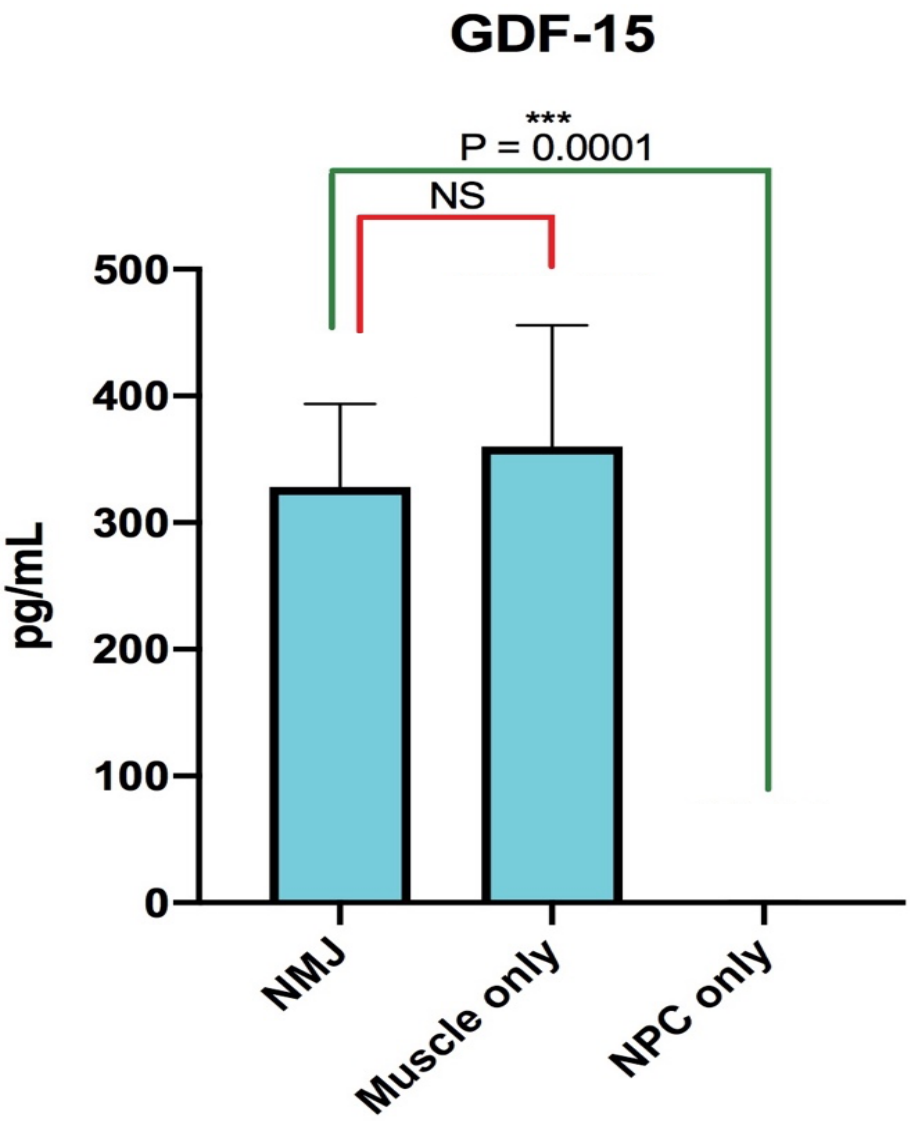

Figure 6.1 GDF-15 in supernatant collected from NMJ, SkMC cultured alone and NPCs cultured alone on Day 7. The above figures illustrate comparisons in the levels of the trophic factors between monoculture and CC conditions. Data is presented as a mean concentration of the trophic factor in each condition with error bars signifying ± SD. n=4 and represents the independent experiments/sample types from which the supernatant was collected. NS (not significant) and represents p= >0.05, ***represents p=0.001-0.0001. The red connectors indicate the comparisons between muscles only vs. co-culture conditions. The green connectors indicate the comparisons between NPC only vs. co-culture conditions.

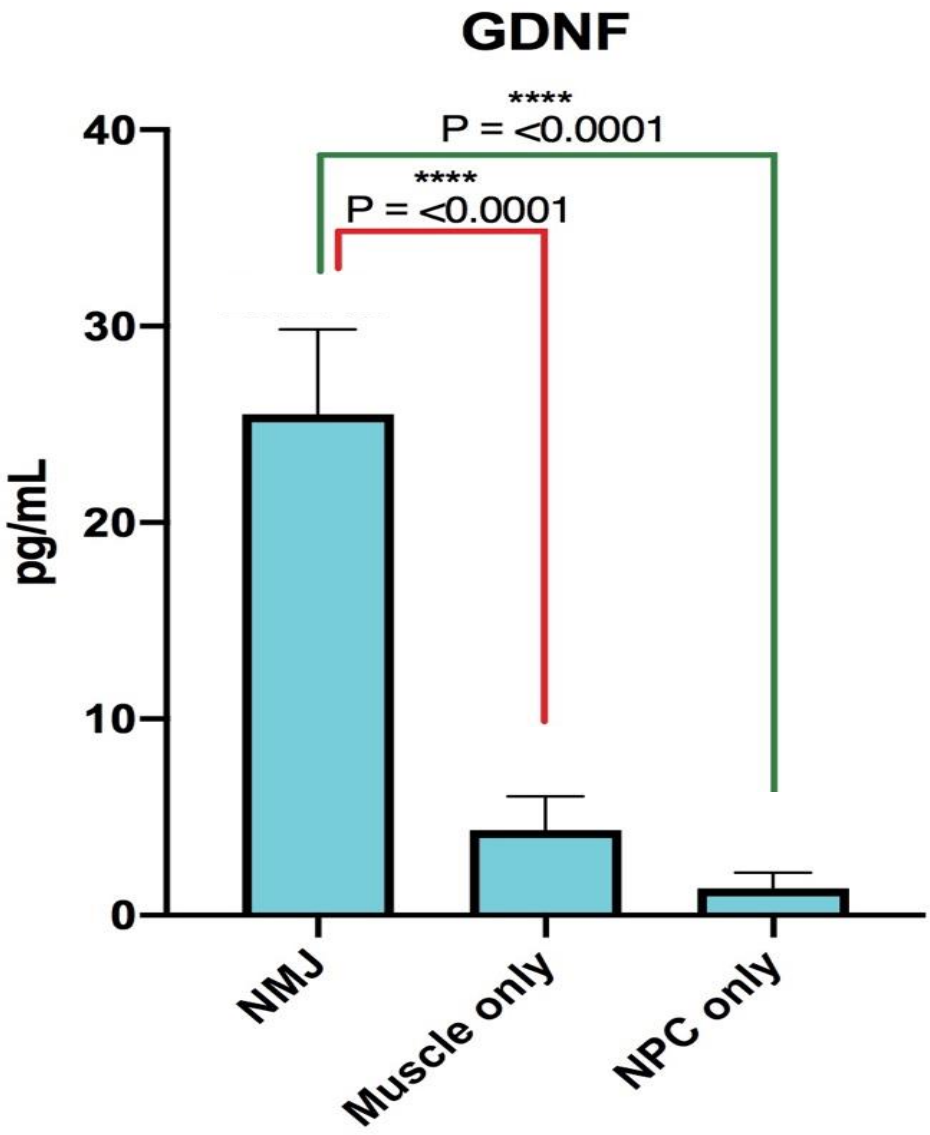

Figure 6.2 GDNF in supernatant collected from NMJ, SkMC cultured alone and NPCs cultured alone on Day 7. The above figures illustrate comparisons in the levels of the trophic factors between monoculture and CC conditions. Data is presented as a mean concentration of the trophic factor in each condition with error bars signifying ± SD. n=4 and represents the independent experiments/sample types from which the supernatant was collected. ****Represents p<0.0001. The red connectors indicate the comparisons between muscles only vs. co-culture conditions. The green connectors indicate the comparisons between NPC only vs. co-culture conditions.

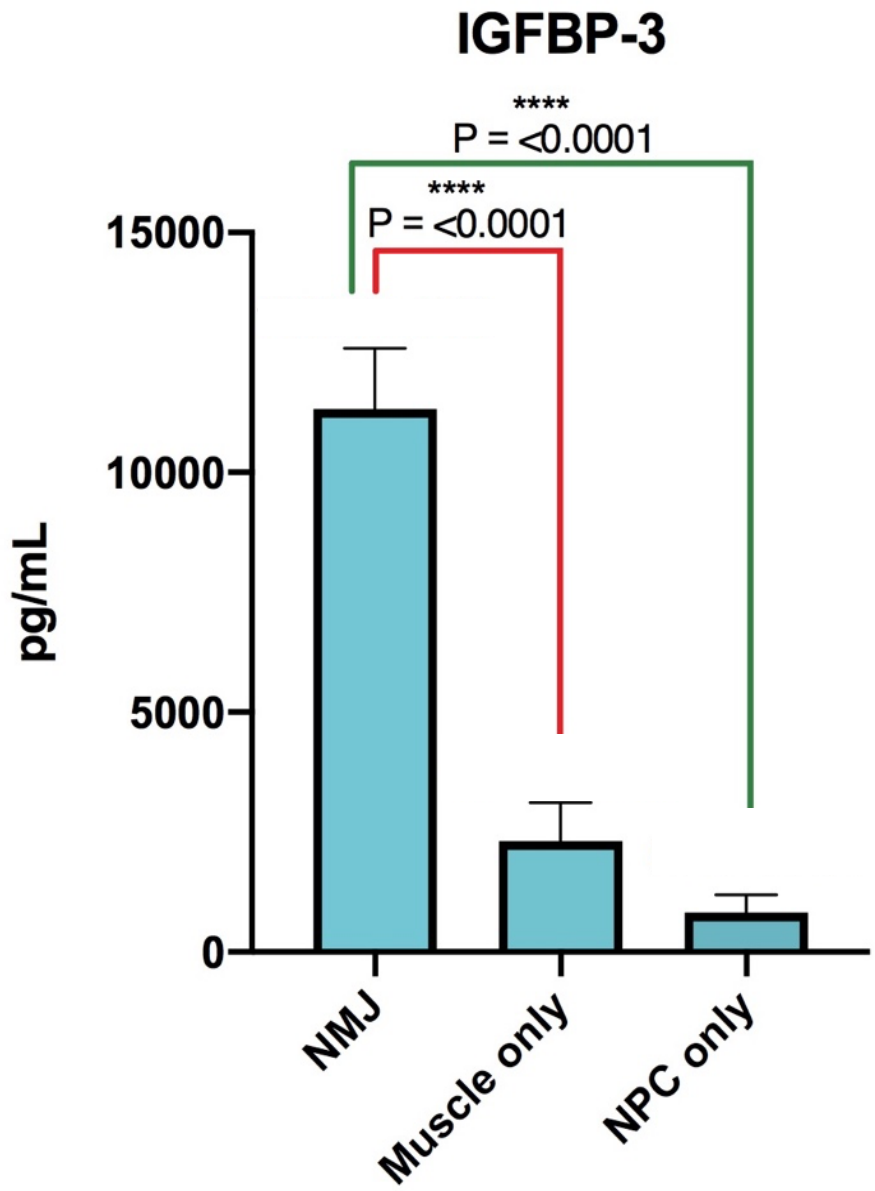

Figure 6.3 IGFBP-3 in supernatant collected from NMJ, SkMC cultured alone and NPCs cultured alone on Day 7. The above figures illustrate comparisons in the levels of the trophic factors between monoculture and CC conditions. Data is presented as a mean concentration of the trophic factor in each condition with error bars signifying ± SD. n=4 and represents the independent experiments/sample types from which the supernatant was collected. ****Represents p<0.0001. The red connectors indicate the comparisons between muscles only vs. co-culture conditions. The green connectors indicate the comparisons between NPC only vs. co-culture conditions.

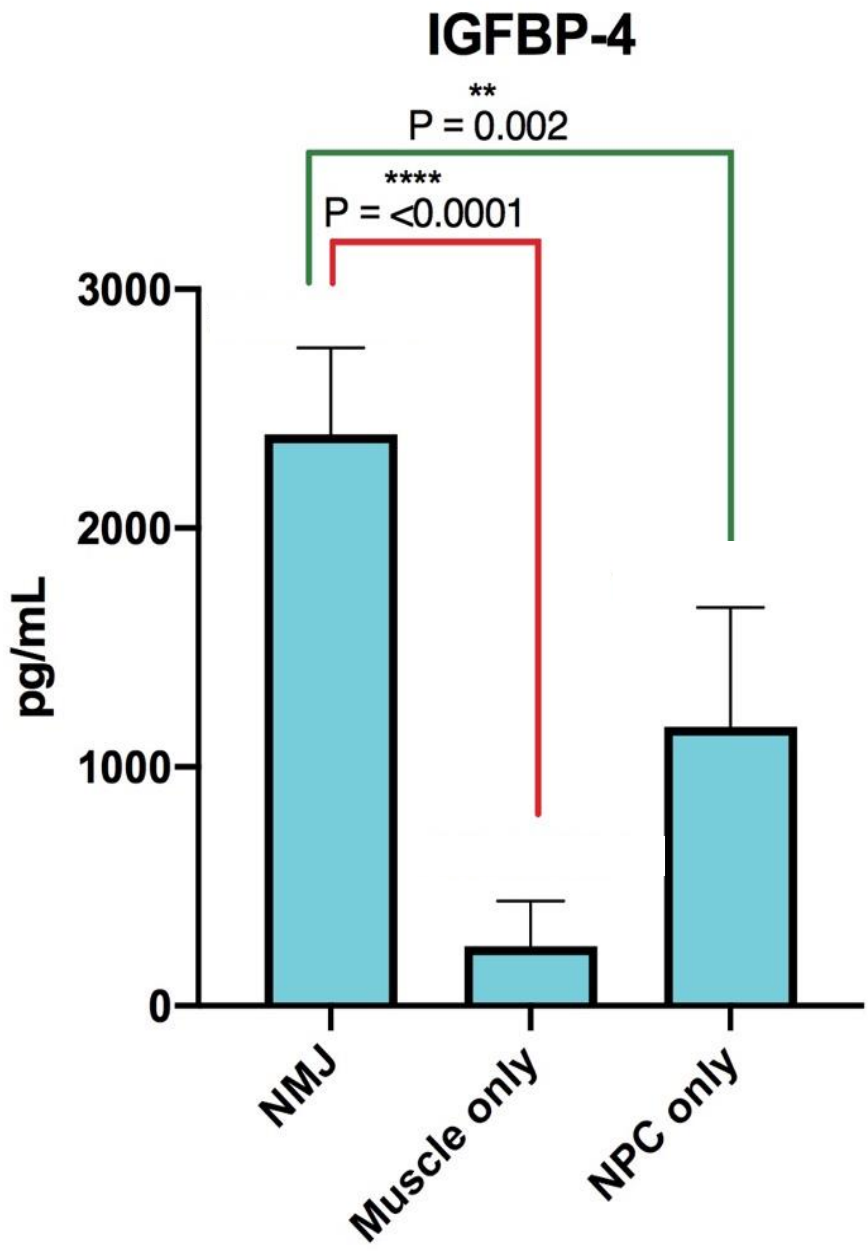

Figure 6.4 IGFBP-4 in supernatant collected from NMJ, SkMC cultured alone and NPCs cultured alone on Day 7. The above figures illustrate comparisons in the levels of the trophic factors between monoculture and CC conditions. Data is presented as a mean concentration of the trophic factor in each condition with error bars signifying ± SD. n=4 and represents the independent experiments/sample types from which the supernatant was collected. **Represents p=0.01-0.001 and ****represents p<0.0001. The red connectors indicate the comparisons between muscles only vs. co-culture conditions. The green connectors indicate the comparisons between NPC only vs. co-culture conditions.

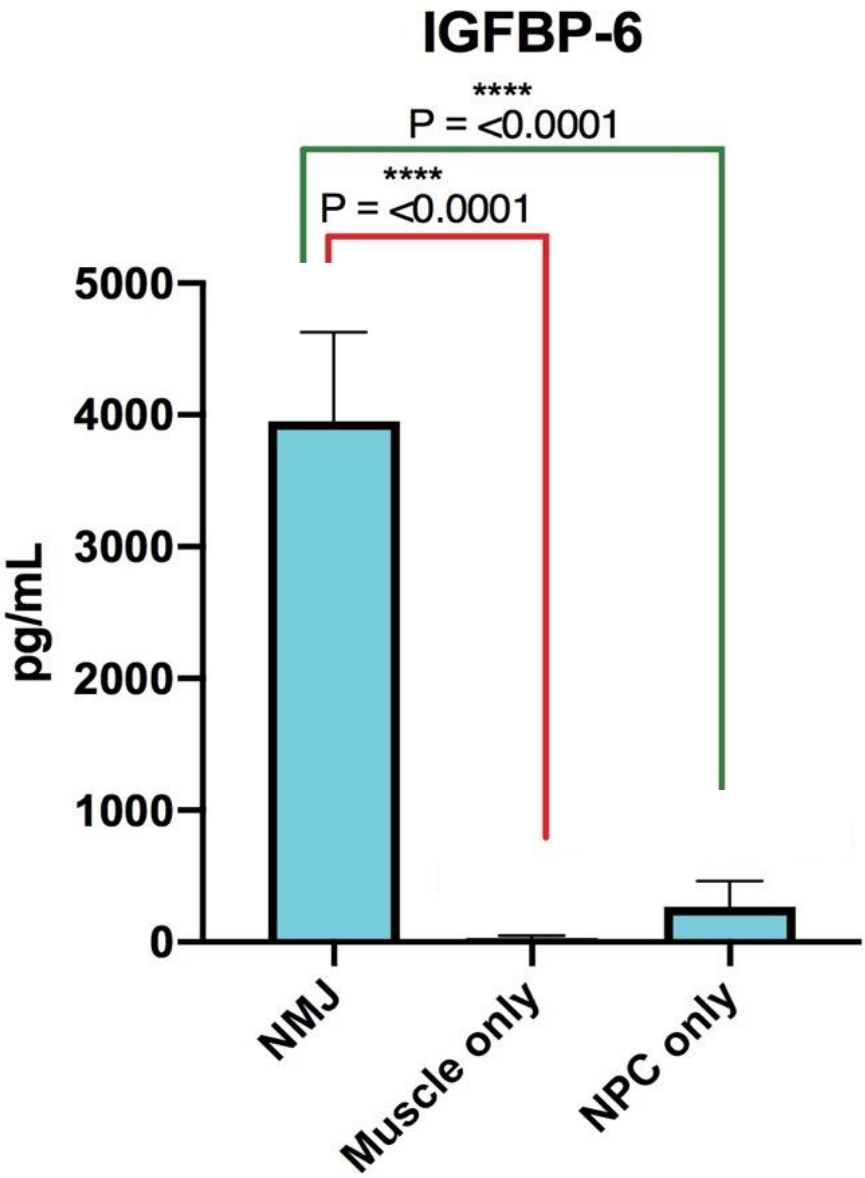

Figure 6.5 IGFBP-6 in supernatant collected from NMJ, SkMC cultured alone and NPCs cultured alone on Day 7. The above figures illustrate comparisons in the levels of the trophic factors between monoculture and CC conditions. Data is presented as a mean concentration of the trophic factor in each condition with error bars signifying ± SD. n=4 and represents the independent experiments/sample types from which the supernatant was collected. ****Represents p<0.0001. The red connectors indicate the comparisons between muscles only vs. co-culture conditions. The green connectors indicate the comparisons between NPC only vs. co-culture conditions.

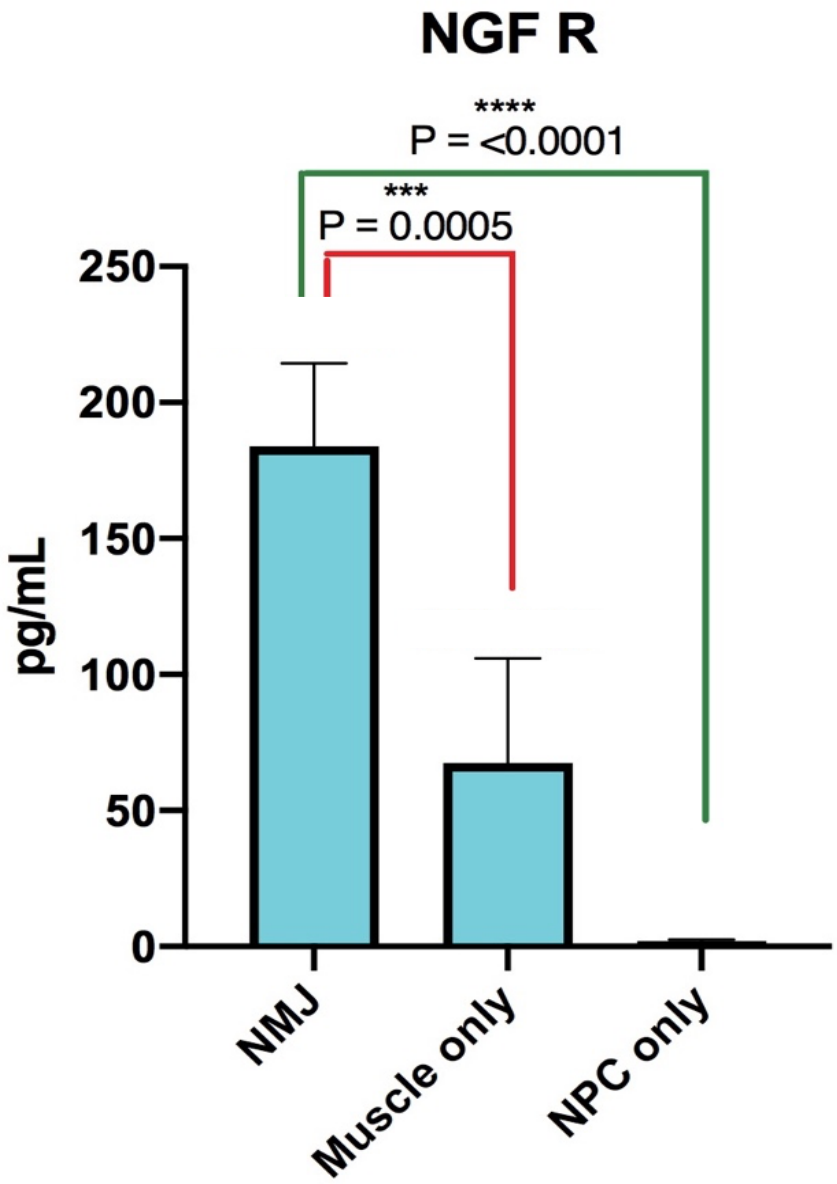

Figure 6.6 NGF R in supernatant collected from NMJ, SkMC cultured alone and NPCs cultured alone on Day 7. The above figures illustrate comparisons in the levels of the trophic factors between monoculture and CC conditions. Data is presented as a mean concentration of the trophic factor in each condition with error bars signifying ± SD. n=4 and represents the independent experiments/sample types from which the supernatant was collected.***Represents p=0.001-0.0001 and ****represents p<0.0001. The red connectors indicate the comparisons between muscles only vs. co-culture conditions. The green connectors indicate the comparisons between NPC only vs. co-culture conditions.

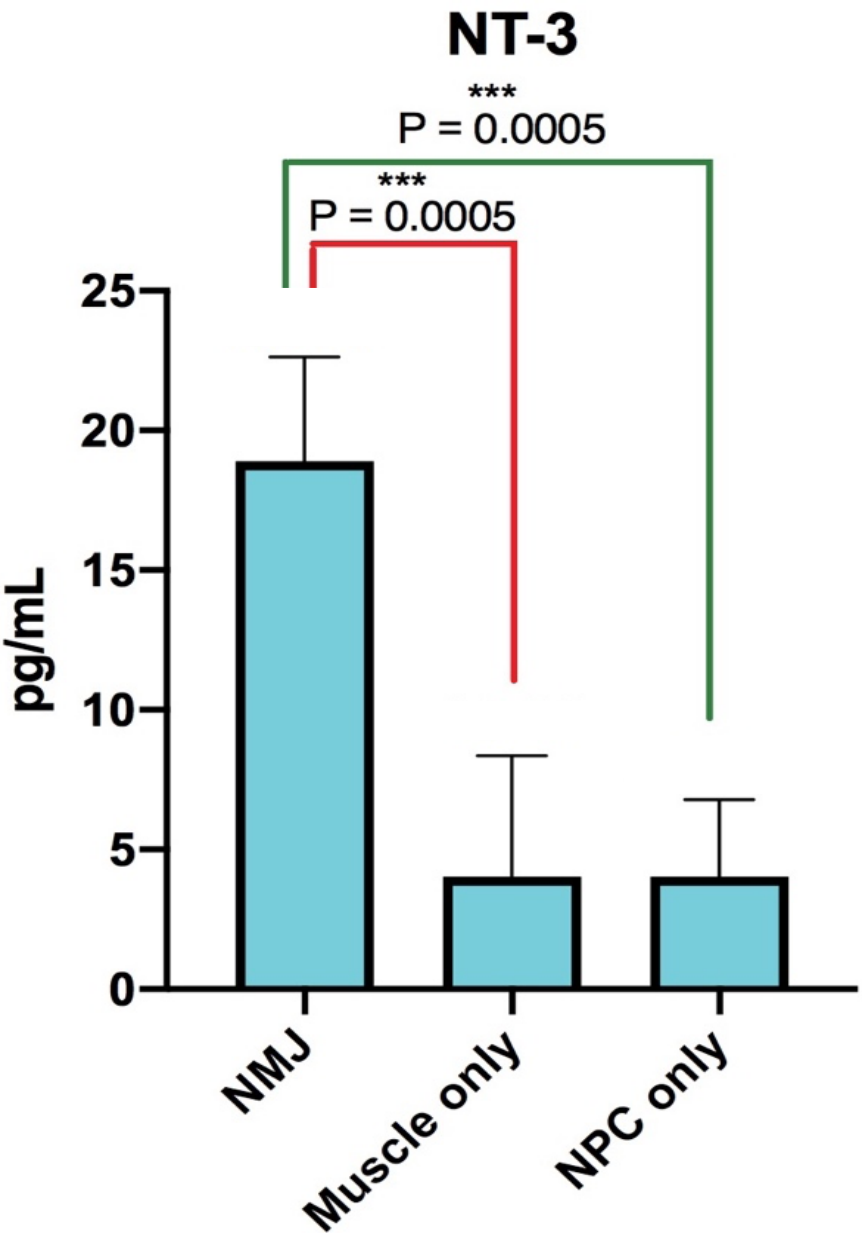

Figure 6.7 NT-3 in supernatant collected from NMJ, SkMC cultured alone and NPCs cultured alone on Day 7. The above figures illustrate comparisons in the levels of the trophic factors between monoculture and CC conditions. Data is presented as a mean concentration of the trophic factor in each condition with error bars signifying ± SD. n=4 and represents the independent experiments/sample types from which the supernatant was collected. ***Represents p=0.001-0.0001. The red connectors indicate the comparisons between muscles only vs. co-culture conditions. The green connectors indicate the comparisons between NPC only vs. co-culture conditions.

The results in this chapter shows the cross-communication system between NPCs and SkMCs and the expressed trophic factors within NMJ. Brain-derived neurotrophic factor, Insulin-like growth factor-binding protein , -3, -4, -6 , Neurotrophin-3, Growth differentiation factor -15 and Glial cell-derived neurotrophic factor were expressed which shows that there is a communication between NPCs and SkMCs hence, some of these factors didn't exist when the cells were cultured alone. Some trophic factors were expressed in higher amounts in NMJ compered to annual culture showing that NPCs and SkMCs enhance certain growth/trophic factors when co-cultured.

6.2 Discussion

Skeletal muscle and motor neurons are tissues that depend on each other, each relying on the other for synaptic stimulation/transmission and support. As a result, the denervation and reinnervation of the muscle can dramatically modify the physiology of muscles and result in the wasting of muscle (Cisterna et al., 2014).

ELISA-based protein microarrays are used for the purpose of developing an understanding of how, without exogenous neural growth factors, this co-culture model was established. This study's results deliver a numerical measurement of 40 neurotrophins and human growth factors which were created in the *in vitro* NMJ co-culture arrangement, compared with factors produced endogenously in aneurally-cultured myotubes and NPCs. The quantification of growth factors was achieved using microarray. The experiments showed *in vitro* NMJs in a co-culture growth factor arrangement. These were supported by endogenous control of precise neurotrophic or growth factors. An examination of the results from Table 6.0, shows the concentrations of several factors in NMJ formation, MN preservation, and the development

of myotubes, which were shown to be higher in the co-culture compared to cultured NPCs and aneural myotube cultures.

Research into the role played by BDNF in NMJs development proposes that the survival of MN and innervation of SkM are improved by BDNF derived from SkM. This experiment showed that BDNF were not expressed in NPCs cultured alone however a small amount were expressed in SkMCs cultured alone and more than 100pg/ml in NMJ. However, transmission at the NMJ is potentiated by BDNF (Yan et al., 1993; Zhang and Poo, 2002). Furthermore, conclusions indicate that high levels of BDNF are expressed by myoblasts during the *in vivo* development of an embryo, which downward regulates with the maturation of NMJ and SkM fibre (Griesbeck et al., 1995). Fascinatingly, studies focusing on chronic exposure to up-regulated BDNF discharged in the current co-culture arrangement permitted the physiological creation and growth of NMJs, typical of NMJ *in vivo* formation. In contrast, nerve-muscle co-culture systems established previously which need the involvement of exogenous BDNF (Das et al., 2010; Smith et al., 2013; Rumsey et al., 2010; Vilmont et al., 2016; Das et al., 2007; Puttonen et al., 2015; Guo et al., 2017; Guo et al., 2014; Guo et al., 2011), might not produce the strong NMJ establishment seen in the NMJ *in vitro* arrangement produced in this project because of inappropriate exogenous BDNF concentrations hindering the maturation of NMJ (Song & Jin, 2015).

Growth differentiation factors (GDFs) belong to a broader family of TGF-β (transforming growth factor-beta) whose role is mostly the control of development. GDF15 (sometimes referred to as non-steroidal anti-inflammatory drug-activated gene (NAG-1) or macrophage inhibitory cytokine 1 (MIC-1), is recognised as having a role to play in the control of lipolysis and tissue injury. In addition, GDF15 plays a role in all-cause mortality and mitochondrial diseases, anorexia linked to cancer, appetite regulation, and weight loss. In the skeletal

muscle, GDFs spur catabolic alterations. It is recognised that growth differentiation factors are connected to several diseases states. For instance, GDF15 has been shown to play a role as a mediator for muscle weakness acquired from an extended stay in the intensive care unit. It has also been shown to have a role in mitochondrial diseases. Therefore, GDF15 are important to examine in this model hence, by showing its existence in the NMJ model this highlights the existing communication between the cells. Furthermore, the GDF15 expression has been linked with mortality. GDNF were indicated in small amounts in NPCs culture and SkMCs culture however, more than double the amount was observed in NMJ showing that the NPCs and SkMCs enhance the expression of GDNF when cultured together. Moreover, GDF15 controls the GFRAL and receptor TGF-β receptor II in the central nervous system. In addition, it has been reported that GDF15 has an advantageous impact on the protection of the cardiac muscle and as an anti-inflammatory. The GDF15's catabolic effect in skeletal muscle could play a role via the GFRAL receptor, in the same way, it works in the central nervous systems, considering that GFRAL is also expressed in the skeletal muscle and the cultured myotubes. Moreover, there is a possibility that GDF15 has the capacity to regulate the catabolism of muscle through an intracellular contrivance which is not known, apart from the ligand-receptor interaction that is yet to be fully explained. Smad3 and FoxO1 maybe some of the GDFs-induced catabolism and oxidative stress, considering that they have been reported to have a detrimental effect on the function of the mitochondria and also prompt apoptosis. When escalated GDFs and MOS, and prompted FoxO to induce catabolism, the result could be loss of muscle fibre. Previously, it has been reported that dysfunctional apoptosis and mitochondria happen to skeletal muscle that is ageing, leading to necrotic and apoptotic fibre loss.

It has been concluded that the GDNF expression is evident in numerous cells and tissues outside the CNS, including Schwann cells and skeletal muscle (Keller-Peck et al., 2001; Baudet et al., 2008). The reults in this chapter showed that GDNF were expressed at a level of more than 5pg/ml in SkMCs cultured alone. Studies done earlier have concluded that GDNF plays a crucial role in sustaining motoneurons in the myogenesis process and also controls the postnatal alteration to single innervation from multi-innervation. Generally, it looks like GDNF expression escalates during the early stages of myogenesis and becomes almost non-existent in skeletal muscle which is mature. A study done more recently has demonstrated with more clarity that the GDNF protein and mRNA exist in both fast-type EDL muscles and slow-type soleus, particularly the latter (Wang et al., 2002) .

From the results obtained from the microarray, it can be seen that there is an elevation of GDNF in the co-cultures to myotube monocultures. GDNF has been noted as a crucial factor that is extremely effective for the survival of MN *in vitro* (Oppenheim et al., 1995). Interestingly GDNF is another illustration of a target-derived factor expressed by SkM with RET tyrosine kinase, it receptor expressed in MNs (Baudet et al., (2008). In the cranial MNs of mice, the conditional ablating of RET tyrosine kinase produces noticeable interruptions to the maturation of MNs and the size of MEP at NMJs is reduced (Baudet et al., 2008).

From experiments using frogs that aimed to produce a nerve-muscle co-culture system, it was concluded that there was an increase in spontaneous synaptic amplitude and frequency in instances where GDNF was used to treat the co-cultures. This is a result that shows the potential role played by GDNF as a retrograde signalling factor (Wang et al., 2002). In addition, research conducted using transgenic mice overexpressing GDNF derived from SkM show a hyper innervation of NMJs (Nguyen et al., 1998). Another study by Keller-Peck et al. (2001) also came to the conclusion that there was motor unit amplification, NMJ hyperinnervation,

and slower eradication of synapse when mice were injected with GDNF in postnatal life. What these conclusions seem to imply is that GDNF derived from SkM has a vital role to play in controlling the maturation of MNT at the NMJ. For this reason, it can be said that the GDNF seen in the co-culture arrangement that this project describes is proof or interaction between pre- and post-synaptic elements of NMJs in the arrangement.

Remarkably, the concentration of five insulin-like growth factor binding proteins (IGFBP -3, -4, -6) that the microarray experiments examined were significantly higher in co-cultures. The main function done by IGFBPs is that of membrane transporter proteins for IGF-1, with nearly every IGF-1 being attached to at least of the seven members of the IGFBP superfamily (Hwa et al., 1999). The superfamily's most common protein is the IGFBP-3, which binds to IGF-1 at a ratio of 1:1. It binds at ~80% of circulating IGF-1 (Adachi et al., 2017). It can be noted that the existence of IGFBP was the leading IGF detected in the monocultures and co-cultures when a comparison was made to other IGFBPs measured during the array experiment. Research into how circulating IGFs are affected by IGFBPs conclude that the activity of the IGFBPs enhances IGF-1 bioavailability (Stewart at al. 1993). For this reason, it can be said that the detected IGFBP up-regulation in the co-culture arrangement backs the notion that the interface between SkMCs and nerve in the arrangement produces the factors required for MN maturation, advanced myofiber differentiation, and production of robust NMJ, illustrative of *in vivo* formation.

The reason why SkM is of specific interest is that it plays the role of a copious source neurotrophic support right across growth (Carrasco & English, 2003). Moreover, there are several neurotrophin receptors expressed by skeletal muscle, making available a foundation for neurotrophin signalling in the muscle section (Chevrel et al., 2006). As can be expected, neurotrophin knockout mice usually show distinctive flaws in both the growth and function

of the muscle. It has also been concluded that neurotrophin- (NT-) 4/5 plays a role in the changes that occur in muscle fibre, the formation of NT-3 muscle spindle, NGF dystrophic muscle pathology. As observed in this experiment NT-3 was expressed in both annually cultured NPCs and SkMCs however, reults indicated more than double the amount observed in NMJ co-culture.

The expression of NT-4/5 depends on neuromuscular synapses activity. In skeletal muscle, the electrical prompting of motor nerves improved the expression of NT-4/5 (Belluardo et al., 2001). Notwithstanding the fact that the expression of NT-4/5 seems to be comparatively robust in skeletal muscle of grown rates, numerous studies, including the present one propose that NT-4/5 expression depends on the type of fibre (Gonzalez et al., 1999; Woolley et al., 2005) In one study, it was concluded that NT-4/5 was evenly distributed in both types of muscle in humans (Mantilla et al., 2004). Yet, another study that used in situ hybridisation and immunohistochemistry came to the conclusion that NT-4/5 was expressed selectively in slow-twitch mice fibres. To the contrary, the Western blot analysis (Sheard et al.,2010) we conduct shows elevated NT-4/5 expression in fast type (tibialis anterior, extensor digitorum longus, gastrocnemius) as opposed to slow-type (soleus) muscles. From the immunohistochemical analysis, NT-4/5 protein in vesicle-type arrangements that are distributed diffusely in the muscle fibres cytosol in the inner tibialis muscle is revealed. On the fringes of the soleus muscle fibres, low degrees of NT-4/5 immunoreactivity were also noted. Furthermore, from a study using Fisher 344 rats, Carrasco and English (Sheard et al.,2010) came to the conclusion that the injection of 1.5g of NT-4/5 into the neonates soleus muscle resulted in the significant acceleration of the normal fast-to-slow myosin heavy chain (MHC) isoform change. This change was prevented from happening by the endogenous NT-

4/5 appropriation using TrkB-IgG. Interestingly, administering an additional TrkB ligand had no impact on the standard process of change in this muscle.

In their study (Sheard et al.,2010), the NT-4/5 mRNA developmental up-regulation in soleus muscle fibres of rats happened earlier in comparison to the MHCI mRNA expression up-regulation linked to the transformation of muscle fibre. What this finding shows is that the expression of NT-4/5 protein is more abundant in the soleus muscle due to the slow-type features. Notwithstanding the reality that the expression pattern of NT-4/5 seems to vary based on animal species and with growth in the postnatal stage, NT-5/5 plays a vital role in sustaining numerous functions, such as the survival of motoneuron, conversion of type of fibre, and the NMJ formation, in skeletal muscle.

It was also noted that NT-3 was elevated significantly in comparison to cultured NPCs and myotube cultures. It has been demonstrated from studies that NT-3 is a crucial synaptic development and function modulator, and is also needed for sustaining post-synaptic and presynaptic apparatus at the NMJ (Belluardo et al., 2001; Gonzalez et al., 1999). Research using NT-3 deficient mice to explore the NM system and NMJs development noted decreases in somal size, even though the αMNs number seemed to develop as expected (Woolley et al., 1999). Supplementary studies revealed reductions in the innervation of MEPs by MNTs and a reduction in the quantities of SkM fibres in NT-3-deficient mice at birth, with a fatal loss of MNTs in the postnatal development Day 7 and total denervation hind limb muscles, and no NMJ was observed to remain in the all the zones of the SkM endplate (Woolley et al., 2005). Moreover, it was noted that mice with reduced NT-3 due to haplo-insufficiency show impairment in the maturation of MNT, lowered synaptic vesicles recycling, and reduction in the diameter of SkM fibre (Sheard et al., 2010). Based on these studies, it could be deduced

that significant elevation in NT-3 expression detected in the co-culture arrangement was as a result of NMJ formation, development, and synaptic activity.

6.3 Conclusion

This report has delivered an analysis of the concentration of 40 human neurotrophins and growth factors in the *in vitro* NMJ system produced from C25 co-cultured NPCs. Results show increased concentrations of 8 factors involved with the development of SkM, MN, and NMJ in the co-culture arrangement, delivering proof the NMJ produced *in vitro* in this project were characteristic of conditions *in vivo*. Finally, the results from the experiments described in this chapter deliver vital understandings regarding this streamlined co-culture arrangement's cellular signalling. In addition, the results show that the co-culture system has the capability to endogenously regulate the formation and development of NMJ, and also make available conditions that permit for the advanced *in vitro* immortalised human myotubes differentiation, through the specific expression of essential neurotrophins and growth factors.

Chapter 7: Establishing physiologically diabetes-specific NMJ platform

7.0 Background

To the best of my knowledge literature on the effect of diabetic myopathy and neuropathy on NMJ modelling as well as muscle function, solely utilising NMJ human co-culture model does not exist. Therefore, the present study seeks to contribute to current efforts to create a novel model that would have significant place within diabetes investigation research.

7.0.0 Introduction

In diabetes, persistent hyperglycaemia induces non-enzymatic reactions (glucose & proteins) forming AGEs which is the primary initiating signals that activates all other pathways of tissue damage associated with diabetes complications through the alteration of the bidirectional communications between muscle and nerve (Chiu et al., 2016). AGEs trigger diabetic impediments in three different processes. First, glycated proteins are rendered dysfunctional through disruption of molecular confirmation, and altering receptor functionality (Yonekura et al., 2005). Secondly, AGEs can form crosslinks intracellularly and extracellularly with various molecules other than proteins, such as nucleic acids and lipids, prompting the advancement of diabetic impairments. Disruption of axonal transmission is one of the characteristics of degenerative nerve fibres, which can be observed as a consequence of glycation alteration of neurofilament and tubulin (Williams et al., 1982). There is evidence suggesting that AGEs aggregation in muscles results in loss of muscle mass, muscle strength, and regenerative muscle abilities (Chiu et al., 2016). Third, the interaction of AGEs with certain receptors in the plasma membrane (known as RAGE) leads to activation of intracellular signalling (NF-κB), which promotes secretion of pro-inflammatory molecules, expression of genes, and eventual development of free radical acids (Singh et al., 2014). The chronic inflammation signals,

initiated by AGE/RAGE carry out the process of diabetes complications initiation, allowing the constitution of a microenvironment that initiates an inflammatory niche. My studies would do much to explore the role of AGEs on soluble factors secretion by motor neuron and muscle during NMJ formation.

Despite decades of diabetes research using animal models and *in vitro* systems no single platform is able to accurately represent T2D, hence diabetic complications remain irreversible. This is mainly due to a failure of the *in vivo* and *in vitro* models (e.g. animal models) to reflect the extremely complex process of human diabetes and its (disease) progression. Therefore, there is a clear unmet need to develop a physiologically relevant *in vitro* NMJ platform to investigate

the specific pathological role of AGEs in cross-talk between muscle and motor neurons in diabetes.

With this goal in mind, this project examines the impact of different concentrations of AGEs on skeletal muscle, specifically the impact on myogenic morphology and differentiation, by developing an operational *in vitro* human model. Additionally, sophisticated co-culture model developed in this project, which simulates *in vivo* human NMJ platform, will be employed (see Figure 1.15). Insofar as my knowledge, this is the pioneer study conducted that uses only wholly pertinent NMJs human model to examine diabetic myopathy and neuropathy. Therefore, this platform brings substantial opportunities for advancement of clinically relevant *in vitro* models of neuromuscular illnesses.

7.0.3 Aims and objectives

To establish a preclinical proof of concept diabetes platform, the co-cultured cells were treated with AGEs to test if they evoked similar deficits to a patient *in vivo*. Therefore, the overall aim was to validate the NMJ system as diabetic specific-model and map out the effects of AGEs on growth factors produced endogenously from the bi-directional communication of SkMCs and NPCs in the co-culture., In this chapter, the effects of a diabetic microenvironment on muscle function, neural progenitor cells differentiation, NMJ integrity and *in vitro* functionality were examined.

The main objectives are:

- Treatment of NMJ system with different concentrations of AGE (50-200 µg/ml).
- Investigate the impact of AGEs on myoblast and NPCs differentiation
- Investigate the effects of AGEs on growth factors produced endogenously from the crosstalk in NMJ platform between of SkMCs and NPCs

7.1 Results

7.1.1 Effects of AGEs on morphological phenotypic of co-cultured cells

NMJs co-culture model was subjected to 50-200µg/ml of AGEs and the control BSA over 7 days of differentiation. starting at a concentration of 50 g/ml, consistent with previous research (Chiu *et al*., 2015; Matou-Nasri *et al*., 2017) and progressing to 100 g/ml, 150 g/ml and 200 g/ml. As a control, BSA was also diluted in DM at concentrations of 150 g/ml and 200 g/ml (dependent on the highest concentration of AGEs used in the present experiment).

AGEs was added with the differentiation media on the first day of co-culture. Subsequently, staining of the myotubes using Texas Red-X Palloidin and ADPI was performed. The fluorescence immunohistochemistry imaging revealed healthy myotubes formation with aligned nuclei in co-culture subjected to the control BSA, while significant myotubes morphological malformations with characteristic increase in myotube area and centrally aggregated nuclei was detected in all treated myotubes (50-200 µg/ml) as illustrated by the white arrows in Figure 7.0; image A1, B1, C1, & E1. Additionally, in treated NMJs system, minor differentiation of motor neurons with shorter axonal formation was detected as illustrated by the red arrows in Figure 7.0; image A2, B2, C2 & E2. In sum, these images portray substantial muscle morphological malformations, centrally clumped nuclei, shorter axonal formation, and diminished motor neurons differentiation compared with controls.

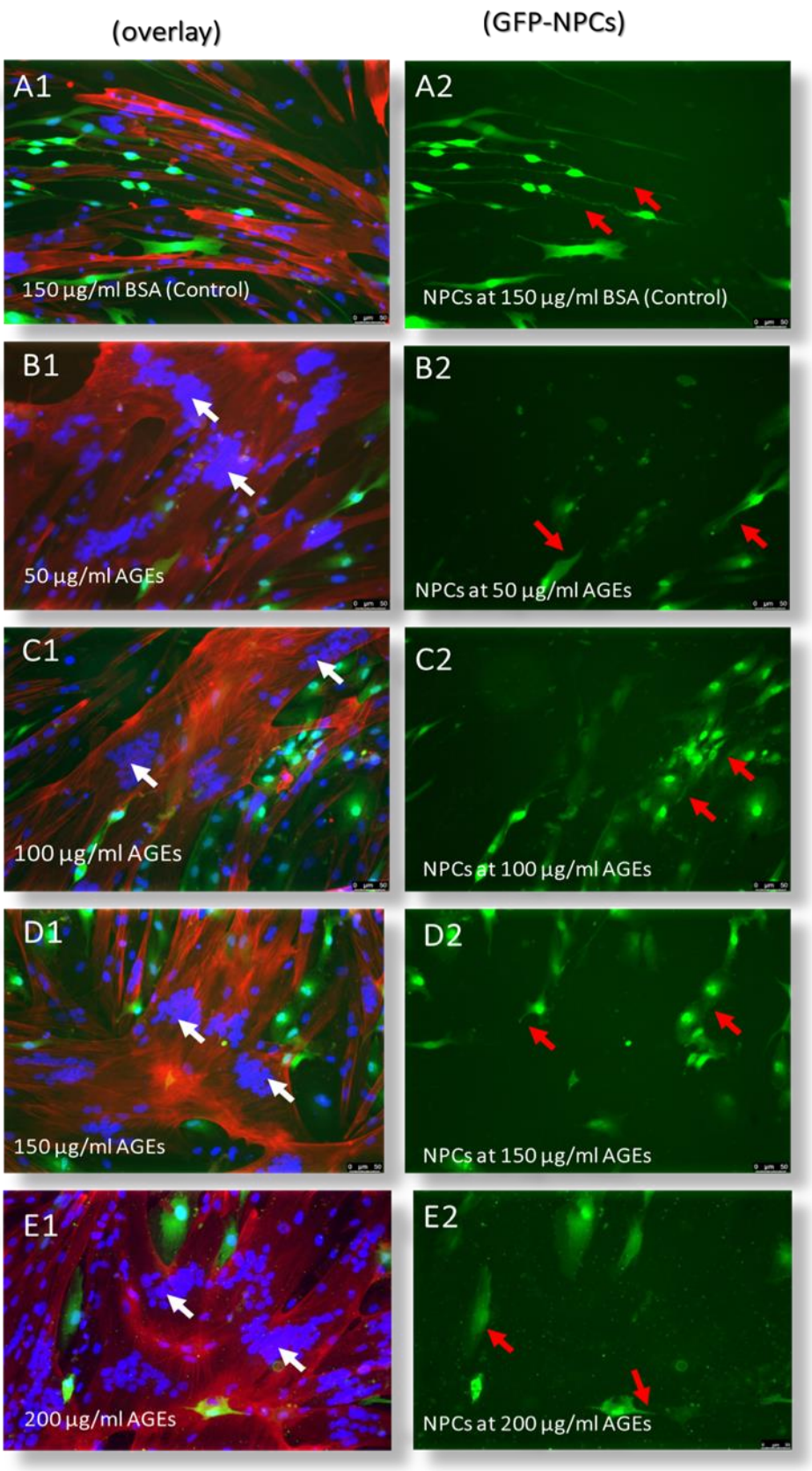
(overlay)
(GFP-NPCs)
A1
150 µg/ml BSA (Control)
A2
NPCs at 150 µg/ml BSA (Control)
B1
50 µg/ml AGEs
B2
NPCs at 50 µg/ml AGEs
C1
100 µg/ml AGEs
C2
NPCs at 100 µg/ml AGEs
D1
150 µg/ml AGEs
D2
NPCs at 150 µg/ml AGEs
E1
200 µg/ml AGEs
E2
NPCs at 200 µg/ml AGEs

Figure 7.0 SkMC co-culture morphological characterisation at day 7 of differentiation following AGEs treatments with different AGEs concentrations and a control group. Image A1, B1, C1, D1 and E1 of overlay panel illustrates representative overlay of co-culture showing morphological differentiation treated with the control BSA (150 mg/ml), AGEs 50, 100, 150 and 200 mg/ml respectively. Myotubes stained with Texas Red-X Phalloidin (red) and nucleus stained with DAPI (blue). Image A2, B2, C2, D2 and E2 of GFP-NPCs panel show GFP-NPCs (green) from the overlaid images. The fluorescence immunohistochemistry imaging showed normal myotubes formation with aligned nuclei in co-culture treated with BSA (A1), while significant myotubes morphological abnormalities with distinct increase in myotube area and centrally clustering nuclei (white arrow) was observed in AGEs treated myotubes (B1C1,D1 and E1). Less differentiation of motoneurons with shorter axonal formation (red arrow) were observed (B2,C2,D2 and E2) compared to control (A2). Images were captured at x20 magnification consisting of at least five random fields of view selected.

7.1.2 Measurement of motor neuron axonal length in co-culture (nerve-muscle)

The axonal length of differentiated motor neurons *in vitro* nerve-muscle co-culture subjected to AGEs were measured over 7 days, analysed with repeated measures ANOVA. The extent of differentiation of motor neurons with regards to AGEs (50-200 μg/ml) treatments or BSA (150 μg/ml) and DM as controls was specified using the measure axonal length (μm) in every 24 hours interval. Owing to inadequate data, 200 μg/ml AGEs treatment data was excluded for the first six days.

In the first set of analysis, the axonal length obtained on the first day exhibited minor variance with decreased axonal length although no statistical significant overall was detected within 24 hours of differentiation. Axonal length in AGE treated media was compared to Baseline treated co-culture. Conversely, the axonal length obtained on the seventh day exhibited significant difference with substantial decrease in axonal length as illustrated by the red arrows in panel (B) Figure 7.1. All concentrations of AGE treatments registered statistically

significant difference relative with Baseline. A split plot ANOVA was performed with Bonferroni post hoc pairwise comparisons showing P values <0.0001 (Figure 7.1).

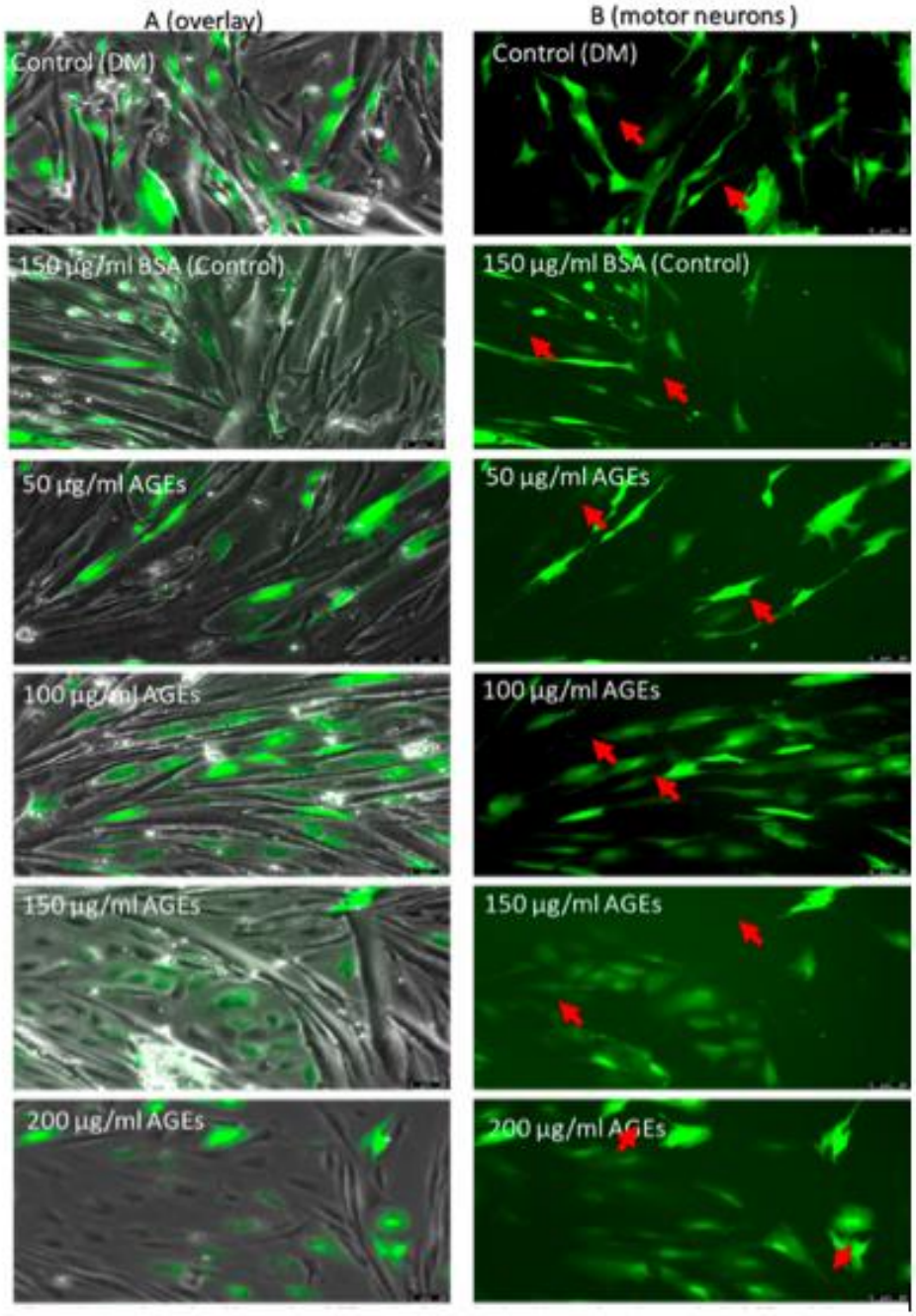

Figure 7.1 Axonal growth and innervation of differentiated myotubes in AGE treated co-culture at day 7 of differentiation. Image Panel (A) display the overlay of representative morphology of SkMC myotube (grey) and GFP-motor neurons (green) in co-culture for DM and BSA 150µg/ml controls, AGE treatments (50, 100, and 150µg/ml) at day 7 of culture. Additionally, image panel (B) show morphology of GFP-motor neurons (green) for the same concentrations from the overlaid images of panel (A). significant decrease in axonal length (red arrow) was observed on day 7 of culture in AGE treated cells compered to control groups. Images were captured at x20 magnification.

Lastly, the axonal length of differentiated motor neurons was quantified at each time interval over the seven days of culture for all treatments (Figure 7.2). Additionally, cells subjected to AGE treatment exhibited significant variation in axonal length compared to controls DM and BSA. The axonal length decreased concentration of AGEs treatment over the 7 days culture period. Repeated measures ANOVA was performed for 7 days measurements in one cell culture type. A series of spANOVA with Bonferroni post hoc pairwise comparison was performed comparing each measurement from the different days with the start point (day 0). The obtained P value for 50, 100, 150 µg/ml was ≤ 0.013.

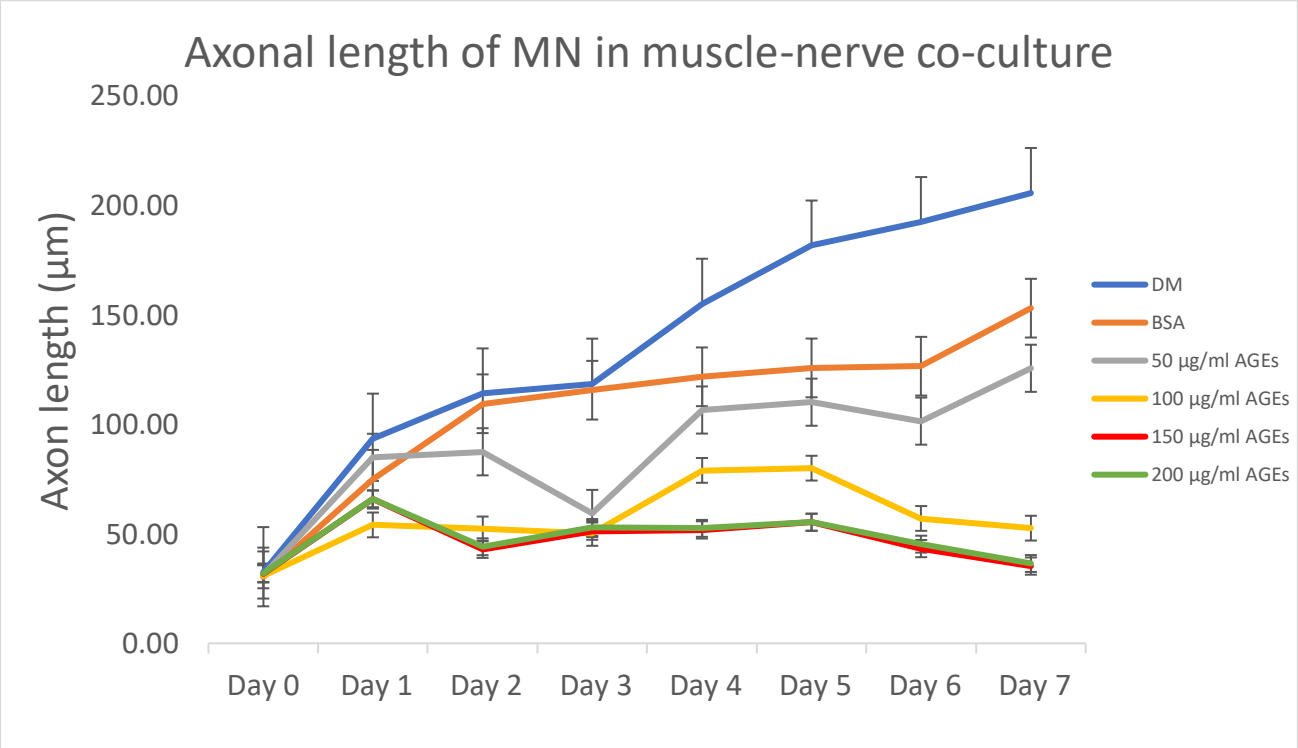

Figure 7.2 Quantitative analysis of axonal length in SkMC co-culture over 7 days of differentiation. Four images taken from a representative co-culture and were analysed for axonal length (mm) on Y-axis vs the differentiation time (in days) on X-axis with respect to different concentrations of AGEs treatments in co-culture. The axonal length decresed with increased concentration of AGEs treatment compared to the controls DM and BSA over the 7 days in *vitro* co-culture ($p<0.013$). Data presented as mean of each condition with error bars ± SD. n= 10. P= .0.05.

7.1.3 Impacts of AGEs on the cross communication between motor neurons and myotubes and microenvironment constituents

To understand how the phenotypic changes in the above figures (Figure 7.0-7.2) were induced, the cross-talk between MN and myotubes and endogenously secreted growth factors in the microenvironment were investigated. On the seventh day the supernatants of both co-culture models were collected to compare the levels of neural/growth factors (NGFs) produced endogenously (40 NGFs) using ELISA-based quantitative microarray. The results revealed that eight of the growth factors studied experienced substantial change ($P<0.05$) between the AGE- and BSA (150 µg/ml)-subjected co-culture models (summarised in Table 7.0). IGF-1 reduced significantly, accounting for 17.4 fewer folds in the co-culture model subjected to AGE treatment. The second-largest decrease was NT-3, which was about 6.8 folds fewer in the co-culture subjected to AGE-treatment. GDNF registered a considerable reduction in folds (-5) in the co-culture subjected to AGE treatment. A substantial reduction in IGFBP-3 of up to 2 folds in the co-culture subjected to AGE treatment was observed. All detected growth factors were reduced (Table 7.0).

Table 7.0. QAH-GF-1 analysis of the GNFs in the supernatants of both co-culture models

	150µg/ml BSA treated co-culture	150µg/ml AGEs treated co-culture	Fold change	P-value	Standard curve (r^2)
AR	0.00 ± 0.00	0.25 ± 0.51	0.00	0.36	0.827
BDNF	112.01 ± 54.50	29.78 ± 34.45	3.76	0.04	0.941
bFGF	36.45 ± 3.28	18.56 ± 10.93	1.96	0.02	0.998
BMP-4	5.80 ± 4.74	1.45 ± 1.02	3.99	0.12	0.999
BMP-5	393.40 ± 285.57	2.80 ± 5.60	140.49	0.03	0.941
BMP-7	3.77 ± 5.46	0.04 ± 0.07	106.03	0.22	0.967
b-NGF	0.50 ± 0.43	0.12 ± 0.20	4.29	0.15	0.998
EGF	0.05 ± 0.01	0.18 ± 0.26	0.29	0.37	0.965
EGF R	29.36 ± 4.05	23.99 ± 13.40	1.22	0.47	0.956
EG-VEGF	0.13 ± 0.27	0.01 ± 0.01	22.33	0.38	0.998
FGF-4	44.64 ± 31.23	18.09 ± 12.18	2.47	0.16	0.997
FGF-7	211.65 ± 47.54	41.58 ± 48.52	5.09	0.00	0.998
GDF-15	328.23 ± 65.59	171.02 ± 92.13	1.92	0.03	0.97
GDNF	25.48 ± 4.34	5.10 ± 5.79	4.99	0.00	0.87
GH	2.58 ± 1.67	0.42 ± 0.74	6.17	0.06	0.996
HB-EGF	0.09 ± 0.19	0.22 ± 0.30	0.43	0.51	0.999
HGF	6413.35 ± 93.09	1968.96 ± 1939.54	3.26	0.00	0.981
IGFBP-1	5.05 ± 0.92	1.78 ± 0.61	2.84	0.00	0.9997
IGFBP-2	7640.45 ± 517.78	5587.73 ± 469.34	1.37	0.00	0.936
IGFBP-3	11315.87 ± 1269.47	4334.02 ± 4663.60	2.61	0.03	0.999
IGFBP-4	2393.25 ± 361.13	1160.80 ± 493.26	2.06	0.01	0.962
IGFBP-6	3952.69 ± 674.41	1471.39 ± 1432.16	2.69	0.02	0.9995
IGF-1	102.62 ± 57.04	5.87 ± 4.52	17.48	0.01	0.9898
Insulin	10239.78 ± 5950.67	5292.31 ± 2264.28	1.93	0.17	0.993
MCSF R	2.14 ± 2.48	0.48 ± 0.70	4.50	0.24	0.984
NGF R	184.01 ± 30.51	57.96 ± 55.21	3.17	0.01	0.996
NT-3	18.91 ± 3.74	2.76 ± 2.36	6.84	0.00	0.978
NT-4	2.69 ± 2.26	1.32 ± 0.73	2.04	0.29	0.999
OPG	864.46 ± 113.11	385.21 ± 141.23	2.24	0.00	0.93
PDGF-AA	260.68 ± 31.63	220.20 ± 185.10	1.18	0.68	0.98
PIGF	270.02 ± 37.28	81.18 ± 73.38	3.33	0.00	0.9998
SCF	7.24 ± 2.01	2.28 ± 1.27	3.17	0.01	0.71
SCF R	4.64 ± 3.06	1.87 ± 1.45	2.48	0.15	0.99
TGFa	0.09 ± 0.06	0.00 ± 0.00	88.59	0.02	0.96
TGFb1	2524.98 ± 1682.32	0.00 ± 0.00	#DIV/0!	0.02	0.92
TGFb3	6.64 ± 2.30	2.01 ± 2.45	3.31	0.03	0.996
VEGF	1131.60 ± 128.28	731.88 ± 102.40	1.55	0.00	0.995

VEGF R2	6.45 ± 5.73	1.38 ± 1.42	4.67	0.14	0.999
VEGF R3	7.46 ± 4.33	2.38 ± 2.39	3.13	0.09	0.83
VEGF-D	0.91 ± 0.20	0.14 ± 0.12	6.49	0.00	0.94

It was decided to focus on eight growth factors (listed below), seen as important factors to consider.

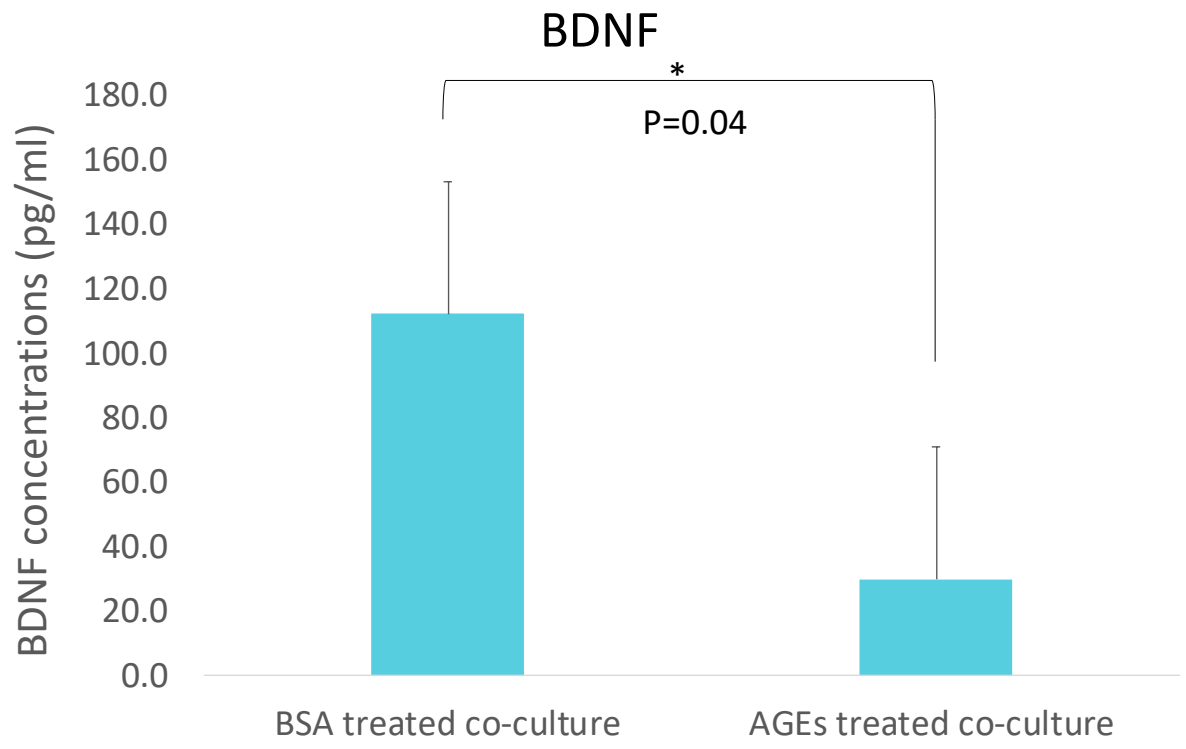

Figure 7.3 BDNF in supernatant collected from BSA treated co-culture and AGEs treated co-culture on day 7 of co-culture. The above figures illustrate comparisons in the levels of the trophic factors between BSA treated and AGEs treated co-culture.. Data is presented as a mean concentration of the trophic factor in each condition with error bars signifying ± SD. n=4 and represents the independent experiments/sample types from which the supernatant was collected. *Represents p=0.05-0.01. The connectors indicate the comparisons between AGE treated co-culture vs. co-culture conditions.

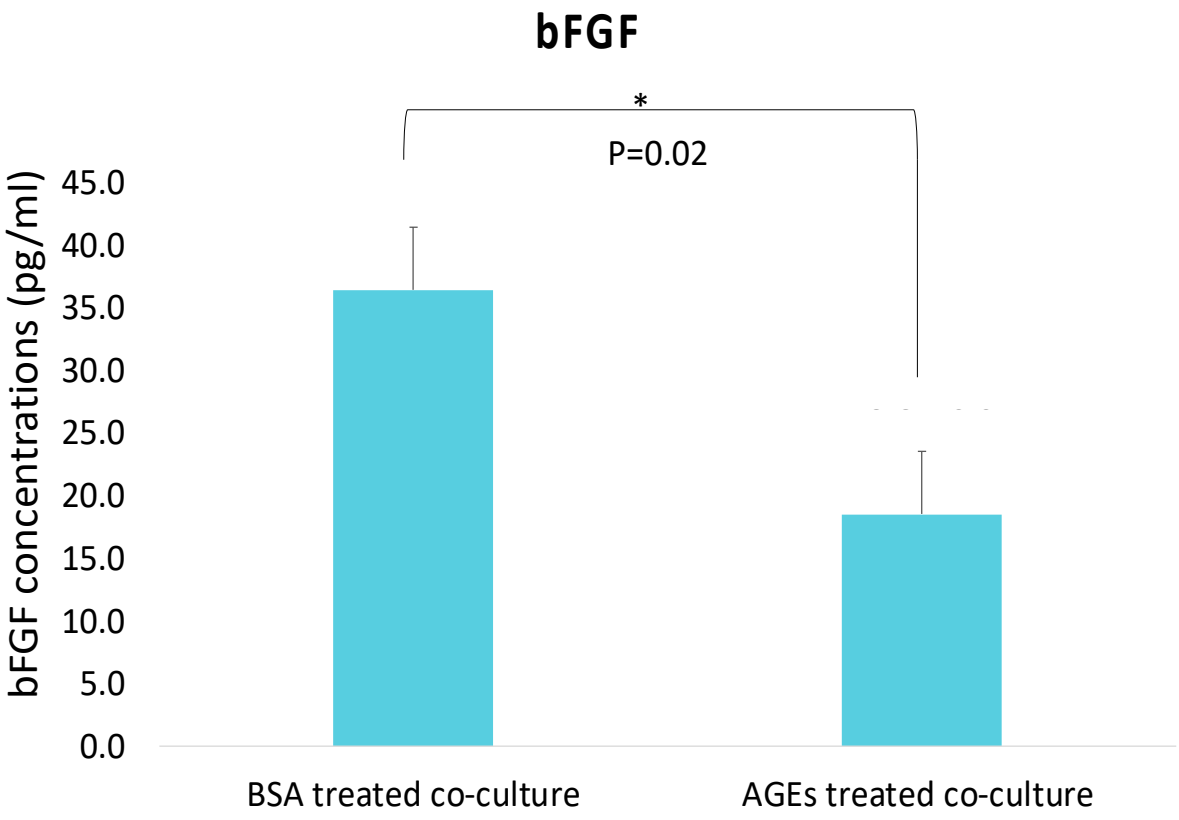

Figure 7.4 bFGF in supernatant collected from BSA treated co-culture and AGEs treated co-culture on day 7 of co-culture. The above figures illustrate comparisons in the levels of the trophic factors between BSA treated and AGEs treated co-culture.. Data is presented as a mean concentration of the trophic factor in each condition with error bars signifying ± SD. n=4 and represents the independent experiments/sample types from which the supernatant was collected. *Represents p=0.05-0.01. The connectors indicate the comparisons between AGE treated co-culture vs. co-culture conditions.

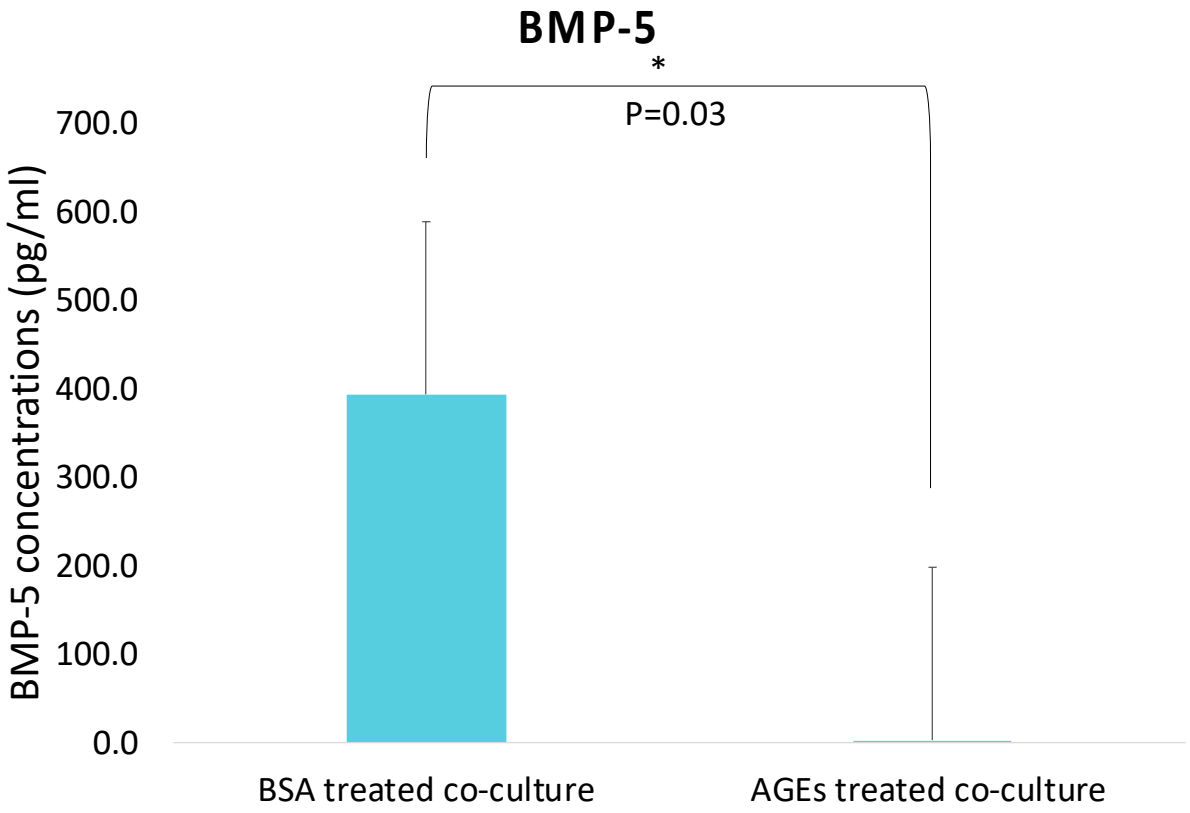

Figure 7.5 BMP-5 in supernatant collected from BSA treated co-culture and AGEs treated co-culture on day 7 of co-culture. The above figures illustrate comparisons in the levels of the trophic factors between BSA treated and AGEs treated co-culture.. Data is presented as a mean concentration of the trophic factor in each condition with error bars signifying ± SD. n=4 and represents the independent experiments/sample types from which the supernatant was collected. *Represents p=0.05-0.01. The connectors indicate the comparisons between AGE treated co-culture vs. co-culture conditions.

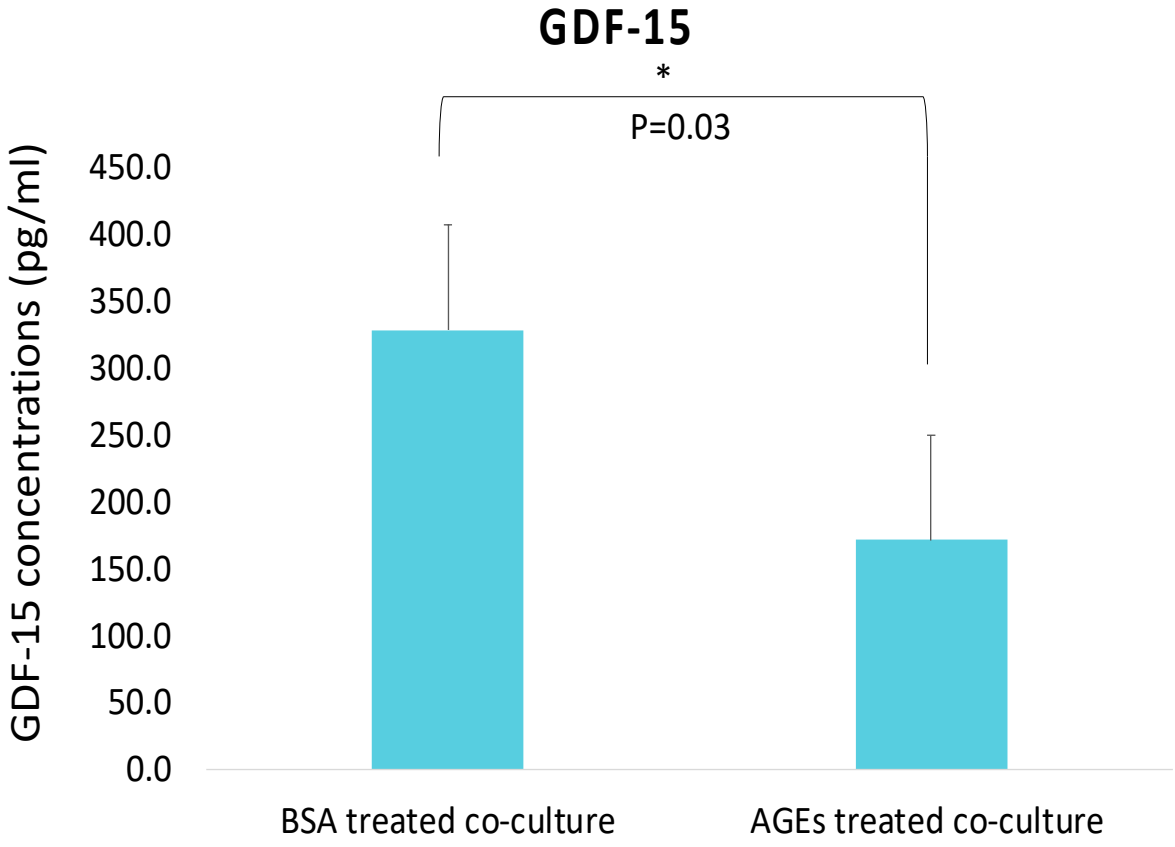

Figure 7.6 GDF-15 in supernatant collected from BSA treated co-culture and AGEs treated co-culture on day 7 of co-culture. The above figures illustrate comparisons in the levels of the trophic factors between BSA treated and AGEs treated co-culture.. Data is presented as a mean concentration of the trophic factor in each condition with error bars signifying ± SD. n=4 and represents the independent experiments/sample types from which the supernatant was collected. *Represents p=0.05-0.01. The connectors indicate the comparisons between AGE treated co-culture vs. co-culture conditions.

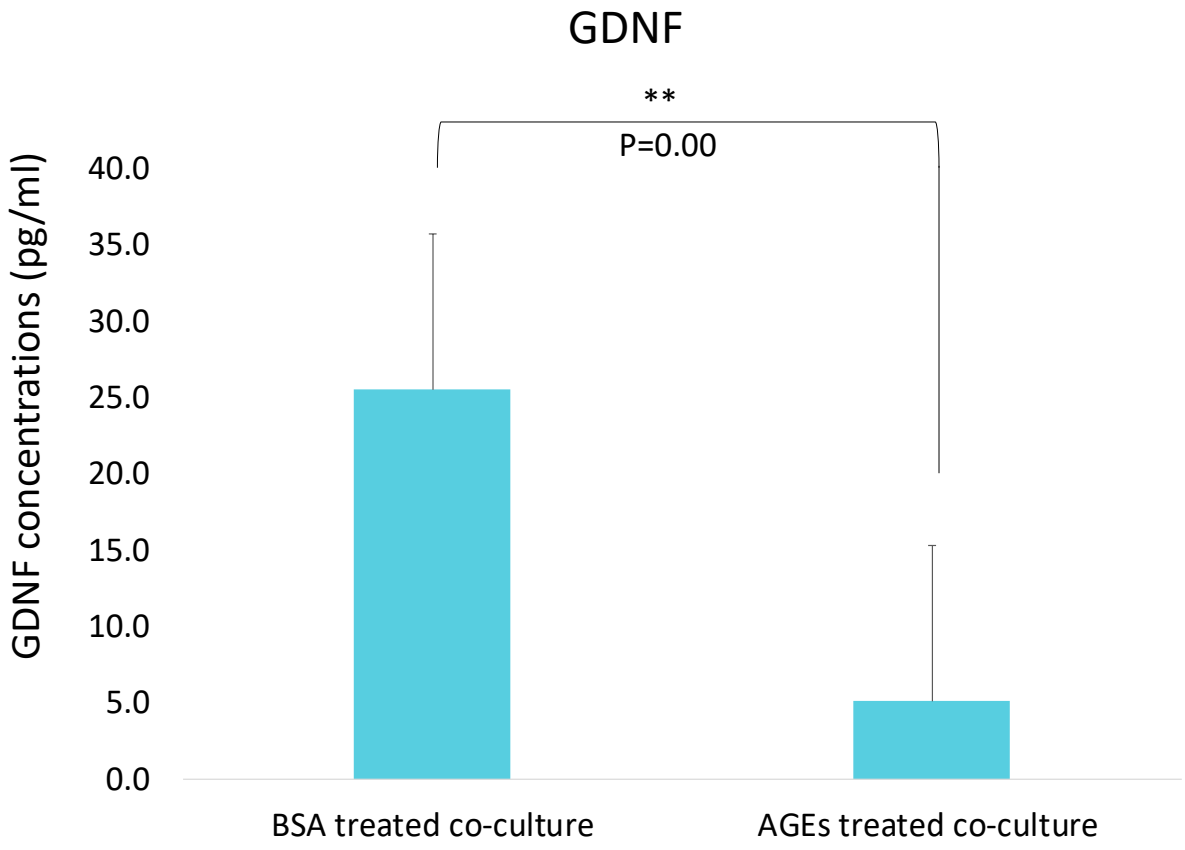

Figure 7.7 GDNF in supernatant collected from BSA treated co-culture and AGEs treated co-culture on day 7 of co-culture. The above figures illustrate comparisons in the levels of the trophic factors between BSA treated and AGEs treated co-culture.. Data is presented as a mean concentration of the trophic factor in each condition with error bars signifying ± SD. n=4 and represents the independent experiments/sample types from which the supernatant was collected. **Represents p=0.01-0.001. The connectors indicate the comparisons between AGE treated co-culture vs. co-culture conditions.

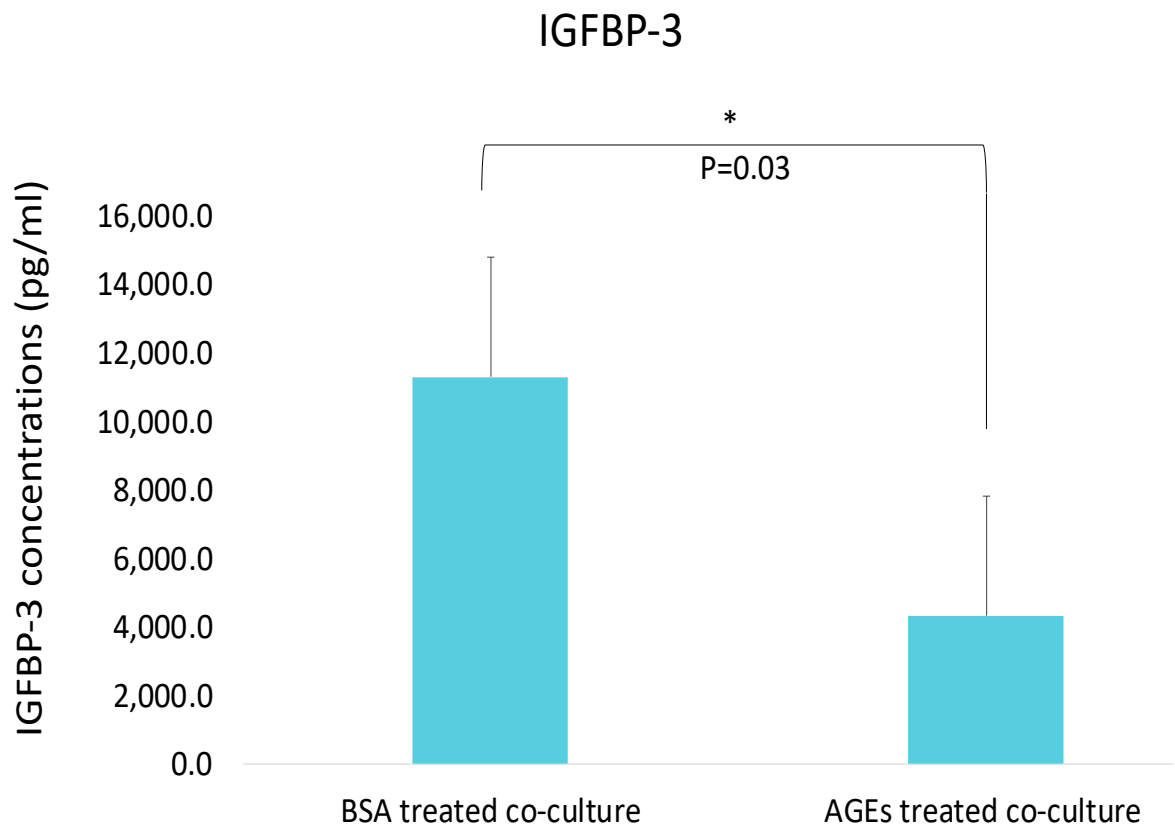

Figure 7.8 IGFBP-3 in supernatant collected from BSA treated co-culture and AGEs treated co-culture on day 7 of co-culture. The above figures illustrate comparisons in the levels of the trophic factors between BSA treated and AGEs treated co-culture.. Data is presented as a mean concentration of the trophic factor in each condition with error bars signifying ± SD. n=4 and represents the independent experiments/sample types from which the supernatant was collected. *Represents p=0.05-0.01. The connectors indicate the comparisons between AGE treated co-culture vs. co-culture conditions.

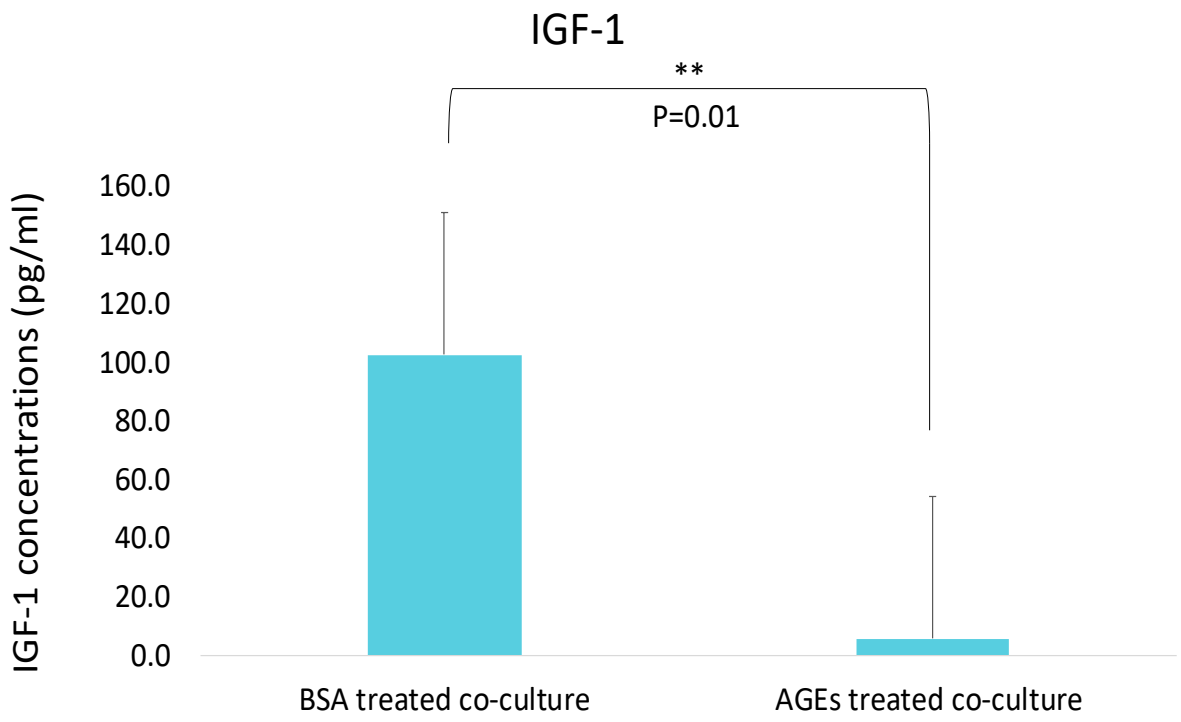

Figure 7.9 IGF-1 in supernatant collected from BSA treated co-culture and AGEs treated co-culture on day 7 of co-culture. The above figures illustrate comparisons in the levels of the trophic factors between BSA treated and AGEs treated co-culture.. Data is presented as a mean concentration of the trophic factor in each condition with error bars signifying ± SD. n=4 and represents the independent experiments/sample types from which the supernatant was collected. **Represents p=0.01-0.001. The connectors indicate the comparisons between AGE treated co-culture vs. co-culture conditions.

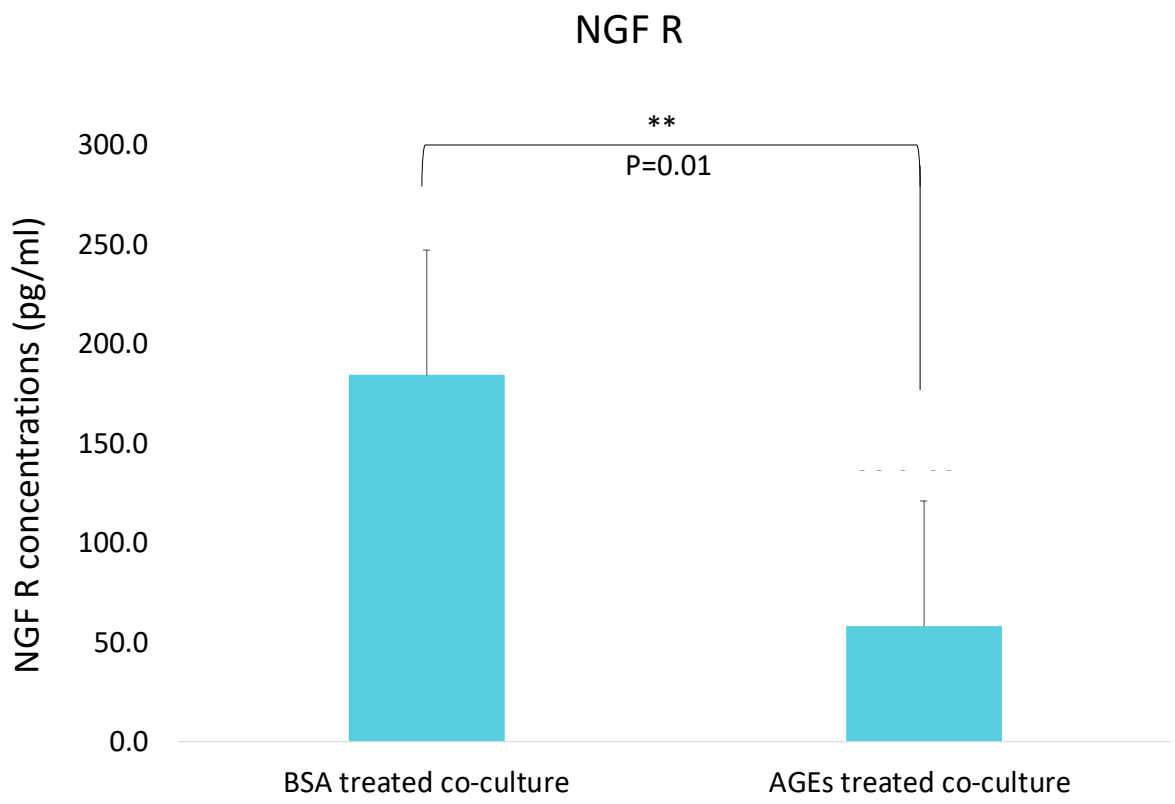

Figure 7.10 NGF R in supernatant collected from BSA treated co-culture and AGEs treated co-culture on day 7 of co-culture. The above figures illustrate comparisons in the levels of the trophic factors between BSA treated and AGEs treated co-culture.. Data is presented as a mean concentration of the trophic factor in each condition with error bars signifying ± SD. n=4 and represents the independent experiments/sample types from which the supernatant was collected. **Represents p=0.01-0.001. The connectors indicate the comparisons between AGE treated co-culture vs. co-culture conditions.

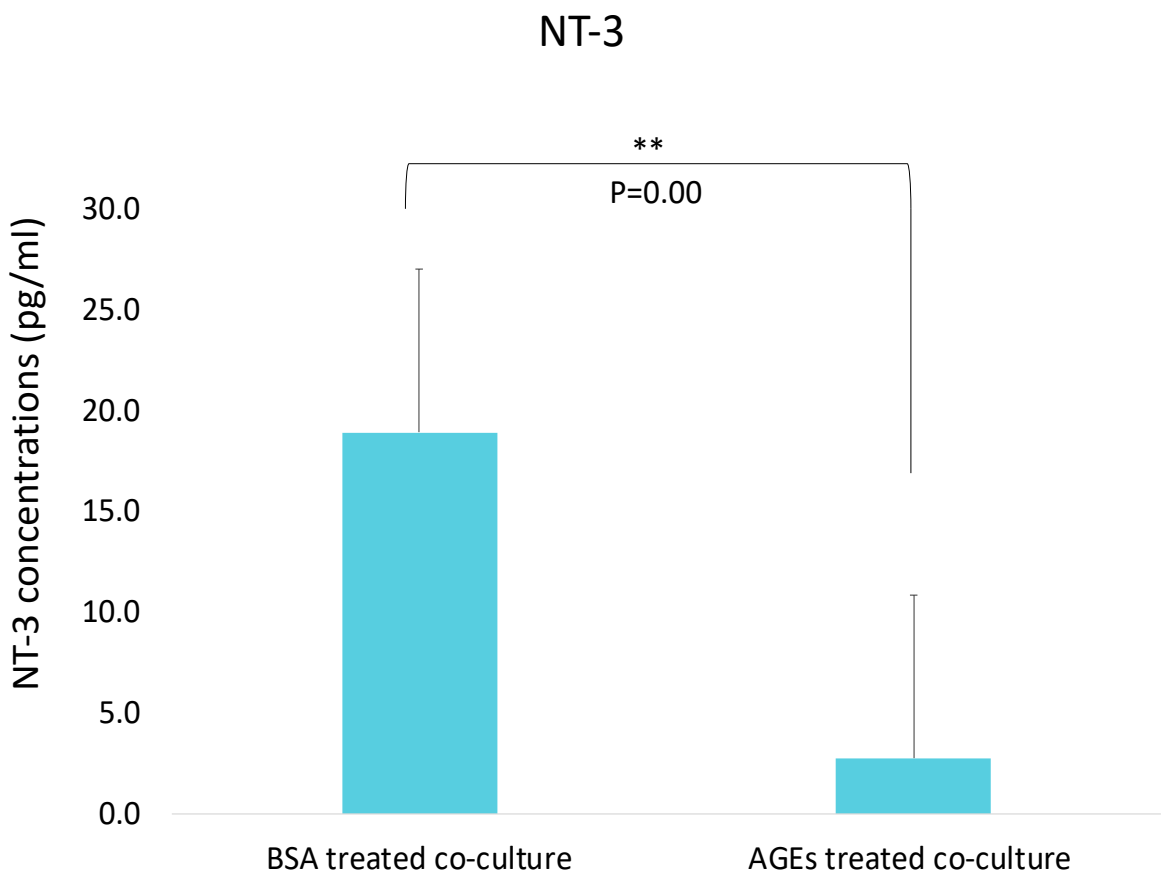

Figure 7.11 NT-3 in supernatant collected from BSA treated co-culture and AGEs treated co-culture on day 7 of co-culture. The above figures illustrate comparisons in the levels of the trophic factors between BSA treated and AGEs treated co-culture.. Data is presented as a mean concentration of the trophic factor in each condition with error bars signifying ± SD. n=4 and represents the independent experiments/sample types from which the supernatant was collected. **Represents p=0.01-0.001. The connectors indicate the comparisons between AGE treated co-culture vs. co-culture conditions.

7.3 Discussion

NMJs serve as the interface between nerves and skeletal muscle. Therefore, in order to maintain the function of NMJs for bidirectional trophic signal and stimulation muscle and motor neuron tissue co-depend on each other. If cross-communication and microenvironment are disturbed, NMJs functioning is affected followed by axon

degeneration, and muscle weakness which results in reduction of NMJs transmission and fibre degradation which leads to development of DMN and DM. Numerous studies have presented evidence of elevated levels of AGEs in diabetes, which hamper the growth and maintenance of human skeletal muscles and motor neurons (Sango et al., 2017; Hunt et al., 2015; Chiu et al., 2015; Nedachi et al., 2008). However, little is known about the mechanisms governing muscle cell growth under elevated AGEs treatment. Ergo, the present study sought to examine the impacts of AGEs on differentiation of skeletal muscle and motor neurons and NMJ functioning in serum-free DM, as serum is not exogenously added and might contain several unknown biological factors which may influence assay reproducibility. The data demonstrated nerve-muscle co-culture model free from serum and neural growth factors in the media subjected to varying concentrations of AGEs, similar outcomes were observed in control co-culture used as control groups. Additionally, the absence of neural growth factors from the co-culture model implies that nerve and muscle cells produce the necessary factors needed to trigger nerve, axonal development and formation of NMJs with myotubes. Given MNs and skeletal muscles are tissues that rely on each other, the transmission and trophic stimulation that occur between them are critical for the development and formation of NMJ. In the present study, immunofluorescent imaging revealed that AGEs result in adverse morphological changes to both myotubes and MNs. Furthermore, it is suggested that muscle contraction and fibre funcitonality are severly affected by these structural alteration in myotubes (Tasfaout et al., 2018; Jungbluth and Gautel, 2014). Typically, the marginal location of nuclei in the myotube axis are esential for the regulation of cellular functions within the muscle (Folker and Baylies, 2013). In the co-culture model subjected to AGEs treatment (the diabetic model), the nuclei centrally clump, resulting in a deficiency in transcriptional and translational by products needed for myofibre survival, which ultimately can affect NMJ

(Cadot et al., 2015). Additionally, the presence of AGEs in the co-culture model (the diabetic model) suggests affected healthy MNs by diminishing their differentiation and their quantity compared to the BSA-treated co-culture model. In confirmation with the findings of our novel study, peer- reviewed studies have reported that AGEs have toxic effects on MNs caused by AGE/RAGE binding, raising the secretion of free radicals and oxidative damage to mitochondria, ultimately resulting in cell death (Sango et al., 2017; Xing et al., 2013). One of the biomarkers of AGEs attack the neural cytoskeleton proteins, resluting in their glycation within in persons with diabetes (Ozturk et al., 2006). These modifications to axonal proteins lead to axonal degeneration. Experiments performed on diabetic mice revealed that they had thinner myelin sheaths and diminished MN differentiation, resulting in dysfunctional MNs and reduction in overall conduction velocity (Gonzalez-Freire et al., 2014). Ergo, these alterations to the structure hamper the function of both myotubes and MNs, ultimately compromising the functionality of the NMJ (such as in DMY and DN). This detrimental morphological changes described above could explain the changes in levels of neural/growth factors (NGFs) when the co-culture model is treated with AGEs. These NGFs could be secreted endogenously in our *in-vitro* NMJ co-culture models (with AGES and BSA), which were measured using ELISA-based microarray experiments. These experiments revealed that the construction and development of in-*vitro* NMJs within the co-culture system were actually strengthened by the endogenous control of certain neurotrophic or growth factors. A few factors involved with MN support, NMJ formation, and, myotube progress were detected to decrease in the co-culture subjected to AGE treatment compared to the one subjected to BSA treatment. A faction of research has reported that NT-3 is a critical regulator of synaptic operation and progression and is vital for the sustenance of presynaptic and postsynaptic frameworks at the NMJ (Gonzalez et al., 1999, Belluardo et al., 2001). Further experiemntal

study has hypothesised that NT-3 functions as a temporary axon path-finding signal for proprioceptive axons both marginally and peripherally *(Genç et al., 2004).* Evidence has demonstrated that a reduction in somal size, while the quantity of MNs usually rose in the initial post-delivery growth of NMJs in mice devoid of NT-3 (Woolley et al., 1999). Mice devoid of NT-3 at birth have been performed and findings revealed that their innervtion of motor end plates by AT is diminished. Demonstrating that the quantity of SkM fibres droped accompanied by a severe postpartum depletion of ATs and also that there is a complete denervation of back limb muscles lacking NMJs in the whole SkM endplate region (Woolley et al., 2005). Additionally, disruption of AT development , decline in SkM fibre diameter, and diminished recovery of synaptic vesicles are all observed in down-regulated NT-3 mice (Sheard et al., 2010). These results perhaps indicate that a drop in NT-3 levels, which was observed in the co-culture model subjected to AGE treatment, results in impairment in NMJ establishment, progession and synaptic action. Our findigns also show reduced levels of GDNF in the AGE-treated co-culture copared to the co-culture subjected to BSA treatment. Susrprisingly, GDNF offers another illustration for a target-derived factor which SkMs express, whie its receptor, Ret, is expressed in the MNs. In mice devoid of Ret, a maldevelopment of AT and decreased motor end plate size have been observed within NMJs (Baudet et al., 2008). Opposing my findings, past experimental studies have suggested that muscle-deprived GDNFs increase substantially at old age (Ulfhake et al., 2000), triggering muscle fibre sprouting and re-innervating as defensive mechanism of cell body size and the chollinergic phenotype of MNs (Edström et al., 2007). The GDNF is an important factor that is thought to be enormously effective when it comes to the survival of MNs *in-vitro* (Oppenheim et al., 1995). Experiment conducted on frogs have reported that GDNF treated co-culture models exhibited an increase in the AP-dependent synaptic current rate and size, suggesting the GDNF's probalble role as

a retrograde-signalling factor (Wang et al., 2002). Hyper-innervated NMJs may have also been detected when SkM-derived GDNF expresion is increasedin transgenic mice (Nguyen et al., 1998). The results suggest that the GDNF derived from SkM may serve as a regulator of AT maturation at the NMJ. Ergo, it is possible that a reduction in GDNF levels implies a diminished interference between pesynaptic and postsynaptic elements of NMJs in the co-culture model subjected to AGE treatment compared to the BSA-treated one. The plausible explanation that the expression of GDNF was reduced but not elevated due to its defensive mechanism that can be activated (causing its increase) in chronic conditions such as marginal neuropathies and ageing. The activated defence mechanism increased the expected reduction therefore it was not recognisable (Lie and Weis, 1998; Yamamoto et al., 1998).

The results of the QAH-GF-1 also revealed a drop in IGF-1 in the co-culture subjected to AGE treatment. IGF-1 is a multitask pleiotropic growth factor, like its neurotrophic counterpart, supporting MN presences and thus muscle size and power while preventing oxidative stress (Maggio et al., 2013; Maggio et al., 2006). Additionally, it has been reported that IGF-1 contributes to healthy synaptic growth, collateral axonal sprouting, nerve terminal flexibility, and axonal rejuvenation (Ishii, 1995; Schmidt, 1996; Ishii et al., 1994). The deterioration of NMJs and MSs can be prevented by introducing IGF-1 into SKMs. In mice, this has been shown to inhibit the force deterioration related to age (Payne et al., 2006). In diabetes, IGFs prompt muscle proliferation instead of prompting muscle differentiation as a coping mechanism to various physiological and pathological conditions, inluding DM (Semenza, 2000; Hanaire-Broutin., 1996). Typically, circulating IGF-1 is up-regulated following damage to the central or peripheral nerve, but in DN, the up-regulation is delayed at the damaged area and there is no increase of IGF-R, adversely diminishing nerve regeneration (Sullivan et al., 2008; Xu and Sima, 2001). Given IGF-1 is transported through binding to IGFBPs, the decrease in IGFBP

levels in this study had a noteworthy effect on IGF-1 (Hwa et al., 1999). Additionally, it has been indicated that IGF-1 bioavailability is bolstered via the activity of IGFBPs (Stewart et al., 1993). These IGFBPs have an efficient compensation process for when there is a drop in levels of one of the IGFBPs, as a result, other IGFBPs are increased automatically, but this process cannot compensate for a drop in more than one of IGFBPs. Nonetheless, in our experiment 3 out of 5 IGFBPs were decreased substantially, resulting in a compromised muscle development and a defective regeneration within our *in-vitro* NMJ model (Sullivan et al 2008;, Xu & Sima, 2001; Ning et al., 2006). Therefore, a further drop in IGF-1 level is linked to the drop in IGFBP levels (3 out of 5) (Hwa et al., 1999). Thusly, the observed down-regulation of IGFBPs and IGF-1 after introducing them to the AGE treated co-culture model supports the notion that the disruption of the interaction between MNs and SkMs by AGEs results in a lack of the GNFs needed for MN development, functional NMJ resemblance in the *in-vivo* foundation, and MC differentiation. In summary, these findings from existing body of knowledge offer key insights into the cellular signalling of our simplified co-culture models (both with AGEs and BSA). Additionally, the results derived from the healthy, BSA-subjected co-culture model exposed the co-culture system's ability to endogenously regulate the formation and progression of NMJ ad also generate the conditions that facilitate progressive differentiation of immortalised human myotubes *in –vitro* occurring through the specific expression of vital GNFs. The results of the AGE-treated co-culture, on the other hand, demonstrated the ability of AGEs to endogenously create functional and structural defects in NMJs, as well as in SkMCs and NPCs *in-vitro* by severely affecting the expression of essential NGFs.

7.4 Conclusions

In conclusion, the use of this new human-based NMJ platform to examine the potential involvement of AGEs in the progress of diabetic myopathy and neuropathy support the hypothesis of this study, as evidenced by the disruption of myotubes morphology and centralised nuclei bundling. Additionally, the findings also confirmed that AGE affected motor neural differentiation which could play a pivotal role in the development of diabetic neuropathy. Ergo, the use of NMJ platform in the present study contributed enormously to this new approach, and it raises the question as to where AGEs damage originate from? From muscle to nerve. With this in mind, further studies are need to answer this question, and the present study could be the first step on this path. This study has successfully established two approaches to co-culture (diabetic and normal) with the utilisation of iHSMMs with NPCs. No exogenous NGFs were introduced to either model, demonstrating that the cross-communication produces simultaneously these NGFs endogenously without the need to add exogenous artificial GNFs, which could influence the outcome of the MN and DMY experiments. The quantitative approaches were used to measure several GNFs in both model to capture the roles they play in the proliferation and differentiation of muscles and nerves and in the functionality of NMJ. In the diabetic model, it became evident that the cross-communication between iHSMMs and NPCs can be severely affected by a significant drop in the expression of these GNFs. These outcomes highlight the damaging role played by AGEs on NMJs, muscles, and nerves. Therefore, it can be concluded that this *in-vitro* simulations of NMJ approaches are superior models for representing in-*vivo* conditions. Successful validation of this model as a preclinical *in vitro* test platform that will replace animal use, provide a more direct bridge between *in vitro* and clinical studies, and serve as a screen for novel therapeutic strategies of diabetic motor neuropathy and diabetic myopathy.

Chapter 8: General discussion and conclusions

8.0 Discussion

This project's predominant aim was to establish and confirm a novel entirely human streamlined nerve-muscle co-culture system platform that has the ability to produce functional in vitro NMJs, with no serum, growth, and/or neurotrophic factors. Thus, it sought to make available a defined platform for the investigation of disease and disorders of the NM system through examining the functionality and formation of the NMJ. In this report, a physical human motor unit platform produced by immortalised skeletal myoblasts and NPCs obtained from hESCs is described. Several objectives are behind the establishment of this unique platform. One of them is the investigation the formation and maintenance of human NMJs and disease. It is also used for the analysis of research into the discovery and toxicity of drugs. The skeletal muscle and neuron co-cultures were with no serum or cocktails of neural growth factors being added. Within a period as short as six to seven days, the formation of myotube started being apparent, and the myotube contractions were documented. When compared to previous studies where the myotube contractions and NMJ formation took 14 days (Vilmont et al., 2016), and sometimes as long as 20 to 25 days (Das et al., 2010) this can be considered quick.

The shorter times indicate progress with regards to the study of the elements of development and for acknowledging the pathophysiological arrangements of disorders linked to NMJ disorders resulting from ageing or disease. What is vital is that this kind of work should be done using human cultures as this could assist in increasing the chances that this can be translated into clinical practice. The majority of cell culture models in the past studies make use of cross-species cell types (Guo et al., 2010; Arnold et al., 2012) and required growth

factors (Guo et al., 2011; Demestre et al., 2015; Das et al., 2010; Guo et al., 2010). In the present model, these were not included, and no adverse effects were noted. Such a conclusion implies that all the necessary factors needed to prompt nerve axonal spouting and NMJ formation with the myotubes were discharged by the nerve and muscle cells. In addition, the elimination of serum, which has anonymous factors that could impact reproducibility, make the toxicity and pharmacology studies' interpretation simpler (Rumsey et al., 2009).

Bidirectional communication between the muscle and nerves strongly supports the formation of NMJ (Zahavi et al., 2015). The process is also supported by neural growth factors (like neurotrophic factor and neurotrophin-3/4 derived from the glial cell line and the neurotrophic factor obtained from the brain), which are discharged by the muscle with the aim of supporting the formation of NMJ, its growth, and maturation (Henderson et al., 1993; Funakoshi et al., 1995). Investigations conducted in the future, making use of this model could detect the main factors discharged from the muscle and nerve to coordinate axonal sprouting, localisation, and maintenance of NMJ. Notwithstanding the reality that models from animals are able to stand for the important parts of human disease's physiological changes (Jensen et al., 2009), there are several advantages offered by *in vitro* human cell cultures since they are created using relevant cell types. Added to this, they can be produced rapidly for high-throughput screening, and when compared to animal models, they are most effective. In addition to the Home Office's commitment to the 3R's in animal research, in conduct to replacement, refinement and reduction (Guo et al., 2011; Demestre et al., 2015).

Once the co-culture model had been established, this project's next objective was to conduct the characterisation of the system with the aim of verifying the incidence of physiological NMJ formation. Before performing the co-culture characterisation, there were experiments done with the aim of determining the best time point, which would indicate that NMJ formation

has reached maturity. For purposes of determining the mature formation of NMJ, peak contraction frequency was employed. The peak was observed to be seven days following the co-culture. Using antibodies for VaChT and ChAT, the characterisation and identification, in the system, of Cholinergic MNs was done, revealing the interface between the systems myotubes and MNs. Such a significant finding is a reflection of NMJ noted *in vivo*, both VaChT and ChAT are needed for the correct development and function of MN (Misgeld et al., 2002; Brandon et al., 2003).

Terminal Schwann cells are also needed together with SkMC and MN during the formation of NMJ *in vivo*. Research done using mice has concluded that the initial stages of NMJ formation can proceed without Schwann cells, even though for suitable synapse development to take place *in vivo*, there has to be an involvement of Schwann cells (Lin et al., 2000; Wolpowitz et al., 2000; Morris et al., 1999; Woldeyesus et al., 1999; Riethmacher et al., 1997). The staining of the co-cultures for Syt1 was done. The Syt1 is a presynaptic calcium sensor shows expression of that presynaptic MNT activity. It is also known for the crucial role it plays in the discharge of neurotransmitters from Ca2+ dependent vesicles (Littleton et al., 1993; Geppert et al., 1994). The ability to identify Syt1 at MNTs in the co-culture system made available more proof that the structural formation of NMJs in the system was successful, as would be anticipated in the *in vivo* signal transmission at NMJ. Then, the characterisation of NMJ was done with the aim of showing that there was a co-localisation of MNs and their terminals, and postsynaptic AChRs at the NMJ MEP (motor end plate). Consequently, this is a process that delivered proof that the physiological *in vitro* NMJ formation noted *in vivo* was obtained through the AChRs identified on the MEP by their characteristic twisting knotted arrangement covered by MNs. This validates the idea that NMJs were being generated by the co-cultures while also showing characteristics consistent with effective maturing.

With the aim of determining whether the NMJs within the system were showing proper structural organisation and postsynaptic development, postsynaptic characterisation of the co-cultures was done. Rapsyn and MuSK observation at MEP implied that the discharge of agrin from the MNT had the ability to prompt the MuSK signalling conduits. From this finding, it can be noted that synaptic communication at NMJ facilitated the effective postsynaptic differentiation, as was indicated by the MuSK, Rapsyn, and AChRs co-localisation.

The co-cultured myotubes also showed morphological features of differentiation at an advanced level. In the co-culture system's physiological sarcomeric development, as shown by the existence of striations on the membrane of the myotube, transversal triads, which can be described as specifically developed excitation-contraction coupling implements with characteristic tight RYRs opposition to DHPRs on the T-tubules and the SR membranes, and the peripheral nuclei were noted. All these are also noted *in vivo* when SkMCs differentiate at an advanced level (Shadrin et al., 2016; Bruusgaard et al., 2003). Therefore, it can be deduced that the advantage of this co-culture arrangement when compared with the usual *in vitro* myoblast cultures and nerve-muscle co-culture models created in the past seems obvious, as they do not show the degree of advanced differentiation of the myotube noted in this co-culture arrangement. So, it can be argued that the co-culture system is a better implement in studying the wasting of SkM as a result of disease (such as cancer cachexia), ageing (such as sarcopenia), and the investigation of disorders linked to MN. By characterising the co-culture system, evidence was made available indicating the interface between myotubes, neurons, and neuroglia, and also a validation of mature NMJs with postsynaptic structural arrangement and presynaptic activity, and advanced myotube differentiation.

After the characterisation, the objective that followed was making sure that the NMJs functioned physiologically and confirmed that the contractions in the myotubes in the co-

culture arrangement were spontaneous and also happening as a result of the NMJ signalling. Agonistic and antagonistic drug-response experiments were used to accomplish this. The experiments were made in such a way that drugs were applied to whole culture. MNs express receptors on soma and dendrites (Ach, GABA & Glutamic acids). They can possibly act on AChRs postsynaptically and on MNs presynaptically on the NMJ, as a result impacting on the frequency of the myotube contraction. However, it is important to consider that the drug can act on the entire surface. Exposure to α-BTX resulted in permanent termination of spontaneous contractions. What this shows is that NMJs within the co-culture reacted as expected to the irrevocable competitive antagonist at the AChRs, as was seen in the *in vivo* NMJ (Domet et al., 1995). In a similar manner, co-cultures treated using tubocurarine also resulted in the termination of myotube contractions. Nonetheless, a difference was noted in that, as opposed to the α-BTX treated cultures, the contractile activity resumed in the co-cultures treated with tubocurarine, Thus, the resumption of contractile activity in the col-cultures is tubocurarine and validates the exact neurotransmission noted in this *in vitro* NMJ arrangement.

Fascinatingly, when bicuculline was used to treat co-cultures, the result was an initial termination of contractions of the myotube before spontaneous activity resumed. From studies involving mice, it has been noted that bicuculline has the capacity to non-competitively block ACh from attaching to AChRs (Demuro et al., 2001; Liu et al., 1994). Therefore, conclusions drawn from this study can be used to propose that bicuculline had the ability to control the activity of NMJ, which was shown in the contraction of myotubes being reduced in the co-culture arrangement by averting ACh from binding with receptors at the postsynaptic NMJ, a situation that shows that signalling at NMJ was responsible for controlling the myotube contractile activity at the co-culture system.

To determine whether the MNs in the system was able to receive the excitatory neurotransmitter, the L-Glut was employed. Even though fleeting (15min), an intense escalation in the frequency of myotubes was detected when the co-cultures were exposed to L-Glut. Since it is generally accepted that the stimulation of SkMC membranes is attained through AChRs, the increase in contraction frequency detected following the applying of L-Glut is an indication that the neurotransmitter stimulated the MNs to escalate the discharge of ACh into the NMJ's synaptic cleft within the co-culture arrangement, in the process prompting the escalated myotube activity.

The inhibitory CNS neurotransmitter GABA is the last treatment applied to the co-cultures. The aim was to find out whether GABA signalling was taking place *in vitro* NMJs in this arrangement. Fascinatingly, a fleeting escalation (10min) in myotube activity was detected after exposure to GABA. In contrast to this result, some research shows that there is a MN receptor expression of $GABA_B$ receptors *in vivo* at NMTs and when they are modulated through GABA, binding may have the effect of lowering the discharge of ACh at MNT (Malomouzh, Petrov, et al., 2015; Malomouzh, Nurullin, et al., 2015). Nonetheless, some questions regarding the full GABA function and the role it plays in the ACh modulation through $GABA_B$ receptors at the presynaptic NMJ still remain (Borodinsky & Spitzer, 2007). On the other hand, studies have concluded that there is an existence of a number of transmitter receptor categories in the initial stages of the embryonic cycle, where $GABA_A$ receptors are expressed on embryonic SkMCs (Borodinsky & Spitzer, 2007). On this basis, it can be said that the role played by GABA at both the mature and embryonic NMJ needs to be explored further before the functions of GABA at the NMJ can be completely appreciated. Eventually, via real-time functional assessment of NMJs in the co-culture system, the proof has been advanced to show that this arrangement can be possibly used as a high-content platform for evaluating

pioneering treatments and modelling of diseases *in vitro*, and also for comprehending how NMJ is formed, develops, and works.

Notwithstanding the fact that the establishment of this model that does not make use of exogenous growth factors and neurotrophins presents a momentous breakthrough in the modelling of NMJ *in vitro*, it comes as no surprise that SkM and MNs are tissues that depend on each other for synaptic transmission/stimulation and trophic support. Moreover, the back and forth communication between MNs and SkM is needed for the establishment of the development of MNs, SkM, and NMJs. The functional assessment of NMJs produced without neurotrophins and growth factors shows that all the factors needed to establish this system were discharged by the cells in the system.

The last objective was to enumerate the co-culture's neurotrophic and growth factor concentration when compared to myotubes that are aneurally-cultured. This was done with the objective of determining whether the endogenous up-regulation of precise tropic factors facilitated the establishment and growth of NMJs, which were produced in the co-culture system. To accomplish this, ELISA-based microarray experiments were used. The results of the experiments showed that there was an escalation in the expression of 22 growth factors. From studies, it has been concluded that BDNF, usually employed *in vitro* NMJ systems, is implicated in the innervation of SkM and survival of MN *in vivo*, together with potentiation of the transmission of signals at the NMJ (Yan et al., 1993; Zhang & Poo, 2002). Thus, it can be noted that the BDNF up-regulation in the co-cultures delivers proof that physiological formation and development of NMJs was allowed by the system through BDNF regulated endogenously, which shows *in vivo* NMJ formation.

From the co-cultures, the up-regulation of FGF-7 was also observed. Notably, this is an organising molecule that can play the role of controlling presynaptic specialisation at the NMJ

(Fox et al., 2007; Umemori et al., 2004). Agrin has the capacity to control the expression of FGF in SkM to facilitate the presynaptic NMJ differentiation (An et al., 2010). Accordingly, high FGF-7 in the co-culture arrangement is an indication that there is an interface between innervated myotubes and MN-secreted agrin during the formation and development of NMJ, as is anticipated *in vivo*.

GDNF is another factor that was up-regulated in the co-cultures. It has been shown that GDNF is vital for *in vitro* MN survival (Oppenheim et al., 1995). Previous research also concludes that GDNF has the capacity to play the role of a retrograde signalling factor (Wang et al., 2002). In addition, experiments involving the overexpression of GDNF in mouse models leads to irregular MN overgrowth (Nguyen et al., 1998; Keller-Peck et al., 2001). The conclusions from these studies show that GDNF is implicated in the maturation of MNT. For this reason, it can be said that the elevated GDNF/GDNf-15 noted in the co-culture system is an indication of the interaction between pre- and postsynaptic NMJs in the arrangement. When the IGFBPs 1, 2, 3, 4, and 6 in the co-cultures were measured, it could be noted that all were substantially raised in the system.

It is generally accepted that IGF-1 plays a fundamental role in the formation of MN, SKM, and NMJ, their development, and maintenance (Dobrowolny et al., 2005; Velloso, 2008). Notably, the elevation of IGFBPs, which play the role of IGF-1 membrane transporter proteins, has also been shown to result in enhanced IGF-1 bioavailability (Stewart et al., 1993). It is on this basis that it could be concluded that the elevated IGFBPs and its binding proteins in the co-culture arrangement imply that there is an interaction between SkMC and SCE, prompted by the up-regulation of these factors to facilitate the MN maturation, myofiber advanced differentiation, and the formation of strong NMJ, illustrative of *in vivo* formation. In the co-cultures, NT-3 which is an essential element of *in vitro* modelling, was elevated. NT-3 and is

implicated in the synaptic function modulation and is needed for maintaining NMJs (Belluardo et al., 2001; Gonzalez et al., 1999).

From animal studies, it has been concluded that NMJ development and maintenance can be disrupted by NT-3, which also results in the reduction in the size of SkM fibres (Woolley et al., 1999; Woolley et al., 2005). Research into NT-3 expression shows its expression depends on the activity and functions of the synapse to regulate the transmission of NM. For this reason, it can be said that the elevated NT-3 recorded in the co-cultures was most likely a result of NMJ formation, development, and synaptic activity.

EGF R, HB-EGF, HGF, OPG, PDGF-AA, PIGF, TGFb3 and VEGF are the last significantly elevated growth factors in the co-cultures. Both PIGF and VEGF belong to the VEGF category of growth factors and are famous for the role they play in vascular growth and development (Ferrara, 2004). Notably, it has been demonstrated that these factors play significant roles in the growth, control, relocation, and survival of MN (Ruiz de Almodovar et al., 2009; Rosenstein et al., 2010). Such factors have also been associated with improvements in the SkM re-innervation following injury. VEGF has been shown to have the capacity to up-regulate NGF and GDNF to facilitate the regeneration of MN axon (Shvartsman et al., 2014), showing that during NMJ formation, growth factors work in synergy. Thus, the recorded PIGF and VEGF up-regulation in the co-cultures implies that these factors were required for the optimal development of MN and NMJ formation system.

The evaluation of the results from the microarray experiments led to useful discernments with regards to cellular signalling of this streamlined co-culture system. Added to this, it was determined that the co-culture system is able to self-regulate the formation of NMJ and

facilitated advanced SkMCs differentiation through the precise essential growth and neurotrophic factors.

The successful confirmation of this model as a preclinical *in vitro* test platform with the capacity to substitute animal use delivers a more explicit connection between clinical and *in vitro* studies. Furthermore, it plays the role of screening for novel treatment approaches for diabetic myopathy and diabetic motor neuropathy. It makes it possible to substitute the employment of diabetic animal models with a suitable human podium which complies with a high-throughput drug screening arrangement which will improve the conversion of preclinical results to human drug trials. The total failure of the ability to translate animal models into therapy that the FDA can approve creates doubt for the translational significance of existing experimental animal models for diabetic myopathy (DM) and diabetic motor neuropathy (DMN). It has been shown (King, 2012) that diabetes has the highest quantity of animals models, which have been extensively employed in diabetes studies. However, the human DMN and DM pathogenesis is still not clear, and therapy options are limited to relief of symptoms. As its performed poorly hence most maintaining patients in a state of dependence on pharmaceuticals. It is on this basis that the failures of the animal models have been brought to the fore in the last several decades by several anti-diabetic medicines. While these models showed promise in animal models, they fail to meet the primary objectives when used in human clinical trials (Colca, 2015; Hedrington & Davis, 2014). The majority of models that have been trialled failed to become rolled out because of ethical considerations linked to extensive manipulation and that they cause pain and distress. They have also been noted to have several serious limitations and disadvantages. Some of these limitations are that it is a challenge to compare studies because different animals are used in the studies, and the tautology renders of diabetes strains are different (Sullivan, 2008).

Notwithstanding strong ethical rationale, very limited substitute *in vitro* models has been established for the study of DM and DMN pathogenesis (Hattangady & Rajadhyaksha, 2009). The leading *in vitro* models in use include primary myoblasts (Chiu et al., 2016) neuroblastoma cell line (Shindo et al., 1996), and dorsal root ganglia neurons (Schmeichel et al., 2003). However, it has been noted that all of these have many disadvantages. For example, muscles (Chiu et al., 2016) and mono cell cultures of neurons (Shindo et al., 1996) are mostly produced using cells derived from animal models. With regards to primary cells, they have been noted to be comparatively heterogeneous and have a restricted ability to expand and undergo phenotypic changes through the progressive expansion of the cells (Mouly et al., 2005).

Added to the challenges noted *in vitro* models is the complicated character of these systems established in media that contains serum, which leads to inconsistency in the experiments. It is, for this reason, that including serum leads to unspecified variables to the arrangement as a result of the differences in the composition of serum between the samples Behringer et al., 2017). This leads to lower experimental reproductively that could have an impact on the results of the experiments. Some evidence has been brought to the fore, showing that the serum used in such arrangements stunted the myelination of motor neurons *in vitro* (Rumsey et al., 2009). Finally, considering that the models discussed above are mono-culture arrangements, the lack of functional innervation and the resulting absence of NMJ formation in these models has a dearth of physiological similarities to humans (Suuronen et al., 2004).

In diabetes, motor nerve and skeletal muscle are the main targets. In addition, the two are tissues that depend on each other for the trophic stimulation back and forth communication which provide a vital link in the human motor system that controls voluntary movements of the muscle. Accordingly, the denervation and re-innervation of muscle have a dramatic altering effect on the function and physiology of muscles (Cisterna et al., 2014). On the other

hand, cell adhesion, muscle-dependent trophic, and axon-guidance signals have a vital role to play in the formation and survival of the NMJs (Steinbeck et al., 2016). This, it can be concluded that NMJ models which make it possible to modulate and analyse NMJs, motor neuron, and muscle concurrently could deliver a more effective and physiologically relevant translational model that will boost the comprehension of DM and DMN.

8.1 Limitations and Future directions

Limitations in this study includes maintaining the NMJ system functional and healthy for more than 10 days. Hence, the NMJ stopped to contract after 10 days furthermore the cells started to lose it shape and die on day 12. This is mainly due to lack of any growth factors and serum to help them surviva for longer time. This issue consequence in limited time to study the cells and can limit the possibility to study a disorder effect on NMJ, SkMCs and Nerve over long periods. In addition, advanced live microscope was necessary to study drug effect on NMJ in order to record contraction frequency over longer periods. Nevertheless, there were some constraints to the current study. Some of this constraints were due to the effect of AGEs on the mono-culture and co-culture, as it would have been beneficial to allow them to develop further if more time was permitted and if it was possibly more applicable to in vivo. Hence, it would/could be appropriate to modify the procedures to allow for DM replacement in order to maintain /keep the cells in the culture for longer. The insufficiency of the media replacement is crucial as it could result

in ultimate death of the cell (most prominently of the co-culture after 5 days of DM). Therefore, if addition time was allowed when sustaining the culture, it would have permitted further analysis. Although most research follow similar procedures in the development of AGEs from BSA, the exact configuration of AGE types inside the final mixture is unidentified. As a result, this could have had a significant effect on its replicability (Hui *et al.,* 2001). Furthermore, both of the models parameters were physically analysed using ImageJ. The axonal analysis of the NPCs in co-culture and the differentiation parameters of the mono-culture was not measured using a definite automated method. The absence of automation due to the high risk of potential human errors and high subjectivity which may reduce the integrity of the results. However, proteomic analysis of myogenin, a marker of myotube differentiation, by western blot analysis, could be used instead to measure the level of myotube differentiation (Murphy *et al*., 2016). Recently, a plugin for the ImageJ software, known as AngleJ, allowed the automated measurement of axonal lengths and therefore reduced subjectivity (Günther *et al*., 2015). Moreover, the co-culture would have greatly benefited from the inclusion of differentiation parameters, to assess the effect of AGEs on myotube differentiation. Unfortunately, the immunofluorescent stain used within the co-culture, phalloidin, stains all filamentous actin and is not a specific marker for myotubes. Consequently, it

would have been impossible to analyse the myotube differentiation using ImageJ. Furthermore, the myotubes could be stained with MHC or, preferably, proteomic analysis used. Confocal microscope was not used for AGEs study due to sensitivity of AGE treated cells. Therefore, confocal microscope was only used for chapter 3 and 4.

While there were some disadvantages to the current experiment, the research delivered many advantages. Although the diverse methodology may be considered to be a constraint, the quantity of immunofluorescence imaging for this study was enormous. The immunofluorescent images discovered different morphological changes between the controls and AGE treated cells. In order to further understand and support the cell's functional capacity, mitochondrial analysis was introduced in conjunction with the images. The Seahorse XF Analyser is frequently used in research, as its measurement of oxygen consumption rate is considered to be extremely accurate (Gusakov *et al*., 2017; Yépez *et al*., 2018). In addition to this, the interpretations observed from the images were converted into quantitative data (differentiation parameters and axonal analysis), therefore, delivering statistical analysis for comparisons. In particular, axonal analysis of NPCs in co-culture stood out as is was based on a large data set of axons, with an average of 75 axons measured per day, for each treatment group.

The results which were obtained via the co-culture, appear to be significantly ensuring to deliver a platform for further development. However, the broader effects of AGEs need to be further investigated. Theoretically, the amplification of multiple targets could be treated at once by the use of a multiplex PCR. Some targets for the co-culture could include proteins related with the maintenance of the axonal structure. Furthermore, targets usually include general protein components of SM such as actin and myosin, and additional proteins linked with the migration and alignment of nuclei. Additionally, the relations between AGEs and RAGE (Ramasamy *et al*., 2005) could be significantly supported by solely evaluating the expression of cell-surface RAGE using flow cytometry (Yoshimaru *et al*., 2008). In order to provide more insight into the pathogenic mechanisms of AGEs (Uy, McGlashan & Shaikh, 2011), the measuring of glucose uptake (Yamamoto *et al.,* 2011) and various ROS from live cells, would be significantly beneficial, however this can be quite difficult. The model also has the potential to become adapted under diabetic conditions, to test the effect of AGEs accumulatively with other factors associated with T2DM. The induction of insulin-resistance in cells is usually cultivated by culturing in high insulin and high glucose media, as seen in previous SM models (Gaster & Beck-Nielsen, 2004; Grabiec *et al*., 2014).

For example, new potential drugs and molecules of interest that are being developed for the treatment of NM and ND disorders such as CMS, LEMS, MG, ALS, SMA, diabetic neuropathy/myopathy, and sarcopenia can be tested on this NMJ model as single or multiple doses over a protracted time interval, mimicking real drug evaluation conditions, which can be used to quantify how the NM system responds to the intervention. The model delivers a realistic replica of live NMJs *in vivo*, approving a quick, accurate, and non-invasive drug testing. Animal testing is known to be an extremely inaccurate method, with many ethical concerns of using animal subjects for drug testing. Studies have shown that only one out of 50 drugs that are tested on animals *in vivo* are suitable for human use, as well as the approval process for drug use in humans based on animal testing being a complex and largely unsuccessful endeavour. In contrast, the functional data generated by this *in vitro* NMJ model can be directly compared to what clinicians may be observing in clinical human trials. Therefore, this model may provide a new guidance for the design of future clinical trials, and significantly decrease the time needed for drug development. Additionally, the delicacy of this model delivers an extremely precise screening tool for new drugs as the model has the competence to quantify the degree of loss-of-function caused by neuromuscular blocking agents with various modes of action. This model also allows for futher

examination into the behaviour of disease progression in the NM system, ensuing a better understanding of a treatment decisions for clinical patients. Moreover, a future version of the NMJ model could be further developed with diseased MNs or SkMCs, and can be additionally used to develop innovative therapies to treat neuromuscular diseases.

However, there is a need for further studies to determine how motor neurons can be used to identify NMJs. The additional tests that can be done in this regard include immunohistochemic markers such as nestin and acetyltransferase or reverse transcriptase polymerase chain reaction (PCR) to identify motor-neuron specific markers (homebox) after RNA isolation (Alves *et al.,* 2015; Yi *et al*., 2018). Innervated NMJs can be determined using immunohistochemical marker and α-Bungarotoxin- tetramethylrhodamine (Kim *et al*., 2008).

8.2 Conclusion

In the platform described in this thesis, neural progenitor cells that were derived from human embryonic stem cells (hESC), were added one day after the culture of myoblasts. Over the course of 7 days, a fully functional mature NMJ was formed. In this model, myoblasts differentiated into myotubes and NPCs differentiated spontaneously into cholinergic motor neurons sprouted axons that branched to form multiple NMJ innervation sites along myotubes which showed extensive spontaneous contractile activity. The obvious advantages of this described model are that it is a much simpler, serum and neural growth factors-free co-culture platform and therefore straightforward to manipulate the system variables, which will allow investigation into MN and NMJ associated diseases including sarcopenia and cancer.

Chapter 7 results establish proof-of-concept that this model could be used as preclinical *in vitro* for diabetes studies thus presents a promising tool to study diabetes mechanisms, and a platform to trial innovative therapies.

This provides further evidence for the high level of functional maturation achieved by co-cultured cells using the described platform. In the system described in this thesis, human immortalised myoblasts were co-cultured with NPCs derived from hESCs. In a period of seven days, myoblasts differentiated into myotubes while NPCs differentiated into motor neurons which sprouted axons that spread out to create several NMJ innervation sites along the myotubes, and the myotubes exhibited extensive contract activity. This is a cell culture platform that could be employed for studying human NMJ growth and disease and could result in a reduction of the use of the animal model in studies of the future. The co-culture model used shows that it can be applied in further diabetes studies. Although the study developed from a mono-culture to a co-culture model, it was never about comparing the two models. AGEs had significant effects on co-culture model based on the parameters measured, which supports the assumption that a co-culture of SkMCs and NPCs plays a significant model in supporting its viability and suitability. Some of the NPCs in the co-culture model differentiated into cells similar to motor neurons morphologically. The human derived and serum free co-culture model can be optimised to be used in many applications. The availability of myotubes and motor neurons enhanced innervation in the muscles, thereby leading to the development of a functional NMJ model. The model increases the number of applications that can be used for NMJ formation and spinal cord, muscle, and motor neurons diseases. Considering the findings of the study, it is evident that co-culture model can be optimised to analyse the development of DN in diabetic model as well as drug efficacy and toxicity tests.

Chapter 9: References

9.0 References

Aagaard, P., Simonson, E. B., Andersen, J. L., Magnusson, P. and Dyhre-Poulsen, P. (2002) 'Increased rate of force development and neural drive of human skeletal muscle following resistance training' *Journal of Applied Physiology,* 93(4), Jan, pp.1318-1326

Aas, V., Bakke, S. S., Feng, Y. Z., Kase, E. T., Jensen, J., Bajpeyi, S., Thoresen, G. H. and Rustan, A. C. (2013) 'Are cultured human myotubes far from home?' *Cell Tissue Res*, 354(3), Dec, pp. 671-682.

Abd Al Samid, M., McPhee, J. S., Saini, J., McKay, T. R., Fitzpatrick, L. M., Mamchaoui, K., Bigot, A., Mouly, V., Butler-Browne, G. and Al-Shanti, N. (2018) 'A functional human motor unit platform engineered from human embryonic stem cells and immortalized skeletal myoblasts.' *Stem Cells Cloning*, 11 pp. 85-93.

Abdul-Ghani, M. and DeFronzo, R. (2010) 'Pathogenesis of Insulin Resistance in Skeletal Muscle'. Journal of Biomedicine and Biotechnology, 2010 pp.1-19.

Adachi, Y., Nojima, M., Mori, M., Yamashita, K., Yamano, H.-O., Nakase, H., Endo, T., Wakai, K., Sakata, K. and Tamakoshi, A. (2017) 'Insulin-like growth factor-1, IGF binding protein-3, and the risk of esophageal cancer in a nested case-control study.' *World journal of gastroenterology*, 23(19) pp. 3488-3495.

Adams, G. R. (2006) 'Satellite cell proliferation and skeletal muscle hypertrophy.' *Appl Physiol Nutr Metab,* 31(6), Oct, pp.782-790

Ahmad, S., Khan, M., Akhter, F., Khan, M., Khan, A., Ashraf, J., Pandey, R. and Shahab, U. (2014) 'Glycoxidation of biological macromolecules: A critical approach to halt the menace of glycation'. *Glycobiology*, 24(11) pp.979-990.

Ahmed, N. (2005) 'Advanced glycation endproducts--role in pathology of diabetic complications.' *Diabetes Res Clin Pract*, 67(1), Jan, pp. 3-21.

Ahmed, N. and Thornalley, P. (2007). Advanced glycation endproducts: what is their relevance to diabetic complications?. *Diabetes, Obesity and Metabolism*, 9(3), pp.233-245.

Allen, R. E. and Boxhorn, L. K. (1989) 'Regulation of skeletal muscle satellite cell proliferation and differentiation by transforming growth factor-beta, insulin-like growth factor 1, and fibroblast growth factor.' *Journal of Cellular Physiology,* 138(2), Jan, pp.311-315

Allen, R. E., Sheehan, S. M., Taylor, R. G., Kendall, T. L. and Rice, G. M. (1995) 'Hepatocyte growth factor activates quiescent skeletal muscle satellite cells in vitro.' *J Cell Physiol,* 165(2), Oct, pp. 307-312

Allen, M., Doherty, T., Rice, C. and Kimpinski, K. (2016) 'Physiology in Medicine: neuromuscular consequences of diabetic neuropathy'. *Journal of Applied Physiology*, 121(1) pp.1-6.

Alves, C., Dariolli, R., Jorge, F., Monteiro, M., Maximino, J., Martins, R., Strauss, B., Krieger, J., Callegaro, D. and Chadi, G. (2015). Gene expression profiling for human iPS- derived motor neurons from sporadic ALS patients reveals a strong association between mitochondrial functions and neurodegeneration.*Frontiers in Cellular Neuroscience*, 9.

Amato, A. A. (2018) 'Myasthenia Gravis and Other Diseases of the Neuromuscular Junction.' *In* Jameson, J. L., Fauci, A. S., Kasper, D. L., Hauser, S. L., Longo, D. L. and Loscalzo, J. (eds.) *Harrison's Principles of Internal Medicine, 20e*. New York, NY: McGraw-Hill Education,

An, M. C., Lin, W., Yang, J., Dominguez, B., Padgett, D., Sugiura, Y., Aryal, P., Gould, T. W., Oppenheim, R. W., Hester, M. E., Kaspar, B. K., Ko, C.-P. and Lee, K.-F. (2010) 'Acetylcholine negatively regulates development of the neuromuscular junction through distinct cellular mechanisms.' *Proceedings of the National Academy of Sciences*, 107(23) pp. 10702-10707.

Andersen, H. (2009) 'Motor function in diabetic neuropathy'. *Acta Neurologica Scandinavica*, 100(4) pp.211-220.

Andreassen, C. S., Jakobsen, J., Flyvbjerg, A. and Andersen, H. (2009) 'Expression of neurotrophic factors in diabetic muscle--relation to neuropathy and muscle strength.' *Brain*, 132(Pt 10), Oct, pp. 2724-2733.

Apel, E. D., Roberds, S. L., Campbell, K. P. and Merlie, J. P. (1995) 'Rapsyn may function as a link between the acetylcholine receptor and the agrin-binding dystrophin-associated glycoprotein complex.' *Neuron*, 15(1), Jul, pp. 115-126.

Apel, E. D., Glass, D. J., Moscoso, L. M., Yancopoulos, G. D. and Sanes, J. R. (1997) 'Rapsyn is required for MuSK signaling and recruits synaptic components to a MuSK-containing scaffold.' *Neuron*, 18(4), Apr, pp. 623-635.

Arnold, A. S., Gueye, M., Guettier-Sigrist, S., Courdier-Fruh, I., Coupin, G., Poindron, P. and Gies, J. P. (2004) 'Reduced expression of nicotinic AChRs in myotubes from spinal muscular atrophy I patients.' *Lab Invest*, 84(10), Oct, pp. 1271-1278.

Arnold, A.-S., Christe, M. and Handschin, C. (2012) 'A Functional Motor Unit in the Culture Dish: Coculture of Spinal Cord Explants and Muscle Cells.' *Journal of Visualized Experiments : JoVE*, (62),p. 3616.

Arvat, E., Broglio, F. and Ghigo, E. (2000) 'Insulin-Like Growth Factor I.' *Drugs & Ageing,* 16(1), Jan, pp.29-40

Arvidsson, U., Riedl, M., Elde, R. and Meister, B. (1997) 'Vesicular acetylcholine transporter (VAChT) protein: a novel and unique marker for cholinergic neurons in the central and peripheral nervous systems.' *J Comp Neurol*, 378(4), Feb 24, pp. 454-467.

Ashby, P. R., Wilson, S. J. and Harris, A. J. (1993) 'Formation of primary and secondary myotubes in aneural muscles in the mouse mutant peroneal muscular atrophy.' *Dev Biol*, 156(2), Apr, pp. 519-528.

Ashraf, J., Ahmad, S., Rabbani, G., Jan, A., Lee, E., Khan, R. and Choi, I. (2014) 'Physicochemical analysis of structural alteration and advanced glycation end products generation during glycation of H2A histone by 3-deoxyglucosone'. *IUBMB Life*, 66(10) pp.686-693.

Ashraf, J., Ahmad, S., Rabbani, G., Hasan, Q., Jan, A., Lee, E., Khan, R., Alam, K. and Choi, I. (2015) '3-Deoxyglucosone: A Potential Glycating Agent Accountable for Structural Alteration in H3 Histone Protein through Generation of Different AGEs'. *PLOS ONE*, 10(2) p.e0116804.

Ashraf, J., Ansari, M., Khan, H., Alzohairy, M. and Choi, I. (2016) 'Green synthesis of silver nanoparticles and characterization of their inhibitory effects on AGEs formation using biophysical techniques'. *Scientific Reports*, 6(1).

Aulehla, A. and Pourquié, O. (2010) 'Signaling gradients during paraxial mesoderm development.' *Cold Spring Harbor perspectives in biology*, 2(2) pp. a000869-a000869.

Baker, J., Liu, J. P., Robertson, E. J. and Efstratiadis, A. (1993) 'Role of insulin-like growth factors in embryonic and postnatal growth.' *Cell*, 75(1), Oct 8, pp. 73-82.

Bandi, E., Jevsek, M., Mars, T., Jurdana, M., Formaggio, E., Sciancalepore, M., Fumagalli, G., Grubic, Z., Ruzzier, F. and Lorenzon, P. (2008) 'Neural agrin controls maturation of the excitation-contraction coupling mechanism in human myotubes developing in vitro.' *Am J Physiol Cell Physiol*, 294(1), Jan, pp. C66-73.

Barker, A. R., & Cicchetti, F. (2012) 'Neuroanatomy and Neuroscience at a Glance, 4th edition. Wiley-Blackwell.

Bartoli, M., Ramarao, M. K. and Cohen, J. B. (2001) 'Interactions of the rapsyn RING-H2 domain with dystroglycan.' *J Biol Chem*, 276(27), Jul 6, pp. 24911-24917.

Barton, E. R., Morris, L., Musaro, A., Rosenthal, N. and Sweeney, H. L. (2002) 'Muscle-specific expression of insulin-like growth factor 1 counters muscle decline in *mdx* mice.' *Journal of Cell Biology,* 157(1), Jan, pp.137-148

Baudet, C., Pozas, E., Adameyko, I., Andersson, E., Ericson, J. and Ernfors, P. (2008) 'Retrograde Signaling onto Ret during Motor Nerve Terminal Maturation.' *The Journal of Neuroscience*, 28(4) pp. 963-975.

Baynes, J. W. (1991) 'Role of oxidative stress in development of complications in diabetes.' *Diabetes*, 40(4), Apr, pp. 405-412.

Behringer, R., et al. (2017). Testing Serum Batches for Mouse Embryonic Stem Cell Culture. Cold Spring Harb Protoc. (12): p.

BEISSWENGER, B., DELUCIA, E., LAPOINT, N., SANFORD, R. and BEISSWENGER, P. (2005) 'Ketosis Leads to Increased Methylglyoxal Production on the Atkins Diet'. *Annals of the New York Academy of Sciences*, 1043(1) pp.201-210.

Belluardo, N., Westerblad, H., Mudo, G., Casabona, A., Bruton, J., Caniglia, G., Pastoris, O., Grassi, F. and Ibanez, C. F. (2001) 'Neuromuscular junction disassembly and muscle fatigue in mice lacking neurotrophin-4.' *Mol Cell Neurosci*, 18(1), Jul, pp. 56-67.

Benatar, M. (2007) 'Lost in translation: treatment trials in the SOD1 mouse and in human ALS.' *Neurobiol Dis*, 26(1), Apr, pp. 1-13.

Bentzinger, C. F., Wang, Y. X. and Rudnicki, M. A. (2012) 'Building muscle: molecular regulation of myogenesis.' *Cold Spring Harb Perspect Biol*, 4(2).

Berry, B.J., Akanda, N., Smith, A.S., Long, C.J., Schnepper, M.T., Guo, X. and Hickman, J.J. (2015). Morphological and functional characterization of human induced pluripotent stem cell-derived neurons (iCell Neurons) in defined culture systems. *Biotechnology progress*, *31*(6), pp.1613-1622.

Bezakova, G., Helm, J. P., Francolini, M. and Lomo, T. (2001) 'Effects of purified recombinant neural and muscle agrin on skeletal muscle fibers *in vivo*.' *J Cell Biol*, 153(7), Jun 25, pp. 1441-1452.

Bezakova, G. and Ruegg, M. A. (2003) 'New insights into the roles of agrin.' *Nat Rev Mol Cell Biol*, 4(4), Apr, pp. 295-308.

Biswal, B., Yetkin, F. Z., Haughton, V. M. and Hyde, J. S. (1995) 'FUNCTIONAL CONNECTIVITY IN THE MOTOR CORTEX OF RESTING HUMAN BRAIN USING ECHO-PLANAR MRI.' *Magnetic Resonance in Medicine*, 34(4), Oct, pp. 537-541.

Bladt, F., Riethmacher, D., Isenmann, S., Aguzzi, A. and Birchmeier, C. (1995) 'Essential role for the *c-met* receptor in the migration of myogenic precursor cells into the limb bud.' *Nature,* Jan, pp.768-771

Bolliger, M. F., Zurlinden, A., Luscher, D., Butikofer, L., Shakhova, O., Francolini, M., Kozlov, S. V., Cinelli, P., Stephan, A., Kistler, A. D., Rulicke, T., Pelczar, P., Ledermann, B., Fumagalli, G., Gloor, S. M., Kunz, B. and Sonderegger, P. (2010) 'Specific proteolytic cleavage of agrin regulates maturation of the neuromuscular junction.' *J Cell Sci*, 123(Pt 22), Nov 15, pp. 3944-3955.

Borodinsky, L. N. and Spitzer, N. C. (2007) 'Activity-dependent neurotransmitter-receptor matching at the neuromuscular junction.' *Proc Natl Acad Sci U S A*, 104(1), Jan 2, pp. 335-340.

Boutet, S. C., Disatnik, M. H., Chan, L. S., Iori, K. and Rando, T. A. (2007) 'Regulation of Pax3 by proteasomal degradation of monoubiquitinated protein in skeletal muscle progenitors.' *Cell,* 130(2), Jan, pp.349-362

Bowe, M. A., Deyst, K. A., Leszyk, J. D. and Fallon, J. R. (1994) 'Identification and purification of an agrin receptor from Torpedo postsynaptic membranes: a heteromeric complex related to the dystroglycans.' *Neuron*, 12(5), May, pp. 1173-1180.

Bowery, N. G., Bettler, B., Froestl, W., Gallagher, J. P., Marshall, F., Raiteri, M., Bonner, T. I. and Enna, S. J. (2002) 'International Union of Pharmacology. XXXIII. Mammalian gamma-aminobutyric acid(B) receptors: structure and function.' *Pharmacol Rev*, 54(2), Jun, pp. 247-264.

Bowman, W. C. (2006) 'Neuromuscular block.' *British journal of pharmacology*, 147 Suppl 1(Suppl 1) pp. S277-S286.

Brandon, E. P., Lin, W., D'Amour, K. A., Pizzo, D. P., Dominguez, B., Sugiura, Y., Thode, S., Ko, C. P., Thal, L. J., Gage, F. H. and Lee, K. F. (2003) 'Aberrant patterning of neuromuscular synapses in choline acetyltransferase-deficient mice.' *J Neurosci*, 23(2), Jan 15, pp. 539-549.

Bril, V. (2014) 'Neuromuscular complications of diabetes mellitus.' *Continuum (Minneap Minn)*, 20(3 Neurology of Systemic Disease), Jun, pp. 531-544.

Brose, N., Petrenko, A. G., Sudhof, T. C. and Jahn, R. (1992) 'Synaptotagmin: a calcium sensor on the synaptic vesicle surface.' *Science*, 256(5059), May 15, pp. 1021-1025.

Bruneau, E. G., Brenner, D. S., Kuwada, J. Y. and Akaaboune, M. (2008) 'Acetylcholine receptor clustering is required for the accumulation and maintenance of scaffolding proteins.' *Curr Biol*, 18(2), Jan 22, pp. 109-115.

Brunner, D., Frank, J., Appl, H., Schoffl, H., Pfaller, W., and Gstraunthaler, G. (2010) 'Serum-free cell culture: The serum-free media interactive online database' *Altex.* 27 (1) pp. 53-62.

Bruusgaard, J. C., Liestol, K., Ekmark, M., Kollstad, K. and Gundersen, K. (2003) 'Number and spatial distribution of nuclei in the muscle fibres of normal mice studied in vivo.' *J Physiol*, 551(Pt 2), Sep 1, pp. 467-478.

Buckingham, M., Bajard, L., Chang, T., Daubas, P., Hadchouel, J., Meilhac, S., Montarras, D., Rocancourt, D. and Relaix, F. (2003) 'The formation of skeletal muscle: from somite to limb.' *Journal of Anatomy*, 202(1), Jan, pp. 59-68.

Buj-Bello, A., Buchman, V. L., Horton, A., Rosenthal, A. and Davies, A. M. (1995) 'GDNF is an age-specific survival factor for sensory and autonomic neurons.' *Neuron*, 15(4), Oct, pp. 821-828.

Bullwinkel, J., Baron-Lühr, B., Lüdemann, A., Wohlenberg, C., Gerdes, J. and Scholzen, T. (2006) 'Ki-67 protein is associated with ribosomal RNA transcription in quiescent and proliferating cells.' *Journal of Cellular Physiology*, 206(3) pp. 624-635.

Cadot, B., Gache, V. and Gomes, E. (2015) 'Moving and positioning the nucleus in skeletal muscle – one step at a time'. *Nucleus*, 6(5) pp.373-381.

Calcutt, N., Cooper, M., Kern, T. and Schmidt, A. (2009) 'Therapies for hyperglycaemia-induced diabetic complications: from animal models to clinical trials'. *Nature Reviews Drug Discovery*, 8(5) pp.417-430.

Callaghan, B., Cheng, H., Stables, C., Smith, A. and Feldman, E. (2012). Diabetic neuropathy: clinical manifestations and current treatments. *The Lancet Neurology*, 11(6), pp.521-534.

Campagna, J. A., Ruegg, M. A. and Bixby, J. L. (1995) 'Agrin is a differentiation-inducing "stop signal" for motoneurons in vitro.' *Neuron*, 15(6), Dec, pp. 1365-1374.

Campagna, J. A., Ruegg, M. A. and Bixby, J. L. (1997) 'Evidence that agrin directly influences presynaptic differentiation at neuromuscular junctions in vitro.' *Eur J Neurosci*, 9(11), Nov, pp. 2269-2283.

Carosio, S., Berardinelli, M. G., Aucello, M. and Musaro, A. (2011) 'Impact of ageing on muscle cell regeneration.' *Ageing Res Rev*, 10(1), Jan, pp. 35-42.

Carrasco, D. I. and English, A. W. (2003) 'Neurotrophin 4/5 is required for the normal development of the slow muscle fiber phenotype in the rat soleus.' *J Exp Biol*, 206(Pt 13), Jul, pp. 2191-2200.

Cassese, A., Esposito, I., Fiory, F., Barbagallo, A., Paturzo, F., Mirra, P., Ulianich, L., Giacco, F., Iadicicco, C., Lombardi, A., Oriente, F., Van Obberghen, E., Beguinot, F., Formisano, P. and Miele, C. (2008). In Skeletal Muscle Advanced Glycation End Products (AGEs) Inhibit Insulin Action and Induce the Formation of Multimolecular Complexes Including the Receptor for AGEs. *Journal of Biological Chemistry*, 283(52), pp.36088-36099.

Chandrasekera, P. (2014). Of rodents and men: Species-specific glucose regulation and type 2 diabetes research. *ALTEX*, pp.157-176.

Chen, J. C. J. and Goldhamer, D. J. (2003) 'Skeletal muscle stem cells.' *Reproductive biology and endocrinology : RB&E*, 1, 11/13, pp. 101-101.

Chevrel, G., Hohlfeld, R. and Sendtner, M. (2006) 'The role of neurotrophins in muscle under physiological and pathological conditions.' *Muscle Nerve*, 33(4), Apr, pp. 462-476.

Chin, M. H., Mason, M. J., Xie, W., Volinia, S., Singer, M., Peterson, C., Ambartsumyan, G., Aimiuwu, O., Richter, L., Zhang, J., Khvorostov, I., Ott, V., Grunstein, M., Lavon, N., Benvenisty, N., Croce, C. M., Clark, A. T., Baxter, T., Pyle, A. D., Teitell, M. A., Pelegrini, M.,

Plath, K. and Lowry, W. E. (2009) 'Induced pluripotent stem cells and embryonic stem cells are distinguished by gene expression signatures.' *Cell Stem Cell*, 5(1), Jul 2, pp. 111-123.

Chipman, P. H., Zhang, Y. and Rafuse, V. F. (2014) 'A stem-cell based bioassay to critically assess the pathology of dysfunctional neuromuscular junctions.' *PloS one*, 9(3) pp. e91643-e91643.

Chiu, C., Yang, R., Sheu, M., Chan, D., Yang, T., Tsai, K., Chiang, C. and Liu, S. (2015) 'Advanced glycation end-products induce skeletal muscle atrophy and dysfunction in diabetic mice via a RAGE-mediated, AMPK-down-regulated, Akt pathway'. *The Journal of Pathology*, 238(3) pp.470-482.

Chiu, C.-Y., Yang, R.-S., Sheu, M.-L., Chan, D.-C., Yang, T.-H., Tsai, K.-S., Chiang, C.-K. and Liu, S.-H. (2016) 'Advanced glycation end-products induce skeletal muscle atrophy and dysfunction in diabetic mice via a RAGE-mediated, AMPK-down-regulated, Akt pathway: AGEs inhibition alleviates diabetic myopathy in mice.' *The Journal of Pathology*, 238(3) pp. 470-482.

Chu, Y.W., Schmitz, S., Choudhury, B., Telford, W., Kapoor, V., Garfield, S., Howe, D. and Gress, R.E. (2008). Exogenous insulin-like growth factor 1 enhances thymopoiesis predominantly through thymic epithelial cell expansion. *Blood, The Journal of the American Society of Hematology*, *112*(7), pp.2836-2846.

Chun, Y., Chaudhari, P. and Jang, Y. (2010) 'Applications of Patient-Specific Induced Pluripotent Stem Cells; Focused on Disease Modeling, Drug Screening and Therapeutic Potentials for Liver Disease'. *International Journal of Biological Sciences*, pp.796-805.

Chung, C.Y., Khurana, V., Auluck, P.K., Tardiff, D.F., Mazzulli, J.R., Soldner, F., Baru, V., Lou, Y., Freyzon, Y., Cho, S. and Mungenast, A.E. (2013). Identification and rescue of α-synuclein toxicity in Parkinson patient–derived neurons. *Science*, *342*(6161), pp.983-987.

Cisterna, B.A., C. Cardozo, and J.C. Saez. (2014) Neuronal involvement in muscular atrophy. Front Cell Neurosci. 8: p. 405.

Cobb, L. J., Salih, D. A., Gonzalez, I., Tripathi, G., Carter, E. J., Lovett, F., Holding, C. and Pell, J. M. (2004) 'Partitioning of IGFBP-5 actions in myogenesis: IGF-independent anti-apoptotic function.' *J Cell Sci*, 117(Pt 9), Apr 1, pp. 1737-1746.

Conboy, I. M. and Rando, T. A. (2002) 'The regulation of Notch signaling controls satellite cell activation and cell fate determination in postnatal myogenesis.' *Developmental Cell,* 3(3), Jan, pp.397-409

Condon, K., Silberstein, L., Blau, H. M. and Thompson, W. J. (1990) 'Differentiation of fiber types in aneural musculature of the prenatal rat hindlimb.' *Dev Biol*, 138(2), Apr, pp. 275-295.

Cooke, I. M. and Grinnell, A. D. (1964) 'EFFECT OF TUBOCURARINE ON ACTION POTENTIALS IN NORMAL AND DENERVATED SKELETAL MUSCLE.' *The Journal of physiology*, 175(2) pp. 203-210.

Copeland, R., Bullen, J. and Hart, G. (2008) 'Cross-talk between GlcNAcylation and phosphorylation: roles in insulin resistance and glucose toxicity'. *American Journal of Physiology-Endocrinology and Metabolism*, 295(1) pp.E17-E28.

Coronado, R., Morrissette, J., Sukhareva, M. and Vaughan, D. M. (1994) 'Structure and function of ryanodine receptors.' *Am J Physiol*, 266(6 Pt 1), Jun, pp. C1485-1504.

Colca, J.R. (2015). Discontinued drug therapies to treat diabetes in 2014. Expert Opin Investig Drugs. 24(9): p. 1241-5.

Collins, T. J. (2007) 'ImageJ for microscopy.' *BioTechniques*, 43(1S) pp. S25-S30.

Court, F. A., Gillingwater, T. H., Melrose, S., Sherman, D. L., Greenshields, K. N., Morton, A. J., Harris, J. B., Willison, H. J. and Ribchester, R. R. (2008) 'Identity, developmental restriction and reactivity of extralaminar cells capping mammalian neuromuscular junctions.' *J Cell Sci*, 121(Pt 23), Dec 1, pp. 3901-3911.

Dalal, M., Ferrucci, L., Sun, K., Beck, J., Fried, L. and Semba, R. (2009). Elevated Serum Advanced Glycation End Products and Poor Grip Strength in Older Community-Dwelling Women. *The Journals of Gerontology Series A: Biological Sciences and Medical Sciences*, 64A(1), pp.132-137.

Daniels, M. P., Lowe, B. T., Shah, S., Ma, J., Samuelsson, S. J., Lugo, B., Parakh, T. and Uhm, C. S. (2000) 'Rodent nerve-muscle cell culture system for studies of neuromuscular junction development: refinements and applications.' *Microsc Res Tech*, 49(1), Apr 1, pp. 26-37.

Das, M., Rumsey, J. W., Gregory, C. A., Bhargava, N., Kang, J. F., Molnar, P., Riedel, L., Guo, X. and Hickman, J. J. (2007) 'Embryonic motoneuron-skeletal muscle co-culture in a defined system.' *Neuroscience*, 146(2), May 11, pp. 481-488.

Das, M., Rumsey, J. W., Bhargava, N., Stancescu, M. and Hickman, J. J. (2010) 'A defined long-term in vitro tissue engineered model of neuromuscular junctions.' *Biomaterials*, 31(18), Jun, pp. 4880-4888.

de Castro, B. M., De Jaeger, X., Martins-Silva, C., Lima, R. D. F., Amaral, E., Menezes, C., Lima, P., Neves, C. M. L., Pires, R. G., Gould, T. W., Welch, I., Kushmerick, C., Guatimosim, C., Izquierdo, I., Cammarota, M., Rylett, R. J., Gomez, M. V., Caron, M. G., Oppenheim, R. W., Prado, M. A. M. and Prado, V. F. (2009) 'The Vesicular Acetylcholine Transporter Is Required for Neuromuscular Development and Function.' *Molecular and Cellular Biology*, 29(19) pp. 5238-5250.

Delaney-Sathy, L., Fessell, D., Jacobson, J. and Hayes, C. (2000) 'Sonography of Diabetic Muscle Infarction with MR Imaging, CT, and Pathologic Correlation'. *American Journal of Roentgenology*, 174(1) pp.165-169.

Delaporte, C., Dautreaux, B. and Fardeau, M. (1986) 'Human myotube differentiation in vitro in different culture conditions.' *Biol Cell*, 57(1) pp. 17-22.

DeMambro, V. E., Clemmons, D. R., Horton, L. G., Bouxsein, M. L., Wood, T. L., Beamer, W. G., Canalis, E. and Rosen, C. J. (2008) 'Gender-specific changes in bone turnover and skeletal architecture in igfbp-2-null mice.' *Endocrinology*, 149(5), May, pp. 2051-2061.

de M. Bandeira, S., da Fonseca, L., da S. Guedes, G., Rabelo, L., Goulart, M. and Vasconcelos, S. (2013) 'Oxidative Stress as an Underlying Contributor in the Development of Chronic Complications in Diabetes Mellitus'. *International Journal of Molecular Sciences*, 14(2) pp.3265-3284.

Demestre, M., Orth, M., Föhr, K. J., Achberger, K., Ludolph, A. C., Liebau, S. and Boeckers, T. M. (2015) 'Formation and characterisation of neuromuscular junctions between hiPSC derived motoneurons and myotubes.' *Stem Cell Research*, 15(2), 2015/09/01/, pp. 328-336.

Demuro, A., Palma, E., Eusebi, F. and Miledi, R. (2001) 'Inhibition of nicotinic acetylcholine receptors by bicuculline.' *Neuropharmacology*, 41(7), Dec, pp. 854-861.

Denoth, J., Stussi, E., Csucs, G. and Danuser, G. (2002) 'Single muscle fiber contraction is dictated by inter-sarcomere dynamics.' *Journal of Theoretical Biology*, 216(1), May, pp. 101-122.

Deshmukh, A. (2016) 'Insulin-stimulated glucose uptake in healthy and insulin-resistant skeletal muscle'. *Hormone Molecular Biology and Clinical Investigation*, 26(1).

Dey, I., Midha, N., Singh, G., Forsyth, A., Walsh, S. K., Singh, B., Kumar, R., Toth, C. and Midha, R. (2013) 'Diabetic Schwann cells suffer from nerve growth factor and neurotrophin-3 underproduction and poor associability with axons.' *Glia*, 61(12), Dec, pp. 1990-1999.

Dixon, T. A., Cohen, E., Cairns, D. M., Rodriguez, M., Mathews, J., Jose, R. R. and Kaplan, D. L. (2018) 'Bioinspired Three-Dimensional Human Neuromuscular Junction Development in Suspended Hydrogel Arrays.' *Tissue Eng Part C Methods*, 24(6), Jun, pp. 346-359.

Dobrowolny, G., Giacinti, C., Pelosi, L., Nicoletti, C., Winn, N., Barberi, L., Molinaro, M., Rosenthal, N. and Musarò, A. (2005) 'Muscle expression of a local Igf-1 isoform protects motor neurons in an ALS mouse model.' *The Journal of cell biology*, 168(2) pp. 193-199.

Dobrowolny, G., Giacinti, C., Pelosi, L., Nicoletti, C., Winn, N., Barberi, L., Molinaro, M., Rosenthal, N. and Musarò, A. (2005) 'Muscle expression of a local Igf-1 isoform protects motor neurons in an ALS mouse model.' *The Journal of cell biology*, 168(2) pp. 193-199.

Domet, M. A., Webb, C. E. and Wilson, D. F. (1995) 'IMPACT OF ALPHA-BUNGAROTOXIN ON TRANSMITTER RELEASE AT THE NEUROMUSCULAR-JUNCTION OF THE RAT.' *Neuroscience Letters*, 199(1), Oct, pp. 49-52.

Drenth, H., Zuidema, S., Bunt, S., Bautmans, I., van der Schans, C. and Hobbelen, H. (2016) 'The Contribution of Advanced Glycation End product (AGE) accumulation to the decline in motor function'. *European Review of Aging and Physical Activity*, 13(1).

D'Souza, D., Al-Sajee, D. and Hawke, T. (2013) 'Diabetic myopathy: impact of diabetes mellitus on skeletal muscle progenitor cells'. Frontiers in Physiology, 4.

Duan, C., Ren, H. and Gao, S. (2010) 'Insulin-like growth factors (IGFs), IGF receptors, and IGF-binding proteins: roles in skeletal muscle growth and differentiation.' *Gen Comp Endocrinol*, 167(3), Jul 1, pp. 344-351.

Dutton, E. K., Uhm, C. S., Samuelsson, S. J., Schaffner, A. E., Fitzgerald, S. C. and Daniels, M. P. (1995) 'Acetylcholine receptor aggregation at nerve-muscle contacts in mammalian cultures: induction by ventral spinal cord neurons is specific to axons.' *J Neurosci*, 15(11), Nov, pp. 7401-7416.

Dyck, P., Albers, J., Andersen, H., Arezzo, J., Biessels, G., Bril, V., Feldman, E., Litchy, W., O'Brien, P. and Russell, J. (2011). Diabetic polyneuropathies: update on research definition, diagnostic criteria and estimation of severity. *Diabetes/Metabolism Research and Reviews*, 27(7), pp.620-628.

Edström, E., Altun, M., Bergman, E., Johnson, H., Kullberg, S., Ramírez-León, V. and Ulfhake, B., (2007). Factors contributing to neuromuscular impairment and sarcopenia during aging. *Physiology & behavior*, *92*(1-2), pp.129-135.

Edwards, J., Vincent, A., Cheng, H. and Feldman, E. (2008) 'Diabetic neuropathy: Mechanisms to management'. *Pharmacology & Therapeutics*, 120(1) pp.1-34.

Elinos, D., Rodríguez, R., Martínez, L. A., Zetina, M. E., Cifuentes, F. and Morales, M. A. (2016) 'Segregation of Acetylcholine and GABA in the Rat Superior Cervical Ganglia: Functional Correlation.' *Frontiers in cellular neuroscience*, 10 pp. 91-91.

Engel, A. G. and Sine, S. M. (2005) 'Current understanding of congenital myasthenic syndromes.' *Current Opinion in Pharmacology*, 5(3), Jun, pp. 308-321.

Englander, L. L. and Rubin, L. L. (1987) 'Acetylcholine receptor clustering and nuclear movement in muscle fibers in culture.' *The Journal of Cell Biology*, 104(1) pp. 87-95.

Ernfors, P., Lee, K. F., Kucera, J. and Jaenisch, R. (1994) 'Lack of neurotrophin-3 leads to deficiencies in the peripheral nervous system and loss of limb proprioceptive afferents.' *Cell*, 77(4), May 20, pp. 503-512.

Faravelli, I., Frattini, E., Ramirez, A., Stuppia, G., Nizzardo, M. and Corti, S. (2014) 'iPSC-Based Models to Unravel Key Pathogenetic Processes Underlying Motor Neuron Disease Development.' *J Clin Med*, 3(4), Oct 17, pp. 1124-1145.

Feher, J. (2017) '3.6 - The Neuromuscular Junction and Excitation–Contraction Coupling.' *In Quantitative Human Physiology (Second Edition)*. Boston: Academic Press, pp. 318-333.

Fernyhough, P., Diemel, L. T., Brewster, W. J. and Tomlinson, D. R. (1995) 'Altered neurotrophin mRNA levels in peripheral nerve and skeletal muscle of experimentally diabetic rats.' *J Neurochem*, 64(3), Mar, pp. 1231-1237.

Fernyhough, P., Diemel, L. T., Hardy, J., Brewster, W. J., Mohiuddin, L. and Tomlinson, D. R. (1995) 'Human recombinant nerve growth factor replaces deficient neurotrophic support in the diabetic rat.' *Eur J Neurosci*, 7(5), May 1, pp. 1107-1110.

Fernyhough, P., Maeda, K. and Tomlinson, D. R. (1996) 'Brain-derived neurotrophic factor mRNA levels are up-regulated in hindlimb skeletal muscle of diabetic rats: effect of denervation.' *Exp Neurol*, 141(2), Oct, pp. 297-303.

Fernyhough, P., Diemel, L. T. and Tomlinson, D. R. (1998) 'Target tissue production and axonal transport of neurotrophin-3 are reduced in streptozotocin-diabetic rats.' *Diabetologia*, 41(3), Mar, pp. 300-306.

Ferrara, N. (2004) 'Vascular endothelial growth factor: basic science and clinical progress.' *Endocr Rev*, 25(4), Aug, pp. 581-611.

Ferris, L. T., Williams, J. S. and Shen, C. L. (2007) 'The effect of acute exercise on serum brain-derived neurotrophic factor levels and cognitive function.' *Med Sci Sports Exerc*, 39(4), Apr, pp. 728-734.

Ferruzza, S., Rossi, C., Sambuy, Y., and Scarino, M. L. (2012) 'Serum-reduced and serum-free media for differentiation of Caco-2 cells' *Altex. 30 (2). pp. 159-168.*

Fischer, L. R., Culver, D. G., Tennant, P., Davis, A. A., Wang, M., Castellano-Sanchez, A., Khan, J., Polak, M. A. and Glass, J. D. (2004) 'Amyotrophic lateral sclerosis is a distal axonopathy: evidence in mice and man.' *Exp Neurol*, 185(2), Feb, pp. 232-240.

FitzPatrick, L.M., Hawkins, K.E., Delhove, J.M., Fernandez, E., Soldati, C., Bullen, L.F., Nohturfft, A., Waddington, S.N., Medina, D.L., Bolaños, J.P. and McKay, T.R. (2018). NF-κB Activity Initiates Human ESC-Derived Neural Progenitor Cell Differentiation by Inducing a Metabolic Maturation Program. *Stem cell reports*, *10*(6), pp.1766-1781.

Florini, J. R., Ewton, D. Z., Magri, K. A. and Mangiacapra, F. J. (1993) 'IGFs and muscle differentiation.' *Adv Exp Med Biol*, 343 pp. 319-326.

Flucher, B. E. and Daniels, M. P. (1989) 'Distribution of Na+ channels and ankyrin in neuromuscular junctions is complementary to that of acetylcholine receptors and the 43 kd protein.' *Neuron*, 3(2), Aug, pp. 163-175.

Folker, E. and Baylies, M. (2013) 'Nuclear positioning in muscle development and disease'. *Frontiers in Physiology*, 4.

Fox, M. A., Sanes, J. R., Borza, D. B., Eswarakumar, V. P., Fassler, R., Hudson, B. G., John, S. W., Ninomiya, Y., Pedchenko, V., Pfaff, S. L., Rheault, M. N., Sado, Y., Segal, Y., Werle, M. J. and Umemori, H. (2007) 'Distinct target-derived signals organize formation, maturation, and maintenance of motor nerve terminals.' *Cell*, 129(1), Apr 6, pp. 179-193.

Frontera, W. R. and Ochala, J. (2015) 'Skeletal Muscle: A Brief Review of Structure and Function.' *Calcified Tissue International*, 96(3), Mar, pp. 183-195.

Funakoshi, H., Belluardo, N., Arenas, E., Yamamoto, Y., Casabona, A., Persson, H. and Ibanez, C. F. (1995) 'Muscle-derived neurotrophin-4 as an activity-dependent trophic signal for adult motor neurons.' *Science*, 268(5216), Jun 9, pp. 1495-1499.

Furman, B. (2015). Streptozotocin-Induced Diabetic Models in Mice and Rats. *Current Protocols in Pharmacology*, pp.5.47.1-5.47.20.

Garcia, C. C., Potian, J. G., Hognason, K., Thyagarajan, B., Sultatos, L. G., Souayah, N., Routh, V. H. and McArdle, J. J. (2012) 'Acetylcholinesterase deficiency contributes to neuromuscular junction dysfunction in type 1 diabetic neuropathy.' *American journal of physiology. Endocrinology and metabolism*, 303(4) pp. E551-E561.

Gautam, M., Noakes, P. G., Mudd, J., Nichol, M., Chu, G. C., Sanes, J. R. and Merlie, J. P. (1995) 'Failure of postsynaptic specialization to develop at neuromuscular junctions of rapsyn-deficient mice.' *Nature*, 377(6546), Sep 21, pp. 232-236.

Gautam, M., Noakes, P. G., Moscoso, L., Rupp, F., Scheller, R. H., Merlie, J. P. and Sanes, J. R. (1996) 'Defective neuromuscular synaptogenesis in agrin-deficient mutant mice.' *Cell*, 85(4), May 17, pp. 525-535.

Gee, S. H., Montanaro, F., Lindenbaum, M. H. and Carbonetto, S. (1994) 'Dystroglycan-alpha, a dystrophin-associated glycoprotein, is a functional agrin receptor.' *Cell*, 77(5), Jun 3, pp. 675-686.

Genç, B., Özdinler, P.H., Mendoza, A.E. and Erzurumlu, R.S. (2004). A chemoattractant role for NT-3 in proprioceptive axon guidance. *PLoS Biol*, *2*(12), p.e403.

Geppert, M., Goda, Y., Hammer, R. E., Li, C., Rosahl, T. W., Stevens, C. F. and Sudhof, T. C. (1994) 'Synaptotagmin I: a major Ca2+ sensor for transmitter release at a central synapse.' *Cell*, 79(4), Nov 18, pp. 717-727.

Gilhus, N. E. (2016) 'Myasthenia Gravis.' *New England Journal of Medicine*, 375(26), Dec, pp. 2570-2581.

Giller, E. L., Jr., Schrier, B. K., Shainberg, A., Fisk, H. R. and Nelson, P. G. (1973) 'Choline acetyltransferase activity is increased in combined cultures of spinal cord and muscle cells from mice.' *Science*, 182(4112), Nov 9, pp. 588-589.

Glass, D. J. (2005) 'Skeletal muscle hypertrophy and atrophy signaling pathways.' *Int J Biochem Cell Biol,* 37(10), Oct, pp.1974-84

Gold, S. M., Schulz, K. H., Hartmann, S., Mladek, M., Lang, U. E., Hellweg, R., Reer, R., Braumann, K. M. and Heesen, C. (2003) 'Basal serum levels and reactivity of nerve growth factor and brain-derived neurotrophic factor to standardized acute exercise in multiple sclerosis and controls.' *J Neuroimmunol*, 138(1-2), May, pp. 99-105.

Gonzalez-Freire, M., de Cabo, R., Studenski, S. A. and Ferrucci, L. (2014) 'The Neuromuscular Junction: Aging at the Crossroad between Nerves and Muscle.' *Front Aging Neurosci*, 6 p. 208.

Gonzalez, M., Ruggiero, F. P., Chang, Q., Shi, Y. J., Rich, M. M., Kraner, S. and Balice-Gordon, R. J. (1999) 'Disruption of Trkb-mediated signaling induces disassembly of postsynaptic receptor clusters at neuromuscular junctions.' *Neuron*, 24(3), Nov, pp. 567-583.

Gould, T. W., Buss, R. R., Vinsant, S., Prevette, D., Sun, W., Knudson, C. M., Milligan, C. E. and Oppenheim, R. W. (2006) 'Complete dissociation of motor neuron death from motor dysfunction by Bax deletion in a mouse model of ALS.' *J Neurosci*, 26(34), Aug 23, pp. 8774-8786.

Grabiec, K., Gajewska, M., Milewska, M., Błaszczyk, M. and Grzelkowska-Kowalczyk, K. (2014) 'The influence of high glucose and high insulin on mechanisms controlling cell cycle progression and arrest in mouse C2C12 myoblasts: the comparison with IGF-I effect'. *Journal of Endocrinological Investigation*, 37(3) pp.233-245.

Griesbeck, O., Parsadanian, A. S., Sendtner, M. and Thoenen, H. (1995) 'Expression of neurotrophins in skeletal muscle: quantitative comparison and significance for motoneuron survival and maintenance of function.' *J Neurosci Res*, 42(1), Sep 1, pp. 21-33.

Grzelkowska-Kowalczyk, K., Wieteska-Skrzeczyńska, W., Grabiec, K. and Tokarska, J. (2012) 'High glucose-mediated alterations of mechanisms important in myogenesis of mouse C2C12 myoblasts'. *Cell Biology International*, 37(1) pp.29-35.

Grzelkowska-Kowalczyk, K. (2014) 'The Effect of High Glucose on Mechanisms Controlling Proliferation of Mouse C2C12 Myoblasts'. *International Journal of Diabetes & Clinical Diagnosis*, 1(1).

Gumy, L., Bampton, E. and Tolkovsky, A. (2008) 'Hyperglycaemia inhibits Schwann cell proliferation and migration and restricts regeneration of axons and Schwann cells from adult murine DRG'. *Molecular and Cellular Neuroscience*, 37(2) pp.298-311.

Guo, X., Das, M., Rumsey, J., Gonzalez, M., Stancescu, M. and Hickman, J. (2010). Neuromuscular junction formation between human stem-cell-derived motoneurons and rat skeletal muscle in a defined system. *Tissue Engineering Part C: Methods*, *16*(6), pp.1347-1355.

Guo, X., Gonzalez, M., Stancescu, M., Vandenburgh, H. H. and Hickman, J. J. (2011) 'Neuromuscular junction formation between human stem cell-derived motoneurons and human skeletal muscle in a defined system.' *Biomaterials*, 32(36), Dec, pp. 9602-9611.

Guo, M., Chen, Y., Du, Y., Dong, Y., Guo, W., Zhai, S., Zhang, H., Dong, S., Zhang, Z., Wang, Y., Wang, P., and Zheng. (2011) 'The bZIP Transcription Factor MoAP1 mediates the oxidative stress response and is critical for pathogenicity of the rice blast fungus magnaporthe oryzae' *PLOS* Pathog 7 (2): e1001302.

Guo, X., Greene, K., Akanda, N., Smith, A., Stancescu, M., Lambert, S., Vandenburgh, H. and Hickman, J. (2014) 'In vitro Differentiation of Functional Human Skeletal Myotubes in a Defined System.' *Biomater Sci*, 2(1), Jan 1, pp. 131-138.

Guo, X., Colon, A., Akanda, N., Spradling, S., Stancescu, M., Martin, C. and Hickman, J. J. (2017) 'Tissue engineering the mechanosensory circuit of the stretch reflex arc with human stem cells: Sensory neuron innervation of intrafusal muscle fibers.' *Biomaterials*, 122, Apr, pp. 179-187.

Haase, G. (2006) 'Motor Neuron Diseases: Cellular and Animal Models.' *In Reviews in Cell Biology and Molecular Medicine*. Wiley-VCH Verlag GmbH & Co.

Hanaire-Broutin, H., Sallerin-Caute, B., Poncet, M.F., Tauber, M., Bastide, R., Chale, J.J., Rosenfeld, R. and Tauber, J.P. (1996). Effect of intraperitoneal insulin delivery on growth hormone binding protein, insulin-like growth factor (IGF)-I, and IGF-binding protein-3 in IDDM. *Diabetologia*, *39*(12), pp.1498-1504.

Hanaire-Broutin, H., Sallerin-Caute, B., Poncet, M. F., Tauber, M., Bastide, R., Rosenfeld, R. and Tauber, J. P. (1996) 'Insulin therapy and GH-IGF-I axis disorders in diabetes: impact of glycaemic control and hepatic insulinization.' *Diabetes Metab*, 22(4), Jul, pp. 245-250.

Happe, C.L., Tenerelli, K.P., Gromova, A.K., Kolb, F. and Engler, A.J. (2017). Mechanically patterned neuromuscular junctions-in-a-dish have improved functional maturation. *Molecular biology of the cell*, *28*(14), pp.1950-1958.

Harper, J. M., Krishnan, C., Darman, J. S., Deshpande, D. M., Peck, S., Shats, I., Backovic, S., Rothstein, J. D. and Kerr, D. A. (2004) 'Axonal growth of embryonic stem cell-derived motor neurons in vitro and in motoneuron-injured adult rats.' *Proc Natl Acad Sci U S A*, 101(18), pp. 7123-7128.

Hattangady, N.G. and M.S. Rajadhyaksha. (2009). A brief review of in vitro models of diabetic neuropathy. Int J Diabetes Dev Ctries.

Hawke, T. J. and Garry, D. J. (2001) 'Myogenic satellite cells physiology to molecular biology.' *J Appl Physiol,* 91(2), Jan, pp.534-551

Hedrington, M.S. and S.N. Davis, (2014). Discontinued in 2013: diabetic drugs. Expert Opin Investig Drugs. 23(12): p. 1703-11.

Henderson, C.E., Camu, W., Mettling, C., Gouin, A., Poulsen, K., Karihaloo, M., Ruilamas, J., Evans, T., McMahon, S.B., Armanini, M.P. and Berkemeier, L. (1993). Neurotrophins promote motor neuron survival and are present in embryonic limb bud. *Nature*, *363*(6426), pp.266-270.

Höke, A. (2012) 'Animal Models of Peripheral Neuropathies'. *Neurotherapeutics*, 9(2) pp.262-269.

Holterman, C. E. and Rudnicki, M. A. (2005) 'Molecular regulation of satellite cell function.' *Cell & Developmental Biology,* 16(4-5), Jan, pp.575-584

Hong, I. H. and Etherington, S. J. (2011) 'Neuromuscular Junction.' *In eLS*. Vol. 1. Chichester: John Wiley & Sons Ltd, Hadwen. (2009) 'Serum-free media for cell culture' *Dr Hadwen trust for human research, retrieved from http://www.drhadwentrust.org/DHT%20-%20FCS%20Free%20Table.pdf.*

Howard, A., McNeil, A., Xiong, F., Xiong, W. and McNeil, P. (2011) 'A Novel Cellular Defect in Diabetes'. *Diabetes*, 60(11) pp.3034-3043.

Hribal, M. L., Nakae, J., Kitamura, T., Shutter, J. R. and Accili, D. (2003) 'Regulation of insulin-like growth factor-dependent myoblast differentiation by Foxo forkhead transcription factors.' *Rockfeller University Press,* 162(4), Jan, pp.535-541

Hsieh-Li, H. M., Chang, J. G., Jong, Y. J., Wu, M. H., Wang, N. M., Tsai, C. H. and Li, H. (2000) 'A mouse model for spinal muscular atrophy.' *Nat Genet*, 24(1), Jan, pp. 66-70.

Hunt, L., Xu, B., Finkelstein, D., Fan, Y., Carroll, P., Cheng, P., Eisenman, R. and Demontis, F. (2015) 'The glucose-sensing transcription factor MLX promotes myogenesis via myokine signaling'. *Genes & Development*, 29(23) pp.2475-2489.

Hwa, V., Oh, Y. and Rosenfeld, R. G. (1999) 'The insulin-like growth factor-binding protein (IGFBP) superfamily.' *Endocr Rev*, 20(6), Dec, pp. 761-787.

Ihara, C., Shimatsu, A., Mizuta, H., Murabe, H., Nakamura, Y. and Nakao, K. (1996) 'Decreased neurotrophin-3 expression in skeletal muscles of streptozotocin-induced diabetic rats.' *Neuropeptides*, 30(4), Aug, pp. 309-312.

Inoue, H., Nagata, N., Kurokawa, H. and Yamanaka, S. (2014) 'iPS cells: a game changer for future medicine.' *Embo j*, 33(5), Mar 3, pp. 409-417.

Ishii, D.N., Glazner, G.W. and Pu, S.F. (1994). Role of insulin-like growth factors in peripheral nerve regeneration. *Pharmacology & therapeutics*, *62*(1-2), pp.125-144.

Ishii, D.N. and Lupien, S.B. (1995)Marwah00. Insulin-like growth factors protect against diabetic neuropathy: effects on sensory nerve regeneration in rats. *Journal of neuroscience research*, *40*(1), pp.138-144.

Jang, J., Yoo, J., Lee, J., Lee, D., Kim, J., Huh, Y., Kim, D., Park, C., Hwang, D., Kim, H., Kang, H. and Kim, D. (2012) 'Disease-specific induced pluripotent stem cells: a platform for human disease modeling and drug discovery'. *Experimental & Molecular Medicine*, 44(3) p.202.

Jensen, K, B., Collins, C, A., Nascimento., E., Tan, D. W., Fyre, M., Itami, S., and Watt, F, M. (2009) 'Lrig1 expression defines a distinct multipotent stem cell population in Mammalian Epidermis'. *Cell stem cell, Elsevier.* 4 (5) pp. 427-439.

Jensen, J., Rustad, P., Kolnes, A. and Lai, Y. (2011) 'The Role of Skeletal Muscle Glycogen Breakdown for Regulation of Insulin Sensitivity by Exercise'. *Frontiers in Physiology*, 2.

Jiang, Z. G., Shen, E. and Dun, N. J. (1990) 'Excitatory and inhibitory transmission from dorsal root afferents to neonate rat motoneurons in vitro.' *Brain Res*, 535(1), Dec 3, pp. 110-118.

Jones, J. I. and Clemmons, D. R. (1995) 'Insulin-like growth factors and their binding proteins: biological actions.' *Endocr Rev*, 16(1), Feb, pp. 3-34.

Jones, G., Meier, T., Lichtsteiner, M., Witzemann, V., Sakmann, B. and Brenner, H. R. (1997) 'Induction by agrin of ectopic and functional postsynaptic-like membrane in innervated muscle.' *Proceedings of the National Academy of Sciences*, 94(6) p. 2654.

Jungbluth, H. and Gautel, M. (2014) 'Pathogenic Mechanisms in Centronuclear Myopathies'. *Frontiers in Aging Neuroscience*, 6. 339.

Kalyani, R., Saudek, C., Brancati, F. and Selvin, E. (2010) 'Association of Diabetes, Comorbidities, and A1C With Functional Disability in Older Adults: Results from the National Health and Nutrition Examination Survey (NHANES), 1999-2006'. *Diabetes Care*, 33(5) pp.1055-1060.

Kalyani, R., Metter, E., Egan, J., Golden, S. and Ferrucci, L. (2014) 'Hyperglycemia Predicts Persistently Lower Muscle Strength With Aging'. *Diabetes Care*, 38(1) pp.82-90.

Kanning, K. C., Kaplan, A. and Henderson, C. E. (2010) 'Motor neuron diversity in development and disease.' *Annu Rev Neurosci*, 33 pp. 409-440.

Kaur, G. and Dufour, J. M. (2012) 'Cell lines: Valuable tools or useless artifacts.' *Spermatogenesis*, 2(1) pp. 1-5.

Kawser H, M., Abdal Dayem, A., Han, J., Kumar Saha, S., Yang, G., Choi, H. and Cho, S. (2016) 'Recent Advances in Disease Modeling and Drug Discovery for Diabetes Mellitus Using Induced Pluripotent Stem Cells'. *International Journal of Molecular Sciences*, 17(2) p.256.

Kelley, D. and Mandarino, L. (2000) 'Fuel selection in human skeletal muscle in insulin resistance: a reexamination'. Diabetes, 49(5) pp.677-683.

Keller-Peck, C. R., Feng, G., Sanes, J. R., Yan, Q., Lichtman, J. W. and Snider, W. D. (2001) 'Glial cell line-derived neurotrophic factor administration in postnatal life results in motor unit enlargement and continuous synaptic remodeling at the neuromuscular junction.' *J Neurosci*, 21(16), Aug 15, pp. 6136-6146.

Kim, W., Hudson, B., Moser, B., Guo, J., Rong, L., Lu, Y., Qu, W., Lalla, E., Lerner, S., Chen, Y., Yan, S., D'agati, V., Naka, Y., Ramasamy, R., Herold, K., Yan, S. And Schmidt, A. (2005) 'Receptor For Advanced Glycation End Products And Its Ligands: A Journey From The Complications Of Diabetes To Its Pathogenesis'. *Annals of the New York Academy of Sciences*, 1043(1) pp.553-561.

Kim, N. and Burden, S. J. (2008) 'MuSK controls where motor axons grow and form synapses.' *Nat Neurosci*, 11(1), Jan, pp. 19-27.

King, R. (2001) 'The role of glycation in the pathogenesis of diabetic polyneuropathy.'. *Molecular Pathology*, (54(6) pp.400–408.

King, A. (2012). The use of animal models in diabetes research. *British Journal of Pharmacology*, 166(3), pp.877-894.

Kobayashi, T. and Askanas, V. (1985) 'Acetylcholine receptors and acetylcholinesterase accumulate at the nerve-muscle contacts of de novo grown human monolayer muscle cocultured with fetal rat spinal cord.' *Exp Neurol*, 88(2), May, pp. 327-335.

Kobayashi, T., Askanas, V. and Engel, W. K. (1987) 'Human muscle cultured in monolayer and cocultured with fetal rat spinal cord: importance of dorsal root ganglia for achieving successful functional innervation.' *J Neurosci*, 7(10), Oct, pp. 3131-3141.

Kondo, T., Asai, M., Tsukita, K., Kutoku, Y., Ohsawa, Y., Sunada, Y., Imamura, K., Egawa, N., Yahata, N., Okita, K. and Takahashi, K. (2013). Modeling Alzheimer's disease with iPSCs reveals stress phenotypes associated with intracellular Aβ and differential drug responsiveness. *Cell stem cell*, *12*(4), pp.487-496.

Kuang, S., Kuroda, K., Grand, F. L. and Rudnicki, M. A. (2007) 'Asymmetric Self-Renewal and Commitment of Satellite Stem Cells in Muscle.' *Cell,* 129(5), Jan, pp.999-1010

Kummer, T. T., Misgeld, T., Lichtman, J. W. and Sanes, J. R. (2004) 'Nerve-independent formation of a topologically complex postsynaptic apparatus.' *The Journal of cell biology*, 164(7) pp. 1077-1087.

Landmesser, L. T. (2001) 'The acquisition of motoneuron subtype identity and motor circuit formation.' *Int J Dev Neurosci*, 19(2), Apr, pp. 175-182.

Lang, T., Streeper, T., Cawthon, P., Baldwin, K., Taaffe, D. R. and Harris, T. B. (2010) 'Sarcopenia: etiology, clinical consequences, intervention, and assessment.' *Osteoporosis International,* 21(4), Feb, pp.543-559

Lavoie, P. A., Collier, B. and Tenehouse, A. (1976) 'Comparison of alpha-bungarotoxin binding to skeletal muscles after inactivity or denervation.' *Nature*, 260(5549), Mar 25, pp. 349-350.

Ledford H. (2011). Translational research: 4 ways to fix the clinical trial. Nature. 477 pp. 526–528.

Lee, K.-Y., Li, M., Manchanda, M., Batra, R., Charizanis, K., Mohan, A., Warren, S. A., Chamberlain, C. M., Finn, D., Hong, H., Ashraf, H., Kasahara, H., Ranum, L. P. W. and Swanson, M. S. (2013) 'Compound loss of muscleblind-like function in myotonic dystrophy.' *EMBO molecular medicine*, 5(12) pp. 1887-1900.

Lees, J. F., Shneidman, P. S., Skuntz, S. F., Carden, M. J. and Lazzarini, R. A. (1988) 'THE STRUCTURE AND ORGANIZATION OF THE HUMAN HEAVY NEUROFILAMENT SUBUNIT (NF-H) AND THE GENE ENCODING IT.' *Embo Journal*, 7(7), Jul, pp. 1947-1955.

Lefebvre, S., Burglen, L., Reboullet, S., Clermont, O., Burlet, P., Viollet, L., Benichou, B., Cruaud, C., Millasseau, P., Zeviani, M., Lepaslier, D., Frezal, J., Cohen, D., Weissenbach, J., Munnich, A. and Melki, J. (1995) 'IDENTIFICATION AND CHARACTERIZATION OF A SPINAL MUSCULAR ATROPHY-DETERMINING GENE.' *Cell*, 80(1), Jan, pp. 155-165.

Le Grand, F. and Rudnicki, M. (2007) 'Skeletal muscle satellite cells and adult myogenesis'. Current Opinion in Cell Biology, 19(6) pp.628-633.

Leinninger, G., Edwards, J., Lipshaw, M. and Feldman, E. (2004) 'Mechanisms of Disease: mitochondria as new therapeutic targets in diabetic neuropathy'. *Nature Clinical Practice Neurology*, 2(11) pp.620-628.

Leto, D. and Saltiel, A. R. (2012) 'Regulation of glucose transport by insulin: traffic control of GLUT4.' *Nat Rev Mol Cell Biol*, 13(6), May 23, pp. 383-396.

Li, M. X., Jia, M., Jiang, H., Dunlap, V. and Nelson, P. G. (2001) 'Opposing actions of protein kinase A and C mediate Hebbian synaptic plasticity.' *Nat Neurosci*, 4(9), Sep, pp. 871-872.

Li, X. J., Du, Z. W., Zarnowska, E. D., Pankratz, M., Hansen, L. O., Pearce, R. A. and Zhang, S. C. (2005) 'Specification of motoneurons from human embryonic stem cells.' *Nat Biotechnol*, 23(2), Feb, pp. 215-221.

Lie, D. C. and Weis, J. (1998) 'GDNF expression is increased in denervated human skeletal muscle.' *Neurosci Lett*, 250(2), Jul 3, pp. 87-90.

Light, N. and Champion, A. E. (1984) 'CHARACTERIZATION OF MUSCLE EPIMYSIUM, PERIMYSIUM AND ENDOMYSIUM COLLAGENS.' *Biochemical Journal*, 219(3) pp. 1017-1026.

Lin, L. F., Doherty, D. H., Lile, J. D., Bektesh, S. and Collins, F. (1993) 'GDNF: a glial cell line-derived neurotrophic factor for midbrain dopaminergic neurons.' *Science*, 260(5111), May 21, pp. 1130-1132.

Lin, S., Maj, M., Bezakova, G., Magyar, J. P., Brenner, H. R. and Ruegg, M. A. (2008) 'Muscle-wide secretion of a miniaturized form of neural agrin rescues focal neuromuscular innervation in agrin mutant mice.' *Proceedings of the National Academy of Sciences*, 105(32) p. 11406.

Lin, W., Burgess, R. W., Dominguez, B., Pfaff, S. L., Sanes, J. R. and Lee, K.-F. (2001) 'Distinct roles of nerve and muscle in postsynaptic differentiation of the neuromuscular synapse.' *Nature*, 410, 04/26/online, p. 1057.

Lin, W., Sanchez, H. B., Deerinck, T., Morris, J. K., Ellisman, M. and Lee, K. F. (2000) 'Aberrant development of motor axons and neuromuscular synapses in erbB2-deficient mice.' *Proc Natl Acad Sci U S A*, 97(3), Feb 1, pp. 1299-1304.

Littleton, J. T., Bellen, H. J. and Perin, M. S. (1993) 'Expression of synaptotagmin in Drosophila reveals transport and localization of synaptic vesicles to the synapse.' *Development*, 118(4) pp. 1077-1088.

Liu, J. P., Baker, J., Perkins, A. S., Robertson, E. J. and Efstratiadis, A. (1993) 'Mice carrying null mutations of the genes encoding insulin-like growth factor I (Igf-1) and type 1 IGF receptor (Igf1r).' *Cell*, 75(1), Oct 8, pp. 59-72.

Liu, Q. Y., Dunlap, V. and Barker, J. L. (1994) 'gamma-Aminobutyric acid type A receptor antagonists picrotoxin and bicuculline alter acetylcholine channel kinetics in cultured embryonic rat skeletal muscle.' *Mol Pharmacol*, 46(6), Dec, pp. 1197-1203.

Liu, Y., Padgett, D., Takahashi, M., Li, H., Sayeed, A., Teichert, R. W., Olivera, B. M., McArdle, J. J., Green, W. N. and Lin, W. (2008) 'Essential roles of the acetylcholine receptor gamma-subunit in neuromuscular synaptic patterning.' *Development*, 135(11), Jun, pp. 1957-1967.

Lopez-Manzaneda, M., Tejero, R., Arumugam, S. and Tabares, L. (2016) 'Synaptotagmin-2, and -1, linked to neurotransmission impairment and vulnerability in Spinal Muscular Atrophy.' *Human Molecular Genetics*, 25(21) pp. 4703-4716.

Low, L. K. and Cheng, H.-J. (2006) 'Axon pruning: an essential step underlying the developmental plasticity of neuronal connections.' *Philosophical Transactions of the Royal Society B: Biological Sciences*, 361(1473), 07/28, pp. 1531-1544.

Luo, D., Renault, V. A. and Rando, T. A. (2005) 'The regulation of Notch signaling in muscle stem cell activation and postnatal myogenesis.' *Cell & Developmental Biology,* 16(4-5), Jan, pp.612-622

Luo, Z., Wang, Q., Dobbins, G. C., Levy, S., Xiong, W. C. and Mei, L. (2003) 'Signaling complexes for postsynaptic differentiation.' *J Neurocytol*, 32(5-8), Jun-Sep, pp. 697-708.

Maeda, M., Ohba, N., Nakagomi, S., Suzuki, Y., Kiryu-Seo, S., Namikawa, K., Kondoh, W., Tanaka, A. and Kiyama, H. (2004) 'Vesicular acetylcholine transporter can be a morphological marker for the reinnervation to muscle of regenerating motor axons.' *Neurosci Res*, 48(3), Mar, pp. 305-314.

Maggio, M., Ceda, G.P., Lauretani, F., Pahor, M., Bandinelli, S., Najjar, S.S., Ling, S.M., Basaria, S., Ruggiero, C., Valenti, G. and Ferrucci, L. (2006). Relation of angiotensin-converting enzyme inhibitor treatment to insulin-like growth factor-1 serum levels in subjects> 65 years of age (the InCHIANTI study). *The American journal of cardiology*, *97*(10), pp.1525-1529.

Maggio, M., De Vita, F., Lauretani, F., Buttò, V., Bondi, G., Cattabiani, C., Nouvenne, A., Meschi, T., Dall'Aglio, E. and Ceda, G.P. (2013). IGF-1, the cross road of the nutritional, inflammatory and hormonal pathways to frailty. *Nutrients*, *5*(10), pp.4184-4205.

Mak, I. WY., Evaniew, N and Ghert, M. (2014) 'Lost in translation: animal models and clinical trials in cancer treatment.' *American Journal Transl Res,* 6 (2) pp. 114-118.

Malomouzh, A. I., Nurullin, L. F. and Nikolsky, E. E. (2015) 'Immunohistochemical evidence of the presence of metabotropic receptors for γ-aminobutyric acid at the rat neuromuscular junctions.' *Doklady Biochemistry and Biophysics*, 463(1), July 01, pp. 236-238.

Malomouzh, A. I., Petrov, K. A., Nurullin, L. F. and Nikolsky, E. E. (2015) 'Metabotropic GABAB receptors mediate GABA inhibition of acetylcholine release in the rat neuromuscular junction.' *J Neurochem*, 135(6), Dec, pp. 1149-1160.

Mamchaoui, K., Trollet, C., Bigot, A., Negroni, E., Chaouch, S., Wolff, A., Kandalla, P. K., Marie, S., Di Santo, J., St Guily, J. L., Muntoni, F., Kim, J., Philippi, S., Spuler, S., Levy, N., Blumen, S. C., Voit, T., Wright, W. E., Aamiri, A., Butler-Browne, G. and Mouly, V. (2011) 'Immortalized pathological human myoblasts: towards a universal tool for the study of neuromuscular disorders.' *Skelet Muscle*, 1 p. 34.

Manabe, Y., Miyatake, S., Takagi, M., Nakamura, M., Okeda, A., Nakano, T., Hirshman, M. F., Goodyear, L. J. and Fujii, N. L. (2012) 'Characterization of an acute muscle contraction model using cultured C2C12 myotubes.' *PloS one*, 7(12) pp. e52592-e52592.

Manske, R. H. F. (1932) 'THE ALKALOIDS OF FUMARACEOUS PLANTS: II. DICENTRA CUCULLARIA (L.) BERNH.' *Canadian Journal of Research*, 7(3), 1932/09/01, pp. 265-269.

Mantilla, C. B., Zhan, W. Z. and Sieck, G. C. (2004) 'Neurotrophins improve neuromuscular transmission in the adult rat diaphragm.' *Muscle Nerve*, 29(3), Mar, pp. 381-386.

Marangi, P. A., Forsayeth, J. R., Mittaud, P., Erb-Vogtli, S., Blake, D. J., Moransard, M., Sander, A. and Fuhrer, C. (2001) 'Acetylcholine receptors are required for agrin-induced clustering of postsynaptic proteins.' *Embo j*, 20(24), Dec 17, pp. 7060-7073.

Marcell, T. J. (2003) 'Review Article: Sarcopenia: Causes, Consequences, and Preventions.' *Journal of Gerontology: Medical Sciences,* 58(10).

Marchand, S., Devillers-Thiery, A., Pons, S., Changeux, J. P. and Cartaud, J. (2002) 'Rapsyn escorts the nicotinic acetylcholine receptor along the exocytic pathway via association with lipid rafts.' *J Neurosci*, 22(20), Oct 15, pp. 8891-8901.

Marty, I., Robert, M., Villaz, M., Dejongh, K. S., Lai, Y., Catterall, W. A. and Ronjat, M. (1994) 'BIOCHEMICAL-EVIDENCE FOR A COMPLEX INVOLVING DIHYDROPYRIDINE RECEPTOR AND

Matou-Nasri, S., Sharaf, H., Wang, Q., Almobadel, N., Rabhan, Z., Al-Eidi, H., Yahya, W. B., Trivilegio, T., Ali, R., Al-Shanti, N. and Ahmed, N. (2017) 'Biological impact of advanced glycation endproducts on estrogen receptor-positive MCF-7 breast cancer cells.' *Biochim Biophys Acta Mol Basis Dis*, 1863(11), Nov, pp. 2808-2820.

Matthews, V. B., Astrom, M. B., Chan, M. H., Bruce, C. R., Krabbe, K. S., Prelovsek, O., Akerstrom, T., Yfanti, C., Broholm, C., Mortensen, O. H., Penkowa, M., Hojman, P., Zankari, A., Watt, M. J., Bruunsgaard, H., Pedersen, B. K. and Febbraio, M. A. (2009) 'Brain-derived neurotrophic factor is produced by skeletal muscle cells in response to contraction and enhances fat oxidation via activation of AMP-activated protein kinase.' *Diabetologia*, 52(7), Jul, pp. 1409-1418.

McComas, A. J., Fawcett, P. R. W., Campbell, M. J. and Sica, R. E. P. (1971) 'ELECTROPHYSIOLOGICAL ESTIMATION OF NUMBER OF MOTOR UNITS WITHIN A HUMAN MUSCLE.' *Journal of Neurology Neurosurgery and Psychiatry*, 34(2) pp. 121-&.

Mears, S. C. and Frank, E. (1997) 'Formation of specific monosynaptic connections between muscle spindle afferents and motoneurons in the mouse.' *J Neurosci*, 17(9), May 1, pp. 3128-3135.

Middlemas, A., Delcroix, J. D., Sayers, N. M., Tomlinson, D. R. and Fernyhough, P. (2003) 'Enhanced activation of axonally transported stress-activated protein kinases in peripheral nerve in diabetic neuropathy is prevented by neurotrophin-3.' *Brain*, 126(Pt 7), Jul, pp. 1671-1682.

Miles, G. B., Yohn, D. C., Wichterle, H., Jessell, T. M., Rafuse, V. F. and Brownstone, R. M. (2004) 'Functional Properties of Motoneurons Derived from Mouse Embryonic Stem Cells.' *The Journal of Neuroscience*, 24(36) pp. 7848-7858.

Milner, L. D. and Landmesser, L. T. (1999) 'Cholinergic and GABAergic inputs drive patterned spontaneous motoneuron activity before target contact.' *J Neurosci*, 19(8), Apr 15, pp. 3007-3022.

Ming, Y., Bergman, E., Edstrom, E. and Ulfhake, B. (1999) 'Evidence for increased GDNF signaling in aged sensory and motor neurons.' *Neuroreport*, 10(7), May 14, pp. 1529-1535.

Mis, K., Grubic, Z., Lorenzon, P., Sciancalepore, M., Mars, T. and Pirkmajer, S. (2017) 'In Vitro Innervation as an Experimental Model to Study the Expression and Functions of Acetylcholinesterase and Agrin in Human Skeletal Muscle.' *Molecules (Basel, Switzerland)*, 22(9) p. 1418.

Misgeld, T., Burgess, R. W., Lewis, R. M., Cunningham, J. M., Lichtman, J. W. and Sanes, J. R. (2002) 'Roles of neurotransmitter in synapse formation: development of neuromuscular junctions lacking choline acetyltransferase.' *Neuron*, 36(4), Nov 14, pp. 635-648.

Mizuno, Y., Chang, H., Umeda, K., Niwa, A., Iwasa, T., Awata, T., Fukada, S., Yamamoto, H., Yamanaka, S., Nakahata, T., and Heike, T. (2010) 'Generation of skeletal muscle stem/progenitor cells from murine induced pluripotent stem cells.' *FASEB Journal,* 24(7), Oct, pp. 2245-2253

Monaco, C. M. F., Perry, C. G. R. and Hawke, T. J. (2017) 'Diabetic Myopathy: current molecular understanding of this novel neuromuscular disorder.' *Curr Opin Neurol*, 30(5), Oct, pp. 545-552.

Monani, U. R., Sendtner, M., Coovert, D. D., Parsons, D. W., Andreassi, C., Le, T. T., Jablonka, S., Schrank, B., Rossoll, W., Prior, T. W., Morris, G. E. and Burghes, A. H. (2000) 'The human centromeric survival motor neuron gene (SMN2) rescues embryonic lethality in Smn(-/-) mice and results in a mouse with spinal muscular atrophy.' *Hum Mol Genet*, 9(3), Feb 12, pp. 333-339.

Moransard, M., Borges, L. S., Willmann, R., Marangi, P. A., Brenner, H. R., Ferns, M. J. and Fuhrer, C. (2003) 'Agrin regulates rapsyn interaction with surface acetylcholine receptors, and this underlies cytoskeletal anchoring and clustering.' *J Biol Chem*, 278(9), Feb 28, pp. 7350-7359.

Morimoto, Y., Kato-Negishi, M., Onoe, H. and Takeuchi, S. (2013) 'Three-dimensional neuron-muscle constructs with neuromuscular junctions.' *Biomaterials*, 34(37), Dec, pp. 9413-9419.

Morley, J. E., Baumgarter, R. N., Roubenoff, R., Mayer, J. and Nair, K. S. (2001) 'Sarcopenia.' *Journal of Laboratory and Clinical Medicine,* 137(4), Feb, pp.231-243

Morris, J. K., Lin, W., Hauser, C., Marchuk, Y., Getman, D. and Lee, K. F. (1999) 'Rescue of the cardiac defect in ErbB2 mutant mice reveals essential roles of ErbB2 in peripheral nervous system development.' *Neuron*, 23(2), Jun, pp. 273-283.

Mouly, V., Aamiri, A., Perie, S., Mamchaoui, K., Barani, A., Bigot, A., Bouazza, B., Francois, V., Furling, D., Jacquemin, V., Negroni, E., Riederer, I., Vignaud, A., St Guily, J. L. and Butler-Browne, G. S. (2005) 'Myoblast transfer therapy: is there any light at the end of the tunnel?' *Acta Myol*, 24(2), pp. 128-133.

Mouly, V., Aamiri, A., Perie, S., Mamchaoui, K., Barani, A., Bigot, A., Bouazza, B., Francois, V., Furling, D., Jacquemin, V., Negroni, E., Riederer, I., Vignaud, A., St Guily, J. L. and Butler-Browne, G. S. (2005) 'Myoblast transfer therapy: is there any light at the end of the tunnel?' *Acta Myol*, 24(2), Oct, pp. 128-133.

Muramatsu, K., Niwa, M., Nagai, M., Kamimura, T., Sasaki, S. and Ishiguro, T. (2012) 'The size of motor neurons of the gastrocnemius muscle in rats with diabetes'. *Neuroscience Letters*, 531(2) pp.109-113.

Murray, L. M., Comley, L. H., Thomson, D., Parkinson, N., Talbot, K. and Gillingwater, T. H. (2008) 'Selective vulnerability of motor neurons and dissociation of pre- and post-synaptic pathology at the neuromuscular junction in mouse models of spinal muscular atrophy.' *Hum Mol Genet*, 17(7), Apr 1, pp. 949-962.

Nedachi, T., Kadotani, A., Ariga, M., Katagiri, H. and Kanzaki, M. (2008) 'Ambient glucose levels qualify the potency of insulin myogenic actions by regulating SIRT1 and FoxO3a in C2C12 myocytes.' *Am J Physiol Endocrinol Metab*, 294(4), Apr, pp. E668-678.

Nelson, P. G., Fields, R. D., Yu, C. and Liu, Y. (1993) 'Synapse elimination from the mouse neuromuscular junction in vitro: a non-Hebbian activity-dependent process.' *J Neurobiol*, 24(11), Nov, pp. 1517-1530.

Neavs (2017) 'Alternatives to animals in science' in research. Retrived 3 March, 2017 from http://www.neavs.org/alternatives/in-research

Nguyen, Q. T., Parsadanian, A. S., Snider, W. D. and Lichtman, J. W. (1998) 'Hyperinnervation of neuromuscular junctions caused by GDNF overexpression in muscle.' *Science*, 279(5357), Mar 13, pp. 1725-1729.

Ning, Y., Schuller, A. G., Bradshaw, S., Rotwein, P., Ludwig, T., Frystyk, J. and Pintar, J. E. (2006) 'Diminished growth and enhanced glucose metabolism in triple knockout mice

containing mutations of insulin-like growth factor binding protein-3, -4, and -5.' *Mol Endocrinol*, 20(9), Sep, pp. 2173-2186.

Nurullin, L. F., Nikolsky, E. E. and Malomouzh, A. I. (2018) 'Elements of molecular machinery of GABAergic signaling in the vertebrate cholinergic neuromuscular junction.' *Acta Histochemica*, 120(3), 2018/04/01/, pp. 298-301.

Obata, K. (2013) 'Synaptic inhibition and γ-aminobutyric acid in the mammalian central nervous system.' *Proceedings of the Japan Academy, Series B*, 89(4) pp. 139-156.

Oda, Y. (1999) 'Choline acetyltransferase: the structure, distribution and pathologic changes in the central nervous system.' *Pathol Int*, 49(11), Nov, pp. 921-937.

Olsen, R. W. and Sieghart, W. (2008) 'International Union of Pharmacology. LXX. Subtypes of gamma-aminobutyric acid(A) receptors: classification on the basis of subunit composition, pharmacology, and function. Update.' *Pharmacol Rev*, 60(3), Sep, pp. 243-260.

Oppenheim, R. W. (1991) 'Cell death during development of the nervous system.' *Annu Rev Neurosci*, 14 pp. 453-501.

Oppenheim, R. W., Houenou, L. J., Johnson, J. E., Lin, L. F., Li, L., Lo, A. C., Newsome, A. L., Prevette, D. M. and Wang, S. (1995) 'Developing motor neurons rescued from programmed and axotomy-induced cell death by GDNF.' *Nature*, 373(6512), Jan 26, pp. 344-346.

Park, J. C., Song, D. Y., Lee, J. S., Kong, I. D., Jeong, S.-W., Lee, B. H., Kang, H. S. and Cho, B. P. (2006) 'Expression of GABAA receptor β2/3 subunits in the rat major pelvic ganglion.' *Neuroscience Letters*, 403(1), 2006/07/31/, pp. 35-39.

Partridge, T. A. (2002) 'Cells that participate in regeneration of skeletal muscle.' *Gene Therapy,* 9(11), Jan, pp.752-753

Patton, B. L., Miner, J. H., Chiu, A. Y. and Sanes, J. R. (1997) 'Distribution and function of laminins in the neuromuscular system of developing, adult, and mutant mice.' *J Cell Biol*, 139(6), Dec 15, pp. 1507-1521.

Payne, A. M., Zheng, Z., Messi, M. L., Milligan, C. E., Gonzalez, E. and Delbono, O. (2006) 'Motor neurone targeting of IGF-1 prevents specific force decline in ageing mouse muscle.' *J Physiol*, 570(Pt 2), Jan 15, pp. 283-294.

Pedersen, B. K. (2011) 'Muscles and their myokines.' *J Exp Biol*, 214(Pt 2), Jan 15, pp. 337-346.

Pette, D. and Staron, R. S. (2000) 'Myosin isoforms, muscle fiber types, and transitions.' *Microsc Res Tech*, 50(6), Sep 15, pp. 500-509.

Phelan, M. C. and Lawler, G. (2001) 'Cell counting.' *Curr Protoc Cytom*, Appendix 3, May, p. Appendix 3A.

Phillips, S. M. (2007) 'Resistance exercise: good for more than just Grandma and Grandpa's muscles.' *Appl Physiol Nutr Metab*, 32(6), Dec, pp. 1198-1205.

Picard, M., White, K. and Turnbull, D. (2013) 'Mitochondrial morphology, topology, and membrane interactions in skeletal muscle: a quantitative three-dimensional electron microscopy study'. *Journal of Applied Physiology*, 114(2) pp.161-171.

Pourquie, O. (2001) 'Vertebrate somitogenesis.' *Annual Review of Cell and Developmental Biology*, 17 pp. 311-350.

POWER, G., DALTON, B., BEHM, D., VANDERVOORT, A., DOHERTY, T. and RICE, C. (2010). Motor Unit Number Estimates in Masters Runners. *Medicine & Science in Sports & Exercise*, 42(9), pp.1644-1650.

Prather, R. S., Lorson, M., Ross, J. W., Whyte, J. J. and Walters, E. (2013) 'Genetically Engineered Pig Models for Human Diseases.' *Annual review of animal biosciences*, 1, 01/03, pp. 203-219.

Punga, A. R. and Ruegg, M. A. (2012) 'Signaling and aging at the neuromuscular synapse: lessons learnt from neuromuscular diseases.' *Curr Opin Pharmacol*, 12(3), Jun, pp. 340-346.

Puttonen, K. A., Ruponen, M., Naumenko, N., Hovatta, O. H., Tavi, P. and Koistinaho, J. (2015) 'Generation of Functional Neuromuscular Junctions from Human Pluripotent Stem Cell Lines.' *Frontiers in cellular neuroscience*, 9 pp. 473-473.

Quadri., 2020 https://slideplayer.com/slide/5276957/

Rajaram, S., Baylink, D. J. and Mohan, S. (1997) 'Insulin-like growth factor-binding proteins in serum and other biological fluids: regulation and functions.' *Endocr Rev*, 18(6), Dec, pp. 801-831.

Ramamurthy, B. and Larsson, L. (2013). Detection of an aging-related increase in advanced glycation end products in fast- and slow-twitch skeletal muscles in the rat. *Biogerontology*, 14(3), pp.293-301.

Ramasamy, R., Vannucci, S., Yan, S., Herold, K., Yan, S. and Schmidt, A. (2005). Advanced glycation end products and RAGE: a common thread in aging, diabetes, neurodegeneration, and inflammation. *Glycobiology*, 15(7), pp.16R-28R.

Ramasamy, R., Yan, S. and Schmidt, A. (2005) 'The RAGE Axis and Endothelial Dysfunction: Maladaptive Roles in the Diabetic Vasculature and Beyond'. *Trends in Cardiovascular Medicine*, 15(7) pp.237-243.

Ramji, N., Toth, C., Kennedy, J. and Zochodne, D. (2007) 'Does diabetes mellitus target motor neurons?'. *Neurobiology of Disease*, 26(2) pp.301-311.

Rashid, G., Benchetrit, S., Fishman, D. and Bernheim, J. (2004) 'Effect of advanced glycation end-products on gene expression and synthesis of TNF-alpha and endothelial nitric oxide synthase by endothelial cells.' *Kidney Int*, 66(3), Sep, pp. 1099-1106

Raybiotech. (2016). Growth neutrophic microarray. Adapted from https://www.raybiotech.com/protein-array

Rayment, I., Holden, H. M., Whittaker, M., Yohn, C. B., Lorenz, M., Holmes, K. C. and Milligan, R. A. (1993) 'STRUCTURE OF THE ACTIN-MYOSIN COMPLEX AND ITS IMPLICATIONS FOR MUSCLE-CONTRACTION.' *Science*, 261(5117), Jul, pp. 58-65.

Reece, J. B., Urry, L. A., Cain, M. L., Wasserman, S. A., Minorsky, P. V. and Jackson, R. B. (2011) *Campbell Biology.* 9th ed. San Francisco: Pearson, pp. 280, 904-905

Reichardt, L. F. (2006) 'Neurotrophin-regulated signalling pathways.' *Philosophical transactions of the Royal Society of London. Series B, Biological sciences*, 361(1473) pp. 1545-1564.

Relaix, F. and Zammit, P. S. (2012) 'Satellite cells are essential for skeletal muscle regeneration: the cell on the edge returns centre stage.' *Development*, 139(16), Aug, pp. 2845-2856.

Ren, K., Crouzier, T., Roy, C. and Picart, C. (2008) 'Polyelectrolyte multilayer films of controlled stiffness modulate myoblast cells differentiation.' *Adv Funct Mater*, 18(9) pp. 1378-1389.

Resistance in Human Type 2 Diabetes: Potential role of AGER1 and SIRT1. *Diabetes Care*, 34(7), pp.1610-1616.

Riebelinng, C., Schelchter, K., Buesen, R., Spielmann, H., Luch, A., and Seiler, A. (2011) 'Defined culture edium for stem cell differentiatio: Applicability of serum-free conditions in the mouse embryonic ste cell test' *Elsevier, 25 (4), Jun, pp. 914-921.*

Riethmacher, D., Sonnenberg-Riethmacher, E., Brinkmann, V., Yamaai, T., Lewin, G. R. and Birchmeier, C. (1997) 'Severe neuropathies in mice with targeted mutations in the ErbB3 receptor.' *Nature*, 389(6652), Oct 16, pp. 725-730.

Ricotti, L., Taccola, S., Bernardeschi, I., Pensabene, V., Dario, P. and Menciassi, A. (2011) 'Quantification of growth and differentiation of C2C12 skeletal muscle cells on PSS-PAH-based polyelectrolyte layer-by-layer nanofilms.' *Biomed Mater*, 6(3), Jun, p. 031001.

Rios, E. and Brum, G. (1987) 'Involvement of dihydropyridine receptors in excitation-contraction coupling in skeletal muscle.' *Nature*, 325(6106), Feb 19-25, pp. 717-720.

Riuzzi, F., Sorci, G., Sagheddu, R. and Donato, R. (2012) 'HMGB1-RAGE regulates muscle satellite cell homeostasis through p38-MAPK- and myogenin-dependent repression of Pax7 transcription'. *Journal of Cell Science*, 125(6) pp.1440-1454.

Rojas Vega, S., Struder, H. K., Vera Wahrmann, B., Schmidt, A., Bloch, W. and Hollmann, W. (2006) 'Acute BDNF and cortisol response to low intensity exercise and following ramp incremental exercise to exhaustion in humans.' *Brain Res*, 1121(1), Nov 22, pp. 59-65.

Rolland, Y., Czerwinski, S., Abellan van Kan, G., Morley, J. E., Cesari, M., Onder, G., Woo, J., Baumgartner, R., Pillard, F. and Boirie, Y. (2008) 'Sarcopenia: Its assessment, etiology, pathogenesis, consequences and future perspectives.' *Journal of Nutrition Health and Aging,* 12(7), Feb, pp.433-450

Roman, W. and Gomes, E. (2017) 'Nuclear positioning in skeletal muscle'. *Seminars in Cell & Developmental Biology*.

Roman, W. and Gomes, E.R. (2018). Nuclear positioning in skeletal muscle. In *Seminars in cell & developmental biology* (Vol. 82, pp. 51-56). Academic Press.

Romero, N. and Bitoun, M. (2011) 'Centronuclear Myopathies'. *Seminars in Pediatric Neurology*, 18(4) pp.250-256.

Rosen, D. R., Siddique, T., Patterson, D., Figlewicz, D. A., Sapp, P., Hentati, A., Donaldson, D., Goto, J., Oregan, J. P., Deng, H. X., Rahmani, Z., Krizus, A., McKennayasek, D., Cayabyab, A., Gaston, S. M., Berger, R., Tanzi, R. E., Halperin, J. J., Herzfeldt, B., Vandenbergh, R., Hung, W. Y., Bird, T., Deng, G., Mulder, D. W., Smyth, C., Laing, N. G., Soriano, E., Pericakvance, M. A., Haines, J., Rouleau, G. A., Gusella, J. S., Horvitz, H. R. and Brown, R. H. (1993) 'MUTATIONS IN CU/ZN SUPEROXIDE-DISMUTASE GENE ARE ASSOCIATED WITH FAMILIAL AMYOTROPHIC-LATERAL-SCLEROSIS.' *Nature*, 362(6415), Mar, pp. 59-62.

Rosenstein, J. M., Krum, J. M. and Ruhrberg, C. (2010) 'VEGF in the nervous system.' *Organogenesis*, 6(2), Apr-Jun, pp. 107-114.

Roubenoff, R. (2000) 'Sarcopenia and its implications for the elderly.' *European Journal of Clinical Nutrition.*' 54(3), Feb, pp.40-47

Rudolf, R., Deschenes, M. R. and Sandri, M. (2016) 'Neuromuscular junction degeneration in muscle wasting.' *Current opinion in clinical nutrition and metabolic care*, 19(3) pp. 177-181.

Ruiz de Almodovar, C., Lambrechts, D., Mazzone, M. and Carmeliet, P. (2009) 'Role and therapeutic potential of VEGF in the nervous system.' *Physiol Rev*, 89(2), Apr, pp. 607-648.

Rumsey, J. W., Das, M., Bhalkikar, A., Stancescu, M. and Hickman, J. J. (2010) 'Tissue engineering the mechanosensory circuit of the stretch reflex arc: Sensory neuron innervation of intrafusal muscle fibers.' *Biomaterials*, 31(32), 2010/11/01/, pp. 8218-8227.

Rumsey, J. W., Das, M., Stancescu, M., Bott, M., Fernandez-Valle, C. and Hickman, J. J. (2009) 'Node of Ranvier Formation on Motoneurons In Vitro.' *Biomaterials*, 30(21), 04/10, pp. 3567-3572.

Rumsey, J.W., et al., Node of Ranvier formation on motoneurons in vitro. Biomaterials (2009). 30(21): p. 3567-72.

RYANODINE RECEPTOR IN TRIAD JUNCTIONS OF SKELETAL-MUSCLE.' *Proceedings of the National Academy of Sciences of the United States of America*, 91(6), Mar, pp. 2270-2274.

Sahashi, K., Hua, Y., Ling, K. K. Y., Hung, G., Rigo, F., Horev, G., Katsuno, M., Sobue, G., Ko, C.-P., Bennett, C. F. and Krainer, A. R. (2012) 'TSUNAMI: an antisense method to phenocopy splicing-associated diseases in animals.' *Genes & development*, 26(16) pp. 1874-1884.

Said, G. (2007) 'Diabetic neuropathy—a review'. *Nature Clinical Practice Neurology*, 3(6) pp.331-340.

Saini, J., McPhee, J.S., Al-Dabbagh, S., Stewart, C.E. and Al-Shanti, N. (2016). Regenerative function of immune system: Modulation of muscle stem cells. *Ageing research reviews*, *27*, pp.67-76.

Sanes, J. R. and Lichtman, J. W. (1999) 'Development of the vertebrate neuromuscular junction.' *Annu Rev Neurosci*, 22 pp. 389-442.

Sanes, J. R. and Lichtman, J. W. (2001) 'Induction, assembly, maturation and maintenance of a postsynaptic apparatus.' *Nat Rev Neurosci*, 2(11), Nov, pp. 791-805.

Sango, K., Mizukami, H., Horie, H. and Yagihashi, S. (2017) 'Impaired Axonal Regeneration in Diabetes. Perspective on the Underlying Mechanism from In Vivo and In Vitro Experimental Studies.' *Frontiers Endocrinology (Lausanne)*, 8 p. 12.

Santhanam, N., Kumanchik, L., Guo, X., Sommerhage, F., Cai, Y., Jackson, M., Martin, C., Saad, G., McAleer, C.W., Wang, Y. and Lavado, A. (2018). Stem cell derived phenotypic human neuromuscular junction model for dose response evaluation of therapeutics. *Biomaterials*, *166*, pp.64-78.

Sareen, D., O'Rourke, J.G., Meera, P., Muhammad, A.K.M.G., Grant, S., Simpkinson, M., Bell, S., Carmona, S., Ornelas, L., Sahabian, A. and Gendron, T. (2013). Targeting RNA foci in iPSC-derived motor neurons from ALS patients with a C9ORF72 repeat expansion. Sci. Transl. Med. 5.

Sargent, B. (2015). Achieving control and reproducibility of cell culture by eliminating serum. Cell culture dish. Retrieved from https://cellculturedish.com/achieving-control-and-reproducibility-of-cell-culture-by-eliminating-serum/

Schiaffino, S. and Mammucari, C. (2011) 'Regulation of skeletal muscle growth by the IGF-1 Akt/PKB pathways: insights from genetic models.' *Skeletal Muscle Journal,* 1(4), Oct, pp.5040

Schmeichel, A.M., J.D. Schmelzer, and P.A. Low. (2003) Oxidative injury and apoptosis of dorsal root ganglion neurons in chronic experimental diabetic neuropathy. Diabetes. 52(1): p. 165-71.

Schmidt, B., Toyka, K.V., Kiefer, R., Full, J., Hartung, H.P. and Pollard, J. (1996). Inflammatory infiltrates in sural nerve biopsies in Guillain-Barré syndrome and chronic inflammatory demyelinating neuropathy. *Muscle & Nerve: Official Journal of the American Association of Electrodiagnostic Medicine*, *19*(4), pp.474-487.

Schnabel, J. (2008) 'Neuroscience: Standard model.' *Nature*, 454(7205), Aug 7, pp. 682-685.

Schneider, C. A., Rasband, W. S. and Eliceiri, K. W. (2012) 'NIH Image to ImageJ: 25 years of image analysis.' *Nature Methods*, 9, 06/28/online, p. 671.

Schonk, D. M., Kuijpers, H. J. H., van Drunen, E., van Dalen, C. H., Geurts van Kessel, A. H. M., Verheijen, R. and Ramaekers, F. C. S. (1989) 'Assignment of the gene(s) involved in the expression of the proliferation-related Ki-67 antigen to human chromosome 10.' *Human Genetics*, 83(3), October 01, pp. 297-299.

Schrank, B., Gotz, R., Gunnersen, J. M., Ure, J. M., Toyka, K. V., Smith, A. G. and Sendtner, M. (1997) 'Inactivation of the survival motor neuron gene, a candidate gene for human spinal muscular atrophy, leads to massive cell death in early mouse embryos.' *Proc Natl Acad Sci U S A*, 94(18), Sep 2, pp. 9920-9925.

Seale, P., Sabourin, L. A., Girgis-Gabardo, A., Mansouri, A., Gruss, P. and Rudnicki, M. A. (2000) 'Pax7 is required for the specification of myogenic satellite cells.' *Cell*, 102(6), Sep 15, pp. 777-786.

Sekido, H., Suzuki, T., Jomori, T., Takeuchi, M., Yabe-Nishimura, C. and Yagihashi, S. (2004) 'Reduced cell replication and induction of apoptosis by advanced glycation end products in rat Schwann cells.' *Biochem Biophys Res Commun*, 320(1), Jul 16, pp. 241-248.

Semba, R., Nicklett, E. and Ferrucci, L. (2010). Does Accumulation of Advanced Glycation End Products Contribute to the Aging Phenotype?. *The Journals of Gerontology Series A: Biological Sciences and Medical Sciences*, 65A(9), pp.963-975.

Semenza, G.L. (2007). Regulation of tissue perfusion in mammals by hypoxia-inducible factor 1. *Experimental physiology*, *92*(6), pp.988-991.

Seok J, Warren HS, Cuenca AG, Mindrinos MN, Baker HV, Xu W, Richards DR., …Tompkins RG. (2013) Inflammation and Host Response to Injury, Large Scale Collaborative Research Program. Genomic responses in mouse models poorly mimic human inflammatory diseases. Proc Natl Acad Sci U S A. 110 pp.3507–3512.

Shadrach, J. and Wagers, A. (2011) 'Stem cells for skeletal muscle repair'. Philosophical Transactions of the Royal Society B: Biological Sciences, 366(1575) pp.2297-2306.

Shadrin, I. Y., Khodabukus, A. and Bursac, N. (2016) 'Striated Muscle Function, Regeneration, and Repair.' *Cellular and molecular life sciences : CMLS*, 73(22), 06/06, pp. 4175-4202.

Sheard, P. W., Bewick, G. S., Woolley, A. G., Shaw, J., Fisher, L., Fong, S. W. and Duxson, M. J. (2010) 'Investigation of neuromuscular abnormalities in neurotrophin-3-deficient mice.' *European Journal of Neuroscience*, 31(1), Jan, pp. 29-41.

Sheehan, S. M. and Allen, R. E. (1999) 'Skeletal muscle satellite cell proliferation in response to members of the fibroblast growth factor family and hepatocyte growth factor.' *Journal of Cellular Physiology,* 181(3), Jan, pp.499-506

Shindo, H., et al. (1996). Modulation of basal nitric oxide-dependent cyclic-GMP production by ambient glucose, myo-inositol, and protein kinase C in SH-SY5Y human neuroblastoma cells. J Clin Invest. 97(3): p. 736-45.

Shvartsman, D., Storrie-White, H., Lee, K., Kearney, C., Brudno, Y., Ho, N., Cezar, C., McCann, C., Anderson, E., Koullias, J., Tapia, J. C., Vandenburgh, H., Lichtman, J. W. and Mooney, D. J. (2014) 'Sustained delivery of VEGF maintains innervation and promotes reperfusion in ischemic skeletal muscles via NGF/GDNF signaling.' *Molecular therapy : the journal of the American Society of Gene Therapy*, 22(7) pp. 1243-1253.

Siegel, A. L., Kuhlmann, P. K. and Cornelison, D. D. (2011) 'Muscle satellite cell proliferation and association: new insights from myofiber time-lapse imaging.' *Skelet Muscle*, 1(1), Feb 2, p. 7.

Siegal, A. L., Kuhlmann, P. K. and Cornelison, D. D. W. (2011) 'Muscle satellite cell proliferation and association: new insights from myofiber time-lapse imaging.' *Skeletal Muscle Journal,* 1(7), Oct, pp. 2044

Siller, R., Greenhough, S., Park, I. H. and Sullivan, G. J. (2013) 'Modelling human disease with pluripotent stem cells.' *Curr Gene Ther*, 13(2), Apr, pp. 99-110.

Simionescu, A. and Pavlath, G. K. (2011) 'Molecular mechanisms of myoblast fusion across species.' *Adv Exp Med Biol*, 713 pp. 113-135.

Singh, V., Bali, A., Singh, N. and Jaggi, A. (2014) 'Advanced Glycation End Products and Diabetic Complications'. *The Korean Journal of Physiology & Pharmacology*, 18(1) p.1.

Singleton, J. R. and Feldman, E. L. (2001) 'Insulin-like Growth Factor-I in Muscle Metabolism and Myotherapies.' *Neurobiology of Disease*, 8(4) Oct, pp. 541-54

Slater, C. R. (2008) 'Reliability of neuromuscular transmission and how it is maintained.' *Handb Clin Neurol*, 91 pp. 27-101.

Sleigh, J. N., Gillingwater, T. H. and Talbot, K. (2011) 'The contribution of mouse models to understanding the pathogenesis of spinal muscular atrophy.' *Dis Model Mech*, 4(4), Jul, pp. 457-467.

Smith, A.S.T., Long, C.J., Pirozzi, K. and Hickman, J.J. (2013). A functional system for high-content screening of neuromuscular junctions in vitro. *Technology*, *1*(01), pp.37-48.

Snow, L., Fugere, N. and Thompson, L. (2007) 'Advanced Glycation End-Product Accumulation and Associated Protein Modification in Type II Skeletal Muscle With Aging'. *The Journals of Gerontology Series A: Biological Sciences and Medical Sciences*, 62(11) pp.1204-1210.

Snow, L. and Thompson, L. (2009). Influence of Insulin and Muscle Fiber Type in Nε-(Carboxymethyl)-Lysine Accumulation in Soleus Muscle of Rats with Streptozotocin-Induced Diabetes Mellitus. *Pathobiology*, 76(5), pp.227-234.

Song, W. and Jin, X. A. (2015) 'Brain-derived neurotrophic factor inhibits neuromuscular junction maturation in a cAMP-PKA-dependent way.' *Neurosci Lett*, 591, Mar 30, pp. 8-12.

Son, Y. J., Trachtenberg, J. T. and Thompson, W. J. (1996) 'Schwann cells induce and guide sprouting and reinnervation of neuromuscular junctions.' *Trends Neurosci*, 19(7), Jul, pp. 280-285.

Souayah, N., Potian, J., Garcia, C., Krivitskaya, N., Boone, C., Routh, V. and McArdle, J. (2009) 'Motor unit number estimate as a predictor of motor dysfunction in an animal model of type 1 diabetes'. *American Journal of Physiology-Endocrinology and Metabolism*, 297(3) pp.E602-E608.

Sousa-Victor, P., Garcia-Prat, L., Serrano, A. L., Perdiguero, E. and Munoz-Canoves, P. (2015) 'Muscle stem cell aging: regulation and rejuvenation.' *Trends Endocrinol Metab*, 26(6), Jun, pp. 287-296.

Southam, K. A., King, A. E., Blizzard, C. A., McCormack, G. H. and Dickson, T. C. (2013) 'Microfluidic primary culture model of the lower motor neuron–neuromuscular junction circuit.' *Journal of Neuroscience Methods*, 218(2), 2013/09/15/, pp. 164-169.

Steinbeck, J. A., Jaiswal, M. K., Calder, E. L., Kishinevsky, S., Weishaupt, A., Toyka, K. V., Goldstein, P. A. and Studer, L. (2016) 'Functional Connectivity under Optogenetic Control Allows Modeling of Human Neuromuscular Disease.' *Cell Stem Cell*, 18(1), Jan 7, pp. 134-143.

Sterne, G. D., Coulton, G. R., Brown, R. A., Green, C. J. and Terenghi, G. (1997) 'Neurotrophin-3-enhanced nerve regeneration selectively improves recovery of muscle fibers expressing myosin heavy chains 2b.' *J Cell Biol*, 139(3), Nov 3, pp. 709-715.

Stewart, C. E., Bates, P. C., Calder, T. A., Woodall, S. M. and Pell, J. M. (1993) 'Potentiation of insulin-like growth factor-I (IGF-I) activity by an antibody: supportive evidence for enhancement of IGF-I bioavailability in vivo by IGF binding proteins.' *Endocrinology*, 133(3), Sep, pp. 1462-1465.

Stifani, N. (2014) 'Motor neurons and the generation of spinal motor neuron diversity.' *Frontiers in cellular neuroscience*, 8 pp. 293-293.

Stockmann, M., Linta, L., Fohr, K. J., Boeckers, A., Ludolph, A. C., Kuh, G. F., Udvardi, P. T., Proepper, C., Storch, A., Kleger, A., Liebau, S. and Boeckers, T. M. (2013) 'Developmental and functional nature of human iPSC derived motor neurons.' *Stem Cell Rev*, 9(4), pp. 475-492.

Stratton, K. (2015). Effect of Electrical Stimulation on Muscle Recruitment as it Relates to Maximal Voluntary Contraction.

Sugimoto, K., Yasujima, M. and Yagihashi, S. (2008). Role of Advanced Glycation End Products in Diabetic Neuropathy. *Current Pharmaceutical Design*, 14(10), pp.953-961.

Sullivan, K. A., Lentz, S. I., Roberts, J. L., Jr. and Feldman, E. L. (2008) 'Criteria for creating and assessing mouse models of diabetic neuropathy.' *Curr Drug Targets*, 9(1), Jan, pp. 3-13.

Suuronen, E. J., McLaughlin, C. R., Stys, P. K., Nakamura, M., Munger, R. and Griffith, M. (2004) 'Functional Innervation in Tissue Engineered Models for In Vitro Study and Testing Purposes.' *Toxicological Sciences*, 82(2) pp. 525-533.

Syverud, B. C., VanDusen, K. W. and Larkin, L. M. (2016) 'Growth Factors for Skeletal Muscle Tissue Engineering.' *Cells, tissues, organs*, 202(3-4) pp. 169-179.

Tanaka, A., Woltjen, K., Miyake, K., Hotta, A., Ikeya, M., Yamamoto, T., Nishino, T., Shoji, E., Sehara-Fujisawa, A., Manabe, Y., Fujii, N., Hanaoka, K., Era, T., Yamashita, S., Isobe, K., Kimura, E. and Sakurai, H. (2013) 'Efficient and reproducible myogenic differentiation from human iPS cells: prospects for modeling Miyoshi Myopathy in vitro.' *PLoS One*, 8(4) p. e61540.

Tasfaout, H., Cowling, B. S. and Laporte, J. (2018) 'Centronuclear myopathies under attack: A plethora of therapeutic targets.' *J Neuromuscul Dis*, 5(4) pp. 387-406.

Tatsumi, R., Anderson, J. E., Nevoret, C. J., Halevy, O. and Allen, R. E. (1998) 'HGF/SF is present in normal adult skeletal muscle and is capable of activating satellite cells.' *Developmental Biology,* 194(1), Jan, pp.114-128

Tedesco, F. S., Dellavalle, A., Manera, J. D.,Messina, G. and Cossu, G. (2010) 'Repairing skeletal muscle: regenerative potential of skeletal muscle stem cells.'*The Journal of Clinical Investigation,* 120(1), Oct, pp.11-17

ter Keurs, H. E., Deis, N., Landesberg, A., Nguyen, T. T., Livshitz, L., Stuyvers, B. and Zhang, M. L. (2003) 'Force, sarcomere shortening velocity and ATPase activity.' *Adv Exp Med Biol*, 538 pp. 583-602; discussion 602.

Thomas, D. R. (2007) 'Loss of skeletal muscle mass in aging: Examining the relation of starvation, sarcopenia and cachexia.' *Clinical Nutrition,* 26(4), Jan, pp.389-399

Thomson, S. R., Wishart, T. M., Patani, R., Chandran, S. and Gillingwater, T. H. (2012) 'Using induced pluripotent stem cells (iPSC) to model human neuromuscular connectivity: promise or reality?' *Journal of Anatomy*, 220(2) pp. 122-130.

Thrailkill, K.M. (2000). Insulin-like growth factor-I in diabetes mellitus: its physiology, metabolic effects, and potential clinical utility. *Diabetes technology & therapeutics*, *2*(1),Spring, pp.69-80.

Tidball, J. G. (2005) 'Inflammatory processes in muscle injury and repair.' *Am J Physiol Regul Integr Comp Physiol*, 288(2), Feb, pp. R345-353.

Tintignac, L. A., Brenner, H. R. and Ruegg, M. A. (2015) 'Mechanisms Regulating Neuromuscular Junction Development and Function and Causes of Muscle Wasting.' *Physiol Rev*, 95(3), Jul, pp. 809-852.

Tomac, A. C., Grinberg, A., Huang, S. P., Nosrat, C., Wang, Y., Borlongan, C., Lin, S. Z., Chiang, Y. H., Olson, L., Westphal, H. and Hoffer, B. J. (2000) 'Glial cell line-derived neurotrophic factor receptor alpha1 availability regulates glial cell line-derived neurotrophic factor signaling: evidence from mice carrying one or two mutated alleles.' *Neuroscience*, 95(4) pp. 1011-1023.

Treanor, J. J., Goodman, L., de Sauvage, F., Stone, D. M., Poulsen, K. T., Beck, C. D., Gray, C., Armanini, M. P., Pollock, R. A., Hefti, F., Phillips, H. S., Goddard, A., Moore, M. W., Buj-Bello, A., Davies, A. M., Asai, N., Takahashi, M., Vandlen, R., Henderson, C. E. and Rosenthal, A. (1996) 'Characterization of a multicomponent receptor for GDNF.' *Nature*, 382(6586), Jul 4, pp. 80-83.

Trnková, L., Dršata, J. and Boušová, I. (2015) 'Oxidation as an important factor of protein damage: Implications for Maillard reaction'. *Journal of Biosciences*, 40(2), Jun, pp.419-439.

Ulfhake, B., Bergman, E., Edstrom, E., Fundin, B. T., Johnson, H., Kullberg, S. and Ming, Y. (2000) 'Regulation of neurotrophin signaling in aging sensory and motoneurons: dissipation of target support?' *Mol Neurobiol*, 21(3), Jun, pp. 109-135.

Umbach, J. A., Adams, K. L., Gundersen, C. B. and Novitch, B. G. (2012) 'Functional Neuromuscular Junctions Formed by Embryonic Stem Cell-Derived Motor Neurons.' *PLoS ONE*, 7(5), 05/04, p. e36049.

Umemori, H., Linhoff, M. W., Ornitz, D. M. and Sanes, J. R. (2004) 'FGF22 and its close relatives are presynaptic organizing molecules in the mammalian brain.' *Cell*, 118(2), Jul 23, pp. 257-270.

Unwin, N. (2013) 'Nicotinic acetylcholine receptor and the structural basis of neuromuscular transmission: insights from Torpedo postsynaptic membranes.' *Q Rev Biophys*, 46(4), Nov, pp. 283-322.

Urazaev, A. K., Magsumov, S. T., Poletayev, G. I., Nikolsky, E. E. and Vyskocil, F. (1995) 'Muscle NMDA receptors regulate the resting membrane potential through NO-synthase.' *Physiol Res*, 44(3) pp. 205-208.

Uribarri, J., Cai, W., Ramdas, M., Goodman, S., Pyzik, R., Chen, X., Zhu, L., Striker, G. and Vlassara, H. (2011). Restriction of Advanced Glycation End Products Improves Insulin

Valdez, G., Tapia, J. C., Kang, H., Clemenson, G. D., Jr., Gage, F. H., Lichtman, J. W. and Sanes, J. R. (2010) 'Attenuation of age-related changes in mouse neuromuscular synapses by caloric restriction and exercise.' *Proceedings of the National Academy of Sciences of the United States of America*, 107(33) pp. 14863-14868.

van der Worp, H. B., Howells, D. W., Sena, E. S., Porritt, M. J., Rewell, S., O'Collins, V. and Macleod, M. R. (2010) 'Can animal models of disease reliably inform human studies?' *PLoS Med*, 7(3), Mar 30, p. e1000245.

Velloso, C. P. (2008) 'Regulation of muscle mass by growth hormone and IGF-I.' *British journal of pharmacology*, 154(3) pp. 557-568.

Vilmont, V., Cadot, B., Ouanounou, G. and Gomes, E. R. (2016) 'A system for studying mechanisms of neuromuscular junction development and maintenance.' *Development*, 143(13), Jul 1, pp. 2464-2477.

Vincent, A., Lang, B. and Newsomdavis, J. (1989) 'AUTOIMMUNITY TO THE VOLTAGE-GATED CALCIUM-CHANNEL UNDERLIES THE LAMBERT-EATON MYASTHENIC SYNDROME, A PARA-NEOPLASTIC DISORDER.' *Trends in Neurosciences*, 12(12), Dec, pp. 496-502.

Vlassara, H., Brownlee, M. and Cerami, A. (1981) 'Nonenzymatic glycosylation of peripheral nerve protein in diabetes mellitus.' *Proc Natl Acad Sci U S A*, 78(8), Aug, pp. 5190-5192.

Vlassara, H. and Palace, M. (2002) 'Diabetes and advanced glycation endproducts'. *Journal of Internal Medicine*, 251(2) pp.87-101.

Wang, C. Y., Yang, F., He, X. P., Je, H. S., Zhou, J. Z., Eckermann, K., Kawamura, D., Feng, L., Shen, L. and Lu, B. (2002) 'Regulation of neuromuscular synapse development by glial cell

line-derived neurotrophic factor and neurturin.' *J Biol Chem*, 277(12), Mar 22, pp. 10614-10625.

Wang, X., Chen, L., Liu, W., Su, B. and Zhang, Y. (2014). *Early Detection of Atrophy of Foot Muscles in Chinese Patients of Type 2 Diabetes Mellitus by High-Frequency Ultrasonography*.

Watanabe, M., Maemura, K., Kanbara, K., Tamayama, T. and Hayasaki, H. (2002) 'GABA and GABA Receptors in the Central Nervous System and Other Organs.' *In* Jeon, K. W. (ed.) *International Review of Cytology*. Vol. 213. Academic Press, pp. 1-47.

Webster, C. and Blau, H. M. (1990) 'Accelerated age-related decline in replicative life-span of Duchenne muscular dystrophy myoblasts: implications for cell and gene therapy.' *Somat Cell Mol Genet*, 16(6), Nov, pp. 557-565.

Wen, Y., Bi, P., Liu, W., Asakura, A., Keller, C. and Kuang, S. (2012) 'Constitutive Notch activation upregulates Pax7 and promotes the self-renewal of skeletal muscle satellite cells.' *Molecular Cell Biology,* 32(12), Jan, pp.2300-2311

Williams, S. K., Howarth, N. L., Devenny, J. J. and Bitensky, M. W. (1982) 'Structural and functional consequences of increased tubulin glycosylation in diabetes mellitus.' *Proc Natl Acad Sci U S A*, 79(21), Nov, pp. 6546-6550.

Wilson, N. and Wright, D. (2014). Experimental motor neuropathy in diabetes. *Diabetes and the Nervous System*, pp.461-467.

Wilson, M.H., Bray, M.G. and Holzbaur, E.L. (2016). Methods for assessing nuclear rotation and nuclear positioning in developing skeletal muscle cells. In *The Nuclear Envelope*(pp. 269-290). Humana Press, New York, NY.

Wilson, S. J. and Harris, A. J. (1993) 'Formation of myotubes in aneural rat muscles.' *Dev Biol*, 156(2), Apr, pp. 509-518.

Woldeyesus, M. T., Britsch, S., Riethmacher, D., Xu, L., Sonnenberg-Riethmacher, E., Abou-Rebyeh, F., Harvey, R., Caroni, P. and Birchmeier, C. (1999) 'Peripheral nervous system defects in erbB2 mutants following genetic rescue of heart development.' *Genes Dev*, 13(19), Oct 1, pp. 2538-2548.

Wolpowitz, D., Mason, T. B., Dietrich, P., Mendelsohn, M., Talmage, D. A. and Role, L. W. (2000) 'Cysteine-rich domain isoforms of the neuregulin-1 gene are required for maintenance of peripheral synapses.' *Neuron*, 25(1), Jan, pp. 79-91.

Wood, S. J. and Slater, C. R. (2001) 'Safety factor at the neuromuscular junction.' *Prog Neurobiol*, 64(4), Jul, pp. 393-429.

Woods, K. A., Camacho-Hubner, C., Savage, M. O. and Clark, A. J. (1996) 'Intrauterine growth retardation and postnatal growth failure associated with deletion of the insulin-like growth factor I gene.' *N Engl J Med*, 335(18), Oct 31, pp. 1363-1367.

Wood, T. L., Rogler, L. E., Czick, M. E., Schuller, A. G. and Pintar, J. E. (2000) 'Selective alterations in organ sizes in mice with a targeted disruption of the insulin-like growth factor binding protein-2 gene.' *Mol Endocrinol*, 14(9), Sep, pp. 1472-1482.

Woolley, A., Sheard, P., Dodds, K. and Duxson, M. (1999) 'Alpha motoneurons are present in normal numbers but with reduced soma size in neurotrophin-3 knockout mice.' *Neurosci Lett*, 272(2), Sep 10, pp. 107-110.

Woolley, A. G., Sheard, P. W. and Duxson, M. J. (2005) 'Neurotrophin-3 null mutant mice display a postnatal motor neuropathy.' *Eur J Neurosci*, 21(8), Apr, pp. 2100-2110.

Wu, H., Xiong, W. C. and Mei, L. (2010) 'To build a synapse: signaling pathways in neuromuscular junction assembly.' *Development*, 137(7), Apr, pp. 1017-1033.

Xing, Y., Zhang, X., Song, X., Lv, Z., Hou, L. and Li, F. (2013) 'Injury of cortical neurons is caused by the advanced glycation end products-mediated pathway.' *Neural Regen Res*, 8(10), Apr 5, pp. 909-915.

Xu, G. and Sima, A.A. (2001). Altered immediate early gene expression in injured diabetic nerve: implications in regeneration. *Journal of Neuropathology & Experimental Neurology*, *60*(10), pp.972-983.

Yamamoto, M., Mitsuma, N., Ito, Y., Hattori, N., Nagamatsu, M., Li, M., Mitsuma, T. and Sobue, G. (1998) 'Expression of glial cell line-derived neurotrophic factor and GDNFR-alpha mRNAs in human peripheral neuropathies.' *Brain Res*, 809(2), Nov 2, pp. 175-181.

Yan, Q., Elliott, J. L., Matheson, C., Sun, J., Zhang, L., Mu, X., Rex, K. L. and Snider, W. D. (1993) 'Influences of neurotrophins on mammalian motoneurons in vivo.' *J Neurobiol*, 24(12), Dec, pp. 1555-1577.

Yi, H., Xie, B., Liu, B., Wang, X., Xu, L., Liu, J., Li, M., Zhong, X. and Peng, F. (2018). Derivation and Identification of Motor Neurons from Human Urine-Derived Induced Pluripotent Stem Cells. *Stem Cells International*, 2018, pp.1-9.

Yin, H., Price, F. and Rudnicki, M. A. (2013) 'Satellite cells and the muscle stem cell niche.' *Physiol Rev*, 93(1), Jan, pp. 23-67.

Yonekura, H., Yamamoto, Y., Sakurai, S., Watanabe, T. and Yamamoto, H. (2005) 'Roles of the receptor for advanced glycation endproducts in diabetes-induced vascular injury.' *J Pharmacol Sci*, 97(3), Mar, pp. 305-311.

Young, H. S., Herbette, L. G. and Skita, V. (2003) 'Alpha-bungarotoxin binding to acetylcholine receptor membranes studied by low angle X-ray diffraction.' *Biophys J*, 85(2), Aug, pp. 943-953.

Yu, S.-C., Klosterman, S. M., Martin, A. A., Gracheva, E. O. and Richmond, J. E. (2013) 'Differential roles for snapin and synaptotagmin in the synaptic vesicle cycle.' *PloS one*, 8(2) pp. e57842-e57842.

Zahavi, E. E., Ionescu, A., Gluska, S., Gradus, T., Ben-Yaakov, K. and Perlson, E. (2015) 'A compartmentalized microfluidic neuromuscular co-culture system reveals spatial aspects of GDNF functions.' *J Cell Sci*, 128(6), Mar 15, pp. 1241-1252.

Zeeshan, A., Chandrasekera, C. and Pippin, J. (2018).). Animal research for type 2 diabetes mellitus, its limited translation for clinical benefit, and the way forward. Alternatives to laboratory animals. *Alternatives to laboratory animals: ATLA*, 46(1), pp.13-22.

Zha, J. and Lackner, M. R. (2010) 'Targeting the Insulin-like Growth Factor Receptor-1R Pathway for Cancer Therapy.' *Clinical Cancer Research,* 16(9), Jan, pp.2512-2517

Zhang, Y., Lin, S., Karakatsani, A., Ruegg, M. A. and Kroger, S. (2015) 'Differential regulation of AChR clustering in the polar and equatorial region of murine muscle spindles.' *Eur J Neurosci*, 41(1), Jan, pp. 69-78.

Zhang, X. and Poo, M. M. (2002) 'Localized synaptic potentiation by BDNF requires local protein synthesis in the developing axon.' *Neuron*, 36(4), Nov 14, pp. 675-688.

Zheng, C., Skold, M. K., Li, J., Nennesmo, I., Fadeel, B. and Henter, J. I. (2007) 'VEGF reduces astrogliosis and preserves neuromuscular junctions in ALS transgenic mice.' *Biochem Biophys Res Commun*, 363(4), Nov 30, pp. 989-993.

Zochodne, D., Ramji, N. and Toth, C. (2008) 'Neuronal Targeting in Diabetes Mellitus: A Story of Sensory Neurons and Motor Neurons'. *The Neuroscientist*, 14(4) pp.311-318.

Öztürk, G., Şekeroğlu, M. R., Erdogan, E. and Ozturk, M. (2006) 'The effect of non-enzymatic glycation of extracellular matrix proteins on axonal regeneration in vitro.' *Acta Neuropathol*, 112(5), Nov, pp. 627-632.

Appendix

Appendix A

Laboratory Equipment

Table 1: Laboratory equipment

Equipment	Company	Catalogue #
3-16KL refrigerated benchtop centrifuge	Sigma Laborzentrifugen	10360
appJET pipette controller	Appleton	AEL540
Axiovert 40 C inverted phase contrast microscope	Zeiss	MIC-990-130D
Axon Instruments GenePix 4000B microarray scanner	Molecular Devices	GENEPIX 4000B-U
BVC control, fluid aspiration system with VacuuHandControl VHC^{pro}	Vacuubrand	727202
Hausser Bright-Line 3100 haemocytometer	Hausser Scientific	3110
JB Nova unstirred water bath	Grant	JBN12
LabGard NU-437 class II, type A2 biosafety cabinet	Nuaire	NU-437-400E
Leica DMI6000 B inverted fluorescence microscope	Leica Microsystems	DMI6000B
Leica TCS SP5 confocal microscope	Leica Microsystems	TCSSP5
M3B stereomicroscope	Wild Heerbrugg	1171
MTS 2/4 digital microtiter shaker	IKA	0003208002
NU-5100E air-jacketed automatic CO_2 incubator	Nuaire	NU5100E
Omni tissue homogenizer (TH) package	Omni International	THP220
Synergy HT microplate reader	BioTek	7091000

Laboratory Plastic ware

Table 2: Laboratory plastic ware

Plasticware	Company	Catalogue #
µ-Dish 35 mm, high glass bottom, D 263® M Schott glass	Ibidi	81158
CRYO.S™ 1 mL, conical bottom internal thread, polypropylene (Cryovial)	Greiner Bio-One	123278
EasYFlask™ 175 cm^2, polystyrene (T175)	Nunc	159910
Microlance™ 3 hypodermic needles 21G x 1.5" (0,8 x 40 mm)	Becton Dickinson	304432
Nalgene® Mr. Frosty™ freezing container	Thermo Scientific	5100-0001
Nunclon™ 6-well x 3mL MultiDish cell culture dish, polystyrene	Nunc	140675
Nunclon™ Delta Surface, petri dish with lid, 150 x 20mm, polystyrene	Nunc	168381
Sterilin™ Sterile sample container – 100 mL, polystyrene	Thermo Scientific	185BM
Tube 15 mL, 120x17mm, polypropylene	Sarstedt	62.554.001
Tube 50 mL, 115x28mm, polypropylene	Sarstedt	62.559

Table 2: Reagents

Reagent	Company	Catalogue #
(+)-Tubocurarine chloride pentahydrate	Sigma-Aldrich	93750
1(S),9(R)-(−)-Bicuculline methiodide (Bicuculline)	Sigma-Aldrich	14343
4′,6-Diamidine-2′-phenylindole dihydrochloride (DAPI)	Sigma-Aldrich	10236276001
Anti-calcium channel L type DHPR alpha 2 subunit antibody [20A] (DHPR)	Abcam	ab2864
Anti-choline acetyltransferase (ChAT)	Sigma-Aldrich	AB144
Anti-glial fibrillary acidic protein (GFAP)	Sigma-Aldrich	G3893
Anti-MUSK antibody (MuSK)	Abcam	ab92950
Anti-neurofilament H antibody (NFH)	Sigma-Aldrich	AB5539
Anti-rapsyn antibody [1234] (rapsyn)	Abcam	ab11423
Anti-ryanodine receptor 1 antibody (RyR)	Sigma-Aldrich	AB9078
Anti-synaptotagmin antibody [ASV30] (Syt1)	Abcam	ab13259
Anti-vesicular acetylcholine transporter (VAChT)	Sigma-Aldrich	ABN100
B27 supplement	Life technologies	12587010
Dexamethasone	Sigma-Aldrich	D4902
Dimethyl sulfoxide (DMSO)	Fisher BioReagents	10103483
Donkey anti-goat IgG (H+L) cross-adsorbed secondary antibody, Alexa Fluor® 568	Invitrogen	A-11057
Donkey serum (DS)	Sigma-Aldrich	D9663
Dulbecco's modified eagle medium (DMEM)	Lonza	12-914F
Dulbecco's modified eagle medium (DMEM)/F12	Gibco, Life Technologie	31331093
Dulbecco's phosphate buffered saline 1X (DPBS)	Lonza	17-512F
Fetuin from fetal bovine serum	Sigma-Aldrich	F3004
Fibroblast growth factor-2	R&D systems	233-FB-025
Gelatin from porcine skin, type A	Sigma-Aldrich	G2500
Gentamicin	Gibco	15710-049
Goat anti-chicken IgY (H+L) cross-adsorbed secondary antibody, DyLight® 488	Invitrogen	SA5-10070
Goat anti-Mouse IgG (H+L) Cross-Adsorbed Secondary Antibody, Alexa Fluor® 555	Invitrogen	A-21422
Goat anti-rabbit IgG (H+L) cross-adsorbed secondary antibody, Alexa Fluor® 568	Invitrogen	A-11011
Goat serum (GS)	Sigma-Aldrich	G9023
Heat-inactivated fetal bovine serum (FBS)	Gibco	10500-064
Heparin	Sigma-Aldrich	H3149
Horse serum (HS)	Sigma-Aldrich	H0146
Human recombinant basic fibroblast growth factor (FGFb)	Gibco	PHG0026
Human recombinant epidermal growth factor (EGF)	Gibco	PHG0311
Human recombinant hepatocyte growth factor (HGF)	Sino Biological Inc.	10463-HNAS
Human recombinant insulin	Sigma-Aldrich	91077C
Knockout serum replacement	Millipore	CC095
Laminin	Gibco, Life Technologie	10828-028
L-Glutamic acid (L-Glut)	Sigma-Aldrich	G1251
L-glutamine	Lonza	17-605E
Matrigel® growth factor reduced basement membrane matrix, *LDEV-free	Corning	354230
Medium 199 with Earle's balanced salt solution	Lonza	12-119F
Mitomycin C	Sigma-Aldrich	M4287
Myosin 4 monoclonal antibody (MF20), Alexa Fluor® 488 (anti-MHC)	eBioscience	53-6503-82
MEM non-essential amino acids	Life technologies	1140050

N2 supplement	Life technologies	17502048
Paraformaldehyde	Sigma-Aldrich	P6148
Penicillin-streptomycin mixture (Pen/Strep)	Lonza	17-602E
Perm/Wash™ buffer (PWB)	BD Biosciences	554723
Plasmocin™ - mycoplasma elimination reagent	InvivoGen	ant-mpp
Poly(vinyl alcohol)	Sigma-Aldrich	341584
Agrin ELISA kit	Sigma-Aldrich	RAB0881-1KT
Rock inhibitor (Y-27632)	Sigma-Aldrich	Y0503-1mg
Skeletal muscle differentiation medium	PromoCell	C-23061
Texas Red®-X phalloidin	Invitrogen	T7471
Triton™ X-100 (TX100)	Sigma-Aldrich	T8787
Trypan Blue, 0.4% solution	Lonza	17-942E
TrypLE™ express enzyme 1X (TrypLE)	Gibco	12605-028
TWEEN® 20	Sigma-Aldrich	P1379
α-Bungarotoxin, Alexa Fluor™ 647 conjugate (α-BTX)	Invitrogen	B35450
γ-Aminobutyric acid (GABA)	Sigma-Aldrich	A2129

Appendix B

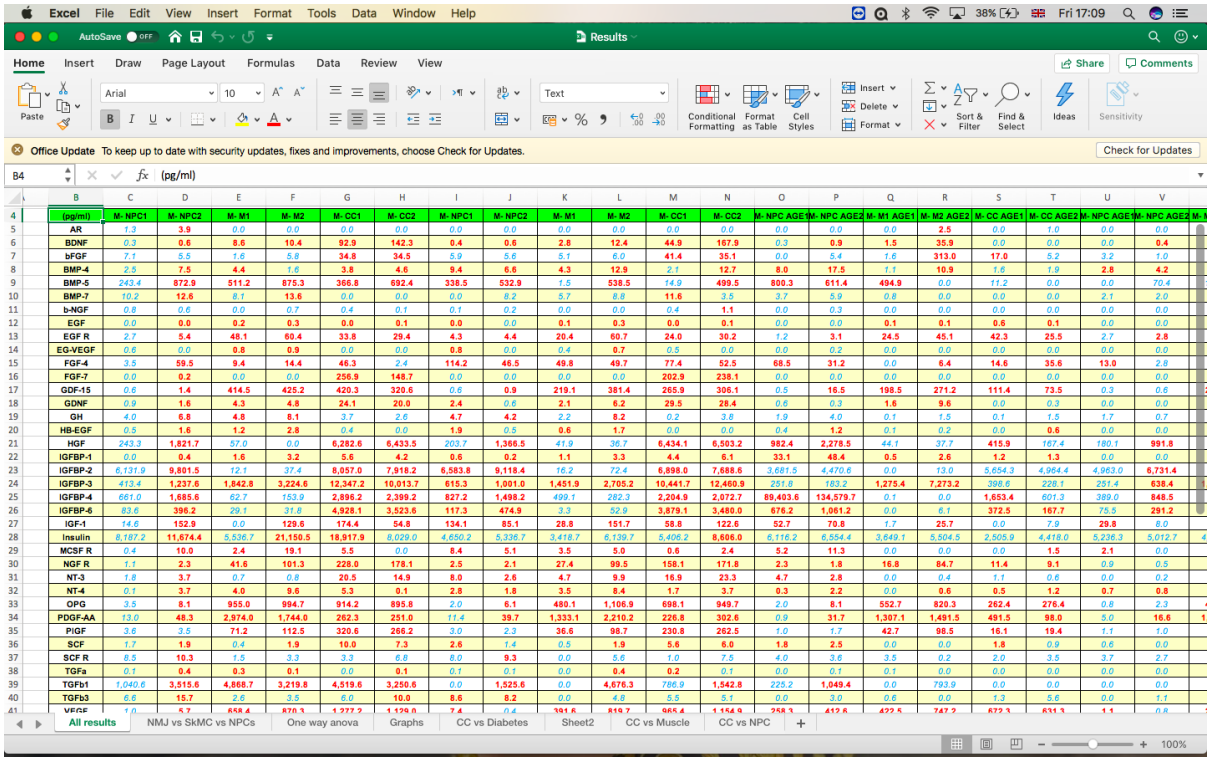

(pg/ml)	M- NPC1	M- NPC2	M- M1	M- M2	M- CC1	M- CC2	M- NPC1	M- NPC2	M- M1	M- M2	M- CC1	M- CC2	M- NPC AGE1	M- NPC AGE2	M- M1 AGE1	M- M2 AGE2	M- CC AGE1	M- CC AGE2	M- NPC AGE1	M- NPC AGE2
AR	1.3	3.9	0.0	0.0	0.0	0.0	0.0	0.0	0.0	0.0	0.0	0.0	0.0	0.0	0.0	2.5	0.0	1.0	0.0	0.0
BDNF	0.3	0.6	8.6	10.4	92.9	142.3	0.4	0.6	2.8	12.4	44.9	167.9	0.3	0.9	1.5	35.9	0.0	0.0	0.0	0.4
bFGF	7.1	5.5	1.6	5.8	34.8	34.5	5.9	5.6	5.1	6.0	41.4	35.1	0.0	5.4	1.6	313.0	17.0	5.2	3.2	1.0
BMP-4	2.5	7.5	4.4	1.6	3.8	4.6	9.4	6.6	4.3	12.9	2.1	12.7	8.0	17.5	1.1	10.9	1.6	1.9	2.8	4.2
BMP-5	243.4	872.9	511.2	875.3	366.8	692.4	338.5	532.9	1.5	538.5	14.9	499.5	800.3	611.4	494.9	0.0	11.2	0.0	0.0	70.4
BMP-7	10.2	12.6	8.1	13.6	0.0	0.0	0.0	8.2	5.7	8.8	11.6	3.5	3.7	5.9	0.8	0.0	0.0	0.0	2.1	2.0
b-NGF	0.8	0.6	0.0	0.7	0.4	0.1	0.1	0.2	0.0	0.0	0.4	1.1	0.0	0.3	0.0	0.0	0.0	0.0	0.0	0.0
EGF	0.0	0.0	0.2	0.3	0.0	0.1	0.0	0.0	0.1	0.3	0.0	0.1	0.0	0.0	0.1	0.1	0.6	0.1	0.0	0.0
EGF R	2.7	5.4	48.1	60.4	33.8	29.4	4.3	4.4	20.4	60.7	24.0	30.2	1.2	3.1	24.5	45.1	42.3	25.5	2.7	2.8
EG-VEGF	0.6	0.0	0.8	0.9	0.0	0.0	0.8	0.0	0.4	0.7	0.5	0.0	0.0	0.2	0.0	0.0	0.0	0.0	0.0	0.0
FGF-4	3.5	59.5	9.4	14.4	46.3	2.4	114.2	46.5	49.8	49.7	77.4	52.5	68.5	31.2	0.0	6.4	14.6	35.6	13.0	2.8
FGF-7	0.0	0.2	0.0	0.0	256.9	148.7	0.0	0.0	0.0	0.0	202.9	238.1	0.0	0.0	0.0	0.0	0.0	0.0	0.0	0.0
GDF-15	0.6	1.4	414.5	425.2	420.3	320.6	0.6	0.9	219.1	381.4	265.9	306.1	0.5	16.5	198.5	271.2	111.4	73.5	0.3	0.6
GDNF	0.9	1.6	4.3	4.8	24.1	20.0	2.4	0.6	2.1	6.2	29.5	28.4	0.6	0.3	1.6	9.6	0.0	0.3	0.0	0.0
GH	4.0	6.8	4.8	8.1	3.7	2.6	4.7	4.2	2.2	8.2	0.2	3.8	1.9	4.0	0.1	1.5	0.1	1.5	1.7	0.7
HB-EGF	0.5	1.6	1.2	2.8	0.4	0.0	1.9	0.5	0.6	1.7	0.0	0.0	0.4	1.2	0.1	0.2	0.0	0.6	0.0	0.0
HGF	243.3	1,821.7	57.0	0.0	6,282.6	6,433.5	203.7	1,366.5	41.9	36.7	6,434.1	6,503.2	982.4	2,278.5	44.1	37.7	415.9	167.4	180.1	991.8
IGFBP-1	0.0	0.4	1.6	3.2	5.6	4.2	0.6	0.2	1.1	3.3	4.4	6.1	33.1	48.4	0.5	2.6	1.2	1.3	0.0	0.0
IGFBP-2	6,131.9	9,801.5	12.1	37.4	8,057.0	7,918.2	6,583.8	9,118.4	16.2	72.4	6,898.0	7,688.6	3,681.5	4,470.6	0.0	13.0	5,654.3	4,964.4	4,963.0	6,731.4
IGFBP-3	413.4	1,237.6	1,842.8	3,224.6	12,347.2	10,013.7	615.3	1,001.0	1,451.9	2,705.2	10,441.7	12,460.9	251.8	183.2	1,275.4	7,273.2	398.6	228.1	251.4	638.4
IGFBP-4	661.0	1,685.6	62.7	153.9	2,896.2	2,399.2	827.2	1,498.2	499.1	282.3	2,204.9	2,072.7	89,403.6	134,579.7	0.1	0.0	1,653.4	601.3	389.0	848.5
IGFBP-6	83.6	396.2	29.1	31.8	4,928.1	3,523.6	117.3	474.9	3.3	52.9	3,879.1	3,480.0	676.2	1,061.2	0.0	6.1	372.5	167.7	75.5	291.2
IGF-1	14.6	152.9	0.0	129.6	174.4	54.8	134.1	85.1	28.8	151.7	58.8	122.6	52.7	70.8	1.7	25.7	0.0	7.9	29.8	8.0
Insulin	8,187.2	11,674.4	5,536.7	21,150.5	18,917.9	8,029.0	4,650.2	5,336.7	3,418.7	6,139.7	5,406.2	8,606.0	6,116.2	6,554.4	3,649.1	5,504.5	2,505.9	4,418.0	5,236.3	5,012.7
MCSF R	0.4	10.0	2.4	19.1	5.5	0.0	8.4	5.1	3.5	5.0	0.6	2.4	5.2	11.3	0.0	0.0	0.0	1.5	2.1	0.0
NGF R	1.1	2.3	41.8	101.3	228.0	178.1	2.5	2.1	27.4	99.5	158.1	171.8	2.3	1.8	16.8	84.7	11.4	9.1	0.9	0.5
NT-3	1.8	3.7	0.7	0.8	20.5	14.9	8.0	2.6	4.7	9.9	16.9	23.3	4.7	2.8	0.0	0.4	1.1	0.6	0.0	0.2
NT-4	0.1	3.7	4.0	9.6	5.3	0.1	2.8	1.8	3.5	8.4	1.7	3.7	0.3	2.2	0.0	0.6	0.5	1.2	0.7	0.8
OPG	3.5	8.1	955.0	984.7	914.2	895.8	2.0	6.1	480.1	1,106.9	698.1	949.7	2.0	8.1	552.7	820.3	262.4	276.4	0.8	2.3
PDGF-AA	13.0	48.3	2,974.0	1,744.0	262.3	251.0	11.4	39.7	1,333.1	2,210.2	226.8	302.6	0.9	31.7	1,307.1	1,491.5	491.5	98.0	5.0	16.6
PlGF	3.6	3.5	71.2	112.5	320.6	266.2	3.0	2.3	36.6	98.7	230.8	262.5	1.0	1.7	42.7	98.5	16.1	19.4	1.1	1.0
SCF	1.7	1.9	0.4	1.9	10.0	7.3	2.6	1.4	0.5	1.9	5.6	6.0	1.8	2.5	0.0	0.0	1.8	0.9	0.6	0.0
SCF R	8.5	10.3	1.5	3.3	3.3	6.8	8.0	9.3	0.0	5.8	1.0	7.5	4.0	3.6	3.5	0.2	2.0	3.5	3.7	2.7
TGFa	0.1	0.4	0.3	0.1	0.0	0.1	0.1	0.1	0.0	0.4	0.2	0.1	0.0	0.1	0.1	0.0	0.0	0.0	0.0	0.0
TGFb1	1,040.6	3,515.6	4,868.7	3,219.8	4,519.6	3,250.6	0.0	1,525.6	0.0	4,676.3	786.9	1,542.8	225.2	1,049.4	0.0	793.9	0.0	0.0	0.0	0.0
TGFb3	6.6	15.7	2.6	3.5	6.0	10.0	8.6	8.2	0.0	4.8	5.5	5.1	0.0	3.0	0.6	0.0	1.3	5.6	0.0	1.1

ELISA- based microarray analysis of supernatant from NPCs vs. supernatant from aneurally-cultured 25-years old immortalised human myoblasts vs. supernatant from co-culture of NPCs cultured with 25-years old immortalised human myoblasts vs. supernatant from co-culture of NPCs cultured with 25-years old immortalised human myoblasts treated with AGEs.

Appendix C

Stem Cells and Cloning: Advances and Applications

Dovepress
open access to scientific and medical research

Open Access Full Text Article

ORIGINAL RESEARCH

A functional human motor unit platform engineered from human embryonic stem cells and immortalized skeletal myoblasts

This article was published in the following Dove Press journal:
Stem Cells and Cloning: Advances and Applications

Marwah Abd Al Samid[1]
Jamie S McPhee[2]
Jasdeep Saini[1]
Tristan R McKay[1]
Lorna M Fitzpatrick[1]
Kamel Mamchaoui[3]
Anne Bigot[3]
Vincent Mouly[3]
Gillian Butler-Browne[3]
Nasser Al-Shanti[1]

[1]Healthcare Science Research Institute, School of Healthcare Science, Manchester Metropolitan University, Manchester, UK; [2]Department of Sport and Exercise Science, Manchester Metropolitan University, Manchester, UK; [3]Center for Research in Myology, Sorbonne Université-INSERM, Paris, France

Background: Although considerable research on neuromuscular junctions (NMJs) has been conducted, the prospect of in vivo NMJ studies is limited and these studies are challenging to implement. Therefore, there is a clear unmet need to develop a feasible, robust, and physiologically relevant in vitro NMJ model.

Objective: We aimed to establish a novel functional human NMJs platform, which is serum and neural complex media/neural growth factor-free, using human immortalized myoblasts and human embryonic stem cells (hESCs)-derived neural progenitor cells (NPCs) that can be used to understand the mechanisms of NMJ development and degeneration.

Methods: Immortalized human myoblasts were co-cultured with hESCs derived committed NPCs. Over the course of the 7 days myoblasts differentiated into myotubes and NPCs differentiated into motor neurons.

Results: Neuronal axon sprouting branched to form multiple NMJ innervation sites along the myotubes and the myotubes showed extensive, spontaneous contractile activity. Choline acetyltransferase and βIII-tubulin immunostaining confirmed that the NPCs had matured into cholinergic motor neurons. Postsynaptic site of NMJs was further characterized by staining dihydropyridine receptors, ryanodine receptors, and acetylcholine receptors by α-bungarotoxin.

Conclusion: We established a functional human motor unit platform for in vitro investigations. Thus, this co-culture system can be used as a novel platform for 1) drug discovery in the treatment of neuromuscular disorders, 2) deciphering vital features of NMJ formation, regulation, maintenance, and repair, and 3) exploring neuromuscular diseases, age-associated degeneration of the NMJ, muscle aging, and diabetic neuropathy and myopathy.

Keywords: motor unit, neuromuscular junctions, human embryonic stem cells, neuronal progenitor cells, human myoblasts

Introduction

Neuromuscular junctions (NMJs) serve as the interface between nerves and skeletal muscles. Maintenance, structure, and formation of NMJs depend on the bidirectional molecular interaction between the muscle and motor neuron.[1] The NMJ consists of a presynaptic motor neuron terminal, a postsynaptic motor end plate and a synaptic cleft. If chemical or molecular communication is disrupted, NMJ deterioration can follow. This involves axon degeneration, synapse disruption, impaired NMJ transmission, and muscle fiber degradation[2] which are the features of neuromuscular diseases, myopathies, and age-associated neuromuscular impairments.[3]

Despite decades of intensive research to characterize the structure and function of NMJs by utilizing animals and ex vivo models,[4] effective treatment of neuromuscular

Correspondence: Nasser Al-Shanti
School of Healthcare Science, Faculty of Science and Engineering, Manchester Metropolitan University, John Dalton Building, Chester Street, M1 5GD Manchester, UK
Tel +44 161 247 5712
Fax +44 161 247 6831
Email n.al-shanti@mmu.ac.uk

submit your manuscript | www.dovepress.com
Dovepress
http://dx.doi.org/10.2147/SCCAA.S178562

and neurodegenerative diseases remains a significant unmet clinical need. This is mainly due to the failure of experimental animal models to reflect complex processes of human aging and disease progression.[5] In order to advance this field, novel, alternative, experimental models are needed.

There has been recent progress toward the development of in vitro co-culture models using human induced pluripotent stem cells (iPSCs);[6,7] mouse,[8] rat,[9] and human primary myoblasts;[10,11] and human embryonic stem cells (hESCs)[12–14] and cross-species models.[15,16] However, existing in vitro motor neuron and skeletal muscle co-culture systems typically require a complex neural growth medium that contains serum and cocktails of around 15 neural growth factors (some of which are derived from animals).[11,12,17] This further complicates drug discovery and toxicology studies due to possible cross-communication of the novel compound with factors contained within the added media, possibly explaining why many promising therapies do not translate to clinics. Another issue with existing models is that muscle contraction is induced by applied electrical or chemical stimulation, which does not replicate the native physiological stimulation required for muscle contractions.[8,17–19] Recent innovation in the use of iPSCs offers the potential to derive myoblasts and motor neurons for use with in vitro NMJ models. However, cells derived from iPSCs may exhibit genetic inconsistency and genetic modification, which limit their use.[20] Recent human iPSC-based studies have failed to recapitulate the severe neuronal loss observed in human neurodegenerative diseases.[21–23] Human skeletal myoblasts which were used in some of the abovementioned models[10,11] were obtained from primary cells (eg, muscle biopsy or surgical samples), but their life span is limited to just a few passages which restricts experimentation and necessitates repeated supply of the primary cells.[24,25] Furthermore, primary cells have varied cell purity[26] and experience phenotypic changes when expanded, rendering primary myoblasts a problematic choice for a consistently reproducible co-culture system.[24,25] Therefore, there is a clear need for a more relevant human experimental model to study motor units and NMJs to overcome the limitations of existing models.

Methods

Human immortalized myoblast cultures

The human immortalized myoblasts cell line ("C25") was obtained from the Institute of Myology.[27] This cell line was established using a biopsy of semi-tendinosis from a 25-year-old male (obtained anonymously from Myobank, a tissue bank affiliated to EuroBioBank which is authorized by the French Ministry of Research [authorization AC-2013-1868]). After attaining 80% confluence, cells were seeded in six-well plates recoated with gelatin (0.5%) at a concentration of 1.5×10^5 cells/mL in growth media. The growth media was supplemented with DMEM from Lonza (Basel, Switzerland), 60% (v/v) Medium 199 with Earle's Balanced Salt Solution from Lonza, 20% (v/v) heat-inactivated FBS from Thermo Fisher Scientific (Waltham, MA, USA), 20% (v/v) L-glutamine from Lonza, 1% (v/v) fetuin from FBS from Sigma-Aldrich (St Louis, MO, USA) 25 µg/mL, recombinant human basic fibroblast growth factor from Thermo Fisher Scientific 0.5 ng/mL, recombinant human EGF from Thermo Fisher Scientific 5 ng/mL, recombinant human hepatocyte growth factor from Sino Biological Inc. (Beijing, China) 2.5 ng/mL, recombinant human insulin from Sigma-Aldrich 5 µg/mL, dexamethasone from Sigma-Aldrich 0.2 µg/mL and gentamicin from Thermo Fisher Scientific.

Neural differentiation of hESCs

Induction of neuroepithelial clusters (NECs)

Mouse embryonic fibroblasts (MEFs; Cell Biolabs, San Diego, CA, USA) were cultured within MEF growth media (summarized in Table 1) and were passaged at a 1:4 ratio. At passage 4 (p4), MEFs were inactivated mitotically using 0.1 µg/mL mitomycin C (Sigma-Aldrich). The Shef3 hESC line was obtained from the UK StemCell Bank under the project SCSC10-48 and maintained on mitotically inactivated MEFs

Table 1 MEF growth media

MEF growth media components	Volume
DMEM from Lonza (Basel, Switzerland)	500 mL
L-glutamine from Lonza	1% (v/v)
Penicillin/streptomycin (Sigma-Aldrich, St Louis, MO, USA)	5 mL (2 mM)
Heat-inactivated FBS from Thermo Fisher Scientific (Waltham, MA, USA)	10% (v/v)

Abbreviation: MEF, mouse embryonic fibroblast.

Table 2 hESC media for cells on MEFs

hESC/MEF cell medium components	Volume
DMEM-F12 (1:1) from Lonza (Basel, Switzerland)	38.5 mL
MEM nonessential amino acids (Thermo Fisher Scientific, Waltham, MA, USA)	0.5 mL (1X)
Penicillin/streptomycin (Sigma-Aldrich, St Louis, MO, USA)	0.5 mL (1X)
bFGF (R&D Systems, Minneapolis, MN, USA) (100 µg/mL)	5 µL (10 ng/mL)
Knockout serum replacement (Thermo Fisher Scientific)	10 mL (20%)

Abbreviations: bFGF, basic fibroblast growth factor; hESC, human embryonic stem cell; MEF, mouse embryonic fibroblast; MEM, Minimum Essential Medium.

in hESC medium (summarized in Table 2) in 96-well plates. hESCs were mechanically passaged every 5–7 days and then conditioned to feeder-free culture by TrypLE Express (Thermo Fisher Scientific) enzyme dissociation and plated at a high density (1:1) onto hESC-qualified Matrigel® (Corning)-coated flasks in mTESR (STEMCELL Technologies). For neural induction, feeder-free hESCs were dissociated with TrypLE and replated in neural induction medium (NIM; summarized in Table 3) in uncoated, V-shaped 96-well plates at a density of 1×10^4 cells/well. Within 24 hours, NECs formed.

Generation of neural rosette-forming progenitor cells (NRPCs)

Medium was replaced daily for 5 days. On day 6, aggregates were replated in 96-well plates in NIM onto 20 µg/mL laminin (Millipore)-coated dishes to allow neural rosette formation (2–3 days).

Expansion of neural progenitor cells

Neural rosette clusters were mechanically isolated and replated in 96-well plates onto laminin-coated dishes in neural expansion medium (NIM plus 1X B27 supplement; Thermo Fisher Scientific). Early- and late-passage neural progenitor cells (NPCs) were cultured in the same conditions and passaged at a 1:3 ratio using TrypLE. To monitor NPCs differentiation into motor neurons, some of the NPCs were transfected with a GFP-reporter lentivirus system.

Immunohistochemistry of NECs, NRPCs, and NPCs

For immunostaining, at each stage of neural differentiation (NECs and NRPCs), cells were sectioned onto glass slides. Sectioned NECs and NRPCs and cultured NPCs in six-well plates were fixed with 4% paraformaldehyde. Fixed sections and NPCs were permeabilized with 0.3% Triton X in PBS and then subsequently blocked with 2% BSA in PBS/Tween 20. The slides were then incubated overnight at 4°C with a primary antibody (MAB2736; R&D Systems). The following day, sections and NPCs were washed with PBS and incubated for 1 hour at room temperature (RT) with goat anti-mouse secondary antibody (Alexa Flour 568-red for NECs, NRPCs and NPCs; Thermo Fisher Scientific) and imaged under a fluorescent microscope (Leica CTR 6000; Leica Microsystems, Wetzlar, Germany).

Table 3 Neural induction medium

NIM components	Volume
DMEM-F12 (1:1) from Lonza (Basel, Switzerland)	48.5 mL
MEM nonessential amino acids (Thermo Fisher Scientific, Waltham, MA, USA)	0.5 mL (1X)
Penicillin/streptomycin (Sigma-Aldrich, St Louis, MO, USA)	0.5 mL (1X)
bFGF (R&D Systems, Minneapolis, MN, USA) (100 µg/mL)	10 µL (20 ng/mL)
N2 supplement (Thermo Fisher Scientific)	0.5 mL (1X)
Heparin (Sigma-Aldrich) (2 mg/mL)	50 µL (2 µg/mL)
Poly (vinyl alcohol) (Sigma-Aldrich)	4 mg/mL

Abbreviations: bFGF, basic fibroblast growth factor; MEM, Minimum Essential Medium; NIM, neural induction medium.

Co-culture of NPCs and human myoblasts

Human myoblasts were incubated over 24 hours at 37°C within a 5% CO_2 environment in six-well plates. Then, the growth media was replaced with co-culture media supplemented with DMEM (500 mL), 10 µg/mL recombinant human insulin, and 10 µg/mL gentamicin. NPCs were present at a concentration of 25×10^3 cells/mL and incubated at 37°C with 5% CO_2 for up to 7 days. At day 7, myotube contractions were observed.

Immunohistochemistry

At day 7, cells were stained with α-Bungarotoxin (α-BTX) (T0195, 1/200; Sigma-Aldrich), and then fixed with 4% paraformaldehyde for 10 minutes at RT. Co-cultures were washed twice with PBS (Thermo Fisher Scientific). After α-BTX staining, cells were washed twice with PBS and permeabilized with 1X perm/wash buffer (BD, Franklin Lakes, NJ, USA) for 30 minutes at RT. Cells were washed twice with PBS and then blocked with PBS containing 1% BSA and 10% goat serum (Thermo Fisher Scientific) for 1 hour at RT. The following antibodies were used: mouse anti-βIII-tubulin (MAB1195, clone #TuJ1, 1/400; R&D Systems), rabbit anti-ryanodine receptor (anti-RyR; AB9078, 1/200; Millipore), goat anti-choline acetyltransferase (anti-ChAT; ABN100, 1/200; Millipore), goat anti-ChAT (AB144, 1/200; Millipore), and mouse anti-dihydropyridine receptor (anti-DHPR; Ab2864, 1/400; Abcam). These antibodies were incubated overnight at 4°C in 1X perm/wash buffer. Co-cultures were washed with PBS and stained with the corresponding secondary antibodies supplemented with DAPI (1/10,000; Sigma-Aldrich) for 1 hour at RT. Stained co-culture cells were visualized using a Leica SP5 confocal microscope sourced by Leica Microsystems for fluorescent microscopy.

Results

A functional human motor unit platform

The present work describes a functional human motor unit platform established using immortalized skeletal myoblasts

and hESCs-derived NPCs that develop into motor neurons in muscle differentiation media (co-culture media) devoid of any complex neural growth factors or serum.

To validate the platform, two monoculture controls were included, one of NPCs and the other of immortalized human myoblasts[27] with co-culture media for 7 days. Cultured GFP-transfected NPCs did not show any morphological changes or motor neuron differentiation, but instead they deteriorated and died (Figure 1A). The human myoblasts stained with phalloidin-DAPI showed normal morphology and differentiation features with centrally and peripherally located nuclei, but the myotubes did not spontaneously contract (Figure 1B).

Derivation of NPCs from hESCs and establishment of the NMJs model

The NPCs were derived from hESCs, as described previously.[28] Neural differentiation of hESCs progressed through three stages of differentiation to NECs (Figure 2A) and NRPCs (Figure 2B) which were stained with Nestin red color. To confirm that differentiated NPCs were homogeneous committed neural lineage, cells were stained with DAPI, anti-GFAP (a specific marker for glial cells) and anti-Nestin. Double-positive staining (DAPI blue and Nestin red) confirmed the formation of NPCs while single DAPI staining was not observed, which confirmed that the differentiated cells were NPCs (Figure 2C). Staining of GFAP was not present, confirming again that all of the cells were NPCs (Figure 2C).

The NPCs were co-cultured with human immortalized myoblasts for 7 days in co-culture media. After myogenic differentiation was initiated, the characteristics of functional motor units began to develop. This included myotube formation and axonal sprouting from the NPCs which subsequently formed NMJs along the myotubes (Figure 2D). The myotubes showed spontaneous muscle contractions from approximately day 7 onwards in the absence of any exogenous electrical and chemical stimuli (Video S1). Due to the force of contractions, some myotubes were detached from the culture plate, causing large spaces within the co-culture. Since the myotubes cultured without NPCs did not contract, they did not detach from the culture plate and did not open up large spaces (Figure 1B).

Characterization of co-cultures

On day 7, the motor neuron formation was assessed using the specific marker for motor neuron differentiation, βIII-tubulin. Figure 3A shows a typical shape of mature motor neurons with axons terminating on myotubes. To further confirm the formation of cholinergic motor neurons, acetyltransferase antibodies (ChAT, a key enzyme for acetylcholine biosynthesis) were used and are shown in green in Figure 3B.

Neurally and aneurally cultured myotubes were characterized by antibody staining against DHPRs and RyRs voltage-gated channels which are located at muscle fiber T-tubules and the sarcoplasmic reticulum, respectively. The DHPR- and RYR-stained images showed transversal triad structures (Figure 3C). These images illustrated mature differentiated myotubes within the co-culture platform with peripherally located nuclei (Figure 3A and B). The aneurally cultured myotubes (control image) differentiated as expected, but did not exhibit appropriate transversal triad structures (Figure 3D).

NMJs display acetylcholine receptor (AChR) clusters along myotubes, and these were assessed by staining for α-BTX, as shown in Figure 3B and E where AChRs are marked by red clusters. As shown in Figure 3A and E, motor neuron axons extend to innervate myotubes and AChR clusters at this same location, marked with α-BTX (red),

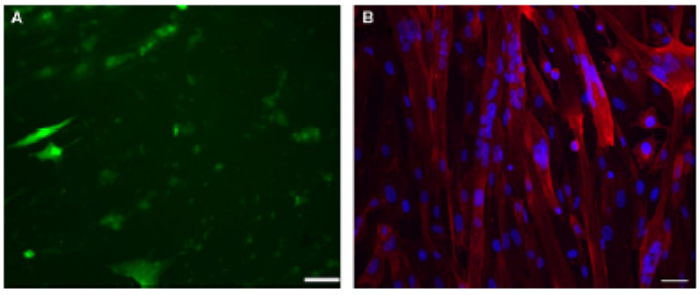

Figure 1 Monoculture of NPCs (**A**) and myoblasts (**B**).
Notes: NPCs and myoblasts were separately cultured for 7 days. The same growth media was used for monocultures and co-cultures. (**A**) A representative image of GFP-transfected NPCs. The NPCs did not exhibit any morphological changes or motor neuron differentiation; instead, they deteriorated and died. (**B**) A representative image of phalloidin-DAPI-stained human myoblasts showed normal morphology and differentiation features with centrally and peripherally located nuclei. Scale bar: 50 μM.
Abbreviation: NPC, neural progenitor cell.

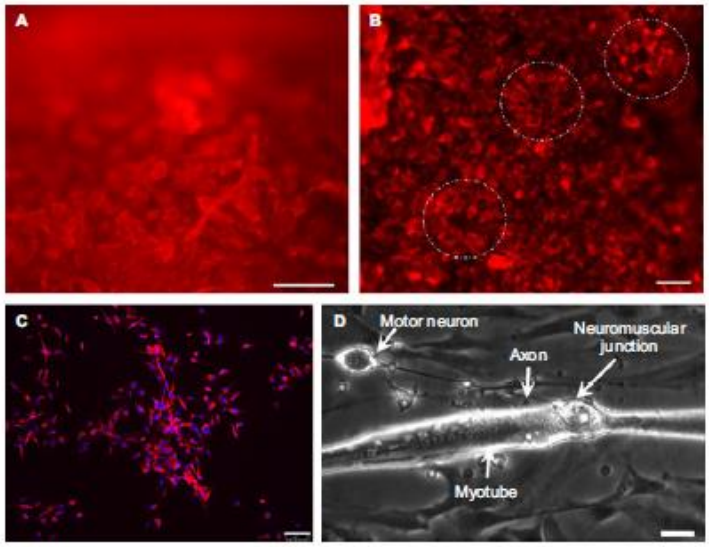

Figure 2 Neural differentiation of hESCs.
Notes: Identification of NPCs from hESCs using Nestin red color as a specific neural differentiation marker. (**A**) NECs. (**B**) NRPCs. (**C**) Nestin-red color for NPCs. (**D**) A representative phase-contrast image of NMJ formation showing an axon extended to contact a myotube. White dotted circle indicates a rosette shape. Scale bars are 100 μM for images (**A**)–(**C**) and 25 μM for image (**D**).
Abbreviations: hESC, human embryonic stem cell; NEC, neuroepithelial cluster; NMJ, neuromuscular junction; NPC, neural progenitor cell; NRPC, neural rosette-forming progenitor cell.

indicating NMJ formation. Spontaneous myotube contractile activity was determined on day 7. The myotubes co-cultured with motor neurons showed high levels of spontaneous contractile activity (Video S1). Muscle contractions were absent from aneural myoblast cultures.

Discussion

Implications and future uses

This report describes a novel functional human motor unit platform engineered from immortalized skeletal myoblasts and NPCs derived from hESCs. This unique platform was established for investigation of human NMJs and motor unit formation, maintenance, and disease, as well as for drug discovery and toxicity research.

The motor neuron and skeletal muscle co-cultures matured without adding complex cocktails of serum or neural growth factors. NMJ formation was observed and spontaneous myotube contractions were recorded (Video S1) over a period as short as 6–7 days, which is very early compared with the 14 days needed in previous studies[16] or where NMJs formed after 20–25 days.[29] These are crucial advances for studying the basic aspects of development and for recognizing pathophysiological systems of NMJ disorders associated with disease or aging. It is important that this type of work is carried out with relevant human cultures to increase the possibility for translation to clinical practice. Most previous cell culture model systems used cross-species cell types[15,19] and required cocktails of serum[30,31] and growth factors.[10,17,19,29] These were absent from the present model without any adverse effects, which suggests that nerve and muscle cells release all of the necessary factors needed to stimulate nerve axonal sprouting and formation of NMJs with myotubes. Moreover, eliminating serum, which contains unknown factors that may affect assay reproducibility, simplifies the interpretation of pharmacology and toxicity studies.[32] Functional NMJ formation is strongly supported by bidirectional communication[1] between nerve and muscle as well as by neural growth factors (such as brain-derived neurotrophic factor, glial cell line-derived neurotrophic factor and neurotrophin-3/4) secreted by muscle to support NMJ formation, maturation and maintenance.[33,34] Future investigations using this model will identify key factors released from nerve and muscle to orchestrate axonal sprouting, localization, and NMJ maintenance.

Although animal models can represent essential parts of physiological changes in a human disease,[35] in vitro human cell cultures offer many advantages because they are formed

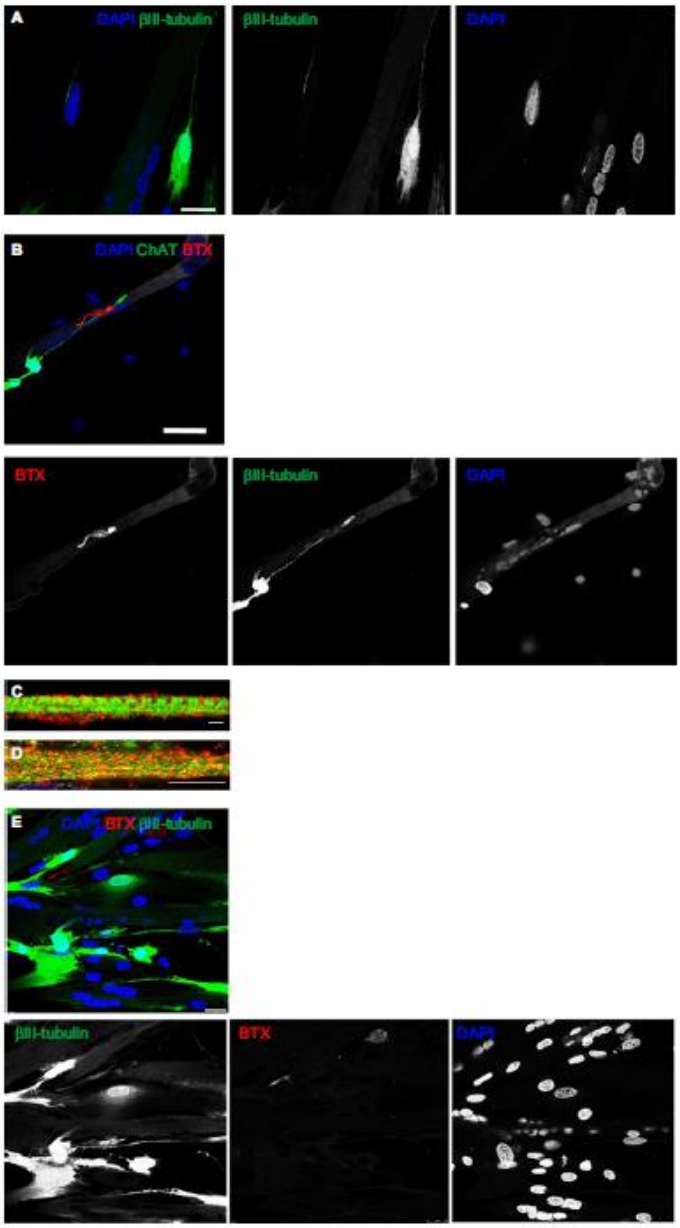

Figure 3 Characterization of muscle–nerve co-cultures.

Notes: (**A** and **B**) Characterization of motor neuron formation. (**A**) A representative image of the co-culture cells stained for βIII-tubulin (green) and DAPI (blue); scale bars: 25 µm. (**B**) A representative image of the co-culture cells stained for ChAT (green), α-BTX (red), and DAPI (blue); scale bars: 75 µm. (**C** and **D**) Characterization of advanced differentiated myotubes. (**C**) A representative image of the co-culture cells stained for DHPR (red), RyR (green), and DAPI (blue); scale bars: 2.5 µm. (**D**) A representative image of the co-culture cells stained for DHPR (red), RyR (green), and DAPI (blue); scale bars: 7.5 µm. (**E**) Characterization of functional NMJs formation. A representative image of the co-culture cells stained for βIII-tubulin (Tuj1; green), α-BTX (red), and DAPI (blue); scale bars: 25 µm.

Abbreviations: α-BTX, α-bungarotoxin; ChAT, choline acetyltransferase; DHPR, dihydropyridine receptor; NMJ, neuromuscular junction; RyR, ryanodine receptor.

of relevant cell types, they can be produced quickly for high-throughput screening, and they are more cost-effective in comparison to animal models.[10,17]

Conclusion

In summary, human immortalized myoblasts were co-cultured with hESCs-derived NPCs. Over the course of 7 days, myoblasts differentiated into myotubes and NPCs sprouted axons that branched to form multiple NMJ innervation sites along myotubes, and myotubes showed extensive, spontaneous contractile activity. This cell culture platform may be used to study human NMJ growth and disease and may reduce the use of animal models in future related research.

Acknowledgment

This work was sponsored by the School of Healthcare Science, Faculty of Science and Engineering, Manchester Metropolitan University (Manchester, UK).

Author contributions

MAS, JSM, and NAS developed the study concept. All the authors contributed to methodology. MAS, JSM, and NAS carried out the investigation. JSM, TRM, and NAS supervised the study. MAS, JSM, and NAS wrote the original draft of the manuscript. MAS, JSM, VM, and NAS reviewed and edited the draft manuscript. All authors contributed to data analysis, drafting or revising the article, gave final approval of the version to be published, and agree to be accountable for all aspects of the work.

Disclosure

The authors report no conflicts of interest in this work.

References

1. Zahavi EE, Ionescu A, Gluska S, Gradus T, Ben-Yaakov K, Perlson E. A compartmentalized microfluidic neuromuscular co-culture system reveals spatial aspects of GDNF functions. *J Cell Sci*. 2015;128(6):1241–1252.
2. Gonzalez-Freire M, de Cabo R, Studenski SA, Ferrucci L. The Neuromuscular Junction: Aging at the Crossroad between Nerves and Muscle. *Front Aging Neurosci*. 2014;6:208.
3. Zhou C, Wu L, Ni F, Ji W, Wu J, Zhang H. Critical illness polyneuropathy and myopathy: a systematic review. *Neural Regen Res*. 2014;9(1):101–110.
4. Wu H, Xiong WC, Mei L. To build a synapse: signaling pathways in neuromuscular junction assembly. *Development*. 2010;137(7):1017–1033.
5. van der Worp HB, Howells DW, Sena ES, et al. Can animal models of disease reliably inform human studies? *PLoS Med*. 2010;7(3):e1000245.
6. Thomson SR, Wishart TM, Patani R, Chandran S, Gillingwater TH. Using induced pluripotent stem cells (iPSC) to model human neuromuscular connectivity: promise or reality? *J Anat*. 2012;220(2):122–130.
7. Berry BJ, Akanda N, Smith AS, et al. Morphological and functional characterization of human induced pluripotent stem cell-derived neurons (iCell Neurons) in defined culture systems. *Biotechnol Prog*. 2015;31(6):1613–1622.
8. Umbach JA, Adams KL, Gundersen CB, Novitch BG. Functional neuromuscular junctions formed by embryonic stem cell-derived motor neurons. *PLoS One*. 2012;7(5):e36049.
9. Smith AS, Long CJ, Pirozzi K, Hickman JJ. A functional system for high-content screening of neuromuscular junctions *in vitro*. *Technology*. 2013;1(1):37–48.
10. Demestre M, Orth M, Föhr KJ, et al. Formation and characterisation of neuromuscular junctions between hiPSC derived motoneurons and myotubes. *Stem Cell Res*. 2015;15(2):328–336.
11. Guo X, Colon A, Akanda N, et al. Tissue engineering the mechanosensory circuit of the stretch reflex arc with human stem cells: Sensory neuron innervation of intrafusal muscle fibers. *Biomaterials*. 2017;122:179–187.
12. Guo X, Greene K, Akanda N, et al. In vitro Differentiation of Functional Human Skeletal Myotubes in a Defined System. *Biomater Sci*. 2014;2(1):131–138.
13. Santhanam N, Kumanchik L, Guo X, et al. Stem cell derived phenotypic human neuromuscular junction model for dose response evaluation of therapeutics. *Biomaterials*. 2018;166:64–78.
14. Happe CL, Tenerelli KP, Gromova AK, Kolb F, Engler AJ. Mechanically patterned neuromuscular junctions-in-a-dish have improved functional maturation. *Mol Biol Cell*. 2017;28(14):1950–1958.
15. Arnold AS, Christe M, Handschin C. A functional motor unit in the culture dish: co-culture of spinal cord explants and muscle cells. *J Vis Exp*. 2012 (62):3616.
16. Vilmont V, Cadot B, Ouanounou G, Gomes ER. A system for studying mechanisms of neuromuscular junction development and maintenance. *Development*. 2016;143(13):2464–2477.
17. Guo X, Gonzalez M, Stancescu M, Vandenburgh HH, Hickman JJ. Neuromuscular junction formation between human stem cell-derived motoneurons and human skeletal muscle in a defined system. *Biomaterials*. 2011;32(36):9602–9611.
18. Miles GB, Yohn DC, Wichterle H, Jessell TM, Rafuse VF, Brownstone RM. Functional properties of motoneurons derived from mouse embryonic stem cells. *J Neurosci*. 2004;24(36):7848–7858.
19. Guo X, das M, Rumsey J, Gonzalez M, Stancescu M, Hickman J. Neuromuscular junction formation between human stem-cell-derived motoneurons and rat skeletal muscle in a defined system. *Tissue Eng Part C Methods*. 2010;16(6):1347–1355.
20. Chin MH, Mason MJ, Xie W, et al. Induced pluripotent stem cells and embryonic stem cells are distinguished by gene expression signatures. *Cell Stem Cell*. 2009;5(1):111–123.
21. Chung CY, Khurana V, Auluck PK, et al. Identification and rescue of α-synuclein toxicity in Parkinson patient-derived neurons. *Science*. 2013;342(6161):983–987.
22. Kondo T, Asai M, Tsukita K, et al. Modeling Alzheimer's disease with iPSCs reveals stress phenotypes associated with intracellular Aβ and differential drug responsiveness. *Cell Stem Cell*. 2013;12(4):487–496.
23. Sareen D, O'Rourke JG, Meera P, et al. Targeting RNA foci in iPSC-derived motor neurons from ALS patients with a C9ORF72 repeat expansion. *Sci Transl Med*. 2013;5(208):ra149.
24. Mouly V, Aamiri A, Périé S, et al. Myoblast transfer therapy: is there any light at the end of the tunnel? *Acta Myol*. 2005;24(2):128–133.
25. Webster C, Blau HM. Accelerated age-related decline in replicative life-span of Duchenne muscular dystrophy myoblasts: implications for cell and gene therapy. *Somat Cell Mol Genet*. 1990;16(6):557–565.
26. Kaur G, Dufour JM. Cell lines: Valuable tools or useless artifacts. *Spermatogenesis*. 2012;2(1):1–5.
27. Mamchaoui K, Trollet C, Bigot A, et al. Immortalized pathological human myoblasts: towards a universal tool for the study of neuromuscular disorders. *Skelet Muscle*. 2011;1:34.
28. Fitzpatrick LM, Hawkins KE, Delhove J, et al. NF-κB Activity Initiates Human ESC-Derived Neural Progenitor Cell Differentiation by Inducing a Metabolic Maturation Program. *Stem Cell Reports*. 2018;10(6):1766–1781.

29. das M, Rumsey JW, Bhargava N, Stancescu M, Hickman JJ. A defined long-term in vitro tissue engineered model of neuromuscular junctions. *Biomaterials*. 2010;31(18):4880–4888.
30. Zhou FM, Hablitz JJ. Layer I neurons of rat neocortex. I. Action potential and repetitive firing properties. *J Neurophysiol*. 1996;76(2):651–667.
31. Walsh K, Megyesi J, Hammond R. Human central nervous system tissue culture: a historical review and examination of recent advances. *Neurobiol Dis*. 2005;18(1):2–18.
32. Rumsey JW, das M, Stancescu M, Bott M, Fernandez-Valle C, Hickman JJ. Node of Ranvier formation on motoneurons in vitro. *Biomaterials*. 2009;30(21):3567–3572.
33. Funakoshi H, Belluardo N, Arenas E, et al. Muscle-derived neurotrophin-4 as an activity-dependent trophic signal for adult motor neurons. *Science*. 1995;268(5216):1495–1499.
34. Henderson CE, Camu W, Mettling C, et al. Neurotrophins promote motor neuron survival and are present in embryonic limb bud. *Nature*. 1993;363(6426):266–270.
35. Jensen J, Hyllner J, Björquist P. Human embryonic stem cell technologies and drug discovery. *J Cell Physiol*. 2009;219(3):513–519.

Stem Cells and Cloning: Advances and Applications

Dovepress
open access to scientific and medical research

Open Access Full Text Article

ORIGINAL RESEARCH

Simplified in vitro engineering of neuromuscular junctions between rat embryonic motoneurons and immortalized human skeletal muscle cells

This article was published in the following Dove Medical Press journal:
Stem Cells and Cloning: Advances and Applications

Jasdeep Saini[1]
Alessandro Faroni[2,3]
Marwah Abd Al Samid[1]
Adam J Reid[2,3]
Adam P Lightfoot[1]
Kamel Mamchaoui[4]
Vincent Mouly[4]
Gillian Butler-Browne[4]
Jamie S McPhee[5]
Hans Degens[1,6,7]
Nasser Al-Shanti[1]

[1]Musculoskeletal Science & Sports Medicine Research Centre, School of Healthcare Science, Manchester Metropolitan University, Manchester, UK; [2]Blond McIndoe Laboratories, Division of Cell Matrix Biology and Regenerative Medicine, School of Biological Sciences, Faculty of Biology Medicine and Health, University of Manchester, Manchester Academic Health Science Centre, Manchester, UK; [3]Department of Plastic Surgery & Burns, University Hospitals of South Manchester, Manchester Academic Health Science Centre, Manchester, UK; [4]Center for Research in Myology, Sorbonne Université–INSERM, Paris, France; [5]Department of Sport and Exercise Science, Manchester Metropolitan University, Manchester, UK; [6]Institute of Sport Science and Innovations, Lithuanian Sports University, Kaunas, Lithuania; [7]University of Medicine and Pharmacy of Targu Mures, Targu Mures, Romania

Correspondence: Jasdeep Saini
School of Healthcare Science, Manchester Metropolitan University, John Dalton Building, E247, Oxford Road, Manchester, M1 5GD, UK
Tel +44 0161 247 5712
Email Jas.Saini2015@gmail.com

Background: Neuromuscular junctions (NMJs) consist of the presynaptic cholinergic motoneuron terminals and the corresponding postsynaptic motor endplates on skeletal muscle fibers. At the NMJ the action potential of the neuron leads, via release of acetylcholine, to muscle membrane depolarization that in turn is translated into muscle contraction and physical movement. Despite the fact that substantial NMJ research has been performed, the potential of in vivo NMJ investigations is inadequate and difficult to employ. A simple and reproducible in vitro NMJ model may provide a robust means to study the impact of neurotrophic factors, growth factors, and hormones on NMJ formation, structure, and function.

Methods: This report characterizes a novel in vitro NMJ model utilizing immortalized human skeletal muscle stem cells seeded on 35 mm glass-bottom dishes, cocultured and innervated with spinal cord explants from rat embryos at ED 13.5. The cocultures were fixed and stained on day 14 for analysis and assessment of NMJ formation and development.

Results: This unique serum- and trophic factor-free system permits the growth of cholinergic motoneurons, the formation of mature NMJs, and the development of highly differentiated contractile myotubes, which exhibit appropriate configuration of transversal triads, representative of in vivo conditions.

Conclusion: This coculture system provides a tool to study vital features of NMJ formation, regulation, maintenance, and repair, as well as a model platform to explore neuromuscular diseases and disorders affecting NMJs.

Keywords: neuromuscular junction, NMJ, coculture, myoblast, myotube, motor neuron, motoneuron

Introduction

Although the neuromuscular junction (NMJ) plays a central role in the pathology of neuromuscular (NM) disorders, current methods to study its role in NM pathology have severe limitations. For instance, most studies on NM diseases rely on in vivo animal models that do not entirely reflect disease in humans.[1] Shortcomings of in vitro models of NM disorders are that they are largely based on cells derived from animals,[2,3] or skeletal muscle cell (SkMC) culture systems that fail to mimic in vivo conditions, particularly due to the lack of functional innervation.[4] Thus, the development of new models to study and manipulate NMJs has the potential to provide significant insight into NM disease pathogenesis and detection, and to test the efficacy of innovative therapies.

To fill this gap, a small number of promising nerve–muscle coculture models have been developed using mouse, rat, primary human myoblasts, human embryonic

http://dx.doi.org/10.2147/SCCAA.S187655

stem cell (hESC) and human induced pluripotent stem cell (hiPSC)-derived cells, and cross-species systems.[5–9] However, some previously established coculture systems suffer from poor experimental reproducibility due to the complexity of the culture system. For example, the use of serum in nerve–muscle coculture systems introduces unspecified variables that can distort the effects of experimental treatments on the system. Further research demonstrates diminished motoneuron myelination in vitro that can be attributed to the use of serum within the culture system.[10]

Coculture systems utilizing primary human skeletal muscle stem cells obtained from muscle biopsies present their own distinct complications as they have limited proliferative capacity and varied cell purity, and experience phenotypic changes when expanded. The phenotypic change is further compounded by progressive cellular senescence during primary cell expansion,[11,12] rendering primary myoblasts a problematic choice for a consistently reproducible coculture system. The use of hESC/hiPSC-derived cells to generate myoblasts[13] and motoneurons[14] may allow for the development of novel coculture systems. However, neuronal cells derived from stem cells are particularly challenging to culture, involving complex media with numerous neurotrophic factors that can have detrimental effects on SkMCs. In addition, cocultures of stem-cell-derived motoneurons and myoblasts result in poorly developed NMJs and have not been maintained for longer than 21 days,[15] which is inadequate for long-duration studies.

This work set out to establish a simplified and easily reproducible nerve–muscle coculture system generating the formation of NMJs. Thus, we developed a novel coculture model devoid of serum and growth/neurotrophic factors. Immortalized human myoblasts were differentiated to mature myotubes while simultaneously being innervated with motoneurons, emanating from neonatal rat spinal cord explants. We observed that this system resulted in the development of highly contractile myotubes that exhibited acetylcholine receptor (AChR) aggregation in the typical twisting knotted structure of mature NMJs that co-localized with motoneuron axon terminals. The success of this system thus offers an easy and reproducible bridge between animal and clinical studies of NM disease and may well serve as a platform to screen the efficacy of novel therapeutic agents.

Experimental procedures

Immortalized human SkMC culture

A non-commercial immortalized human skeletal muscle cell (SkMC) line was generated at the Institute of Myology (Paris, France). The cell line was established using primary human myoblasts obtained anonymously from Myobank, a tissue bank affiliated to Eurobiobank, which has an agreement from the French Ministry of Research (authorization number AC-2013-1868). The primary myoblasts originated from biopsies of the semitendinosus muscle of a 25-year-old man, free of genetic defects and disease. Myoblast immortalization was achieved using transduction with both telomerase-expressing and cyclin-dependent kinase 4-expressing vectors.[37] A 1-mL frozen vial containing a suspension of 1×10^6 SkMCs in 90% FBS and 10% dimethyl sulfoxide (DMSO) was thawed and resuspended in 10 mL of complete growth media (GM)[37] to induce SkMC proliferation.

Cells were incubated at 37°C with a 5% CO_2 atmosphere until 80% confluent. Subsequently, cells were washed twice with Dulbecco's phosphate-buffered saline (DPBS) (Lonza, Basel, Switzerland). Cells were disassociated using 2 mL of TrypLE™ Express Enzyme (Thermo Fisher Scientific, Waltham, MA, USA) and incubated at 37°C in 5% CO_2 for 5 minutes. The cells were counted and then seeded on a 35-mm glass-bottom µ-Dish (ibidi®, Martinsried, Germany) at a density of 350 cells/mm^2, and incubated at 37°C with a 5% CO_2 atmosphere for 24 hours.

Following incubation in GM, cells were washed twice with DPBS and switched to a simplified differentiation medium (DM) consisting of 99% (v/v) DMEM, 1% (v/v) L-glutamine, 10 µg/mL recombinant human insulin, and 10 µg/mL gentamicin. The cells were incubated for 24 hours in DM at 37°C with a 5% CO_2 atmosphere before plating the rat embryo spinal cord explants.

Isolation of rat embryonic spinal cord explants

Ethical approval for the animal work was obtained from the animal facility under a general S1 Home Office license at the University of Manchester. Animal welfare was in accordance with the guidelines detailed in the Animals Scientific Procedures Act 1986, which regulates the use of living vertebrates and cephalopods in scientific procedures within the UK. Time-mated Sprague–Dawley rats from Charles River (Oxford, UK) were killed with CO_2 when embryos were between embryonic development day 13 and 14. Embryo dissection was performed in a 100-mm dish under a binocular microscope using 21-gage needles. The spinal cord was dissected in one piece from the embryo and surrounding connective tissue removed, ensuring that the dorsal root ganglia (DRGs) remained attached to the spinal cord. The spinal cord was sliced transversally into ~1–2 mm^3 explants.

Coculture

DM was removed from the dishes and the cells were washed twice with DPBS; 500 µL DM was added to each dish. Five evenly spaced explants were placed in each dish and incubated for 3 hours at 37°C with a 5% CO_2 atmosphere. Once explants were slightly attached to the SkMCs, an additional 500 µL DM was added to each dish and then incubated for 24 hours. After 24 hours of incubation, a further 1 mL of DM was added to each dish. As the myocytes fuse into immature myotube between 24 and 48 hours, sprouting neurites from the explants innervate the cells at this stage of development. Cocultures were maintained by changing half the DM every 48 hours. Live cells were visualized using a Leica DMI6000 B inverted microscope (Leica Microsystems, Milton Keynes, UK). In addition, real-time myotube contractions were video-captured with phase-contrast microscopy on day 7 at 24 frames per second. Cell fixation for immunocytochemistry was performed on day 14.

Immunocytochemistry

Cells were washed twice with DPBS and fixed in 4% paraformaldehyde for 10 minutes at 21°C. Fixed cells were washed thrice with DPBS and permeabilized with 1× perm/wash buffer (BD Biosciences, Franklin Lakes, NJ, USA), and incubated for 30 minutes at 21°C, followed by a final wash with DPBS. Cells were then incubated for 1 hour in a blocking solution of 0.2% Triton X-100 with 10% normal goat serum (GS) or 10% normal donkey serum (DS) (all from Sigma-Aldrich, St Louis, MO, USA). Blocking solution was removed and cells were washed once with DPBS. The primary antibody in a diluent consisting of 3% GS or DS with 0.05% Tween-20 (Sigma-Aldrich, St Louis, MO, USA) was added to the cells and incubated for 18–24 hours at 4°C. Following primary antibody incubation, the cells were washed thrice with DPBS before incubation with the corresponding secondary antibodies for 1 hour at 21°C. Confirmation of myotube innervation and NMJ formation was assessed via confocal microscopy using the Leica TCS SP5 confocal microscope (Leica Microsystems, Wetzlar, Germany).

Quantification of NMJ morphologies

Innervated and aneural cultures were fixed and stained as described above. Various NMJ morphologies were quantified using previously established NMJ morphology development classifications (ie, mature, fragmented, faint, premature, denervated).[38–41] Twenty random fields of view were assessed at 20× magnification using the Leica TCS SP5 confocal microscope for each data set.

Triad quantification

Innervated and aneural cultures were fixed and stained as described above. Verification of triad formation was assessed using the Leica TCS SP5 confocal microscope. Thirty random fields of view were assessed at 40× magnification.

Results

Characterization of cholinergic motoneurons

An appropriate NMJ is characterized by the connection of cholinergic motoneurons via endplates with SkMCs.[16] In our coculture, motoneurons and myotubes were identified by their staining for choline acetyltransferase (ChAT) and myosin heavy chain (MHC), respectively. Indeed, they were often co-localized (Figure 1) and, together with the numerous motoneuron axon terminals in contact with differentiated myotubes, suggest innervation of the SkMCs. There were also some myotubes with multiple points of contact with

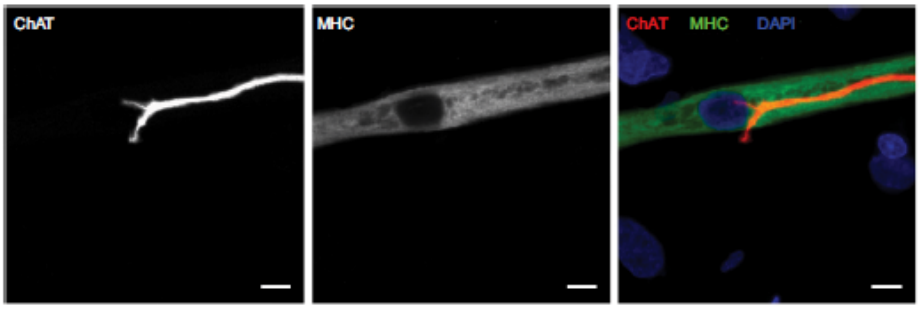

Figure 1 Cholinergic motoneurons co-localize with myotubes at day 14.
Notes: Representative images of human myotube cocultured with embryonic rat motoneuron stained for choline acetyltransferase (ChAT) (red), myosin heavy chain (MHC) (green), and DAPI (blue). Scale bars =7.5 µm.

axon terminals, similar to what is seen in early postnatal muscle development. During in vivo development, myotubes are innervated by multiple branching axons, which extend from many motoneurons. As development progresses, axon pruning occurs and hundreds of mature muscle fibers are innervated by single motoneurons, creating a functional motor unit.[17] Importantly, the development of the cocultures appeared similar to what is observed in vivo before axon pruning occurs.

NMJ formation

Having confirmed the co-localization of cholinergic motoneurons with differentiated myotubes, subsequent experiments were performed to verify that synaptic connections were indeed formed between the motoneurons and myotubes. NMJs are distinguishable by highly clustered AChRs on the myotube membrane in close proximity of motoneuron axons. Motoneurons were identified by staining for β-III-tubulin and AChR clusters were identified with fluorescently labeled α-bungarotoxin (α-BTX) (Figure 2). In the cocultures, numerous axon terminals co-localized with AChR aggregations on the myotube membrane. These clusters of AChRs had the typical twisting-knotted configuration, as seen in vivo, while sparse, unstructured and disjointed AChRs were observed on the membranes of myotubes that were aneurally cultured.

The efficacy of NMJ formation in the coculture system was much better than that in aneurally cultured myotubes, as reflected by a larger proportion of mature NMJs (Figure 3).

Spontaneous myotube contractions

The first spontaneous muscle contractions were detected in the myotubes ~3 days after co-culturing the SkMCs with rat embryo spinal cord explants. We believe this is the first time spontaneous contractions have been observed at this early stage of development in a nerve–muscle coculture system. Despite the fact that myotube contractions were observed as early as 72 hours, only individual arrhythmically contracting myotubes were observed at this time point, with the most vigorously contracting myotubes closest to the explant. The cocultures progressively displayed an increase in both the number of contracting myotubes and the frequency of contractions. By day 7 post coculture, networks of myotubes were contracting simultaneously in a rhythmic manner (Video S1), suggesting that the myotube network functioned as a single motor unit, receiving bursts of stimulation from the motoneurons. Contracting myotubes separated from the culture plate adopted the morphological characteristics of three-dimensional tubes. Conversely, aneurally cultured myotubes did not contract and maintained a flat two-dimensional morphology, firmly fixed to the culture plate surface. These observations indicate that the observed NMJs are in fact functional. However, even at this time point, multiple innervations were still visible on a large proportion (83.4±12.6%, n=20) of the innervated myotubes.

Characterization of innervated myotubes

Mature myotubes in vivo display triads that are arranged in a repetitive transversal manner. Triads consist of a T-tubule with terminal cisternae on each side.[18] T-tubules were identified by staining for the dihydropyridine receptor (DHPR), a voltage-dependent calcium channel located in the T-tubule membrane,[19] and the terminal cisternae were identified by staining for the ryanodine receptor (RyR), which is located on the membrane of the sarcoplasmic reticulum.[20] By day 14, about 32% of the cocultured myotubes had well-developed triads (Figure 4A), whereas none of the aneurally cultured SkMCs exhibited the triad structure (Figure 4B, C).

Discussion

We developed a serum-free coculture of immortalized human myoblasts and embryonic rat spinal cord explants

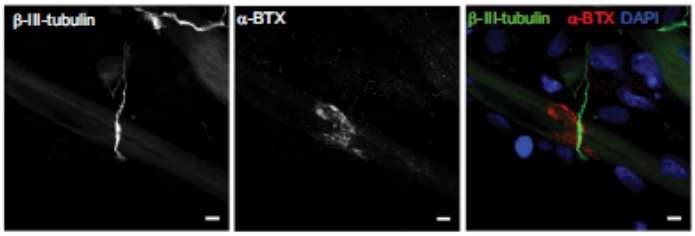

Figure 2 Characterization of neuromuscular junction formation at day 14.
Notes: Representative images of coculture stained for β-III-tubulin (green), α-bungarotoxin (α-BTX) (red), and DAPI (blue). Scale bars =5 μm.

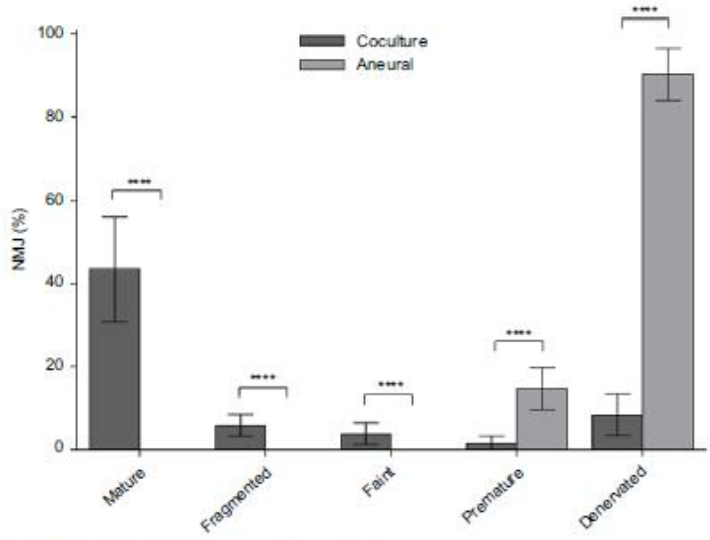

Figure 3 Percentage of various neuromuscular junction (NMJ) morphologies at day 14.
Notes: Cocultured and aneurally cultured myotubes. Results are expressed as mean ± SD, n=4, analyzed with unpaired *t*-test; ****P<0.0001.

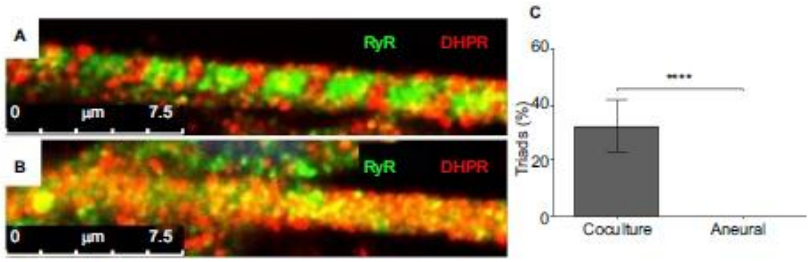

Figure 4 Characterization of myotubes at day 14.
Notes: Representative images of (**A**) a myotube cocultured with embryonic rat spinal cord and (**B**) an aneurally cultured myotube. Myotubes were stained for ryanodine receptor (RyR) (green) and dihydropyridine receptor (DHPR) (red); scale bars =7.5 µm. (**C**) The percentage of myotubes with triads from cocultured and aneurally cultured myotubes. Results are expressed as mean ± SD, n=10, analyzed with unpaired *t*-test; ****P<0.0001.

that successfully produced abundant functional NMJs, as reflected by the structural differentiation and coordinated contractions of myotubes. This coculture model can be used as a model platform to test the efficacy of agents to modulate NMJ structure and function. This may be particularly useful in studies on NM diseases.

Neurons generated in this coculture model were derived from ~1–2 mm transversally sliced spinal cord explants with intact DRGs.[9,21] Preliminary experiments with mechanically disassociated embryo spinal cords to create a neuronal cell suspension, or coculture of myoblasts with the ventral horn only without the DRGs, showed poorer results than the coculture with entire rat embryonic spinal cord explants. The poorer result was reflected by a delayed initiation of spontaneous myotube contractions, higher incidence of arrhythmic contractions, lower contraction frequency, and lower abundance of NMJs that were poorly developed or had a failed junction assembly in comparison to the myoblast plus complete embryonic spinal cord segment coculture (data not shown). While this suggests that both motor and sensory neurons[22] are required for correct innervation of myotubes and NMJ formation, it is more likely that the

progenitor and supporting cell types, such as glial cells, in the DRGs are crucial for correct innervation. Indeed, Schwann cells perform vital functions in motoneuron development, differentiation, and maintaining NMJ integrity.[23] Subsequently, we cocultured myoblasts with rat embryonic spinal cord explants.

In line with previous observations,[24] we found that innervated myotubes in our coculture system were in an advanced state of differentiation and exhibited endogenously stimulated contractility, something not seen in the aneurally cultured SkMCs. The innervation appears to be important, as while treatment of aneurally cultured human myotubes with the secretome of a rat-nerve/human-muscle coculture secretome did increase AChR clustering, it failed to induce advanced myotube differentiation and contractile activity.[25,26] In fact, early research found that myotubes that failed to become innervated within a nerve–muscle coculture system not only failed to differentiate, but eventually even deteriorated, despite nerve-derived secretions in the culture environment.[27]

In our coculture model, myotube contractions were observed as early as 72 hours post coculture, which we believe is the first time contractile functionality has been observed in any nerve–muscle coculture system. This indicates that functional NMJs were already present at this time point, as myotubes require nervous input to induce contraction.[28] Over time, the contraction frequency increased and the contractions occurred synchronously by day 7 (Video S1). At day 14, the cocultured innervated myotubes also displayed the regular appearance, every 2.4 µm, of transversal triads, peripherally located nuclei and actin–myosin striations, all morphological characteristics of advanced differentiation seen in vivo.[29,30] The advanced differentiation of innervated myotubes illustrates the strength of this coculture system over typical aneural in vitro SkMC cultures, which fail to achieve advanced stages of development. Our coculture model thus provides a promising tool to elucidate the significance of the integrity of the NMJ in conditions such as NM disorders.

Our coculture model not only resembled the in vivo skeletal muscle more than aneurally cultured SkMC, but was also simple and reproducibly generated large quantities of functional NMJs. In contrast to our simple model, which already has functional NMJs after 3 days of coculture, other nerve–muscle coculture models require various culture media formulations to separately differentiate myotubes and motoneurons for at least 10 days before co-culturing can even start,[31] and need another 21 days of co-culturing before NMJs form.[5] These lengthy protocols lead to avoidable postponements, possible unintended variation to experimental procedures, and a larger risk of contamination. In our model, however, coculture can start immediately, and after only 3 days, viable NMJs are already detectable.

In addition, other nerve–muscle coculture systems require serum or trophic factors, such as brain-derived neurotrophic factor or insulin-like growth factor-1, to induce spontaneous myotube contractions, myotube innervation, and functional NMJ formation.[5,31–33] Our coculture media were devoid of serum, neurotrophic factors, and growth factors, which will drastically reduce experimental variability. The simplicity of our system makes it ideal for high-throughput research of agents that may affect NMJ formation and myotube differentiation.

High throughput is also facilitated by the fact that a single pregnant rat can yield up to 100 embryo spinal cord explants. This also reduces between-experiment variation as the same spinal cord can be used for different experimental conditions and time points. Although our cocultures were characterized on day 14, preliminary viability experiments revealed that persistent myotube contractions continued to occur as late as day 30, with the potential for further extended viability. Even though the lack of extended viability of other nerve–muscle models[34] has been improved,[32] they still only generated immature NMJs with a speckled AChR morphology and myotubes without advanced differentiation. Clearly, our system is an improvement on these coculture systems as we did see advanced myotube differentiation and a large number of functional NMJs.

Another advantage of our heterologous coculture model is that antibodies specific for rat or human can be used to study both presynaptic and postsynaptic regions of the NMJ. One such application is illustrated by the exploitation of species-specific immunocytochemical staining against acetylcholinesterase (AChE) to differentiate between AChE originating from the human SkMCs and rat neuronal cells at the NMJ.[35] Alternative chimeric cocultures have demonstrated similar advantages. For instance, a coculture model consisting of chick SkMCs innervated by rat neurons was stained using species-specific antibodies to determine that agrin, which is a vital element in the development of the NMJ, is secreted from both SkMCs and motoneurons into the synaptic cleft of NMJs.[36] Fully human homologous hESC/hiPSC-derived SkMC and motoneuron coculture models would be of great interest. However, these systems are still in their infancy and require significant optimization before they parallel the formation of functional NMJs and express the level of differentiation demonstrated in our coculture model.

Conclusion

We have developed an easy and reproducible serum-free coculture of immortalized human myoblasts and embryonic rat spinal cord explants that induces a rapid formation of functional NMJs. The model can be a used as a high-throughput platform to assess the impact of interventions on NM integrity and drug testing.

Acknowledgments

This work was sponsored by the School of Healthcare Science, Faculty of Science and Engineering, Manchester Metropolitan University (Manchester, UK). Thank you to the Lumley Trust, which paid for the animal costs.

Author contributions

JS, AF, AJR, HD, and NAS developed the study concept. All the authors contributed to experimental procedures. JS, AF, and NAS carried out the investigation. AJR, JSM, HD, and NAS supervised the study. JS, HD, APL, and NAS wrote the original draft of the manuscript. JS, MAAS, JSM, HD, and NAS reviewed and edited the draft manuscript. All authors contributed to data analysis and drafting or revising the article, gave final approval of the version to be published, and agree to be accountable for all aspects of the work.

Disclosure

The authors report no conflicts of interest in this work.

References

1. van der Worp HB, Howells DW, Sena ES, et al. Can animal models of disease reliably inform human studies? *PLoS Med*. 2010;7(3):e1000245.
2. Haase G. Motor neuron diseases: cellular and animal models. In: Meyers RA, editor. *Reviews in Cell Biology and Molecular Medicine*. Weinheim: Wiley-VCH Verlag GmbH & Co. KGaA; 2006.
3. Prather RS, Lorson M, Ross JW, Whyte JJ, Walters E. Genetically engineered pig models for human diseases. *Annu Rev Anim Biosci*. 2013;1(1):203–219.
4. Suuronen EJ, Mclaughlin CR, Stys PK, Nakamura M, Munger R, Griffith M. Functional innervation in tissue engineered models for in vitro study and testing purposes. *Toxicol Sci*. 2004;82(2):525–533.
5. Demestre M, Orth M, Föhr KJ, et al. Formation and characterisation of neuromuscular junctions between hiPSC derived motoneurons and myotubes. *Stem Cell Res*. 2015;15(2):328–336.
6. Umbach JA, Adams KL, Gundersen CB, Novitch BG. Functional neuromuscular junctions formed by embryonic stem cell-derived motor neurons. *PLoS One*. 2012;7(5):e36049.
7. Harper JM, Krishnan C, Darman JS, et al. Axonal growth of embryonic stem cell-derived motoneurons in vitro and in motoneuron-injured adult rats. *Proc Natl Acad Sci USA*. 2004;101(18):7123–7128.
8. Guo X, Greene K, Akanda N, et al. In vitro differentiation of functional human skeletal myotubes in a defined system. *Biomater Sci*. 2014;2(1):131–138.
9. Arnold A-S, Christe M, Handschin C. A functional motor unit in the culture dish: co-culture of spinal cord explants and muscle cells. *J Vis Exp*. 2012;62(62):3616.
10. Rumsey JW, Das M, Stancescu M, Bott M, Fernandez-Valle C, Hickman JJ. Node of Ranvier formation on motoneurons in vitro. *Biomaterials*. 2009;30(21):3567–3572.
11. Mouly V, Aamiri A, Périé S, et al. Myoblast transfer therapy: is there any light at the end of the tunnel? *Acta Myol*. 2005;24(2):128–133.
12. Webster C, Blau HM. Accelerated age-related decline in replicative life-span of Duchenne muscular dystrophy myoblasts: implications for cell and gene therapy. *Somat Cell Mol Genet*. 1990;16(6):557–565.
13. Tanaka A, Woltjen K, Miyake K, et al. Efficient and reproducible myogenic differentiation from human iPS cells: prospects for modeling Miyoshi myopathy in vitro. *PLoS One*. 2013;8(4):e61540.
14. Stockmann M, Linta L, Föhr KJ, et al. Developmental and functional nature of human iPSC derived motoneurons. *Stem Cell Rev*. 2013;9(4):475–492.
15. Li XJ, Du ZW, Zarnowska ED, et al. Specification of motoneurons from human embryonic stem cells. *Nat Biotechnol*. 2005;23(2):215–221.
16. Sanes JR, Lichtman JW. Development of the vertebrate neuromuscular junction. *Annu Rev Neurosci*. 1999;22:389–442.
17. Low LK, Cheng HJ. Axon pruning: an essential step underlying the developmental plasticity of neuronal connections. *Philos Trans R Soc Lond B Biol Sci*. 2006;361(1473):1531–1544.
18. Marty I, Robert M, Villaz M, et al. Biochemical evidence for a complex involving dihydropyridine receptor and ryanodine receptor in triad junctions of skeletal muscle. *Proc Natl Acad Sci USA*. 1994;91(6):2270–2274.
19. Rios E, Brum G. Involvement of dihydropyridine receptors in excitation-contraction coupling in skeletal muscle. *Nature*. 1987;325(6106):717–720.
20. Coronado R, Morrissette J, Sukhareva M, Vaughan DM. Structure and function of ryanodine receptors. *Am J Physiol*. 1994;266(6 Pt 1):C1485–C1504.
21. Kobayashi T, Askanas V, Engel WK. Human muscle cultured in monolayer and cocultured with fetal rat spinal cord: importance of dorsal root ganglia for achieving successful functional innervation. *J Neurosci*. 1987;7(10):3131–3141.
22. Mears SC, Frank E. Formation of specific monosynaptic connections between muscle spindle afferents and motoneurons in the mouse. *J Neurosci*. 1997;17(9):3128–3135.
23. Riethmacher D, Sonnenberg-Riethmacher E, Brinkmann V, Yamaai T, Lewin GR, Birchmeier C. Severe neuropathies in mice with targeted mutations in the ErbB3 receptor. *Nature*. 1997;389(6652):725–730.
24. Feher J, editor. The neuromuscular junction and excitation–contraction coupling. In: *Quantitative Human Physiology*. 2nd ed. Boston: Academic Press; 2017:318–333.
25. Bandi E, Jevšek M, Mars T, et al. Neural agrin controls maturation of the excitation-contraction coupling mechanism in human myotubes developing in vitro. *Am J Physiol Cell Physiol*. 2008;294(1):C66–C73.
26. Arnold A-S, Gueye M, Guettier-Sigrist S, et al. Reduced expression of nicotinic AChRs in myotubes from spinal muscular atrophy I patients. *Lab Investig*. 2004;84(10):1271–1278.
27. Askanas V, Kwan H, Alvarez RB, et al. De novo neuromuscular junction formation on human muscle fibres cultured in monolayer and innervated by foetal rat spinal cord: ultrastructural and ultrastructural--cytochemical studies. *J Neurocytol*. 1987;16(4):523–537.
28. Hong IHK, Etherington SJ, editors. Neuromuscular junction. In: *eLS*. Vol. 1. Chichester: John Wiley & Sons; 2011.
29. Bruusgaard JC, Liestøl K, Ekmark M, Kollstad K, Gundersen K. Number and spatial distribution of nuclei in the muscle fibres of normal mice studied *in vivo*. *J Physiol*. 2003;551(2):467–478.
30. Shadrin IY, Khodabukus A, Bursac N. Striated muscle function, regeneration, and repair. *Cell Mol Life Sci*. 2016;73(22):4175–4202.
31. Guo X, Gonzalez M, Stancescu M, Vandenburgh HH, Hickman JJ. Neuromuscular junction formation between human stem cell-derived motoneurons and human skeletal muscle in a defined system. *Biomaterials*. 2011;32(36):9602–9611.

32. das M, Rumsey JW, Bhargava N, Stancescu M, Hickman JJ. A defined long-term in vitro tissue engineered model of neuromuscular junctions. *Biomaterials*. 2010;31(18):4880–4888.
33. Rumsey JW, das M, Bhalkikar A, Stancescu M, Hickman JJ. Tissue engineering the mechanosensory circuit of the stretch reflex arc: sensory neuron innervation of intrafusal muscle fibers. *Biomaterials*. 2010;31(32):8218–8227.
34. das M, Rumsey JW, Gregory CA, et al. Embryonic motoneuron-skeletal muscle co-culture in a defined system. *Neuroscience*. 2007;146(2):481–488.
35. Jevsek M, Mars T, Mis K, Grubic Z. Origin of acetylcholinesterase in the neuromuscular junction formed in the in vitro innervated human muscle. *Eur J Neurosci*. 2004;20(11):2865–2871.
36. Lieth E, Fallon JR. Muscle agrin: neural regulation and localization at nerve-induced acetylcholine receptor clusters. *J Neurosci*. 1993;13(6):2509–2514.
37. Mamchaoui K, Trollet C, Bigot A, et al. Immortalized pathological human myoblasts: towards a universal tool for the study of neuromuscular disorders. *Skelet Muscle*. 2011;1(1):34.
38. Valdez G, Tapia JC, Kang H, et al. Attenuation of age-related changes in mouse neuromuscular synapses by caloric restriction and exercise. *Proc Natl Acad Sci USA*. 2010;107(33):14863–14868.
39. Lee KY, Li M, Manchanda M, et al. Compound loss of muscleblind-like function in myotonic dystrophy. *EMBO Mol Med*. 2013;5(12):1887–1900.
40. Kummer TT, Misgeld T, Lichtman JW, Sanes JR. Nerve-independent formation of a topologically complex postsynaptic apparatus. *J Cell Biol*. 2004;164(7):1077–1087.
41. Sahashi K, Hua Y, Ling KK, et al. Tsunami: an antisense method to phenocopy splicing-associated diseases in animals. *Genes Dev*. 2012;26(16):1874–1884.

Supplementary material

Video S1 Phase-contrast video-micrograph of spontaneously contracting human myotubes that were cocultured with embryonic rat spinal cord explants at day 7. Representative video of innervated myotubes contracting within the coculture system without external stimulation. Scale bar =100 µm.